様式 2-4-1

日米科学技術協力事業「脳研究」分野
グループ共同研究実施報告書　　〔研究分野：　3　〕

１．グループ共同研究代表者

所属機関・職名・氏名
所属機関・部局　東北大学大学院・医学系研究科・精神神経生物学分野
職名　教授
(ﾌﾘｶﾞﾅ)　ソラ　イチロウ
氏名　曽良　一郎
所属機関所在地　〒980-8574　宮城県仙台市青葉区星陵町1-1
連絡先　TEL:　022-717-7808
E-mail: isora@mail.tains.tohoku.ac.jp

２．研究課題名

（和文）ヒトゲノム解析および遺伝子改変動物モデルを用いた
薬物依存の分子遺伝学的研究

（英文）Molecular genetics of substance abuse with human genome scanning and transgenic animal models

３．日本側グループ組織（代表者及び分担者の所属・職・氏名）

東北大学大学院・医学系研究科・精神神経生物学分野
教授　曽良　一郎

４．米国側グループ組織（代表者及び分担者の所属・職・氏名）

米国国立衛生研究所(NIH)付属薬物依存研究所
分子神経生物学研究部門・部門長・ウール、ジョージ

５．研究期間　平成　17　年　4　月　1 日～平成　20　年　3　年　31　日

６．研究の概要，成果及び意義（1000 字）

代表的な依存性薬物である覚せい剤はモノアミントランスポーター、麻薬はオピオイド受容体を標的分子とする。日本側代表の曽良は、米国側代表のNIH薬物依存研究所のUhl博士と遺伝子改変マウスモデルの解析を分担して緊密な共同研究を行い、モノアミントランスポーター欠損マウスでは五つの英文原著論文、オピオイド受容体欠損マウスでは十の英文原著論文を発表した。

メタンフェタミン(MAP)は代表的な覚せい剤であり、モノアミントランスポーターを標的分子として薬物依存を引き起こす。モノアミントランスポーター欠損マウスのMAPに対する解析によりにドーパミントランスポーター(DAT)が、依存形成の指標である行動感作や体温上昇などの神経毒性に他のモノアミントランスポーターよりも重要な役割を果たしていることを明らかにした。モルヒネ、ヘロインなどのオピオイドは、オピオイド受容体を標的分子として鎮痛効果や薬物依存を引き起こす。従来の薬理学的手法では作用機序が十分に解明されていなかったオピオイド系薬物の作用メカニズムについてオピオイド受容体欠損マウスを用いて、オピオイド神経伝達の関与について明らかにした。

日本側代表の曽良が参加する本邦における薬物依存の多施設共同研究コンソーシアムJapanese Genetics Initiative for Drug Abuse (JGIDA)は、これまでに覚せい剤依存の病因・脆弱性遺伝

子について多数の報告を行ってきた。本共同研究では、数万個の遺伝子の関与を検討するためにDNAマイクロアレイを用いた全ゲノムの相関解析を行い、覚せい剤依存の脆弱性候補遺伝子を見いだした。全ゲノム相関解析の成果は精神医学の領域では最も評価の高いArch Gen Psychiatryに発表した。

本邦は他国と比較して依存性薬物の規制に成功している数少ない国であるが、近年は若年層を中心として依存性薬物の乱用・依存は増加している。欧米・アジア諸国、ことに米国では薬物乱用・依存は極めて重大な社会問題を引き起こしおり、多大な国家的対策を必要としている。本研究の成果は未だ病態が十分に明らかではない薬物依存のメカニズムの解明に貢献できたと考えられる。

７．その他（実施上の問題点，特記事項等）

特になし

◎参考資料があれば，添付ください。

1. Ikeda K, Ide S, Han W, Hayashida M, Uhl GR, Sora I. How individual sensitivity to opiates can be predicted by gene analyses. **Trends Pharmacol Sci** 26(6): 311-317 (2005)
2. Wu HE, Sun HS, Terashivili M, Schwasinger E, Sora I, Scott Hall F, Uhl GR, Tseng LF. *dextro*- and *levo*-morphine attenuate opioid delta and kappa receptor agonist produced analgesia in mu-opioid receptor knockout mice. **Eur J Pharmacol**. 531(1-3):103-107 (2006)
3. Yamada H, Shimoyama N, Sora I, Uhl RG, Fukuda Y, Moriya H, Shimoyama M. Morphine can produce analgesia via spinal kappa opioid receptors in the absence of mu opioid receptors. **Brain Research.** 1083:61-69 (2006)
4. Kasai S, Han W, Ide S, Hata H, Takamatsu Y, Yamamoto H, Uhl GR, Sora I, Ikeda K. Involvement of the 3' non-coding region of the mu opioid receptor gene in morhine-induced analgesia. **Psychiatry Clin Neurosci.** 60: S11-17 (2006)
5. Han W, Kasai S, Hata H, Takahashi T, Takamatsu Y, Yamamoto H, Uhl GR, Sora I, Ikeda K. Intracisternal A-Particle Element in the 3' Noncoding Region of the Mu Opioid Receptor Gene in CXBK Mice: A New Genetic Mechanism Underlying Differences in Opioid Sensitivity. **Pharmacogenetics and Genomics** 16(6):451-460 (2006)
6. Han W, Hata H, Imbe H, Liu QR, Takamatsu Y, Koizumi M, Murphy NP, Senba E, UhI GR, Sora I, Ikeda K. Increased body weight in mice lacking mu-opioid receptors. **Neuroreport** 17(9):941-944 (2006)
7. Ide S, Minami M, Ishihara K, Uhl GR, Sora I, Ikeda K. Mu opioid receptor-dependent and independent components in effects of tramadol. **Neuropsychopharmacology** 51(3):651-658 (2006)
8. Yamashita M, Fukushima S, Shen H, Hall FS, Uhl GR, Numachi Y, Kobayashi H, Sora I. Norepinephrine transporter blockade can normalize the prepulse inhibition deficits found in dopamine transporter knockout mice. **Neuropsychopharmacology** 31(10):2132-2139. (2006)
9. Harburg GC, Hall FS, Harrist AV, Sora I, Uhl GR and Eisch AJ. Knockout of the mu opioid receptor enhances the survival of adult-generated hippocampal granule cell neurons. **Neuroscience.** 144(1):77-87(2007)
10. Fukushima S, Shen H, Hata H, Ohara A, Ohmi K, Ikeda K, Numachi Y, Kobayashi H, Hall FS, Uhl GR, Sora I. Methamphetamine-induced locomotor activity and sensitization in dopamine transporter and vesicular monoamine transporter 2 double mutant mice. **Psychopharmacology.** 193(1):55-62(2007)
11. Yamamoto H, Kamegaya E, Hagino Y, Imai K, Fujikawa A, Tamura K, Enokiya T, Yamamoto T, Takeshima T, Koga H, Uhl GR, Ikeda K, Sora I. Genetic deletion of vesicular monoamine transporter-2 (VMAT2) reduces dopamine transporter activity in mesencephalic neurons in primary culture. **Neurochemistry International.** 51: 237–244(2007)
12. Numachi Y, Ohara A, Yamashita M, Fukushima S, Kobayashi H, Hata H, Watanabe H, Hall FS, Lesch KP, Murphy DL, Uhl GR, Sora I. Methamphetamine-induced hyperthermia and lethal toxicity: role of the dopamine and serotonin transporters. **Eur J Pharmacol.** 572: 120-128(2007)
13. Job MO, Tang A, Hall FS, Sora I, Uhl GR, Bergeson SE, Gonzales RA. Mu opioid receptor regulation of ethanol-induced dopamine response in the ventral striatum: evidence of genotype specific sexual dimorphic epistasis. **Biol Psychiatry.** 62 (6): 627-634 (2007)
14. Ide S, Minami M, Ishihara K, Uhl GR, Satoh M, Sora I, Ikeda K. Abolished thermal and mechanical antinociception but retained visceralchemical antinociception induced by butorphanol in m-opioidreceptor knockout mice. **Neuropharmacology.** 54 : 1182–1188 (2008)
15. Perona MT, Waters S, HallFS, Sora I, Lesch KP, Murphy DL, Caron M, Uhl GR. Animal models of depression in dopamine, serotonin, and norepinephrine transporter knockout mice: prominent effects of dopamine transporter deletions. **Behav Pharmacol.** 19(5-6):566-74(2008)
16. Uhl GR, Drgon T, Liu QR, Johnson C, Walther D, Ujike H, Komiyama T, Harano M, Sekine Y , Inada T, Ozaki N, Iyo M, Iwata N , Yamada M, Sora I, Chen CK, Liu HC, Lin SK. Genome-wide association for methamphetamine dependence: convergent results from two samples. **Arch Gen Psychiatry.** 65(3):345-355 (2008)

Review TRENDS in Pharmacological Sciences Vol.26 No.6 June 2005

How individual sensitivity to opiates can be predicted by gene analyses

Kazutaka Ikeda[1], Soichiro Ide[1,2], Wenhua Han[1], Masakazu Hayashida[3], George R. Uhl[4] and Ichiro Sora[1,5]

[1]Department of Molecular Psychiatry, Tokyo Institute of Psychiatry, 2-1-8 Kamikitazawa, Setagaya-ku, Tokyo 156-8585, Japan
[2]Laboratory of Neuropharmacology, Department of Pharmaceutical Sciences, Hiroshima International University, 5-1-1 Hirokoshingai, Kure, Hiroshima 737-0112, Japan
[3]Surgical Center Research Hospital, The Institute of Medical Science, The University of Tokyo, 4-6-1 Shirokanedai, Minato-ku, Tokyo 108-8639, Japan
[4]Molecular Neurobiology, National Institute on Drug Abuse, Baltimore, MD 21224, USA
[5]Division of Psychobiology, Department of Neuroscience, Tohoku University Graduate School of Medicine, 1-1 Seiryo-machi, Sendai 980-8574, Japan

Opiate analgesics are widely used and abused drugs. Individual differences in opiate sensitivity can hamper effective pain treatments and increase risks of drug abuse. Although genetic factors might affect individual differences in opiate sensitivity, scientific evidence for specific genetic mechanisms that underlie these differences has been sparse. Recent studies using inbred and knockout mice have revealed that the mu opioid peptide (MOP) receptor encoded by the *Oprm1* gene has a mandatory role in the analgesic and addictive properties of opiate drugs. Increasing evidence suggests that differences in *Oprm1* gene sequences affect the amount of *Oprm1* mRNA and sensitivity to opiates, and >100 polymorphisms have been identified in the human *OPRM1* gene, some of which are related to vulnerability to drug dependence in some populations. Rapid advances in this research field are leading to improved understanding of the relationships between gene polymorphisms and opiate sensitivities that will enable more-accurate prediction of the opiate sensitivity and opiate requirements in individual patients.

Opiates, pain and addiction: individual differences

Opiate drugs are used widely for the treatment of pain. However, sensitivity to opiates can vary widely among individuals and thus effective pain treatment is often hampered by significant differences in opiate sensitivity [1]. Several recent studies have suggested that polymorphisms in the human *OPRM1* gene, which encodes the mu opioid peptide (MOP) receptor, might contribute to this wide variation in opiate sensitivity [2–4]. Thus, studies on the relationship between *OPRM1* gene patterns and opiate sensitivity might lead to the development of methods for predicting opiate sensitivity and opiate requirements for individual patients. In this review, we will summarize current knowledge about the relationships between *OPRM1* gene polymorphisms and opiate sensitivity, including rapidly accumulating data from both animal and human studies.

Current status of the clinical use of opiates

Opiates, such as morphine and fentanyl, are arguably the most important human analgesics and have long been used to alleviate a variety of types of pain, including acute (e.g. perioperative) and chronic (e.g. cancer) pain [1,5–7]. However, this clinical benefit is associated with several difficulties. For example, insufficient doses of opiates that fail to provide adequate pain relief are often identified in clinical settings, whereas high doses of opiates can result in adverse side-effects that include nausea, vomiting, constipation and life-threatening respiratory depression [1,5–7]. Furthermore, chronic and/or inappropriate use of opiates increases the risk of problematic adverse effects that include tolerance to the analgesic effects of opiates, the development of physical opiate dependence and the development of addiction to opiates. Clinical observations have confirmed, however, that many such adverse effects can be avoided when opiates are used appropriately [5]. Proper administration of opiates to meet the needs of individual patients is therefore crucial.

Despite the importance of using the correct administration protocol for opiates, predicting the optimal dose for individual patients is difficult. As mentioned earlier, the sensitivity to opiates varies widely among individual subjects [8,9]. For example, the minimal effective analgesic concentration (MEAC) of the potent MOP receptor agonist fentanyl required for analgesia varies from 0.2 to 2.0 ng ml^{-1} among patients [9]. Similarly, MEACs for other MOP receptor agonists, including morphine, pethidine, alfentanil and sufentanil, vary among patients by factors of 5 to 10 [9,10]. Because of this variability, a plasma opiate concentration that can produce satisfactory pain relief without adverse effects in some patients might provide under-dosing (with failure of pain relief) or overdosing (with serious adverse effects) in other patients (Figure 1). Although some of these differences in sensitivity can be related to differences in environmental

Corresponding author: Ikeda, K. (ikedak@prit.go.jp).
Available online 3 May 2005

 0165-6147/$ - see front matter doi:10.1016/j.tips.2005.04.001

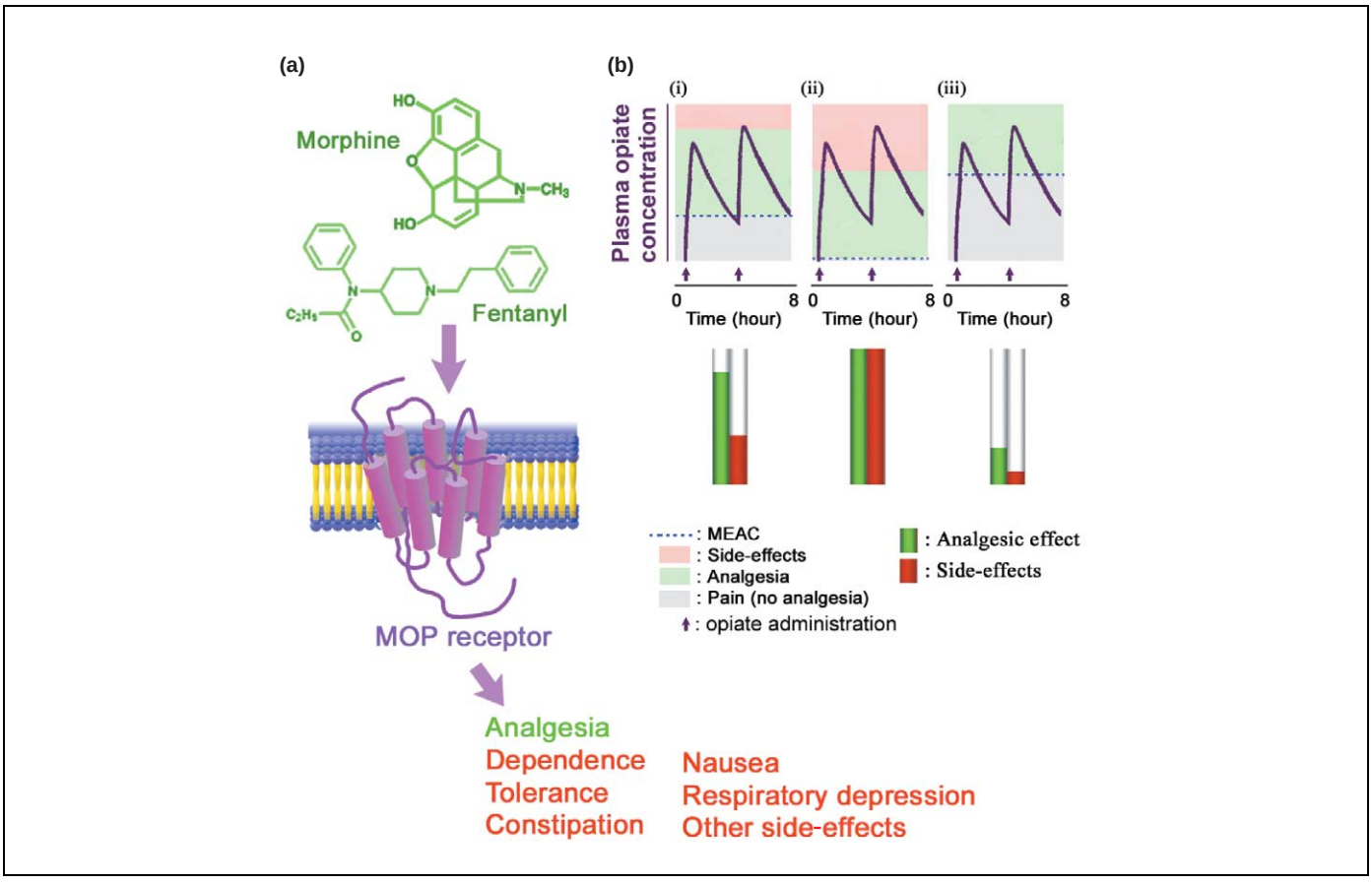

Figure 1. Individual differences in opiate sensitivity. **(a)** Opiate analgesics, such as morphine and fentanyl, act mainly on mu opioid peptide (MOP) receptors and induce analgesia together with adverse side-effects such as dependence, tolerance, constipation, nausea and respiratory depression. **(b)** Opiate sensitivity differs among individuals at least partly because of the differences in the *OPRM1* gene. Although the plasma opiate concentration after its administration (arrows) changes in the same manner in different patients (i–iii), the clinical response can differ between patients because of 5–10-fold inter-patient differences in the minimal effective analgesic concentration (MEAC) (dashed blue line). Gray, green and red zones indicate ranges of the plasma opiate concentration that produce no analgesia, satisfactory analgesia and severe side-effects, respectively. An opiate dose that provides satisfactory pain relief in some patients (i) can thus be an overdose (associated with severe side-effects) in others (ii) or, conversely, an 'under-dose' (associated with persistent pain) in others (iii). Green and red bars indicate the magnitudes of the analgesic effect and side-effects, respectively.

factors, pain severity, age, emotional state and prior pain experience, much of this variation in opiate sensitivity is likely to be due to genetic factors [3,4,11,12]. Analyzing the effects of human genetic variations on traits as complex as pain can require large samples. Ethical constraints limit pain research in humans and thus animal models continue to provide powerful templates for elucidating how genetic differences might affect opiate sensitivity in humans. Recent data from both rodent and human studies summarized later reveal evidence for genetic mechanisms that underlie variations in the *OPRM1* gene that could contribute to human individual differences in opiate sensitivity.

MOP receptor expression levels and opiate sensitivity

Opiates exert their pharmacological actions through opioid peptide receptors, which exist as mu, delta and kappa subtypes [6]. Several studies on mice that lack the *Oprm1* gene have now provided evidence that the MOP receptor is the subtype that is essential for the analgesic effects, rewarding effects and most of the side-effects of most clinically useful opiate drugs [13,14]. In several independently tested strains of MOP receptor knockout mice, morphine does not exert any analgesic effect even though normal complements of delta and kappa opioid peptide receptors are present. Homozygous and heterozygous MOP receptor knockout mice that display 0% and 50% of the levels of MOP receptors identified in wild-type mice display complete abolition and partial reductions, respectively, of the analgesic effects of morphine. Analgesia produced by morphine thus depends crucially on MOP receptor densities [13]. In addition, nociceptive sensitivity is increased in MOP receptor knockout mice compared with that in wild-type mice. Thus, the densities of *Oprm1* expression can affect pain sensitivity even without the presence of opiates [15]. Individual variation in MOP receptor densities has also been recognized in humans [3,4,11]. Identification of the genetic mechanisms that control the variation in *OPRM1* expression might thus improve our understanding of the individual differences in responses to opiates and/or pain sensitivity.

Genetic mechanisms underlying mouse strain differences in opiate sensitivity

Mice have been systematically bred so that many strains are available, and have been subjected to detailed genomic characterization. Thus, mouse genome sequences and many of the variations that distinguish common strains are known. Mice of the same strain are identical in genotype and similar in phenotype whereas mice of

different strains have different genotypes and therefore often show different phenotypes. Differences found among mouse strains provide models for differences among humans, where consanguineous marriage is rare and genetic variations are substantial. Comparative studies of different mouse strains that elucidate the genetic differences that account for strain-to-strain differences in phenotype thus provide insights into possible genetic mechanisms for variation in opiate sensitivity among humans [4,16]. One approach involves mapping mouse inter-strain genetic variations and correlating these variations with inter-strain differences in sensitivity to opiates.

Such comparisons among different mouse strains reveal significant correlations between *Oprm1* expression levels and responses to morphine [4]. The gene loci responsible for differences in response to morphine among different inbred strains have also been mapped using quantitative trait locus (QTL) approaches [11]. Results from QTL studies suggest that allelic variations in the vicinity of the *Oprm1* gene are linked to variations in the analgesic effect of morphine. In addition, the genetic mechanisms that underlie the reduced opiate sensitivity identified in CXBK mice have also been revealed by studies of their *Oprm1* gene (Figure 2). The CXBK mouse is an inbred strain derived from F2 intercrosses between C57BL/6By (B6) and BALB/cBy mice. CXBK mice have been used widely for >20 years as a model for reduced MOP receptor expression because CXBK mice exhibit significantly reduced responses to opiate agonists and reduced binding of opioids, compared with the parent strains [2]. CXBK mice thus display a phenotype similar to those displayed by heterozygous MOP receptor knockout mice [17]. Recently, it was shown that CXBK mice possess a longer *Oprm1* mRNA and express this mRNA at lower levels than either of their progenitor strains [18]. There is an ~5.3-kilobase (kb) insertion in the 3′ untranslated region (UTR) of the CXBK mouse *Oprm1* gene [19]. This 3′UTR provides differential regulation of the rate of translation and degradation of *Oprm1* mRNAs through differential interactions with proteins that bind to 3′UTR sequences. These observations in CXBK mice are consistent with clinical reports that suggest that other human diseases, such as myotonic dystrophy and Fukuyama-type congenital muscular dystrophy, are associated with variations in 3′UTR sequences of other genes [20]. The sequences inserted into the 3′ UTR of CXBK mouse lines are thus likely to explain the reduced levels of *Oprm1* mRNA expression and the reduced sensitivity to morphine in these mice. CXBK mice thus provide a useful model for exploring the contribution of 3′UTR variation to the regulation of the *Oprm1* gene. It is likely that such investigations of the genetic mechanisms that underlie mouse inter-strain differences in opiate sensitivity will be helpful in exploring genomic variations that might be responsible for individual differences in opiate sensitivity in humans.

Structure and polymorphisms of the *Oprm1* gene

The mouse *Oprm1* gene is >53 kb long. Exon splice junctions are found at sites that correspond to the

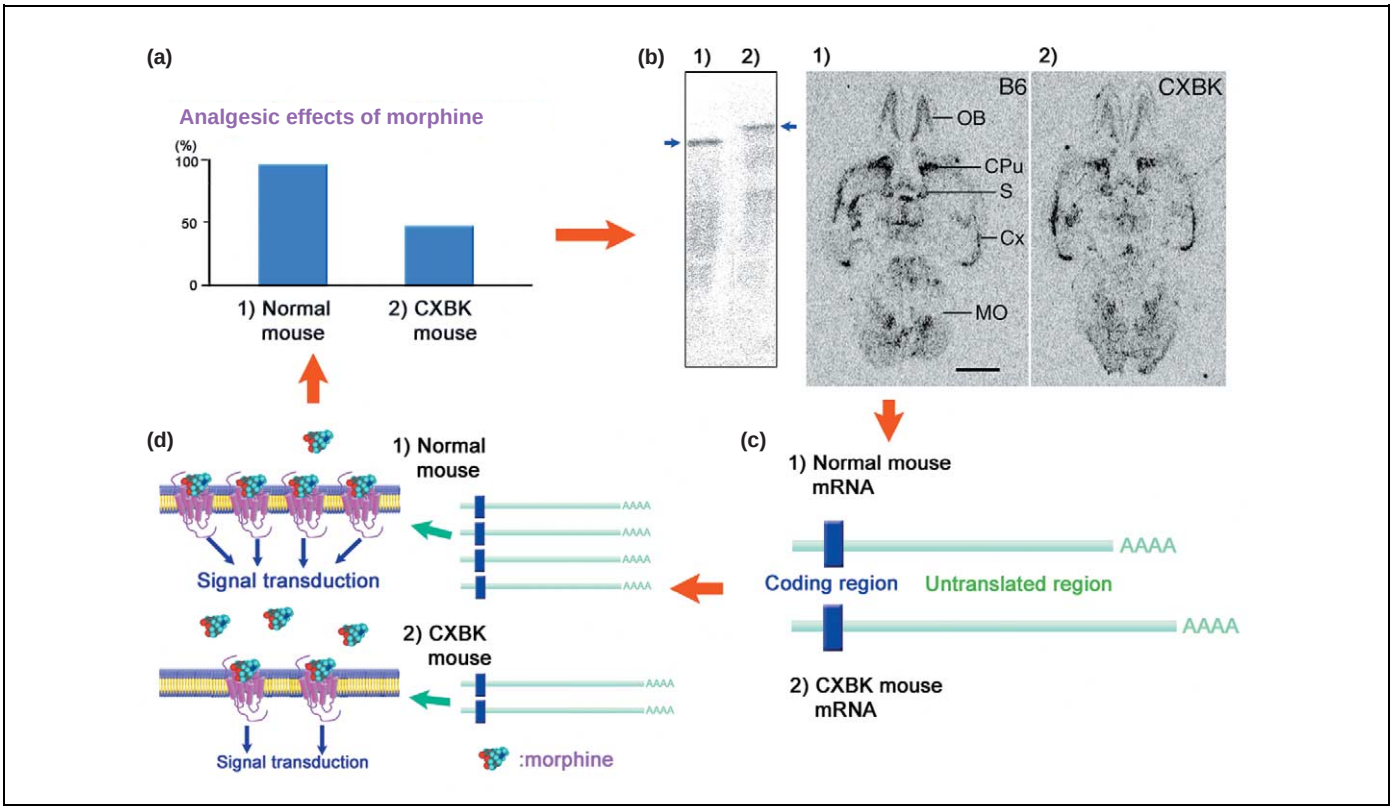

Figure 2. Mechanisms that underlie reduced morphine effects in CXBK mice. **(a)** CXBK mice show less analgesic effects of morphine than other strains in anti-nociceptive tests. **(b)** It has been revealed that the CXBK mouse has an abnormally long *Oprm1* mRNA (arrow in second lane of northern blot in left-hand panel). Furthermore, a reduced level of *Oprm1* mRNA (black) is seen in the CXBK mouse brain without a change in distribution (*in situ* hybridization in right-hand panel). **(c)** The untranslated region of *Oprm1* mRNA in CXBK mice is longer than that of other mouse strains. **(d)** It is thought that longer *Oprm1* mRNA in CXBK mice causes reduced expression of MOP receptors and thus less signal transduction. Abbreviations: B6, C57BL/6By mice; CPu, caudate–putamen; Cx, cerebral cortex; MO, medulla oblongata; OB, olfactory bulb; S, septum.

junctions of the first intracellular loop (Arg95), second extracellular loop (Gly213) and C-terminal cytoplasmic region (Gln386/Leu387) of the MOP receptor [21]. Intron 1 is >26 kb in length, whereas intron 2 is 773 base pairs (bp) and intron 3 is >12 kb in length. Based on currently identified gene structures, distal and proximal candidate promoter regions have been identified in the *Oprm1* gene [4,21]. Studies using techniques that include rapid amplification of the cDNA 5′ ends have suggested that transcription is initiated at two sites that lie −793 and −268 bp from the translational start site [22]. The cDNA sequence of the mouse *Oprm1* gene thus begins 268 or 793 nucleotides from the initiating ATG codon, contains an open reading frame of 389 amino acids and encodes a 44.5-kDa protein. Some research groups have reported the existence of several splicing variants [23], and northern blot analyses have revealed a predominant *Oprm1* transcript, MOR-1 [18].

Current models of the 3′UTRs of the mouse and human MOR-1 mRNAs indicate approximate 10-kb and 13.6-kb lengths, respectively. Based on the results obtained from studies of CXBX mice noted earlier, it is possible that polymorphisms in these large *Oprm1* UTRs and introns could contribute to individual differences in modulating *Oprm1* expression.

Cloning of the rhesus monkey *OPRM1* coding region reveals 98% homology with the human *OPRM1* coding region. A single nucleotide polymorphism (SNP), C77G, in the *OPRM1* gene in rhesus monkeys alters an N-terminal region amino acid [24], and this SNP provides a homolog for the relatively common A118G variant identified in the human *OPRM1* gene [25] (see later). Studies of the rhesus monkey variant suggest that, compared with C77-containing alleles, G77-containing alleles are associated with higher β-endorphin affinity, lower blood cortisol levels and higher aggressive threat scores that provide a striking analogy with findings associated with the G118-containing alleles identified in humans [25] (see later). The similarity of the phenotypes induced by the C77G rhesus monkey and A118G human SNPs supports the notion that the non-human primate might serve as a particularly useful experimental model for the investigation of SNP functions in the human *OPRM1* genes that display rhesus monkey homologs.

Re-sequencing human *OPRM1* genomic sequences from many individuals has now identified >100 polymorphisms (Figure 3). These polymorphisms are more frequent in the non-protein-coding exonic regions than in the translated exonic sequences. However, at least ten SNPs have been reported in *OPRM1* translated regions [25–30]. The A118G variant is the most frequent coding region variant in most samples. However, its frequency differs substantially from individuals in one population to individuals in other populations. For example, the frequency of this polymorphism is ~45% in Asian populations but between 5% and 25% in both European- and African-American populations [25,27–31]. At least 41 SNPs have been reported in the 5′UTR and 5′ flanking regions of *OPRM1* [26,31]. Sequences between nucleotides −4500 and −2500 are substantially conserved in humans and mice, which suggests that this region in the genome might have particular relevance for *OPRM1* gene regulation [4]. Interestingly, little sequence variation in this region has been reported. Eight SNPs have been identified in the relatively short intron 2 (773 bp), which is equivalent to nearly one mutation per 100 bp ([26,27,30]; S. Ide, PhD thesis, Kyoto University, 2004). These findings are consistent with the observation that intronic sequences might be subjected to lower selection pressure than coding regions [32]. Fifty-four SNPs have been identified in the 3′UTR and 3′ flanking regions of *OPRM1* (S. Ide, PhD thesis, Kyoto University, 2004). These polymorphisms are good candidates to be correlated with *OPRM1* mRNA stability and opiate sensitivity because levels of gene expression can be regulated by DNA sequences located in both the 3′UTR and the 5′UTR [20].

These sequence variants represent possible sites for differential gene regulation, and also provide markers for haplotype blocks (sets of polymorphisms that are linked closely enough to be inherited as a unit) that can be identified as a result of their linkage disequilibrium (the condition in which the haplotype frequencies in a population deviate from the values they would have if the genes at each locus were combined at random). These patterns of linkage disequilibrium provide correlations among many neighboring alleles. They identify haplotypes that reflect groups of nearby variants that tend to be found together in members of the population. Association or linkage disequilibrium mapping is also a relatively powerful tool for identifying gene variants that contribute to individual differences in complex traits and diseases (e.g. breast cancer) [33–35]. The linkage disequilibrium relationships in the *OPRM1* gene have been analyzed [26,28,31,36–38]. There are several linkage disequilibrium relationships in the *OPRM1* gene, although the degree of recombination in the gene might be increased relative to that of other genes because of its relatively telomeric position on chromosome 6 (6q24–q25). In exon 1 of *OPRM1*, several SNPs show significant linkage disequilibrium [28,36,37], and form a block with only several haplotypes. Three other linkage disequilibrium blocks cover regions that range from exon 1 to the 3′UTR (S. Ide *et al.*, unpublished). These relatively large linkage disequilibrium blocks indicate that a relatively restricted number of all of the possible combinations of variants at the *OPRM1* locus are actually found. These studies identify differences in polymorphism patterns that include those that might alter the levels of *OPRM1* gene expression.

Human *OPRM1* gene polymorphisms and the associations with various opiate effects

Differences in the *OPRM1* gene are thus likely to affect opiate analgesia, tolerance and dependence [4,11]. Other mouse studies indicate that *Oprm1* variants might have roles in addictions not only to opiates, but also to alcohol and non-opiate abused drugs [39–44]. Several studies have demonstrated associations between the frequencies of polymorphisms in the human *OPRM1* gene and opiate dependence in various populations [26,30,36–38,45]. In these association studies, the A118G *OPRM1* SNP has been studied most intensively. This missense SNP changes the N-terminal region amino acid asparagine to

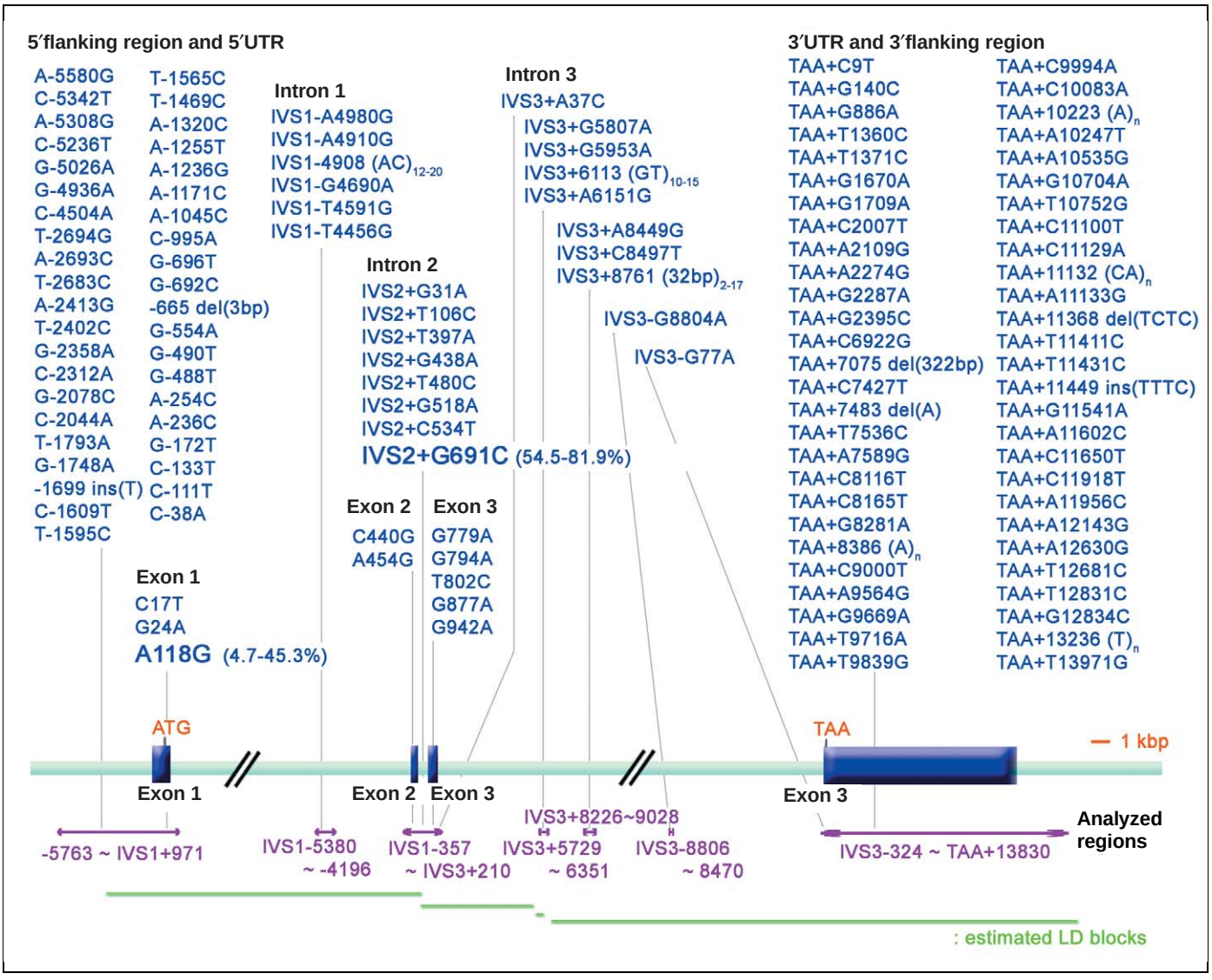

Figure 3. Polymorphisms and estimated linkage disequilibrium (LD) blocks in the human *OPRM1* gene. All exons, parts of the 5′ and 3′flanking regions and parts of the introns of the *OPRM1* gene have been analyzed (as illustrated by double-headed purple arrows under the scheme of the *OPRM1* gene) ([25–30]; S. Ide, PhD thesis, Kyoto University, 2004). Polymorphisms in the *OPRM1* gene are indicated by blue letters. The allelic frequencies of some polymorphisms are extremely different among populations (e.g. A118G in exon 1 and IVS2+G691C in intron 2) ([25–30]; S. Ide, PhD thesis, Kyoto University, 2004). Furthermore, it has been revealed that the polymorphisms in the *OPRM1* gene are well linked, and four linkage disequilibrium blocks are estimated to exist in the *OPRM1* gene (the green lines under the analyzed regions). Abbreviations: del, deletion; ins, insertion; IVS, intervening sequence.

aspartic acid, thus decreasing the number of sites for N-linked glycosylation of the MOP receptor from five to four. The A118G SNP is reported to increase the affinity of MOP receptor for β-endorphin by perhaps threefold [25]. Several studies have demonstrated associations between the frequencies of the A118G *OPRM1* genomic polymorphisms and opiate [30,38], alcohol [25,29] or poly-drug [26,37] dependence. However, conflicting and/or inconsistent results have also been reported [36,46].

Significant findings using other *OPRM1* SNPs include the relationship between the SNP IVS2 (intervening sequence 2) +C691G and methamphetamine dependence in Japanese samples (S. Ide *et al.*, unpublished). Most previous studies analyzed polymorphisms in protein-coding regions or 5′UTRs, with particular focus on missense SNPs that change amino acid sequences [36–38]. Although only a few studies have analyzed SNPs in introns or 3′UTRs [26,30,31], this work suggests that polymorphisms in human intronic and 3′UTR *OPRM1* regions might have substantial roles in altering transcription, production of splice variants and/or stabilization of *OPRM1* mRNA. Further studies are required to confirm the effects of polymorphisms in these regions on opiate sensitivity.

In addition to the reported correlations with vulnerability to dependence on addictive substances, associations of other phenotypes with *OPRM1* polymorphisms have also been examined. Significant associations between the A118G SNP and decreased potency of a major metabolite of morphine, morphine-6-glucuronide, have been reported [47,48]. Alterations in markers for stress responses that include basal cortisol levels, cortisol responses to opioid peptide receptor blockade, and cortisol responses to stimulation by adrenocorticotropic hormone (ACTH), have also been associated with *OPRM1* polymorphisms [24,46,49]. Diseases that have been associated

with *OPRM1* polymorphisms in at least one study include schizophrenia, epilepsy and other psychogenic disorders [38,50,51]. Interestingly, although analgesia is among the most important actions of opiate drugs, there are currently few reports of the relationships between *OPRM1* polymorphisms and human pain or analgesia [52].

Future directions

In the current status of pain treatment, doses of opiates that are appropriate for individual patients are identified only after time-consuming trial-and-error adjustments or titrations with multiple incremental doses [1,5]. It is exciting to envisage a time when the rapidly accumulating data regarding the relationships between *OPRM1* genomic variants and opiate sensitivity enable us to use increasingly accurate methods to predict opiate sensitivity. Indeed, determining appropriate doses and achieving satisfactory analgesia without the need to induce adverse effects would be a breakthrough for pain treatment.

Differences in the *OPRM1* gene can affect the sensitivity not only to opiate drugs but also to endogenous opioid peptides, such as endomorphins, enkephalins and endorphins, and to endogenous morphine that has been found to be synthesized in animal tissue [53,54]. Individual differences in the sensitivity to these endogenous ligands of the MOP receptor can be related to differences in pain sensitivity and emotion.

To predict most accurately the appropriate opiate doses, correlations between *OPRM1* genomic polymorphisms and pain and opiate sensitivity need to be even more fully elucidated in normal humans and in those with acute or chronic pain. Other loci should also be tested. Each of these goals presents challenges. Although cancer pain seriously affects large numbers of cancer patients, it is challenging to deduce gene-sensitivity relationships from data sampled from patients with cancer pain because the mechanism, severity and nature of cancer pain can differ substantially from patient to patient [5]. Patients with acute postoperative pain that follows standardized surgical procedures might be more optimal subjects for studies investigating gene–opiate sensitivity relationships, particularly when their pain reports are more uniform. Studies on human research volunteers who receive carefully controlled thermal, electrical or mechanical noxious stimuli would also be likely to reduce the influences of non-genetic factors.

Studies of polymorphisms in other genes related to pain and opiate function can also help to better understand the relative roles of *OPRM1* variants. Because mu, delta and kappa opioid peptide receptors are each coupled with several effector systems including adenylyl cyclases, voltage-dependent Ca^{2+} channels and G-protein-activated inwardly rectifying K^{+} (GIRK) channels through their interactions with $G_{i/o}$ proteins [55], variations in the genes that encode other molecular components of opiate signal transduction pathways should also be examined to identify the extent to which they affect sensitivity to opiates. Studies of the genes that encode opiate metabolizing enzymes are also worth examining. Because most opiate drugs are metabolized by cytochrome P450 enzymes (CYPs), including CYP2D6, the genes that encode these metabolic enzymes are worthy of examination [56]. Furthermore, there are several anti-opioid systems, such as nociceptin/orphanin FQ and glutamate-mediated systems [57], that influence the effects of opioids. Similarly, a variety of neuropeptides that act as excitatory neurotransmitters on pain-transmitting neurons, including substance P, calcitonin gene-related peptide, somatostatin and cholecystokinin, might modulate opiate analgesic potency. Differences in the genes related to these systems might also affect sensitivity to opiates.

Comprehensive analyses of polymorphisms in each of the relevant genes will enable more-precise estimation of individual sensitivities to opiates, improve the quality of pain treatment and reduce the risk of adverse opiate effects. Rapid advances and more-precise data on the relationship between individual gene polymorphism patterns and opiates will, in the near future, lead to more-thorough understanding of this important relationship, and enable precise prediction of opiate sensitivity and opiate requirements in individual patients.

Acknowledgements

This study was supported by the Japanese Ministry of Health, Labour and Welfare; the Japanese Ministry of Education, Culture, Sports and Science; and NIDA-IRP, NIH, DHSS. We thank Athina Markou and Mark Geyer for fruitful discussions.

References

1 Ready, L.B. (2000) Acute Perioperative Pain. In *Anesthesia* (5th edn) (Miller, R.D., ed.), pp. 2323–2350, Churchill Livingstone
2 Han, W. *et al*. (2004) A possible genetic mechanism underlying individual and interstrain differences in opioid actions: focus on the mu opioid receptor gene. *Ann. New York Acad. Sci.* 1025, 370–375
3 Mogil, J.S. (1999) The genetic mediation of individual differences in sensitivity to pain and its inhibition. *Proc. Natl. Acad. Sci. U. S. A.* 96, 7744–7751
4 Uhl, G.R. *et al*. (1999) The mu opiate receptor as a candidate gene for pain: polymorphisms, variations in expression, nociception, and opiate responses. *Proc. Natl. Acad. Sci. U. S. A.* 96, 7752–7755
5 Rowlingson, J.C. and Murphy, T.M. (2000) Chronic Pain. In *Anesthesia* (5th edn) (Miller, R.D., ed.), pp. 2351–2379, Churchill Livingstone
6 Inturrisi, C.E. (2002) Clinical pharmacology of opioids for pain. *Clin. J. Pain.* 18, S3–13
7 Goldstein, F.J. (2002) Adjuncts to opioid therapy. *J. Am. Osteopath. Assoc.* 102, S15–S21
8 Polomano, R.C. *et al*. (2001) Evidence for opioid variability, Part 1: a biological perspective. *Semin. Perioper. Nurs.* 10, 3–16
9 Glass, P.S.A. *et al*. (2000) Intravenous Drug Delivery Systems. In *Anesthesia* (5th edn) (Miller, R.D., ed.), pp. 377–411, Churchill Livingstone
10 Camu, F. and Vanlersberghe, C. (2002) Pharmacology of systemic analgesics. *Best Pract. Res. Clin. Anaesthesiol.* 16, 475–488
11 Mogil, J.S. *et al*. (2000) Pain genes?: natural variation and transgenic mutants. *Annu. Rev. Neurosci.* 23, 777–811
12 Kim, H. *et al*. (2004) Genetic influence on variability in human acute experimental pain sensitivity associated with gender, ethnicity and psychological temperament. *Pain* 109, 488–496
13 Sora, I. *et al*. (2001) Mu opiate receptor gene dose effects on different morphine actions: evidence for differential *in vivo* mu receptor reserve. *Neuropsychopharmacology* 25, 41–54
14 Kieffer, B.L. and Gaveriaux-Ruff, C. (2002) Exploring the opioid system by gene knockout. *Prog. Neurobiol.* 66, 285–306
15 Sora, I. *et al*. (1997) Opiate receptor knockout mice define mu receptor roles in endogenous nociceptive responses and morphine-induced analgesia. *Proc. Natl. Acad. Sci. U. S. A.* 94, 1544–1549

16 Koide, T. *et al*. (2000) Multi-phenotype behavioral characterization of inbred strains derived from wild stocks of *Mus musculus*. *Mamm. Genome* 11, 664–670
17 Ikeda, K. *et al*. (1999) Unique behavioural phenotypes of recombinant-inbred CXBK mice: partial deficiency of sensitivity to mu- and kappa-agonists. *Neurosci. Res.* 34, 149–155
18 Ikeda, K. *et al*. (2001) The untranslated region of mu-opioid receptor mRNA contributes to reduced opioid sensitivity in CXBK mice. *J. Neurosci.* 21, 1334–1339
19 Han, W. *et al.* (2004) Characterization of the 3′-untranslated region of the mouse mu opioid receptor gene: insertion of an intracisternal A particle (IAP) sequence in CXBK mice. *SFN2004 Abstract*
20 Conne, B. *et al*. (2000) The 3′ untranslated region of messenger RNA: a molecular 'hotspot' for pathology? *Nat. Med.* 6, 637–641
21 Law, P.Y. *et al*. (2000) Molecular mechanisms and regulation of opioid receptor signaling. *Annu. Rev. Pharmacol. Toxicol.* 40, 389–430
22 Wei, L.N. and Loh, H.H. (2002) Regulation of opioid receptor expression. *Curr. Opin. Pharmacol.* 2, 69–75
23 Pasternak, G.W. (2004) Multiple opiate receptors: deja vu all over again. *Neuropharmacology* 47, 312–323
24 Miller, G.M. *et al*. (2004) A mu-opioid receptor single nucleotide polymorphism in rhesus monkey: association with stress response and aggression. *Mol. Psychiatry* 9, 99–108
25 Bond, C. *et al*. (1998) Single-nucleotide polymorphism in the human mu opioid receptor gene alters beta-endorphin binding and activity: possible implications for opiate addiction. *Proc. Natl. Acad. Sci. U. S. A.* 95, 9608–9613
26 Hoehe, M.R. *et al*. (2000) Sequence variability and candidate gene analysis in complex disease: association of mu opioid receptor gene variation with substance dependence. *Hum. Mol. Genet.* 9, 2895–2908
27 Bergen, A.W. *et al*. (1997) Mu opioid receptor gene variants: lack of association with alcohol dependence. *Mol. Psychiatry* 2, 490–494
28 Gelernter, J. *et al*. (1999) Genetics of two mu opioid receptor gene (*OPRM1*) exon I polymorphisms: population studies, and allele frequencies in alcohol- and drug-dependent subjects. *Mol. Psychiatry* 4, 476–483
29 Smolka, M. *et al*. (1999) mu-opioid receptor variants and dopaminergic sensitivity in alcohol withdrawal. *Psychoneuroendocrinology* 24, 629–638
30 Shi, J. *et al*. (2002) Sequence variations in the mu-opioid receptor gene (*OPRM1*) associated with human addiction to heroin. *Hum. Mutat.* 19, 459–460
31 Ide, S. *et al*. (2004) Gene polymorphisms of the mu opioid receptor in methamphetamine abusers. *Ann. New York Acad. Sci.* 1025, 316–324
32 Pesole, G. *et al*. (2002) UTRdb and UTRsite: specialized databases of sequences and functional elements of 5′ and 3′ untranslated regions of eukaryotic mRNAs. Update 2002. *Nucleic Acids Res.* 30, 335–340
33 Zabetian, C.P. *et al*. (2003) The structure of linkage disequilibrium at the DBH locus strongly influences the magnitude of association between diallelic markers and plasma dopamine beta-hydroxylase activity. *Am. J. Hum. Genet.* 72, 1389–1400
34 Risch, N. (2000) Searching for genes in complex diseases: lessons from systemic lupus erythematosus. *J. Clin. Invest.* 105, 1503–1506
35 Hartikainen, J.M. *et al*. (2005) An autosome-wide scan for linkage disequilibrium-based association in sporadic breast cancer cases in eastern Finland: three candidate regions found. *Cancer Epidemiol. Biomarkers Prev.* 14, 75–80
36 Crowley, J.J. *et al*. (2003) A genetic association study of the mu opioid receptor and severe opioid dependence. *Psychiatr. Genet.* 13, 169–173
37 Luo, X. *et al*. (2003) Haplotypes at the *OPRM1* locus are associated with susceptibility to substance dependence in European-Americans. *Am. J. Med. Genet. B Neuropsychiatr. Genet.* 120B, 97–108
38 Tan, E.C. *et al*. (2003) Mu opioid receptor gene polymorphism and neuroleptic-induced tardive dyskinesia in patients with schizophrenia. *Schizophr. Res.* 65, 61–63
39 Lichtman, A.H. *et al*. (2001) Opioid and cannabinoid modulation of precipitated withdrawal in delta(9)-tetrahydrocannabinol and morphine-dependent mice. *J. Pharmacol. Exp. Ther.* 298, 1007–1014
40 Becker, A. *et al*. (2002) Rewarding effects of ethanol and cocaine in mu opioid receptor-deficient mice. *Naunyn Schmiedebergs Arch. Pharmacol.* 365, 296–302
41 Berrendero, F. *et al*. (2002) Attenuation of nicotine-induced antinociception, rewarding effects, and dependence in mu-opioid receptor knock-out mice. *J. Neurosci.* 22, 10935–10940
42 Contarino, A. *et al*. (2002) Lack of reward and locomotor stimulation induced by heroin in mu-opioid receptor-deficient mice. *Eur. J. Pharmacol.* 446, 103–109
43 Hall, F.S. *et al*. (2001) Ethanol consumption and reward are decreased in mu-opiate receptor knockout mice. *Psychopharmacology (Berl.)* 154, 43–49
44 Hall, F.S. *et al*. (2004) mu-Opioid receptor knockout mice display reduced cocaine conditioned place preference but enhanced sensitization of cocaine-induced locomotion. *Brain Res. Mol. Brain Res.* 121, 123–130
45 LaForge, K.S. *et al*. (2000) Opioid receptor and peptide gene polymorphisms: potential implications for addictions. *Eur. J. Pharmacol.* 410, 249–268
46 Hernandez-Avila, C.A. *et al*. (2004) Association study of personality factors and the Asn40Asp polymorphism at the mu-opioid receptor gene (*OPRM1*). *Psychiatr. Genet.* 14, 89–92
47 Lotsch, J. *et al*. (2002) The polymorphism A118G of the human mu-opioid receptor gene decreases the pupil constrictory effect of morphine-6-glucuronide but not that of morphine. *Pharmacogenetics* 12, 3–9
48 Lotsch, J. *et al*. (2002) Does the A118G polymorphism at the mu-opioid receptor gene protect against morphine-6-glucuronide toxicity? *Anesthesiology* 97, 814–819
49 Wand, G.S. *et al*. (2002) The mu-opioid receptor gene polymorphism (A118G) alters HPA axis activation induced by opioid receptor blockade. *Neuropsychopharmacology* 26, 106–114
50 Urraca, N. *et al*. (2004) Mu opioid receptor gene as a candidate for the study of obsessive compulsive disorder with and without tics. *Am. J. Med. Genet. B Neuropsychiatr. Genet.* 127, 94–96
51 Wilkie, H. *et al*. (2002) Association of mu-opioid receptor subunit gene and idiopathic generalized epilepsy. *Neurology* 59, 724–728
52 Compton, P. *et al*. (2003) Association between human mu-opioid receptor gene polymorphism, pain tolerance, and opioid addiction. *Am. J. Med. Genet. B Neuropsychiatr. Genet.* 121B, 76–82
53 Poeaknapo, C. *et al*. (2004) Endogenous formation of morphine in human cells. *Proc. Natl. Acad. Sci. U. S. A.* 101, 14091–14096
54 Stefano, G.B. *et al*. (2000) Endogenous morphine. *Trends Neurosci.* 23, 436–442
55 Ikeda, K. *et al*. (2002) Molecular mechanisms of analgesia induced by opioids and ethanol: is the GIRK channel one of the keys? *Neurosci. Res.* 44, 121–131
56 Rogers, J.F. *et al*. (2002) Pharmacogenetics affects dosing, efficacy, and toxicity of cytochrome P450-metabolized drugs. *Am. J. Med.* 113, 746–750
57 Ueda, H. (2004) Locus-specific involvement of anti-opioid systems in morphine tolerance and dependence. *Ann. New York Acad. Sci.* 1025, 376–382

Available online at www.sciencedirect.com
SCIENCE DIRECT
European Journal of Pharmacology 531 (2006) 103–107
www.elsevier.com/locate/ejphar

dextro- and *levo*-morphine attenuate opioid δ and κ receptor agonist produced analgesia in μ-opioid receptor knockout mice

Hsiang-en Wu [a], Han-Sen Sun [a], Maia Terashivili [a], Emma Schwasinger [a], Ichiro Sora [b], F. Scott Hall [c], George R. Uhl [c], Leon F. Tseng [a,*]

[a] *Department of Anesthesiology, Medical College of Wisconsin, Milwaukee, Wisconsin 53226, USA*
[b] *Department of Neuroscience, Tohoku University, Graduate School of Medicine, Sendai 980-8574, Japan*
[c] *Molecular Neurobiology Branch, National Institute on Drug Abuse-IRP, NIH/DHSS, Baltimore, Maryland 21224, USA*

Received 25 August 2005; received in revised form 8 December 2005; accepted 12 December 2005

Abstract

We have demonstrated that the antianalgesia induced by *dextro*-morphine and *levo*-morphine is not mediated by the stimulation of μ-opioid receptors in male CD-1 mice. We now report that the *dextro*-morphine and *levo*-morphine attenuated antinociception produced by δ-opioid receptor agonist deltorphin II and κ-opioid receptor agonist U50,488H given spinally in the male μ-opioid receptor knockout mice. The tail-flick response was used for the antinociceptive test. Intrathecal injection of *levo*-morphine (3 nmol) markedly inhibited the tail-flick response in wild type, partially in heterozygous, but not in homozygous μ-opioid receptor knockout mice. Intrathecal pretreatment with *dextro*-morphine (33 fmol) or *levo*-morphine (0.3 nmol) for 45 min also attenuated *levo*-morphine-produced antinociception in wide type mice. Intrathecal pretreatment with *dextro*-morphine (33 fmol) or *levo*-morphine (0.3 nmol) for 45 min attenuated the tail-flick inhibition produced by deltorphin II (12.8 nmol) and U50,488H (123.3 nmol) in wide type, heterozygous and homozygous μ-opioid receptor knockout mice. The findings provide additional evidence that μ-opioid receptors are not involved in the antianalgesia induced by *dextro*-morphine and *levo*-morphine.

Keywords: Antianalgesia; Analgesia; Opioid; Spinal cord; Knockout mice

1. Introduction

We have previously reported that intrathecal (i.t.) pretreatment with naturally occurring *levo*-morphine at a picomolar dose or synthetic *dextro*-morphine at an extremely low femtomolar dose attenuates the antinociception produced by *levo*-morphine (Wu et al., 2004, 2005). The phenomenon of the attenuation of *levo*-morphine-produced analgesia by *dextro*-morphine or *levo*-morphine pretreatment has been defined as antianalgesia. The antianalgesia induced by *dextro*-morphine or *levo*-morphine against *levo*-morphine-produced antinociception is blocked by the pretreatment with the non-opioid receptor antagonist *dextro*-naloxone (Iijima et al., 1978) or the glial inhibitor propentofylline (Sweitzer et al., 2001), indicating that the effects of *dextro*-morphine and *levo*-morphine to induce antianalgesia is mediated by the stimulation of a novel and non-opioid receptor on glial cells (Wu et al., 2004, 2005).

The use of the transgenic μ-opioid receptor knockout mice has proven to be a useful experimental approach to opioid and pain researches. Mice that lack μ-opioid receptor gene have been generated by disrupting exon 1 (Sora et al., 1997), exon 2 (Matthes et al., 1996) or exon 2 and 3 (Loh et al., 1998). The antinociception produced by the μ-opioid receptor agonist *levo*-morphine or endomorphin-1 is reduced in heterozygous μ-opioid receptor knockout (+/−) mice and virtually abolished in homozygous μ-opioid receptor knockout (−/−) mice (Mizoguchi et al., 1999). Common adverse effects of *levo*-morphine such as respiratory depression, constipation and locomotor hyperactivity are reduced or eliminated in these −/− mice (Matthes et al.,

* Corresponding author. Medical College of Wisconsin, Department of Anesthesiology, Medical Education Building, Room M4308, 8701 Watertown Plank Road, Milwaukee, WI 53226, USA. Tel: +1 414 456 5686; fax: +1 414 456 6507.
E-mail address: ltseng@post.its.mcw.edu (L.F. Tseng).

0014-2999/$ - see front matter © 2005 Elsevier B.V. All rights reserved.
doi:10.1016/j.ejphar.2005.12.012

1998; Roy et al., 1998; Tian et al., 1997). Chronic treatment with *levo*-morphine does not induce place preference or withdrawal signs (Matthes et al., 1996). The genetic approach clearly demonstrates that pharmacological and biological actions of *levo*-morphine and other μ-opioid receptor agonists are mediated by the activation of μ-opioid receptor.

We have previously demonstrated that antianalgesia induced by *dextro*-and *levo*-morphine is mediated by the activation of a non-opioidergic mechanism in male CD-1 mice (Wu et al., 2004, 2005). We found that intrathecal pretreatment with a sub-analgesic dose of *levo*-morphine attenuates the antinociception induced by opioid μ-receptor agonist [D-Ala^2, *N*-Me-Phe^4, Gly-ol^5]enkephalin, δ-receptor agonist deltorphin II and κ-receptor agonist *trans*-(1S,2S)-3,4-Dichloro-*N*-methyl-*N*-[2-(1-pyrolidinyl)cyclohexyl]benzeneacetamide hydrochloride (U50,488H) (Wu et al., 2004). Present experiments were then undertaken to determine the effect of *dextro*-and *levo*-morphine on the induction of antianalgesia against the antinociception produced by opioid δ-receptor and κ-receptor agonists in wide type (+/+), heterozygous (+/−), and homozygous (−/−) μ-opioid receptor mice. We now report that pretreatment with an ultra-low, femtomolar dose of *dextro*-morphine and sub-analgesic dose of *levo*-morphine attenuate the analgesia produced by subsequent injection of δ opioid receptor agonist deltorphin II or κ opioid receptor agonist U50,488H produced analgesia in wide type (+/+), heterozygous (+/−), and homozygous (−/−) μ-opioid receptor knockout mice. The findings provide additional evidence that μ-opioid receptors are not involved in the antianalgesia induced by *dextro*-morphine and *levo*-morphine against antinociception produced by opioid μ-, δ- and κ-receptor agonist.

2. Materials and methods

2.1. Animals

The μ-opioid receptor knockout mice used in this report, in which the exon 1 of the μ-opioid receptor gene has been deleted, has been previously described (Sora et al., 1997). The μ-opioid receptor exon-1 knockout (−/−) mice were first generated by heterozygous (+/−) × heterozygous (+/−) crosses of mice from C57BL congenic background strain producing wild (+/+), heterozygous (+/−), and homozygous (−/−) knockout littermates. Mice were genotyped by tail biopsy tissue. Male mice, 16 to 20 weeks of age and weighing 20–25 g with genotype identified were used. Animals were housed one to five mice per cage based on their birthday and genotype in a room maintained at 22±0.5 °C with an alternating 12-h light–dark cycle. Food and water were available ad libitum. Each animal was used only once. All experiments were approved by and conformed to the guidelines of the Animal Care Committee of the Medical College of Wisconsin.

2.2. Assessment of analgesia

Analgesic responses were measured with the tail-flick test (D'Amour and Smith, 1941). To measure the latency of the tail-flick response, mice were gently held with the tail put on the apparatus (Model TF6, EMDIE Instrument Co., Maidens, VA). The tail-flick response was elicited by applying radiant heat to the dorsal surface of the tail. The heat stimulus was set to provide a pre-drug tail-flick response time of 3 to 4 s and the cutoff time was set at 10 s to avoid tissue damage.

2.3. Experimental protocols

Drugs were injected intrathecally (i.t.) in an injection volume of 5 μl according to the procedure of Hylden and Wilcox (1980) using a 25-μl Hamilton syringe with a 30-gauge needle. The first experiment was to determine the effect of *levo*-morphine given i.t. on the production of the tail-flick inhibition in wide type (+/+), heterozygous (+/−), and homozygous (−/−) μ-opioid receptor knockout mice. The second experiment was to determine the effects of *dextro*-morphine and *levo*-morphine given i.t. on the tail-flick inhibition produced by i.t.-administered *levo*-morphine in wide type (+/+) mice. Third experiment was to determine the effects of *dextro*-morphine and *levo*-morphine given i.t. on the tail-flick inhibition produced by opioid δ-receptor agonist deltorphin II and κ-receptor agonist U50,488H in wide type (+/+), heterozygous (+/−), and homozygous (−/−) μ-opioid receptor knockout mice.

2.4. Drugs

levo-Morphine sulfate, *dextro*-morphine base and *dextro*-naloxone were obtained from National Institute of Drug Abuse (Baltimore, MD). *levo*-naloxone and U50,488H were purchased from Sigma (St. Louis, MO). Deltorphin II was purchased from Phoenix Pharmaceuticals, Inc. (Belmont, CA). *levo*-morphine, *levo*-naloxone, *dextro*-naloxone, and U50,488H were dissolved in 0.9% saline. The *dextro*-morphine was dissolved in 10 N hydrochloric acid and then titrated with 1 N sodium hydroxide to pH 7.4, which then diluted to intended dose in 0.9% saline. Deltorphin II was dissolved in 0.9% saline containing 10% hydroxypropyl-β-cyclodextrin.

2.5. Statistical analysis

The analgesic responses (tail-flick latencies) were presented as the mean±S.E.M. Two-way analysis of variance (ANOVA) followed by Bonferroni's post-tests was used to test the differences between groups. The GraphPad Prism software was used to perform the statistics (version 4.1; GraphPad Software, Inc., San Diego, CA).

3. Results

3.1. Effects of levo-morphine given intrathecally (i.t.) on the production of the tail-flick inhibition in wide type (+/+), heterozygous (+/−), and homozygous (−/−) μ-opioid receptor knockout mice

Groups of male wide type (+/+), heterozygous (+/−), and homozygous (−/−) μ-opioid receptor knockout mice were

injected i.t. with *levo*-morphine (3.0 nmol) or vehicle and the tail-flick responses were measured at 15 min after injection. Intrathecal injection of *levo*-morphine markedly inhibited the tail-flick response in wild type (+/+), partially inhibited in heterozygous (+/−), but not in homozygous (−/−) μ-opioid receptor knockout mice. The tail-flick latencies show no significant difference among wild type (+/+), heterozygous (+/−) and homozygous (−/−) μ-opioid receptor knockout mice injected with vehicle (Fig. 1).

3.2. Effects of pretreatment with dextro-morphine or levo-morphine given i.t. on the tail-flick inhibition produced by i.t.-administered levo-morphine in wide type (+/+) mice

We have previously demonstrated that pretreatment with *dextro*-morphine at a femtomolar dose and *levo*-morphine at a picomolar dose attenuates the tail-flick inhibition produced by *levo*-morphine in male CD-1 mice (Wu et al., 2005). The present study was conducted to confirm that *dextro*-morphine and *levo*-morphine also attenuate the tail-flick inhibition produced by *levo*-morphine in wide type (+/+) mice. Groups of wide type (+/+) mice were pretreated i.t. with *dextro*-morphine (33 fmol), *levo*-morphine (0.3 nmol), or vehicle 45 min before i.t. administration of *levo*-morphine (3.0 nmol) and the tail-flick responses were measured thereafter. Intrathecal injection of *levo*-morphine 3.0 nmol caused an increase of tail-flick inhibition in mice pretreated with the vehicle. The tail-flick inhibition developed in 5 to 10 min, reached a maximum (8.65±0.40 s) at 15 min, declined slowly and returned to the control level in 60 min. The tail-flick inhibitions produced by *levo*-morphine observed at 5 to 20 min after injection were markedly attenuated by the i.t. pretreatment with *dextro*-morphine or *levo*-morphine (Fig. 2).

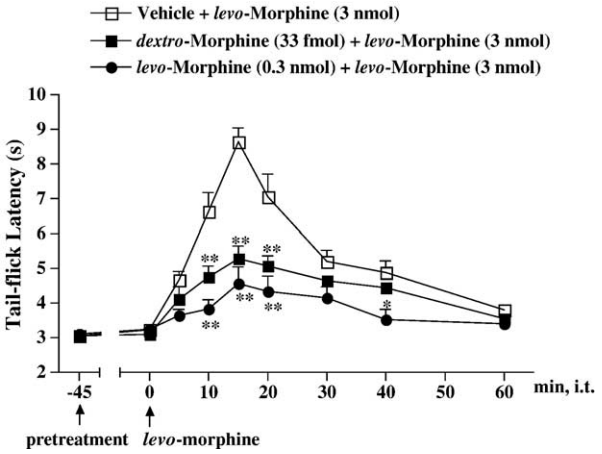

Fig. 2. Effects of pretreatment with *dextro*-morphine or *levo*-morphine given i.t. on the tail-flick inhibition produced by i.t.-administered *levo*-morphine in wide type (+/+) mice. Groups of wide type (+/+) mice were pretreated i.t. with *dextro*-morphine (33 fmol), *levo*-morphine (0.3 nmol) or vehicle 45 min before i.t. administration of *levo*-morphine (3.0 nmol) and the tail-flick latency was measured at different times thereafter. Each point represents the mean and the vertical bar represents the S.E.M. with 7 to 8 mice in each group. The two-way ANOVA followed by Bonferroni's post-test was used to test the difference between groups. The F interaction, treatment, time=6.12, 55.15, 34.81; * $P<0.05$, ** $P<0.001$.

3.3. Effects of pretreatment with dextro-morphine or levo-morphine given i.t. on the tail-flick inhibition produced by i.t.-administered δ-opioid receptor agonist deltorphin II in wide type(+/+), heterozygous (+/−), and homozygous(−/−) μ-opioid receptor knockout mice

Groups of wide type (+/+), heterozygous (+/−), and homozygous (−/−) μ-opioid receptor knockout mice were

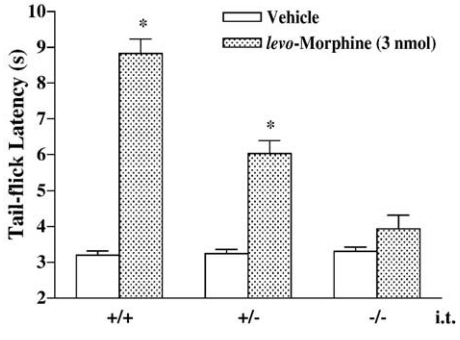

Fig. 1. The tail-flick responses to *levo*-morphine or vehicle given i.t. in wide type (+/+), heterozygous (+/−), and homozygous (−/−) μ-opioid receptor knockout mice. Groups of wide type (+/+), heterozygous (+/−), and homozygous (−/−) μ-opioid receptor knockout mice were injected i.t. with *levo*-morphine (3 nmol), or vehicle (5 μl) and the tail-flick responses were then measured at 15 min thereafter. Each column represents the mean and vertical bar represents the S.E.M. with 7 to 10 mice in each group. The two-way ANOVA followed by Bonferroni's post-test was used to test the difference between groups. The F interaction, treatment, genotype=31.67, 137.5, 29; * $P<0.001$.

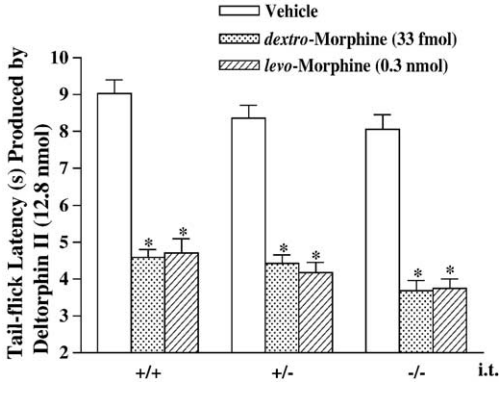

Fig. 3. Effects of pretreatment with *dextro*-or *levo*-morphine given i.t. on the tail-flick inhibition produced by i.t.-administered deltorphin II in wide type (+/+), heterozygous (+/−), and homozygous (−/−) μ-opioid receptor knockout mice. Groups of wide type (+/+), heterozygous (+/−), and homozygous (−/−) μ-opioid receptor knockout mice were pretreated i.t. with *dextro*-morphine (33 fmol), *levo*-morphine (0.3 nmol) or vehicle 45 min before i.t. administration of deltorphin II (12.8 nmol) and the tail-flick latency was measured at 10 min thereafter. Each column represents the mean and the vertical bar represents the S.E.M. with 8 to 10 mice in each group. The two-way ANOVA followed by Bonferroni's post-test was used to test the difference between groups. The F interaction, treatment, genotype=0.19, 170.4, 6.39; * $P<0.001$.

pretreated i.t. with *dextro*-morphine (33 fmol), *levo*-morphine (0.3 nmol), or saline vehicle 45 min before i.t. injection of δ-opioid receptor agonist deltorphin II (12.8 nmol) and the tail-flick responses were measured 10 min thereafter. Intrathecal injection of deltorphin II markedly produced tail-flick inhibition in wide type (+/+), heterozygous (+/−) and homozygous (−/−) μ-opioid receptor knockout mice pretreated i.t. with vehicle. The tail-flick inhibition produced by deltorphin II was markedly attenuated to the same extent by the pretreatment with *dextro*-morphine or *levo*-morphine in wide type (+/+), heterozygous (+/−), and homozygous (−/−) μ-opioid receptor knockout mice (Fig. 3).

3.4. Effects of pretreatment with dextro-morphine or levo-morphine given i.t. on the tail-flick inhibition produced by i.t.-administered κ-opioid receptor agonist U50,488H in wide type (+/+), heterozygous (+/−), and homozygous (−/−) μ-opioid receptor knockout mice

Groups of wide type (+/+), heterozygous (+/−), and homozygous (−/−) μ-opioid receptor knockout mice were pretreated i.t. with *dextro*-morphine (33 fmol), *levo*-morphine (0.3 nmol), or vehicle 45 min before i.t. injection of a κ-opioid receptor agonist U50,488H (123.2 nmol) and the tail-flick responses were measured 10 min thereafter. Intrathecal injection of U50,488H markedly produced tail-flick inhibition in wide type (+/+), heterozygous (+/−) and homozygous (−/−) μ-opioid receptor knockout mice pretreated i.t. with saline vehicle. The tail-flick inhibition produced by U50,488H was markedly attenuated to the same extent by the pretreatment with *dextro*-morphine or *levo*-morphine in wide type(+/+), heterozygous (+/−), and homozygous (−/−) μ-opioid receptor knockout mice (Fig. 4).

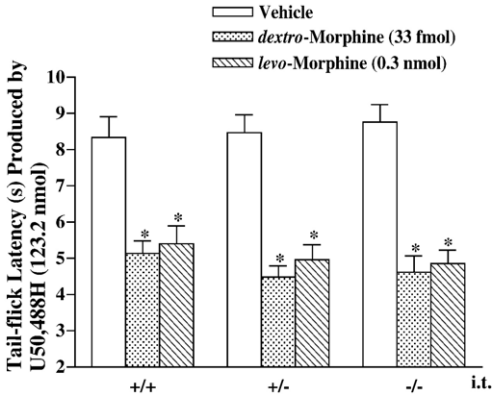

Fig. 4. Effects of pretreatment with *dextro*- or *levo*-morphine given i.t. on the tail-flick inhibition produced by i.t.-administered U50,488H in wide type (+/+), heterozygous (+/−), and homozygous (−/−) μ-opioid receptor knockout mice. Groups of wide type (+/+), heterozygous (+/−), and homozygous (−/−) μ-opioid receptor knockout mice were pretreated i.t. with *dextro*-morphine (33 fmol), *levo*-morphine (0.3 nmol) or vehicle 45 min before i.t. administration of U50,488H (123.2 nmol) and the tail-flick latency was measured at 10 min thereafter. Each column represents the mean and the vertical bar represents the S.E.M. with 8 to 10 mice in each group. The two-way ANOVA followed by Bonferroni's post-test was used to test the difference between groups. The F interaction, treatment, genotype = 0.42, 65.48, 0.40; * $P < 0.001$.

4. Discussions

4.1. Lack of analgesic response to levo-morphine in μ-opioid receptor knockout mice

We found in the present study that the spinally administered *levo*-morphine-produced antinociception was reduced partially in heterozygous (+/−) and completely abolished in homozygous (−/−) μ-opioid receptor knockout mice. The result is consistent with the findings of previous studies that the antinociception produced by μ-opioid receptor agonists *levo*-morphine or endomorphin-1 given systemically or supraspinally is markedly reduced in heterozygous (+/−) μ-opioid receptor knockout mice and virtually abolished in homozygous (−/−) knockout mice (Loh et al., 1998; Sora et al., 1997; Mizoguchi et al., 1999). The finding gives support to the view that the antinociception produced by *levo*-morphine or endomorphin-1 is mediated by the stimulation of μ-opioid receptors.

4.2. Both dextro-morphine and levo-morphine induces anti-analgesia against levo-morphine-produced antinociception in wide type (+/+) mice

We have previously demonstrated that pretreatment with *dextro*-morphine at a femtomolar dose level or *levo*-morphine at a picomolar dose range attenuates the antinociception produced by *levo*-morphine in CD-1 mice. The phenomenon has been defined as antianalgesia. *dextro*-Morphine was found to be at least 17,000-fold more potent than *levo*-morphine in inducing antianalgesia against *levo*-morphine-produced antinociception. The antianalgesia induced by *dextro*-morphine and *levo*-morphine is not mediated by the activation of opioidergic mechanism (Wu et al., 2005). *dextro*-Morphine, which does not have any affinity and efficacy to μ-opioid receptors and therefore, does not produce any μ-opioid receptor mediated analgesic and other *levo*-morphine-like effects (Jacquet et al., 1977) produces potent antianalgesia against *levo*-morphine produced antinociception. Pretreatment with *dextro*-naloxone, which does not have any μ-opioid receptor blocking activity (Iijima et al., 1978), blocks the *dextro*-morphine and *levo*-morphine-induced antianalgesia. Inhibition of glial activation by pretreatment with glial inhibitor propentofylline also blocks the antianalgesia induced by *dextro*-morphine and *levo*-morphine. We have therefore proposed that the antianalgesia induced by *dextro*-morphine and *levo*-morphine is mediated by the stimulation of a novel and non-opioid receptor on glial cells (Wu et al., 2005).

4.3. dextro-Morphine and levo-morphine produce antianalgesia against antinociception produced by opioid δ-receptor agonist deltorphin II and κ-receptor agonist U50,488H in μ-opioid receptor knockout (−/−) mice

We have previously demonstrated that pretreatment with *levo*-morphine attenuates the tail-flick inhibition produced by μ-opioid receptor agonist [D-Ala^2,*N*-Me-Phe^4,Gly-ol^5]-enkephalin, δ-opioid receptor agonist deltorphin II or κ-opioid receptor

agonist U50,488H in male CD-1 mice, indicating that the *levo*-morphine-induced antianalgesia is non-selective and is generalized to attenuate the antinociception produced by μ-, δ- and κ-opioid receptor agonists (Wu et al., 2004). Present study was then conducted to determine if *dextro*-morphine and *levo*-morphine can attenuate the tail-flick inhibition produced by opioid δ-receptor agonist deltorphin II or κ-receptor agonist U50,488H in wide type (+/+), heterozygous (+/−) and homozygous (−/−) μ-opiod receptor knockout mice. We found in the present study that both *dextro*-morphine and *levo*-morphine induced antianalgesia equally well in wide type (+/+), heterozygous (+/−) and homozygous (−/−) μ-opioid receptor knockout mice. The findings provide additional evidence that μ-opioid receptors are not required for the antianalgesia induced by *dextro*-morphine and *levo*-morphine against antinociception produced by opioid μ-, δ- and κ-receptor agonist.

It is concluded that pretreatment with *dextro*-morphine or *levo*-morphine given spinally induces antianalgesia against antinociception produced by opioid δ-receptor agonist deltorphin II or κ-opioid receptor agonist U50,488H in wide type (+/+), heterozygous (+/−) and homozygous (−/−) μ-opioid receptor knockout mice. Thus μ-opioid receptors are not involved in the antianalgesia induced by *dextro*-morphine and *levo*-morphine.

Acknowledgements

This work was supported by grant DA12588 from the National Institute of Health, National Institute on Drug Abuse (PI: Leon F.Tseng).

References

D'Amour, F.E., Smith, D.L., 1941. A method for determining loss of pain sensation. J. Pharmacol. Exp. Ther. 72, 74–79.

Hylden, J.L.K., Wilcox, G.L., 1980. Intrathecal morphine in mice: a new technique. Eur. J. Pharmacol. 167, 313–316.

Iijima, I., Minamikawa, J-I., Jacobsen, A.E., Brossi, A., Rice, K.E., 1978. Studies in the (+)-morphine series-5. Synthesis and biological properties of (+)-naloxone. J. Med. Chem. 21, 398–400.

Jacquet, Y.F., Klee, W.A., Rice, K.C., Iijima, I., Minamikawa, J., 1977. Stereospecfic and nonstereospecific effects of (+)-and (−)-morphine: evidence for a new class of receptors? Science 198, 842–845.

Loh, H.H., Liu, H.S., Cavalli, A., Yang, W., Chen, Y.F., Wei, L.N., 1998. μ-opioid receptor knockout in mice: effects on ligand-induced analgesia and morphine lethality. Mol. Brain Res. 54, 321–326.

Matthes, H.W.D., Maldonado, R., Simonin, F., Valverde, O., Slowe, S., Kitchen, I., Befort, K., Dierich, A., Le Meur, M., Dolle, P., Tzavara, E., Hanoune, J., Roques, B.P., Kieffer, B.L., 1996. Loss of morphine-induced analgesia, reward effect and withdrawal symptoms in mice lacking the μ-opioid-receptor gene. Nature 383, 819–823.

Matthes, H.W.D., Smadja, C., Valverde, O., Vonesch, J.L., Foutz, A.S., Boudinot, E., Denavit-Saubie, M., Severini, C., Negri, L., Roques, B.P., Maldonado, R., Kieffer, B.L., 1998. Activity of the delta-opioid receptor is partially reduced, whereas activity of the kappa-receptor is maintained in mice lacking the mu-receptor. J. Neurosci. 18, 7285–7295.

Mizoguchi, H., Narita, M., Oji, D.E., Suganuma, C., Nagase, H., Sora, I., Uhl, G.R., Cheng, E.Y., Tseng, L.F., 1999. μ-Opioid receptor gene-dose dependent reductions in G-protein activation in the pons/medulla and antinociception induced by endomorphins in μ-opioid receptor knockout mice. Neuroscience 94, 203–207.

Roy, S., Liu, H.C., Loh, H.H., 1998. Mu-opioid receptor-knockout mice: the role of mu-opioid receptor in gastrointestinal transit. Brain Res. Mol. Brain Res. 56, 281–283.

Sora, I., Takahashi, N., Funada, M., Ujike, H., Revay, R.S., Donovan, D.M., Miner, L.L., Uhl, G.R., 1997. Opiate receptor knockout mice define μ receptor roles in endogenous nociceptive response and morphine-induced analgesia. Proc. Natl. Acad. Sci. U. S. A. 94, 1544–1549.

Sweitzer, S.M., Schubert, P., DeLeo, J.A., 2001. Propentofylline, a glial modulating agent, exhibits antiallodynic properties in a rat model of neuropathic pain. J. Pharmacol. Exp. Ther. 297, 1210–1217.

Tian, M., Broxmeyer, H.E., Fan, Y., Lai, Z., Zhang, S., Aronica, S., Cooper, S., Bigsby, R.M., Steinmetz, R., Engle, S.J., Mestek, A., Pollock, J.D., Lehman, M.N., Jansen, H.T., Ying, M., Stambrook, P.J., Tischfield, J.A., Yu, L., 1997. Altered hematopoiesis, behavior, and sexual function in mu opioid receptor-deficient mice. J. Exp. Med. 185, 1517–1522.

Wu, H., Thompson, J., Sun, H., Leitermann, R.J., Fujimoto, J.M., Tseng, L.F., 2004. Nonopioidergic mechanism mediating morphine-induced antianalgesia in the mouse spinal cord. J. Pharmacol. Exp. Ther. 310, 240–246.

Wu, H., Thompson, J., Sun, H., Terashvili, M., Tseng, L.F., 2005. Antianalgesia: stereo-selecitve action of dextro-morphine over levo-morphine on glia in the mouse spinal cord. J. Pharmacol. Exp. Ther. 314, 1101–1108.

available at www.sciencedirect.com

SCIENCE DIRECT®

www.elsevier.com/locate/brainres

BRAIN RESEARCH

Research Report

Morphine can produce analgesia via spinal kappa opioid receptors in the absence of mu opioid receptors

Hiroaki Yamada[a,b], *Naohito Shimoyama*[c], *Ichiro Sora*[d], *George R. Uhl*[e], *Yasuichiro Fukuda*[a], *Hideshige Moriya*[b], *Megumi Shimoyama*[a,*]

[a]*Department of Autonomic Physiology, Chiba University Graduate School of Medicine, 1-8-1 Inohana, Chuo-ku, Chiba, Chiba-ken 260-8670, Japan*
[b]*Department of Orthopedic Surgery, Chiba University Graduate School of Medicine, Japan*
[c]*Department of Pain Medicine and Palliative Care, National Cancer Center Hospital, Japan*
[d]*Department of Neuroscience, Division of Psychobiology, Tohoku University Graduate School of Medicine, Japan*
[e]*Molecular Neurobiology Branch, NIDA, NIH, DHSS, USA*

ARTICLE INFO

Article history:
Accepted 25 January 2006
Available online 10 March 2006

Keywords:
Opioid receptor
Morphine
Analgesia
Knockout mouse
Tail flick test

Abbreviations:
i.c.v., intracerebroventricular
i.t., intrathecal
s.c., subcutaneous
ED_{50}, median effective dose
nor-BNI, nor-binaltorphimine
DPDPE, [D-Pen2,D-Pen5]enkephalin

ABSTRACT

Previous studies have demonstrated the virtual lack of analgesia in mu opioid receptor knockout mice after systemic administration of morphine. Thus, it has been suggested that analgesic actions of morphine are produced via the mu opioid receptor, despite its ability to bind to kappa and delta receptors in vitro. However, it is not clear whether the results of these studies reflect the effect of morphine in the spinal cord. In the present study, we report study of the analgesic actions of spinally-administered morphine and other opioid receptor agonists in mu opioid receptor knockout and wild type mice. Morphine produced a dose-dependent antinociceptive effect in the tail flick test in the knockout mice, although higher doses were needed to produce antinociception than in wild type mice. The antinociceptive effect of morphine was completely blocked by naloxone (a non-selective opioid antagonist) and nor-binaltorphimine (nor-BNI, a selective kappa-opioid receptor antagonist), but not by naltrindole (a selective delta-opioid receptor antagonist). U-50,488H (a selective kappa-opioid receptor agonist) also produced a dose-dependent antinociceptive effect in knockout mice but presented lower analgesic potency in knockout mice than in wild type mice. Analgesic effects of [D-Pen2,D-Pen5]enkephalin (DPDPE, a selective delta-opioid receptor agonist) were observed in wild type mice but abolished in knockout mice. SNC80 (a selective delta-opioid receptor agonist) was not antinociceptive even in wild type mice. The present study demonstrated that morphine can produce thermal antinociception via the kappa opioid receptor in the spinal cord in the absence of the mu opioid receptor. Lower potency of U50,488H in mu opioid receptor knockout mice suggests interaction between kappa and mu opioid receptors at the spinal level.

* *Corresponding author*. Fax: +81 43 226 2034.
E-mail address: shimoyama@faculty.chiba-u.jp (M. Shimoyama).

0006-8993/$ – see front matter © 2006 Elsevier B.V. All rights reserved.
doi:10.1016/j.brainres.2006.01.095

1. Introduction

Morphine is a prototypical opioid agonist most frequently used clinically to produce analgesia. Morphine is weakly selective to the mu opioid receptor and also possesses affinity to the delta and kappa opioid receptors. Thus, morphine was long thought to act on all three receptor types to produce analgesia. This has been supported by in vivo pharmacological studies (Heyman et al., 1987; Takemori and Portoghese, 1987; Omote et al., 1991). Pharmacological studies also suggested possible interactions among opioid receptors, in particular, those between the mu and delta receptors in producing analgesia (Larson et al., 1980; Vaught et al., 1982; Malmberg and Yaksh, 1992). The generation of mu opioid receptor knockout mice approximately a decade ago and those of the other opioid receptors that followed led to better understanding of the mechanism of opioid analgesia. Surprisingly, the analgesic effects of morphine were abolished or strongly reduced in mu receptor knockout mice, indicating that the mu receptor was mandatory for the analgesic effects of morphine and that the delta or kappa receptor alone could not mediate morphine's analgesic actions (Matthes et al., 1996; Sora et al., 1997b, 2001; Loh et al., 1998; Schuller et al., 1999; Hosohata et al., 2000; Hall et al., 2003). In the initial studies, morphine was administered systemically most probably with the assumption that systemic morphine acts both in the brain and the spinal cord. Studies utilizing the intracerebroventricular (i.c.v.) route also showed the ineffectiveness of morphine in mu receptor knockout mice reflecting the results of studies with systemic administration (Loh et al., 1998; Schuller et al., 1999; Hosohata et al., 2000). On the other hand, there have been indications by studies that when morphine is administered systemically in animals, its direct action is predominantly in the brain (Manning and Franklin, 1998; Heinricher et al., 2001). In these studies, the analgesic effects of systemic morphine were completely reversed by blocking pathways within the brain. Furthermore, Honda et al. (2004) showed that the analgesic effects of systemic and i.c.v. morphine were attenuated by muscarinic antagonists, while the antagonist had no effect on the actions of intrathecal morphine. Thus systemic administration may not reflect the actions of morphine in the spinal cord, and morphine needs to be administered intrathecally (i.t.) to specifically observe its spinal actions. Although some studies have suggested the ineffectiveness of intrathecal morphine in mu receptor knockout mice (Schuller et al., 1999; Hosohata et al., 2000), there have been no studies that fully looked at the effect of intrathecal morphine on acute thermal pain in these mice. The present study was designed to examine the analgesic effects of spinally administered morphine in mu receptor knockout mice and to determine the possible molecular target of morphine in the absence of the mu opioid receptor.

2. Results

Baseline tail flick latencies of wild type and mu receptor knockout mice were 2.93 ± 0.26 s (n = 58) and 3.00 ± 0.26 s (n = 70), respectively, and were not significantly different.

2.1. *The antinociceptive effect of spinal morphine in mu receptor knockout mice and its blockade with naloxone*

Morphine given i.t. produced a dose-dependent antinociceptive effect in both wild type mice (Fig. 1A) and mu receptor knockout mice (Fig. 1B). The dose required to produce a significant effect was higher in knockout mice than in wild type mice. The median effective doses (ED_{50}) of morphine were 0.17 μg (0.07–0.35 μg, 95% confidence limits) and 5.00 μg (3.01–9.00 μg, 95% confidence limits) in wild type and knockout mice, respectively (Fig. 2), and were significantly different. Doses of morphine at 10 μg and above could not be examined in knockout mice because they yielded a paradoxical pain behavior (intermittent bouts of biting and scratching of affected dermatomes), which has previously been described in rats (Yaksh et al., 1986; Yaksh and Harty, 1988). This pain behavior has been shown to be non-reversible by naloxone (a non-selective opioid antagonist), thus is not mediated by opioid receptors. The concomitant spinal administration of naloxone (10 μg) completely blocked the antinociceptive effect of morphine in knockout

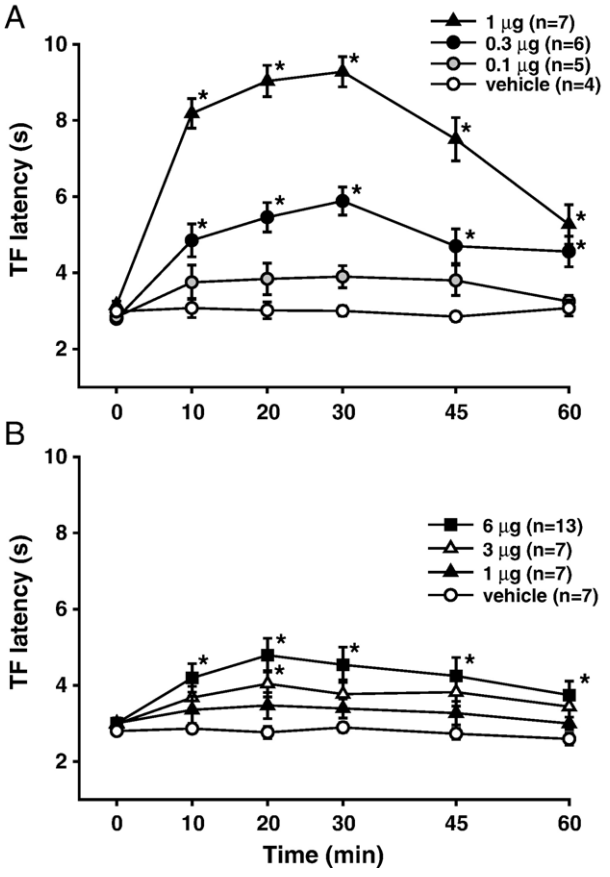

Fig. 1 – Time courses of the antinociceptive effect of morphine in wild type (A) and mu opioid receptor knockout (B) mice. Tail flick latencies were measured prior to and every 10–15 min during a period of 60 min after intrathecal administration of morphine. Values are expressed in mean ± SE. *Significantly different from vehicle control.

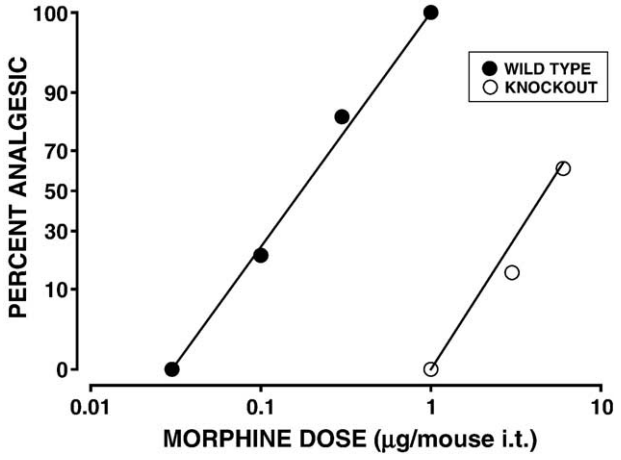

Fig. 2 – Dose-dependent antinociceptive effects of morphine in wild type and mu opioid receptor knockout mice. Mice were tested by the tail flick test. ED_{50} values of morphine were 0.17 μg (0.07–0.35 μg, 95% confidence limits) and 5.00 μg (3.01–9.00 μg, 95% confidence limits) in wild type and knockout mice, respectively.

mice (Fig. 3). This indicated that the effect was mediated by opioid receptors.

2.2. *The involvement of kappa opioid receptors*

In order to determine whether kappa opioid receptors are involved in the antinociceptive effects of morphine in mu receptor knockout mice, we first examined the antinociceptive effects produced by spinal kappa receptor activation in the knockout mice. The selective kappa receptor agonist, U50,488H, given i.t. produced a dose-dependent antinociceptive effect in the knockout mice, but required a 2-fold increase in dose to produce effects similar to those in wild type mice (Fig. 4). The ED_{50} values of U50,488H were 18.0 μg (14.8–22.9 μg,

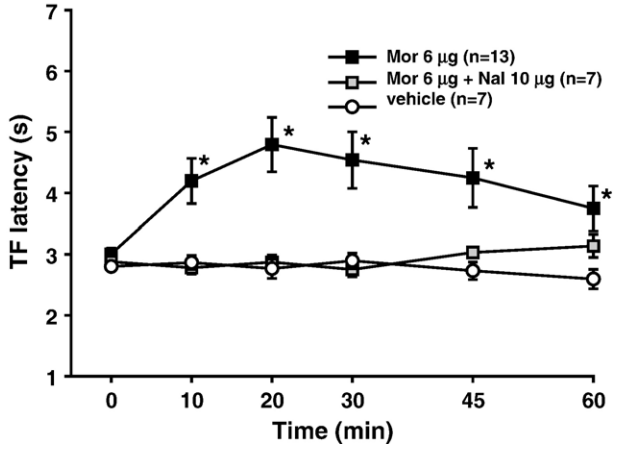

Fig. 3 – Reversal of the antinociceptive effect of morphine (Mor, 6 μg) by the non-selective opioid receptor antagonist, naloxone (Nal, 10 μg) in mu opioid receptor knockout mice. Naloxone was administered concomitantly with morphine. Values are expressed in mean ± SE. *Significantly different from vehicle control.

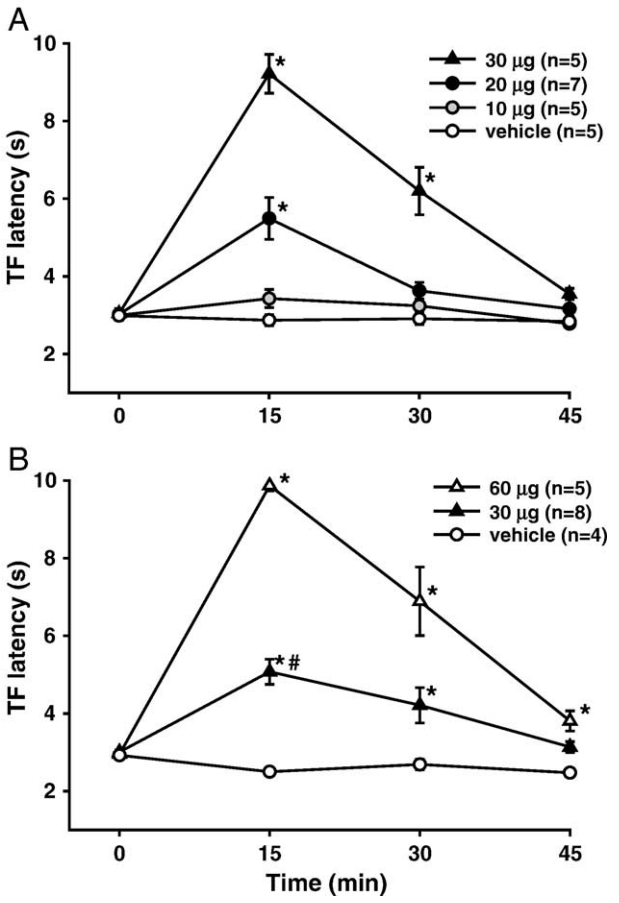

Fig. 4 – Time courses of the antinociceptive effect of the selective kappa receptor agonist, U50,488H in wild type (A) and mu opioid receptor knockout (B) mice. Tail flick latencies were measured prior to and every 15 min during a period of 45 min after intrathecal administration of U50,488H. Values are expressed in mean ± SE. *Significantly different from vehicle control. #Significantly different from wild type mice administered U50,488H at the same dose (30 μg).

95% confidence limits) and 29.3 μg (23.8–47.1 μg, 95% confidence limits) in wild type and knockout mice, respectively (Fig. 5), and were significantly different. Nonetheless, the results demonstrated that kappa receptor activation produced potent analgesic effects in mu receptor knockout mice. This indicated that the kappa receptor is functional in these mice and suggested that the kappa receptor may mediate morphine's analgesic effects in mu receptor knockout mice. Next, we examined whether the analgesic effects of morphine in the knockout mice could be reversed by a selective kappa receptor antagonist, nor-binaltorphimine (nor-BNI, 7.5 μg i.t.). The analgesic effects of morphine were completely blocked by nor-BNI, indicating that the effects were mediated by the kappa opioid receptor (Fig. 6).

2.3. *The involvement of delta opioid receptors*

We next examined the effects of spinal delta receptor activation in mu receptor knockout mice. A selective peptidic delta agonist, [D-Pen2,D-Pen5]enkephalin (DPDPE), given i.t.,

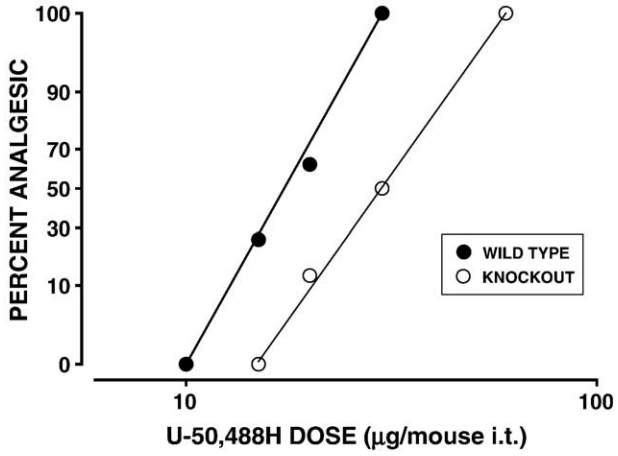

Fig. 5 – Dose-dependent antinociceptive effects of U50,488H in wild type and mu opioid receptor knockout mice. Mice were tested by the tail flick test. The ED_{50} values of U50,488H were 18.0 μg (14.8–22.9 μg, 95% confidence limits) and 29.3 μg (23.8–47.1 μg, 95% confidence limits) in wild type and knockout mice, respectively.

produced dose-dependent analgesic effects (1–3 μg) in wild type mice (Fig. 7A) while no analgesic effects were observed in mu receptor knockout mice at 10 times higher doses (10–30 μg) (Fig. 7B). In contrast to the effects of DPDPE, a selective non-peptidic delta agonist SNC80 given i.t. at a high dose of 45 μg (100 nmol) produced no antinociceptive effects in wild type mice (Fig. 8). A three-fold increase in dose to 135 μg produced overt paralysis of the hind limbs and the tail, which became apparent within a few minutes after administration and resembled effects of local anesthetics. Due to the paralysis, antinociceptive effects could not be tested at this dose. The paralysis was not reversed by naloxone (10 mg/kg s.c., 15 min prior to administration of SNC80) and therefore was likely a non-specific effect due to the very high

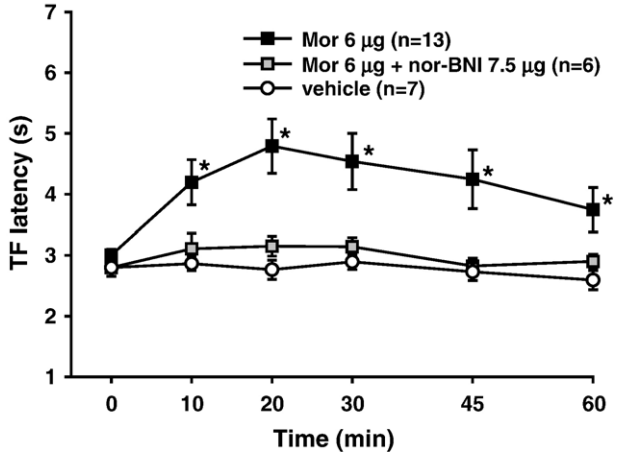

Fig. 6 – Reversal of the antinociceptive effect of morphine (Mor, 6 μg) by the selective kappa opioid receptor antagonist, nor-BNI (7.5 μg) in mu opioid receptor knockout mice. Nor-BNI was administered concomitantly with morphine. Values are expressed in mean ± SE. *Significantly different from vehicle control.

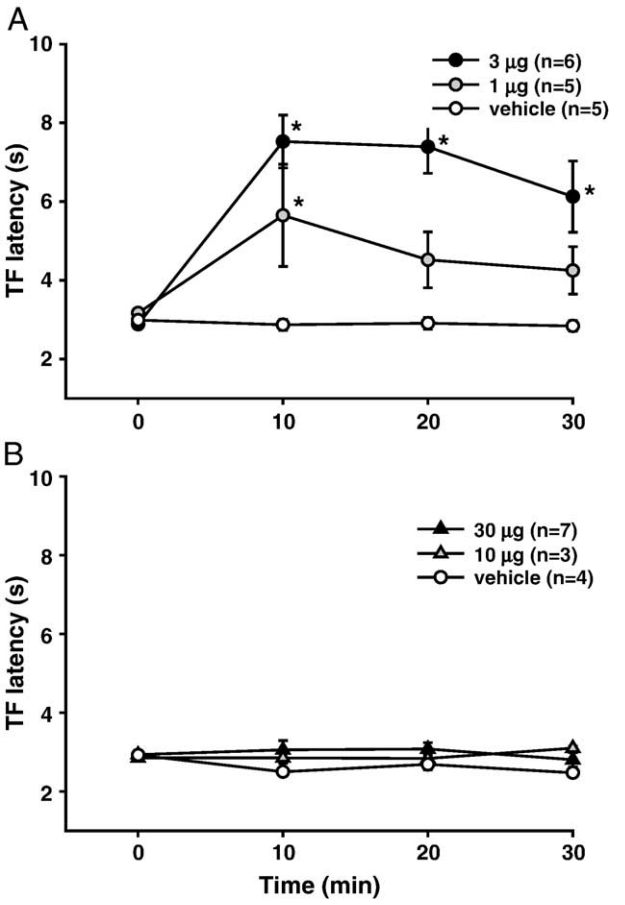

Fig. 7 – Time courses of the effect of the selective peptidic delta receptor agonist, DPDPE on tail flick latencies in wild type (A) and mu opioid receptor knockout (B) mice. Tail flick latencies were measured prior to and every 10 min during a period of 30 min after intrathecal administration of DPDPE. Values are expressed in mean ± SE. *Significantly different from vehicle control.

dose. Thus, SNC80 did not produce observable antinociceptive effects in wild type mice, and was not tested in knockout mice. Although these results revealed differences in actions between delta agonists in wild type mice, they indicated that, at least in mu receptor knockout mice, spinal delta receptor activation does not produce analgesia. Thus, the analgesic effects of morphine in the knockout mice were not likely mediated by delta receptors. To confirm this, we examined the effect of naltrindole, a selective delta receptor antagonist, on the analgesic effects of morphine in mu receptor knockout mice. Naltrindole had no effect on morphine's analgesic effects (Fig. 9).

3. Discussion

The present study demonstrated that morphine can produce thermal antinociception via the kappa receptor in the spinal cord in the absence of the mu receptor. This is the first study that demonstrated analgesic effects of morphine in mu receptor knockout mice after spinal administration. The dose

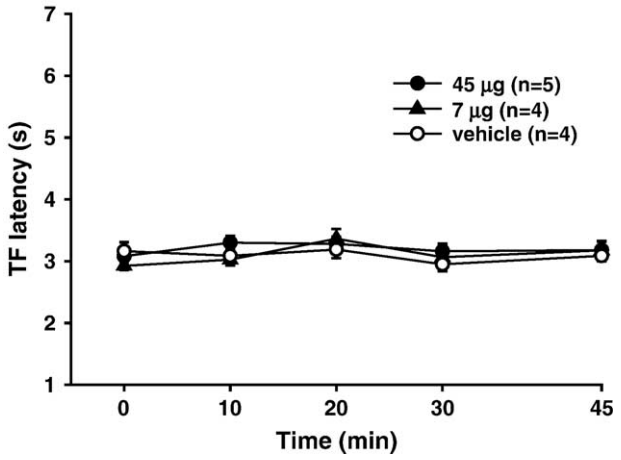

Fig. 8 – Time courses of the effect of the selective non-peptidic delta receptor agonist, SNC80 on tail flick latencies in wild type mice. Tail flick latencies were measured prior to and every 15 min during a period of 45 min after intrathecal administration of SNC80. Values are expressed in mean ± SE.

that produced a potent effect in wild type mice (1 µg) was without effect in knockout mice, but a higher dose (6 µg) produced a mild nonetheless significant analgesic effect. Further increase in dosage could not be investigated because of the manifestation of paradoxical pain behavior (see Results). Although a few previous reports showed the lack of morphine's analgesic effects in the tail flick test after spinal administration, these studies only examined doses that produced submaximal analgesic response in wild type mice and higher doses were not investigated (Schuller et al., 1999; Hosohata et al., 2000). In contrast to the analgesic effects of intrathecal morphine observed in the present study, i.c.v. morphine at an extremely high dose of 120 µg has been reported to be without effect in mu receptor knockout mice (Loh et al., 1998). Thus, it appears that there is some difference between the brain and the spinal cord in the types of opioid receptors that morphine recruits to produce analgesia. The lack of recruitment of kappa receptors in the brain might be explained, at least in part, by the difference in kappa receptor agonists' analgesic potency in the brain and the spinal cord (Porreca et al., 1987; Millan et al., 1989; Miaskowski et al., 1991; Nakazawa et al., 1991). While systemic morphine has been demonstrated to be without effect at normal analgesic doses (~6 mg/kg), Sora et al. (1997b) observed a modest trend of reduced thermal nociception at a cumulated dose of 56 mg/kg and Loh et al. (1998) reported an ED_{50} value of approximately 400 mg/kg in the tail flick test. Thus extremely high doses of morphine can produce analgesia in mu receptor knockout mice even after systemic administration and this may be reflecting the analgesic effects produced by the spinal action of morphine. The requirement of such extremely high systemic doses may be attributable to the difference between the brain and the spinal cord in the relative magnitude of morphine's action after systemic administration. Previous reports have suggested that the direct action of systemic morphine to produce analgesia is predominantly in the brain (Manning and Franklin, 1998; Heinricher et al., 2001; Honda et al., 2004).

The analgesic effects of morphine in mu receptor knockout mice were mediated by the kappa receptor and not by the delta receptor. This was demonstrated by the complete reversal of morphine's effect by nor-BNI and the lack of antagonism by naltrindole. It should be noted that there is always the issue of selectivity even with the use of selective antagonists such as nor-BNI and naltrindole. However, in the present study, we used these antagonists in mu-receptor knockout mice, thus the possible actions of the antagonists at the mu receptor can be excluded. Furthermore, although the possibilities of nor-BNI having some actions at the delta receptor and naltrindole likewise at the kappa receptor cannot be excluded, since nor-BNI completely blocked the effect of morphine while naltrindole had no effect, it is plausible to conclude that the effect of morphine was mediated only by the kappa receptor. This indicated that spinal kappa receptors are functional in the absence of mu receptors, which was also confirmed by the analgesic effects of the selective kappa agonist U50,488H in mu receptor knockout mice. However, while U50,488H produced potent analgesic effects in the knockout mice, morphine only exerted a limited effect in these mice at the doses investigated. Although this limited effectiveness may have been merely due to insufficient dosing, alternatively, it may have been due to a ceiling effect of morphine at the kappa receptor. As mentioned above, higher doses of morphine could not be studied because of the manifestation of "paradoxical pain behavior" at these doses. Thus, the possibility that morphine has limited efficacy at the kappa receptor could not be investigated in this study.

On the other hand, in the present study we observed that U50,488H, was less potent in mu receptor knockout mice than in wild type mice, indicating that the mu receptor plays some role in the analgesic effects of U50,488H. Although U50,488H is highly selective to the kappa receptor in vitro, spinally administered U50,488H in vivo might have directly activated mu receptors as well as kappa receptors, and this may have caused the difference between its effects in wild type and mu

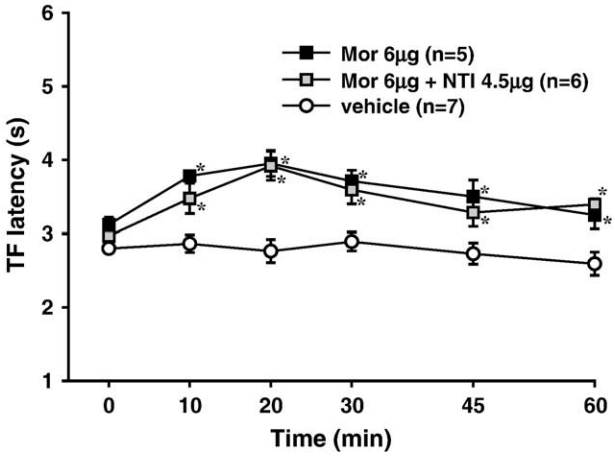

Fig. 9 – The effect of the selective delta opioid receptor antagonist, naltrindole (NTI, 4.5 µg) on the antinociceptive effect of morphine (Mor, 6 µg) in mu opioid receptor knockout mice. Naltrindole was administered concomitantly with morphine. Values are expressed in mean ± SE. *Significantly different from vehicle control.

receptor knockout mice. However, it has been shown that analgesic effects of U50,488H are abolished in kappa receptor knockout mice, indicating that U50,488H is selective in vivo as well as in vitro (Simonin et al., 1998). Furthermore, the analgesic effects of U50,488H were maintained in mu receptor knockout mice after systemic and i.c.v. administration (Loh et al., 1998; Matthes et al., 1998; Fuchs et al., 1999; Sora et al., 1999). Thus, it is unlikely that the difference in response between knockout and wild type mice was due to in vivo kappa selectivity, but was likely due to a mechanism more specific to the spinal cord. A possible mechanism is the interactions between the spinal kappa and mu receptors. Interactions may exist at the cellular and/or at the circuit level in the spinal dorsal horn. Co-expression of mu and kappa receptors have been shown in some neurons of the dorsal root ganglion (Ji et al., 1995) and such co-expression may also exit in neurons of the dorsal horn. Such neurons may be a site of cellular interaction. However, kappa agonist induced G-protein activation and adenylcyclase inhibition in spinal cord and/or brain preparations of mu receptor knockout mice were not different from wild type mice, indicating that signal transduction induced by kappa receptor activation was not affected by the absence of mu receptors (Matthes et al., 1998). Thus cellular interaction between the mu and kappa receptors does not seem very likely. Another possible mode of interaction between opioid receptor types that has been proposed is the involvement of endogenous opioid peptide release (Scherrer et al., 2004). In the spinal dorsal horn, multiple endogenous opioid peptides are expressed within complex neural circuits and this raises the possibility of interactions among opioid receptors and endogenous opioid peptides. The release of an endogenous opioid peptide, dynorphin, has been demonstrated after the spinal administration of opioid peptides such as endomorphin and [DMT^1] DALDA (Ohsawa et al., 2001; Szeto et al., 2003). Thus, a speculation may be that kappa receptor activation causes downstream release of endogenous opioid peptides such as endomorphin or enkaphalin that activate the mu receptor. Although the lack of mu receptors themselves is most certainly the predominant cause of the high dose requirement to produce morphine analgesia in mu receptor knockout mice, the lack of such possible interaction between the kappa and mu receptors may also have contributed to some extent.

Prototypical peptidic delta agonists (DPDPE and deltorphin II) have been utilized to demonstrate analgesic effects produced by delta receptor activation. In the present study, the analgesic effects of DPDPE observed in wild type mice were abolished in mu receptor knockout mice. This indicated that mu receptors are essential for DPDPE analgesia, which is in accordance with previous reports (Sora et al., 1997a; Scherrer et al., 2004). The results may appear to support the existence of functional mu/delta interaction suggested by previous pharmacological studies (Larson et al., 1980; Vaught et al., 1982; Malmberg and Yaksh, 1992). However, a recent study by Scherrer et al. (2004) showed that DPDPE and deltorphin II given i.c.v. were fully analgesic against acute thermal pain in mice lacking delta receptors, while being without effect in mu receptor knockout mice. Furthermore, pure delta receptor activation in the brain by these agonists utilizing mu and kappa receptor combinatorial knockout mice caused very small antinociceptive effects in the hot plate test and no effect in the tail flick test (Scherrer et al., 2004). These findings indicated that, in spite of high delta receptor selectivity in vitro, these peptidic agonists possess very low in vivo delta selectivity and that their analgesic effects were predominantly produced by direct activation of mu receptors. Since the lack of effect of DPDPE in mu receptor knockout mice in the present study may also have been due to its very low in vivo selectivity, we also examined the effects of SNC80, a selective non-peptidic delta receptor agonist. SNC80 is a potent and full agonist in the GTP gammaS binding assay at the delta receptor (Hosohata et al., 2000). Because of its non-polar nature, SNC80 is expected to have better diffusion properties in nervous tissues as compared to polar peptidic delta agonists. Contrary to our expectations, SNC80 produced no analgesia in wild type mice even at a high dose of 45 μg. A dose three times higher produced non-opioid mediated regional paralysis. Our findings are in contrast to the report by Bilsky et al. (1995) who showed that SNC80 produced dose-dependent antinociceptive effects in acute thermal pain models after systemic, intrathecal and intracerebroventricular administration in mice. On the other hand, Gallantine and Meert (2005) showed that SNC80 administered systemically in rats produced no antinociceptive effects in the tail flick test even at a high dose of 80 mg/kg, while producing analgesic effects in inflammatory pain and chemically-induced visceral pain at lower doses. SNC80 given s.c. also produced potent anxiolytic effect mediated by the delta receptor, suggesting that SNC80 was systemically active (Saitoh et al., 2004). Furthermore, other selective non-peptidic delta agonists have been shown to lack antinociceptive effects in acute thermal pain models while significantly reducing inflammatory pain and chemically-induced visceral pain (Kamei et al., 1995; Petrillo et al., 2003). The lack of analgesic effects of non-peptidic delta agonists in acute thermal pain together with the lack of delta receptor mediation in the analgesic effects of DPDPE and deltorphin II as shown in the above studies may put forward a possibility that, although the delta receptor has been thought to mediate thermal antinociception in a degree similar to the mu receptor, in reality, we were merely observing the effect of mu receptor activation by the peptidic "delta agonists". On the other hand, Zhu et al. (1999) reported that the thermal antinociceptive effects of DPDPE and deltorphin II given spinally were markedly reduced in delta receptor knockout mice, indicating that the spinal delta receptor is the major target of these agonists. Thus, further studies are needed to demonstrate whether delta receptor activation in the spinal cord does or does not produce potent thermal antinociception. At any rate, the results of the present study indicated that delta receptor activation at least in mu receptor knockout mice does not produce thermal antinociception whether the cause is minimal thermal antinociception in wild type mice to begin with or the existence of mu/delta interactions. This is in accordance with our finding that, despite morphine's affinity to both kappa and delta receptors, its analgesic effects in mu receptor knockout mice were mediated only by the kappa receptor and not by the delta receptor.

In summary, we demonstrated that, in the spinal cord, the thermal antinociception produced by morphine is mediated by the mu receptor at normal analgesic doses, but is also

mediated by the kappa receptor at higher doses. Lower potency of U50,488H in mu receptor knockout mice as compared to wild type mice may suggest interaction between kappa and mu receptors at the spinal level. The finding that the kappa receptor is a molecular target of morphine at higher doses suggests that the kappa receptor may play a role in the analgesia of high-dose morphine regimens used in cancer pain treatment.

4. Experimental procedures

Experiments were conducted in accordance with the National Institute of Health Guide for the Care and Use of Laboratory Animals (1996) and were approved by the Institutional Animal Use Committee of Chiba University Graduate School of Medicine.

4.1. *Animals*

Adult male mice were used in all experiments. Mu receptor knockout mice were generated as described previously (Sora et al., 1997b). Congenic mu opioid receptor knockout mice backcrossed with C57BL/6 mice were used in the study (Hall et al., 2003). Wild type C57BL/6J mice with the same genetic background (CLEA Japan, Tokyo, Japan) were used as control. All mice were housed in plastic cages in controlled laboratory conditions with the temperature maintained at 23–25 °C and light in 12 h cycles (on at 7:00 and off at 19:00). Mice had food and water available ad libitum except during behavioral testing.

4.2. *Drugs*

Morphine hydrochloride was purchased from Takeda Chemical Industries, Osaka, Japan. U50,488H, DPDPE, naloxone hydrochloride, nor-BNI dihydrochloride and naltrindole hydrochloride were purchased from Sigma Chemicals, St. Louis, MO, U.S.A. SNC 80 was purchased from Tocris, Ellisville, MO, U.S.A. DPDPE and U50,488H were dissolved in distilled water and SNC80 was dissolved in 50% DMSO in distilled water with pH adjusted to 4.5 by hydrochloric acid. Other drugs were dissolved in saline. Vehicle was used as control for each drug.

4.3. *Drug administration*

Intrathecal administrations were performed in unanesthetized mice at the L5–L6 intervertebral space as follows. A mouse was placed in a handmade mouse holder and was held gently by its pelvic bone. Drug solution was administered into the intrathecal space by a 30-gauge needle connected to a 10-μl Hamilton syringe by polyethylene tubing. A flick of the tail was used as an indication that the needle had penetrated the dura mater (Hylden and Wilcox, 1980). All drugs were administered intrathecally in a volume of 3–5 μl. In preliminary studies, we found that repeating direct intrathecal injections to the same mouse resulted in unreliable effectiveness of drugs. Thus, opioid receptor antagonists were administered concomitantly with morphine in the same drug solution to avoid repeated intrathecal injections. The effect of intrathecal naloxone has been reported to be present as early as at 5 min post-administration and still present at 30 min post-administration (Yaksh and Rudy, 1977; Shimoyama et al., 1997). The peak effect of intrathecal nor-BNI has been reported to be 15 min post-administration and pretreatment times used were 15 to 25 min in previous studies (Takemori et al., 1988; Nakazawa et al., 1991; Dawson-Basoa and Gintzler, 1996). Intrathecal naltrindole has been reported to be effective between 15 and 45 min post-administration (Drower et al., 1991). Thus concomitant administration of the antagonists with morphine can be justified since the peak effect of intrathecal morphine was observed at 20 to 30 min post-administration.

4.4. *Behavioral testing*

Testings were performed during the day portion of the circadian cycle (07:00–19:00 h). The tail-flick test was used to evaluate antinociceptive responses to thermal pain. During testing, a mouse was loosely wrapped in a soft towel and was held gently by the experimenter's hand. The tail flick response was elicited by applying radiant heat to the dorsal surface of the tail. The intensity of the heat stimulus was adjusted so that naive wild type mice flicked their tails with latencies in a range of 3.0 ± 0.5 s. Cut off latency was set at 10 s to avoid tissue damage. Tail flick latencies were measured twice with an interval of 30 s, and the mean of the two latencies was used as the datum for each time point. Tail flick latencies were measured prior to (baseline latency) and every 10–15 min during a period up to 60 min after intrathecal administration of each drug (response latency). The experimenter was blinded to drug treatment throughout the study. To construct a dose response curve, the percentage of analgesic responders in the group was calculated. An analgesic responder was defined as one whose mean response tail-flick latency was 1.5 or more times the baseline latency value.

4.5. *Statistical analysis*

Comparisons between groups were performed using two-way ANOVAs for repeated measures or Student's *t* test when appropriate. Data were expressed as means ± SE. A *P* values less than 0.05 was considered significant. The quantal dose-response data were analyzed using the BLISS-21 computer program. This program maximizes the log-likelihood function to fit a parallel set of Gaussian normal sigmoid curves to the dose-response data and provides ED50 values and 95% confidence limits (Umans and Inturrisi, 1981).

Acknowledgments

This study was supported in part by a Grant-in-Aid for Scientific Research (15591617) from the Ministry of Education, Culture, Sports, Science and Technology, Japan (MS), a Grant-in-Aid for Cancer Research (Study Group on Palliative Care and Psycho-oncology in Cancer Treatment) from the Ministry of

Health and Welfare, Japan (NS) and NIDA intramural research program (GRU).

REFERENCES

Bilsky, E.J., Calderon, S.N., Wang, T., Bernstein, R.N., Davis, P., Hruby, V.J., McNutt, R.W., Rothman, R.B., Rice, K.C., Porreca, F., 1995. SNC 80, a selective, nonpeptidic and systemically active opioid delta agonist. J. Pharmacol. Exp. Ther. 273, 359–366.

Dawson-Basoa, M.E., Gintzler, A.R., 1996. Estrogen and progesterone activate spinal kappa-opioid receptor analgesic mechanisms. Pain 64, 607–615.

Drower, E.J., Stapelfeld, A., Rafferty, M.F., de Costa, B.R., Rice, K.C., Hammond, D.L., 1991. Selective antagonism by naltrindole of the antinociceptive effects of the delta opioid agonist cyclic[D-penicillamine2-D-penicillamine5]enkephalin in the rat. J. Pharmacol. Exp. Ther. 259, 301–725.

Fuchs, P.N., Roza, C., Sora, I., Uhl, G.R., Raja, S.N., 1999. Characterization of mechanical withdrawal responses and effects of mu-, delta- and kappa-opioid agonists in normal and mu-opioid receptor knockout mice. Brain Res. 821, 480–486.

Gallantine, E.L., Meert, T.F., 2005. A comparison of the antinociceptive and adverse effects of the mu-opioid agonist morphine and the delta-opioid agonist SNC80. Basic Clin. Pharmacol. Toxicol. 97, 39–51.

Hall, F.S., Li, X.F., Goeb, M., Roff, R., Hoggatt, H., Sora, I., Uhl, G.R., 2003. Congenic C57BL/6 mu opiate receptor (MOR) knockout mice: baseline and opiate effects. Genes Brain Behav. 2, 114–121.

Heinricher, M.M., Schouten, J.C., Jobst, E.E., 2001. Activation of brainstem N-methyl-D-aspartate receptors is required for the analgesic actions of morphine given systemically. Pain 92, 129–138.

Heyman, J.S., Mulvaney, S.A., Mosberg, H.I., Porreca, F., 1987. Opioid delta-receptor involvement in supraspinal and spinal antinociception in mice. Brain Res. 420, 100–108.

Honda, K., Ando, S., Koga, K., Takano, Y., 2004. The spinal muscarinic receptor subtypes contribute to the morphine-induced antinociceptive effects in thermal stimulation in mice. Neurosci. Lett. 371, 235–238.

Hosohata, Y., Vanderah, T.W., Burkey, T.H., Ossipov, M.H., Kovelowski, C.J., Sora, I., Uhl, G.R., Zhang, X., Rice, K.C., Roeske, W.R., Hruby, V.J., Yamamura, H.I., Lai, J., Porreca, F., 2000. Delta-opioid receptor agonists produce antinociception and [35S]GTPgammaS binding in mu receptor knockout mice. Eur. J. Pharmacol. 388, 241–248.

Hylden, J.L., Wilcox, G.L., 1980. Intrathecal morphine in mice: a new technique. Eur. J. Pharmacol. 67, 313–316.

Ji, R.-R., Zhang, Q., Law, P.Y., Low, H.H., Elde, R., Hokfelt, T., 1995. Expression of mu-, delta-, and kappa-opioid receptor-like immunoreactivities in rat dorsal root ganglia after carrageenan-induced inflammation. J. Neurosci. 15, 8156–8166.

Kamei, J., Saitoh, A., Ohsawa, M., Suzuki, T., Misawa, M., Nagase, H., Kasuya, Y., 1995. Antinociceptive effects of the selective non-peptidic delta-opioid receptor agonist TAN-67 in diabetic mice. Eur. J. Pharmacol. 276, 131–135.

Larson, A.A., Vaught, J.L., Takemori, A.E., 1980. The potentiation of spinal analgesia by leucine enkephalin. Eur. J. Pharmacol. 61, 381–383.

Loh, H.H., Liu, H.-C., Cavalli, A., Yang, W., Chen, Y.-F., Wei, L.-N., 1998. Mu-opioid receptor knockout mice: effects on ligand-induced analgesia and morphine lethality. Mol. Brain Res. 54, 321–326.

Malmberg, A.B., Yaksh, T.L., 1992. Isobolographic and dose–response analyses of the interaction between intrathecal mu and delta agonists: effects of naltrindole and its benzofuran analog (NTB). J. Pharmacol. Exp. Ther. 263, 264–275.

Manning, B.H., Franklin, K.B.J., 1998. Morphine analgesia in the formalin test: reversal by microinjection of quaternary naloxone into the posterior hypothalamic area or periaqueductal gray. Behav. Brain Res. 92, 97–102.

Matthes, H.W.D., Maldonado, R., Simonin, F., Valverde, O., Slowe, S., Kitchen, I., Befort, K., Dierich, A., Meur, M.L., Dollé, P., Tzavara, E., Hanoune, J., Roques, B.P., Kieffer, B.L., 1996. Loss of morphine-induced analgesia, reward effect and withdrawal symptoms in mice lacking the mu-opioid-receptor gene. Nature 383, 819–823.

Matthes, H.W.D., Smadja, C., Valverde, O., Vonesch, J.-L., Foutz, A.S., Boudinot, E., Denavit-Saubié, M., Severini, C., Negri, L., Roques, B.P., Maldonado, R., Kieffer, B.L., 1998. Activity of the delta-opioid receptor is partially reduced, whereas activity of the kappa-receptor is maintained in mice lacking the mu-receptor. J. Neurosci. 18, 7285–7295.

Miaskowski, C., Taiwo, Y.O., Levine, J.D., 1991. Contribution of supraspinal mu- and delta-opioid receptors to antinociception in the rat. Eur. J. Pharmacol. 205, 247–252.

Millan, M.J., Czlonkowski, A., Lipkowski, A., Herz, A., 1989. Kappa-opioid receptor-mediated antinociception in the rat: II. Supraspinal in addition to spinal sites of action. J. Pharmacol. Exp. Ther. 251, 342–350.

Nakazawa, T., Furuya, Y., Kaneko, T., Yamatsu, K., 1991. Spinal kappa receptor-mediated analgesia of E-2078, a systemically active dynorphin analog, in mice. J. Pharmacol. Exp. Ther. 256, 76–81.

Ohsawa, M., Mizoguchi, H., Narita, M., Nagase, H., Kampine, J.P., Tseng, L.F., 2001. Differential antinociception induced by spinally administered endomorphin-1 and endomorphin-2 in the mouse. J. Pharmacol. Exp. Ther. 298, 592–597.

Omote, K., Kitahara, L.M., Nakatani, K., Collins, J.G., 1991. Delta receptor involvement in morphine suppression of noxiously evoked activity of spinal WDR neurons in cats. Brain Res. 554, 299–303.

Petrillo, P., Angelici, O., Bingham, S., Ficalora, G., Garnier, M., Zaratin, P.F., Petrone, G., Pozzi, O., Sbacchi, M., Stean, T.O., Upton, N., Dondio, G.M., Scheideler, M.A., 2003. Evidence for a selective role of the delta-opioid agonist 8R-(4bS*,8aalpha, 8abeta,12bbeta)]7,10-Dimethyl-1-methoxy-11-(2-methylpropyl)oxycarbonyl 5,6,7,8,12,12b-hexahydro-(9H)-4,8-methanobenzofuro [3,2-e] pyrrolo [2,3-g] isoquinoline hydrochloride (SB-235863) in blocking hyperalgesia associated with inflammatory and neuropathic pain responses. J. Pharmacol. Exp. Ther. 307, 1079–1089.

Porreca, F., Mosberg, H.I., Omnaas, J.R., Burks, T.F., Cowan, A., 1987. Supraspinal and spinal potency of selective opioid agonists in the mouse writhing test. J. Pharmacol. Exp. Ther. 240, 890–894.

Saitoh, A., Kimura, Y., Suzuki, T., Kawai, K., Nagase, H., Kamei, J., 2004. Potential anxiolytic and antidepressant-like activities of SNC80, a selective delta-opioid agonist, in behavioral models in rodents. J. Pharmacol. Sci. 95, 374–380.

Scherrer, G., Befort, K., Contet, C., Becker, J., Matifas, A., Kieffer, B.L., 2004. The delta agonists DPDPE and deltorphin II recruit predominantly mu receptors to produce thermal analgesia: a parallel study of mu, delta and combinatorial opioid receptor knockout mice. Eur. J. Neurosci. 19, 2239–2248.

Schuller, A.G.P., King, M.A., Zhang, J., Bolan, E., Pan, Y.-X., Morgan, D.J., Chang, A., Czick, M.E., Unterwald, E.M., Pasternak, G.W., Pintar, J.E., 1999. Retention of heroin and morphine-6beta-glucuronide analgesia in a new line of mice lacking exon 1 of MOR-1. Nat. Neurosci. 2, 151–156.

Shimoyama, M., Shimoyama, N., Inturrisi, C.E., Elliott, K.J., 1997. Gabapentin enhances the antinociceptive effects of spinal morphine in rat tail-flick test. Pain 72, 375–382.

Simonin, F., Valverde, O., Smadja, C., Slowe, S., Kitchen, I., Dierich, A., Meur, M.L., Roques, B.P., Maldonado, R., Kieffer, B.L., 1998. Disruption of the kappa-opioid receptor gene in mice enhances sensitivity to chemical visceral pain, impairs pharmacological actions of the selective kappa-agonist U50,488H and attenuates morphine withdrawal. EMBO J. 17, 886–897.

Sora, I., Funada, M., Uhl, G.R., 1997a. The mu-opioid receptor is necessary for [D-Pen2,D-Pen5]enkephalin-induced analgesia. Eur. J. Pharmacol. 324, R1–R2.

Sora, I., Takahashi, N., Funada, M., Ujike, H., Revay, R.S., Donovan, D.M., Miner, L.L., Uhl, G.R., 1997b. Opiate receptor knockout mice define mu receptor roles in endogenous nociceptive responses and morphine-induced analgesia. Proc. Natl. Acad. Sci. U. S. A. 94, 1544–1549.

Sora, I., Li, X.F., Funada, M., Kinsey, S., Uhl, G.R., 1999. Visceral chemical nociception in mice lacking mu-opioid receptors: effects of morphine, SNC80 and U-50,488. Eur. J. Pharmacol. 366, R3–R5.

Sora, I., Elmer, G., Funada, M., Pieper, J., Li, X.F., Hall, F.S., Uhl, G.R., 2001. Mu opiate receptor gene dose effects on different morphine actions: evidence for differential in vivo mu receptor reserve. Neuropsychopharmacology 25 (1), 41–54.

Szeto, H.H., Soong, Y., Wu, D., Qian, X., Zhao, G.-M., 2003. Endogenous opioid peptides contribute to antinociceptive potency of intrathecal [Dmt1]DALDA. J. Pharmacol. Exp. Ther. 305, 696–702.

Takemori, A.E., Portoghese, P.S., 1987. Evidence for the interaction of morphine with kappa and delta opioid receptors to induce analgesia in beta-funaltrexamine-treated mice. J. Pharmacol. Exp. Ther. 243, 91–94.

Takemori, A.E., Ho, B.Y., Naeseth, J.S., Portoghese, P.S., 1988. Nor-binaltorphimine, a highly selective kappa-opioid antagonist in analgesic and receptor binding assays. J. Pharmacol. Exp. Ther. 246, 255–258.

Umans, J.G., Inturrisi, C.E., 1981. Pharmacodynamics of subcutaneously administered diacetylmorphine, 6-acetylmorphine and morphine in mice. J. Pharmacol. Exp. Ther. 218, 409–415.

Vaught, J.L., Rothman, R.B., Westfall, T.C., 1982. Mu and delta receptors: their role in analgesia in the differential effects of opioid peptides on analgesia. Life Sci. 30, 1443–1455.

Yaksh, T.L., Harty, G.J., 1988. Pharmacology of the allodynia in rats evoked by high dose intrathecal morphine. J. Pharmacol. Exp. Ther. 244, 501–507.

Yaksh, T.L., Rudy, T.A., 1977. Studies on the direct spinal action of narcotics in the production of analgesia in the rat. J. Pharmacol. Exp. Ther. 202, 411–428.

Yaksh, T.L., Harty, G.J., Onofrio, B.M., 1986. High doses of spinal morphine produce a nonopiate receptor-mediated hyperesthesia: clinical and theoretic implications. Anesthesiology 64, 590–597.

Zhu, Y., King, M.A., Schuller, A.G.P., Nitsche, J.F., Reidl, M., Elde, R.P., Unterwald, E., Pasternak, G.W., Pintar, J.E., 1999. Retention of supraspinal delta-like analgesia and loss of morphine tolerance in delta opioid receptor knockout mice. Neuron 24, 243–252.

Intracisternal A-particle element in the 3′ noncoding region of the mu-opioid receptor gene in CXBK mice: a new genetic mechanism underlying differences in opioid sensitivity

Wenhua Han[a,*], Shinya Kasai[a,*], Harumi Hata[a,b], Takehiro Takahashi[a], Yukio Takamatsu[a], Hideko Yamamoto[a], George R. Uhl[c], Ichiro Sora[a,b] and Kazutaka Ikeda[a]

Objectives **CXBK mice, recombinant inbred mice derived from C57BL/6By and BALB/cBy progenitors, display reduced morphine-induced analgesia. Earlier we reported that CXBK mice expressed a reduced amount of the major transcript, MOR-1 mRNA, of the mu-opioid receptor gene. The CXBK MOR-1 mRNA contains a normal coding region and an abnormally long untranslated region.**

Methods and results **To identify the nucleotide-sequence difference between the CXBK MOR-1 mRNA and that of the progenitors, we first characterized the 3′ untranslated region of the MOR-1 mRNA, which was largely unknown. A 3′ rapid amplification of cDNA ends-PCR analysis revealed that the 3′ untranslated region of the C57BL/6By MOR-1 mRNA was 10 181 nucleotides transcribed from an exon. Next, we compared the MOR-1 genes in C57BL/6By, CXBK, and BALB/cBy mice, and found a 5293 nucleotide insertion only in CXBK mice. The inserted sequence was a variant of the intracisternal A-particle elements that exist in the mouse genome at approximately 1000 sites. Reverse transcription–PCR analyses revealed that the intracisternal A-particle element was transcribed as a part of the CXBK MOR-1 mRNA. No other differences were found in the MOR-1 mRNA between CXBK and BALB/cBy mice, whereas 100 nucleotides differed between C57BL/6By and CXBK mice aside from the intracisternal A-particle insertion. Finally, CXBK mice displayed reduced morphine responses compared with BALB/cBy mice.**

Conclusions **Our data suggest that differences in the MOR-1 3′ untranslated region appear to cause the CXBK phenotype. This genetic mechanism underlying the CXBK phenotype may provide good insight into the possible genetic mechanisms underlying individual differences in opioid sensitivity in humans. *Pharmacogenetics and Genomics* 16:451–460 © 2006 Lippincott Williams & Wilkins.**

Pharmacogenetics and Genomics 2006, **16**:451–460

Keywords: CXBK mouse, mu-opioid receptor, 3′ untranslated region, intracisternal A-particle, morphine, analgesia

[a]Division of Psychobiology, Tokyo Institute of Psychiatry, Tokyo, Japan, [b]Department of Psychobiology, Tohoku University Graduate School of Medicine, Sendai, Japan and [c]Molecular Neurobiology Branch, National Institute on Drug Abuse-International Research Program, National Institute of Health, Box 5180, Baltimore, MD, USA.

Correspondence and requests for reprints to Kazutaka Ikeda, Division of Psychobiology, Tokyo Institute of Psychiatry, 2-1-8 Kamikitazawa, Setagaya-ku, Tokyo 156-8585, Japan.
Tel: +81-3-3304-5701 (ext. 508); fax: +81-3-3329-8035;
e-mail: ikedak@prit.go.jp

This study was supported by the Japanese Ministry of Health, Labour and Welfare (H16-Iyaku-029 and H17-pharmaco-001); the Japanese Ministry of Education, Culture, Sports, Science, and Technology; and NIDA-IRP, NIH, DHSS.

Received 3 August 2005 **Accepted** 30 January 2006

Introduction

Opioids are the most powerful pain relievers used for major surgeries and pain associated with cancer. However, individual differences in opioid sensitivity limit the effective pain treatment. Opioids exert their pharmacological actions through their specific receptors, designated mu-, delta-, and kappa-subtypes [1]. Studies on mice lacking the mu-opioid receptor (MOR) demonstrated that, among these three subtypes, MOR is a mandatory component for opioid actions [2,3]. For example, deletion of MOR eliminates the antinociceptive effects of morphine; and heterozygous MOR knockout (KO) mice, which have 50% of the receptor density found in wild-type mice, show lower but still significant morphine analgesia [4,5]. These findings suggest that the gene encoding MOR (*Oprm1*) is the best candidate gene contributing to the individual differences in sensitivity to opioids [6].

The MOR cDNAs and genes of several species have been cloned (reviewed in [7]). The mouse *Oprm1* gene spans over 250 kb and consists of multiple exons that combine to yield several isoforms [8]. Among these isoforms, MOR-1 mRNA with exon splice junctions at the first intracellular loop (Arg^{95}), the second extracellular loop (Gly^{213}), and the cytoplasmic C-terminal region

*These authors contributed equally to this study.

1744-6872

(Gln^{386}/Leu^{387}) [9] is approximately 12 kb in length and the most abundant transcript [8,10,11]. In addition, studies on rapid amplification of the cDNA 5′-end demonstrated two transcriptional initiation sites, −793 base pairs (bp) and −268 bp from the translation start site of the MOR-1 mRNA [12,13]. The 3′ untranslated region (UTR) of the mouse MOR-1 mRNA is long, being over 10 kb; however, the sequence of this 3′UTR has not been characterized.

To understand the genetic mechanisms underlying human individual differences in opioid sensitivity, investigation of the mechanisms responsible for mouse inter-strain differences in such sensitivity is one promising approach. The CXBK mouse strain, a recombinant inbred strain derived from an F_2 intercross between C57BL/6 (B6) and BALB/c (BALB) mice, has been widely used as a MOR-deficient mouse strain for more than 30 years (reviewed in [14]). The CXBK mice exhibit reduced opioid binding [15] and reduced responses to MOR agonists [16]. The CXBK mice also display a phenotype similar to that of heterozygous MOR-KO mice [16], and possess an abnormally long MOR-1 mRNA that is expressed at lower levels than that of the progenitor strains [11]. However, the genetic basis of the CXBK phenotype remains to be elucidated.

In the present study, we determined the complete 3′UTR sequence of the mouse MOR-1 mRNA for the first time, and identified genetic differences in this mRNA between CXBK mice and their progenitors.

Materials and methods

Animals

C57BL/6By, CXBK, and BALB/cBy mice were purchased from The Jackson Laboratory (Bar Harbor, Maine, USA). C57BL/6J mice were purchased from CLEA Japan Inc. (Tokyo, Japan). C57BL/6By, CXBK, and BALB/cBy mice were used in the genetic experiments, and C57BL/6J, CXBK, and BALB/cBy mice were used in the behavioral tests. The mice were housed five per cage in an environment maintained at 22 ± 2°C, with a relative humidity of $55 \pm 5\%$ and a 12 h light/12 h dark cycle (lights on 8:00 a.m. to 8:00 p.m.). The mice had free access to a standard laboratory diet and water *ad libitum*. The experimental procedures were approved by the Institutional Animal Care and Use Committee of Tokyo Institute of Psychiatry.

Molecular cloning of the murine MOR-1 3′UTR

A bacterial artificial chromosome (BAC) library containing 129/SvJ mouse genomic DNAs (Incyte Genomics Inc., California, USA) was screened for *Oprm1* genomic DNA sequences. BAC clones containing *Oprm1* genomic sequences were isolated by hybridization with ^{32}P-labeled *Oprm1* gene fragments prepared from B6 mouse genomic DNA by polymerase chain reaction (PCR) amplification with the following primers: sense primer, 5′-AACTGCTCCATTGCCCTAACTGGGT-3′; and antisense primer, 5′-GGATTTTGCTCAGAATGGTGGCATG-3′ (1434–2205 bp, GenBank accession number U19380). A QIAGEN Plasmid Purification Kit (QIAGEN K.K., Tokyo, Japan) was used to purify the positive clone. This BAC clone was sequenced with the aid of a series of oligonucleotide primers designed according to the initially reported exon 4 sequence of the *Oprm1* gene [10] and sequences analyzed in the present study.

3′ Rapid amplification of cDNA ends (RACE)–PCR analysis

3′ RACE was conducted by using the components of a 3′-Full RACE Core Set (TaKaRa, Tokyo, Japan). The poly(A) RNA, which was prepared from B6 mouse brain by use of a Message RNA Isolation Kit (Stratagene, La Jolla, California, USA), was reverse-transcribed with the Oligo(dT)-Adaptor Primer included in the set. Two rounds of PCR amplification were conducted by using the Adaptor Primer (AP) along with mouse *Oprm1* gene-specific primers F1, 5′-AAGTATTTCCCTGGGAACCTGGGTATT-3′ (outer) and F2, 5′-CTGTGTGACTGGTGATGTGCCAGAATCCAC-3′ (inner), designed according to the sequences of the BAC clone. The AP-primed cDNAs were subjected to the first-round PCR amplification with the AP and F1 primers under the following conditions: 94°C for 5 min; 35 cycles of 94°C for 1 min, 60°C for 1 min, and 74°C for 3 min; and 74°C for 7 min. The PCR products were purified by using a QIAquick PCR Purification Kit (QIAGEN K.K., Tokyo, Japan), and then subjected to the second-round PCR amplification (nested PCR). Nested PCR was conducted with the AP and F2 primers under the same conditions. The products from the second-round PCR amplification were cloned into pCR2.1 plasmid vector (Invitrogen, Carlsbad, California, USA) and sequenced.

PCR of genomic DNA

Genomic DNAs were prepared from mouse tail or liver, and subjected to the PCR amplification by use of an Expand Long Template PCR system (Roche, Mannheim, Germany) with the primers described below. The reaction mixture was prepared according to the instructions of the manufacturer. The PCR conditions were as follows: 94°C for 2 min; 30 cycles of 94°C for 20 s, 60°C for 30 s, and 68°C for 8 min + T s [T = 0 (cycles, 1–10); T = (cycle no. − 10) × 20 (cycles, 11–30)]; and 68°C for 7 min. With reference to the sequences from the BAC clone, the designed primers were the following: F3, 5′-AGAAGACAACCATCAATGTGTTCTCTGATG-3′; F4, 5′-CTACCCAGCTGGTTCTTTCCATACAAGCTA-3′; F5, 5′-AACTCTTGGCGATCCTTCTGCCTCGGACTC-3′; R3, 5′-CAAGTCATGCCTAAGTTGAATGAATGAGTC-3′; R4, 5′-CTAGGCATACGTCATCTGGATTAATGT-

CAT-3′; R7, 5′-GTGATCTGTAGAGATCTGCCTGTT TTCAGC-3′.

Sequence analysis

The PCR products were purified by using the QIAquick PCR Purification Kit and then sequenced with a PRISM 3100 genetic analyzer (Applied Biosystems, Foster City, California, USA). DNASTAR 5.0 software (DNAstar, Madison, Wisconsin, USA) was used to analyze and assemble nucleotide sequences.

Reverse transcriptase (RT)–PCR analysis

Poly(A) RNA was isolated from B6 and CXBK mouse brains by using the Message RNA Isolation Kit. First-strand cDNA was synthesized by using poly(A) RNA with random hexamer or oligo(dT) primers and SurperScript II RNase H free reverse transcriptase (Invitrogen, Carlsbad, California, USA). The PCR amplification was conducted with the primers shown below and KOD Taq Polymerase (TOYOBO, Osaka, Japan). The following thermal cycle conditions recommended by the manufacturer were adopted: 94°C for 5 min; 35 cycles of 94°C for 1 min, 60°C for 1 min, and 74°C for 3 min; and 74°C for 7 min. With reference to the sequences of the BAC clone and sequences obtained from mouse genomic DNA, the following primers were designed: F6, 5′-TTCAAGGA-TATGAGAAAGACTGGAACTGAC-3′; F7, 5′-AAGTAT TTCCCTGGGAACCTGGGTATTCCT-3′; F8, 5′-TCAG TGACTTTAGATTTTGTTTGT-3′; R6, 5′-AGGGCCAA CGAATTCATGTAAACAAATAAC-3′; R7, 5′-GTGATCT GTAGAGATCTGCCTGTTTTCAGC-3′; R8, 5′-CTCG CTGCCTAGATTTTACTGA-3′; IAPF, 5′-CACACTGG GGATTTGACCTC-3′; IAPR, 5′-AGCCATTTCTCACT TCCGTTCC-3′.

Behavioral tests

The analgesic (antinociceptive) effects of morphine were examined by conducting tail-flick and hot-plate tests, which were slightly modified versions of the original methods developed by D'Amour and Smith [17] and Woolfe and MacDonald [18], respectively, as previously described [16]. The B6, CXBK, and BALB mice were used in both experiments. Morphine hydrochloride solution (10 mg/ml, Takeda Chemical Industries Ltd., Osaka, Japan) was diluted to 1 mg/ml with sterile saline on every experimental day. Morphine was injected intraperitoneally (i.p.) into the mice at 20 min intervals with an ascending cumulative dosing regimen producing total drug doses of 3, 10, 30, and 100 mg/kg. In the tail-flick test, the mice were loosely wrapped in an adsorbent towel and placed on the tail-flick apparatus (Model MK-330A, Muromachi Kikai Co., Tokyo, Japan). A light beam was focused on the tail, and the latency to vigorous tail flicking in response to a heat stimulus was measured within a 15 s cut-off time to minimize tissue damage. In the hot-plate test, the animals were placed on a metal plate maintained at 52 ± 0.2°C, and the latency to hindpaw licking as a response to the heat stimulus was measured within a 60 s cut-off time. The analgesic effects were expressed as the percentage of the maximal possible effect (%MPE), which was calculated as follows: %MPE = 100% × {[(post drug latency)–(pre drug latency)]/[(cut-off time)–(pre drug latency)]}.

Statistical analyses

The ED_{50} values were determined by constructing cumulative dose–response curves for morphine antinociception in B6, CXBK, and BALB mice. A computer-assisted probit and relative potency analyses were used to calculate the ED_{50} values in each mouse strain. The results of ED_{50} values were analyzed with unpaired *t*-test to examine significant differences between mouse strains. A two-way repeated measures analysis of variance (ANOVA), followed by a Scheffé's F *post-hoc* test and a repeated-measures ANOVA was used to examine significance of differences between groups in the behavioral tests. $P < 0.05$ was considered to be statistically significant.

Results

To obtain genomic sequences corresponding to the 3′-terminal region of the MOR-1 mRNA, we screened a BAC library containing 129/SvJ mouse genomic DNAs with the 5′-end fragment (772 bp) of the mouse *Oprm1* exon 4 as a hybridization probe. Some BAC clones that were strongly hybridized with the probe were obtained, and one of these BAC clones was subjected to DNA sequencing with the series of oligonucleotide primers. An approximately 15-kb genomic sequence downstream from the MOR-1 stop codon was deduced by sequencing (GenBank accession number AB180894).

3′ RACE–PCR was conducted to identify the transcriptional 3′-end of the mouse MOR-1 mRNA. In the first-round PCR, multiple bands about 600 bp, 850 bp, and 1.2 kbp in size were amplified from both B6 and CXBK samples (Fig. 1a). All fragments were then subjected to the second PCR amplification with the nested primer. A single fragment, about 180 bp in length, was amplified from both samples (Fig. 1b). This PCR product was sequenced, and a cleavage/polyadenylation site was found at 10 177 nucleotides downstream from the stop codon (Fig. 1c). A polyadenylation signal sequence (AATAAA) was also found 23 nucleotides upstream from the cleavage/polyadenylation site. These results well agree with the vast majority of eukaryotic polyadenylation signal sequences, which contain the consensus sequence AATAAA between 10 and 35 nucleotides upstream from the actual cleavage/polyadenylation site [19]. Considering the 793 bases of the 5′UTR [20] and the 1197 bases of the entire coding region [9], the putative length of the MOR-1 mRNA is 12167 bases, which is in accord with the previous results obtained from Northern blot analysis

[8,10,11]. According to this sequence, the 3′UTR of the mouse MOR-1 mRNA was considered to be transcribed from only exon 4 of the *Oprm1* gene (Fig. 1d).

Next, RT–PCR analyses were conducted to confirm the results of the 3′ RACE–PCR analysis. The cDNAs were synthesized from poly(A) RNAs of the B6 and CXBK mouse brains, and subjected to PCR. The locations of the primers are shown in Fig. 1(d). The F6 and R6 primer set, located within exon 4 of the *Oprm1* gene, amplified the predicted-size DNA fragments (563 bp) from both B6 and CXBK mouse samples. In contrast, the PCR product was not obtained by amplification with the cDNAs as the template and the F7 and R7 primer set matching sites located upstream and downstream from the cleavage/polyadenylation site that we identified (Fig. 1e), although PCR fragments of approximately 800 bp were obtained from both B6 and CXBK mouse genomic DNAs with the

Fig. 1

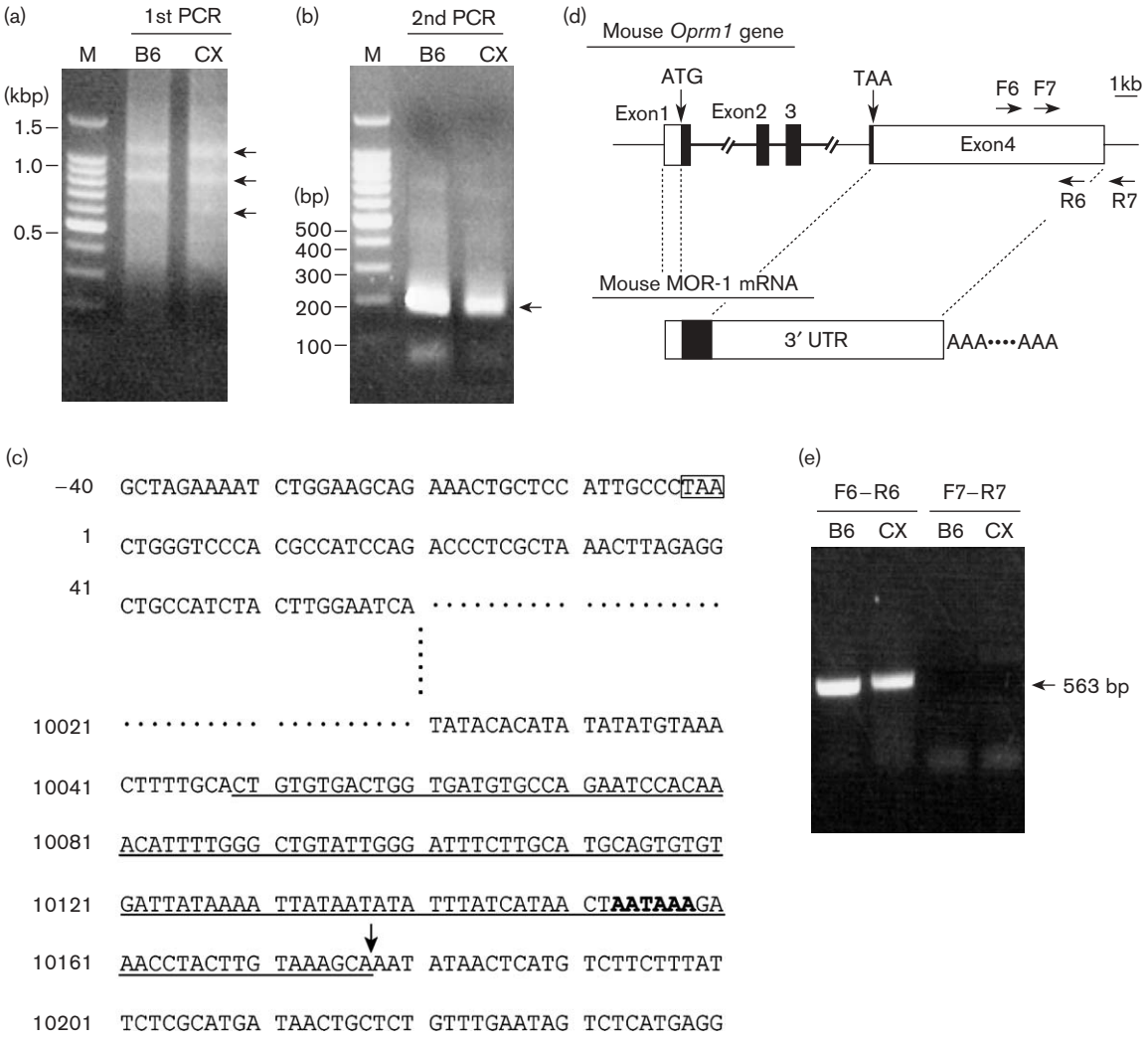

3′ RACE–PCR analysis of murine MOR-1 mRNA. (a) First-round PCR amplification in the 3′-RACE–PCR analysis. The cDNA samples obtained from C57BL/6By (B6) and CXBK (CX) mouse brains were subjected to first-round PCR with the primer F1 and Adaptor Primer. The PCR products were separated by electrophoresis along with 100-bp incremental ladder markers (M) in 1.0% agarose gels. (b) Second-round PCR with the nested primer F2 and Adaptor Primer. A single fragment of approximately 200 bp was detected in both B6 and CX mice. (c) Genomic sequence corresponding to the 3′-end region of the mouse MOR-1 mRNA. The sequence of the product from the second-round PCR amplification is underlined. The TAA nucleotide sequence (−3 to −1) corresponds to the translation termination. The putative polyadenylation sequence is indicated in bold type. The position of the cleavage/polyadenylation site is indicated by the arrow. (d) Schematic representation of the mouse *Oprm1* gene and its transcript. The coding regions and UTRs of the *Oprm1* gene and MOR-1 mRNA are represented by closed and open boxes, respectively, and thick lines indicate the introns. (e) RT–PCR analysis of the 3′UTR of the MOR-1 mRNA. The poly(A) RNA samples prepared from the B6 and CX mouse brains were reverse-transcribed, and subjected to PCR with MOR-1 specific primers shown by the arrows in (d). The F6–R6 and F7–R7 sets indicate amplifications with the F6 and R6 primers and the F7 and R7 primers, respectively. The predicted-size PCR fragment was amplified with the F6–R6, but not with the F7–R7, primer set in both B6 and CX mice.

same primer set (data not shown). These data support the results of the 3′ RACE–PCR analysis regarding the cleavage/polyadenylation site of the mouse MOR-1 mRNA.

Messenger RNA degradation/stabilization is one of the mechanisms that control gene expression [21]. Well-characterized *cis*-acting elements that are the possible binding sites for RNA-binding proteins and regulate mRNA stability are AU-rich elements (AREs) found in the 3′UTRs of mRNAs [22]. Typically these elements are composed of a variable number of the AUUUA pentamer and/or UUAUUUA(U/A)(U/A) nonamer. In the 3′UTR of the 129/SvJ mouse MOR-1 cDNA, there are many of these motifs (Table 1). Six AUUUA motifs and 1 UUAUUUAUU motif were found in the last 2.0 kb of the 3′UTR. This finding is in accordance with previous results showing that AUUUA elements are densely located in the 3′-terminal regions of 3′UTRs [23]. Furthermore, we used an *Oprm1* region corresponding to the MOR-1 3′UTR to search for other *cis*-acting elements by using TRANSFAC version 6.0, the database of transcription factors, and found a large number of putative transcription factor-binding sites in the region corresponding to the MOR-1 3′UTR (data not shown).

The genomic DNAs prepared from B6, CXBK, and BALB mice were analyzed by the Expand Long Template PCR system using three primer sets (shown by arrows in Fig. 2(a)) covering the whole MOR-1 3′ noncoding region. PCRs were carried out in duplicate wells independently to avoid misreading the sequences. The F3 and R3 primer set and F5 and R7 primer set amplified the predicted-size DNA fragments (6.6 kb and 3.7 kb, respectively) from all three mouse strain samples, whereas the F4 and R4 primer set amplified a longer DNA fragment (6.6 kb) only in CXBK mice and predicted-size DNA fragment (562 bp) in B6 and BALB mice (Fig. 2b). All fragments were subjected to DNA sequencing, and the obtained sequences were analyzed by DNASTAR software (The GenBank accession numbers of complete MOR-1 3′UTR sequences of B6, CXBK, and BALB mice are AB180895, AB180892, and AB180893, respectively). The whole length of the 3′UTR sequence of the CXBK MOR-1 mRNA was 15 503 nucleotides, which was 5322 and 5299 bases longer than that of the B6 and BALB MOR-1 mRNA, respectively. The extra DNA sequence of the MOR-1 3′UTR in CXBK mice corresponded to the nucleotides between 6667 and 11 965 bp downstream from the stop codon. The sequence was composed of the 5293-bp insertion and 6-bp duplicate of the endogenous gene sequence 5′-TATCCC-3′ at the site of insertion (indicated by the underline in Fig. 2(a)).

Table 1 The positions of putative core motifs of AU-rich elements (AREs) in the 129/SvJ mouse MOR-1 3′UTR

Core motifs of AREs	Positions in 3′UTR
AUUUA	600, 1038, 1487, 1698, 2081, 3945, 4177, 4360, 4508, 4847, 5694, 5979, 6345, 6386, 6819, 6877, 6932, 8341, 8493, 8613, 8779, 8879, 10140
UUAUUUA(U/A)(U/A)	4175, 8877

A BLAST search of the GenBank DNA sequences identified the inserted 5293-bp sequence as an intracisternal A-particle (IAP) transposon. This IAP element inserted in the 3′ noncoding region of the CXBK *Oprm1* gene (CXBK-IAP) belonged to the IΔ1 type of IAP elements [24], which contains a diagnostic 4-kb *Hin*dIII restriction fragment (Fig. 3a). The IΔ1 type is the most abundant deleted-element type of IAP in the mouse genome [25]. Sequence analysis revealed that the CXBK-IAP contained long terminal repeats (LTRs) at both 5′- and 3′-flanking regions and that these repeats on both ends were identical. The LTRs of the CXBK-IAP were 400 bp in length and consisted of typical U3, R, and U5 regions bracketed by the characteristic 4-bp perfect inverted repeats (5′-TGTT/AACA-3′) (Fig. 3b). Previous findings showed the length of the U3 and U5 regions in the IAP LTRs to be conserved as 220 ± 4 bp and 55 ± 2 bp, respectively [26]. In the case of the CXBK-IAP, the LTRs had a 215-bp U3 region that contained a typical CAT box and a possible TATA box, and a 57-bp U5 region.

To know whether the transcript of the *Oprm1* gene in CXBK mice possesses the IAP element, we conducted RT–PCR analysis on the CXBK mouse brain mRNAs with the primers corresponding to the MOR-1 3′UTR (F8 and R8 primers) and the CXBK-IAP region (IAPF and IAPR primers) (Fig. 4a). As controls, RT–PCR analysis was also conducted on the B6 mouse samples. Whereas both the F8 and IAPR primer set and the IAPF and R8 primer set amplified the predicted-size PCR fragments (811 bp and 845 bp, respectively) from the CXBK mouse sample, neither of these primer sets yielded a PCR product from the B6 mouse sample (Fig. 4b). These results indicate that the CXBK-IAP element inserted in the 3′ noncoding region of the *Oprm1* gene was completely transcribed as a part of the MOR-1 mRNA in CXBK mice. This finding is in accord with earlier results obtained by Northern blot analysis showing that the MOR-1 mRNA in CXBK mice was longer than that in B6 mice [11].

The genomic sequence encompassing the whole MOR-1 mRNA was compared among B6, CXBK, and BALB mice (Table 2). In the 5′ noncoding region, a single nucleotide differed between B6 and CXBK mice, and no nucleotide differed between CXBK and BALB mice. In the coding region (1197 bp), the nucleotide sequences were identical among all three strains. In the sequence of the 3′ noncoding region except for the CXBK-IAP insertion and the 6-bp endogenous gene duplication (10 181 bp),

Fig. 2

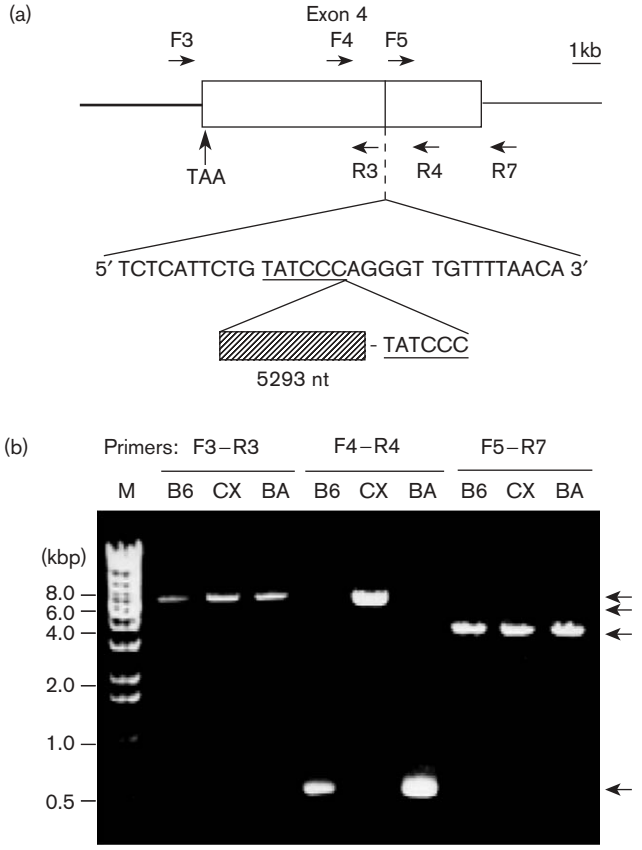

Increased length of the 3′ noncoding region of the CXBK *Oprm1* gene. (a) Structure of exon 4 of the *Oprm1* gene in CXBK mice. The coding and 3′ noncoding region of exon 4 of the mouse *Oprm1* gene are represented by a closed and open box, respectively. Arrows indicate the positions and directions of the primers used in the PCR analysis. The 5293-bp insertion in the 3′ noncoding region of the *Oprm1* gene is represented by the striped box. The underlined 6-bp sequences (TATCCC) are the duplicated endogenous sequences at the divergent site. (b) PCR analysis of genomic DNA. Genomic DNA samples of B6, CXBK (CX), and BALB (BA) mice were subjected to PCR with the 3 pairs of primers shown by arrows in (a), and the products were electrophoresed on a 1% agarose gel along with 1 kb incremental DNA markers (M). Amplifications with both the F3 and R3 primer set and the F5 and R7 primer set gave the same results among B6, CX, and BA mice. However, in amplification with the F4 and R4 primer set, a long product was detected only in CXBK mice, whereas the products in B6 and BA mice were short.

99 nucleotides differed between B6 and CXBK mice, whereas the nucleotide sequences were identical between CXBK and BALB mice. These results suggest that the *Oprm1* gene in CXBK mice was derived from BALB mice and that the CXBK-IAP was inserted in the *Oprm1* gene during the establishment of the CXBK mouse strain.

Since nucleotide sequences of the *Oprm1* exons were identical between the CXBK and BALB mice except for the insertion of the CXBK-IAP element in the 3′ noncoding region, comparison of the morphine analgesic effect in CXBK mice with that in BALB mice could help to determine the contribution of the CXBK-IAP element to the CXBK phenotype. Additionally, comparison of morphine analgesic effect in B6 mice with that in BALB mice could provide the contribution of 100 nucleotides differences between B6 and BALB mice in the analgesic effect of morphine. The analgesic effects of morphine in B6, CXBK, and BALB mice were examined by the tail-flick and hot-plate tests. The two-way repeated measures ANOVA revealed significant effects of morphine ($F_{4,16} = 129.57$, $P < 0.001$; $F_{4,16} = 119.16$, $P < 0.001$), mouse strain ($F_{2,16} = 16.89$, $P = 0.001$; $F_{2,16} = 18.19$, $P < 0.001$), and a significant interaction between morphine concentration and mouse strain ($F_{8,64} = 4.03$, $P = 0.006$; $F_{8,64} = 6.63$, $P < 0.001$) in both the tail-flick (Fig. 5a) and hot-plate (Fig. 5b) tests, respectively. All three mouse strains displayed antinociception by administration of morphine in both tail-flick test {$F_{4,30} = 86.36$, $P < 0.001$ (B6); $F_{4,20} = 19.63$, $P < 0.001$ (CXBK); $F_{4,30} = 51.25$, $P < 0.001$ (BALB)} and hot-plate test {$F_{4,30} = 105.87$, $P < 0.001$ (B6); $F_{4,20} = 17.60$, $P < 0.001$ (CXBK); $F_{4,30} = 34.48$, $P < 0.001$ (BALB)} (repeated-measures ANOVA). However, the analgesic effect of morphine was smaller in CXBK mice than in B6 and BALB mice. The differences in the morphine analgesia between

Fig. 3

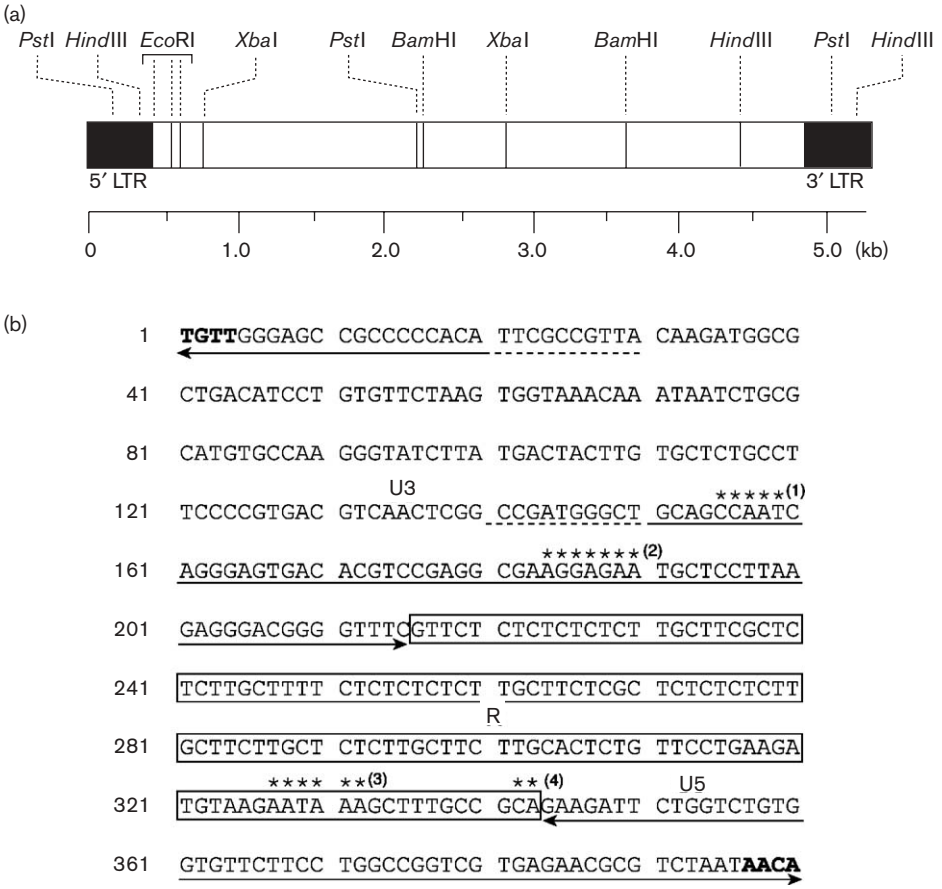

Characteristic features of the CXBK-IAP element. (a) Structure and restriction map of the CXBK-IAP element. The IAP internal region is represented by the open box, and the LTRs of the CXBK-IAP element are indicated by closed boxes. Locations of restriction sites are shown by vertical lines. (b) Complete sequence of the LTR in the CXBK-IAP element. The total size of the CXBK-IAP is 391 bp. The LTR of the CXBK-IAP consists of three sub-domains: U3 (215 bp, underlined with arrow), R (128 bp, open box) and U5 (57 bp, underlined with arrow). The 4-bp terminal inverted repeats (5′-TGTT/AACA-3′) are indicated in bold type. Typical regulatory elements are shown by asterisks: 1, CCAAT box; 2, TATA box; 3, AATAAA polyadenylation signal; 4, CA cleavage/polyadenylation site.

BALB and CXBK mice were significant at the 10 mg/kg and 30 mg/kg doses of morphine in the tail-flick test ($P < 0.001$ and $P < 0.05$, respectively; Scheffé's *post-hoc* test) and at the 3 mg/kg and 10 mg/kg doses of morphine in the hot-plate test ($P < 0.01$ and $P < 0.001$, respectively; Scheffé's *post-hoc* test). There were approximately three to five-fold rightward shifts in the dose–response curves for morphine antinociception in CXBK mice compared with B6 and BALB mice, yielding significantly greater morphine ED_{50} values for CXBK mice than for B6 mice ($t_{4.22} = 3.34$, $P < 0.05$; $t_{4.07} = 2.96$, $P < 0.05$; Welch's *t*-test) and for BALB mice ($t_{4.14} = 3.75$, $P < 0.05$; $t_{4.19} = 3.11$, $P < 0.05$; Welch's *t*-test) in the tail-flick and hot-plate tests, respectively (Table 3). The relative potencies of morphine for B6 or CXBK mice based on BALB mice (BALB ED_{50}/B6 or CXBK ED_{50}) were 0.67 or 0.17 in the tail-flick test, respectively. The ED_{50} value for B6 mice was 1.5-fold greater than that for BALB mice in the tail-flick test, but this difference was not significant ($t_{11} = 1.80$, $P = 0.099$; Student's *t*-test).

Discussion

In the present study, we characterized the complete 3′UTR of the mouse MOR-1 mRNA for the first time. The present results, together with the previous findings on the 5′UTR and exon-intron junctions, revealed the exon–intron structure of the *Oprm1* gene. As the transcript from the mouse *Oprm1* gene over 10 kb in size is MOR-1 mRNA only [8], this especially long 3′UTR is considered to be specific to the MOR-1 isoform. These findings in the mouse *Oprm1* gene are consistent with our recent findings in the human *OPRM1* gene [27]. Considering the fact that some elements in the 3′UTR can regulate the rate of translation and degradation of mRNAs through 3′UTR sequence-binding proteins [28,29], it is reasonable to predict that the long 3′UTR

Fig. 4

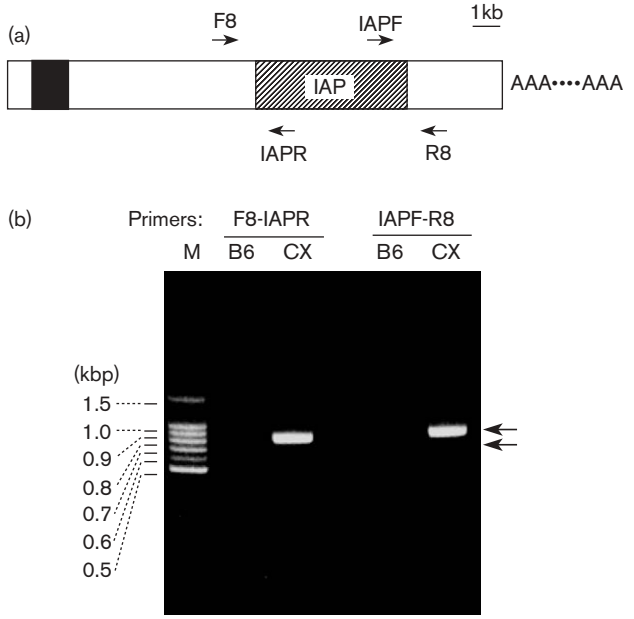

Characterization of MOR-1/CXBK-IAP fusion transcript in CXBK mice. (a) Schematic representation of the MOR-1/CXBK-IAP fusion transcript in CXBK mice. The coding region and the UTRs are represented by closed and open boxes, respectively. The CXBK-IAP insertion is indicated by the striped box. Arrows indicate the positions and directions of the primers used in the RT–PCR analysis. (b) RT–PCR analysis with the primers located in the region of the CXBK-IAP insert. The cDNAs prepared from the B6 and CXBK mouse brains were amplified with two primer sets, F8 and IAPR primers, and IAPF and R8 primers. The PCR products were electrophoresed on an agarose gel along with 100-bp incremental ladder markers (M). The PCR fragments were detected only in CXBK mice with both primer sets.

Table 2 Number of nucleotide differences in the 4 *Oprm1* exons among B6, CXBK and BALB mice

	Regions of the mouse *Oprm1* gene		
	5′-noncoding	CDS	3′-noncoding
B6/BA	1	0	99
B6/CX (IAP(–))	1	0	99
CX (IAP(–))/BA	0	0	0

Nucleotide sequences of the *Oprm1* gene were compared among B6, CXBK (CX) and BALB (BA) mice. 5′ noncoding, CDS and 3′ noncoding refer to the 5′ noncoding region, the coding region, and the 3′ noncoding region except for the IAP element, respectively.

Fig. 5

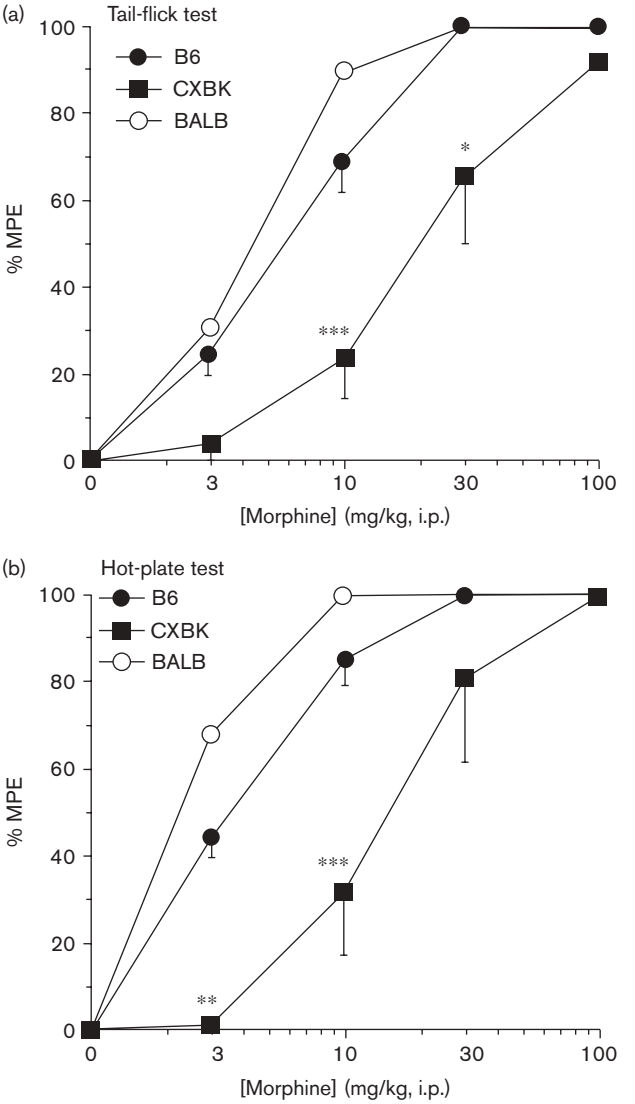

Reduced analgesic effects of morphine in CXBK mice. (a) Dose-dependent antinociceptive effects of morphine in B6, CXBK, and BALB mice in the tail-flick test. (b) Dose-dependent antinociceptive effects of morphine in B6, CXBK, and BALB mice in the hot-plate test. Each point represents the mean ± SEM ($n = 5–7$). The antinociceptive effect of morphine on B6, CXBK, and BALB mice was significant in both tests. However, the effect was significantly smaller in the CXBK mice than in their progenitor strains, B6 and BALB mice, in both tail-flick and hot-plate tests. Asterisks indicate statistically significant difference from the corresponding value for BALB mice ($^{*}P<0.05$, $^{**}P<0.01$, $^{***}P<0.001$, Scheffé's *post-hoc* test).

of the MOR-1 mRNA may participate in regulating the gene expression and thus affect opioid sensitivity. Actually, it has already been demonstrated that the especially long 3′UTR of the MOR-1 mRNA may contain physiologically relevant elements for regulating the receptor expression [27,30]. Therefore, the present findings including identification of the AUUUA motifs and transcription factor-binding sites, which may act as *cis*-acting elements, might lead to the discovery of functional elements in the MOR-1 3′UTR.

CXBK mice showed reduced MOR-1 mRNA levels compared with B6 and BALB mice, and the CXBK MOR-1 mRNA possessed a coding region identical to that in the MOR-1 mRNA of the progenitor mice [11]. The UTR regions of genes are well known to influence their expression via regulating their transcription, mRNA stability and translation. In the case of the *Oprm1* gene, the consensus sequences of some transcription factor

Table 3 Analgesic effects of i.p. morphine in B6, CXBK, and BALB strain mice in the tail-flick and hot-plate tests

	ED_{50}(mg/kg)	
	Tail-flick test	Hot-plate test
B6	5.87 ± 0.82	3.76 ± 0.37
CXBK	22.60 ± 4.94*	15.09 ± 3.81*
BALB	3.95 ± 0.64	3.06 ± 0.59

Each ED_{50} value was determined as mean ± SEM by constructing cumulative dose–response curves and computer-assisted probit analysis in each mouse strain and test. Asterisks indicate statistically significant differences from the corresponding values of B6 and BALB mice ($P<0.05$; Welch's *t*-tests).

binding sites are also located at the 5′UTR promoter/enhancer regions [9]. The nucleotide at −202 upstream from the start codon in the *Oprm1* gene is different between B6 and CXBK mice. The nucleotide is next to a transcription factor Sp1-binding site. Lee *et al.* reported that the nucleotide difference affects the Sp1 binding and MOR-1 transcription levels [31]. However, in the present study, we found that CXBK and BALB mice had the same MOR-1 mRNA sequence except for the IAP insertion into the 3′ noncoding region and that CXBK mice showed remarkably reduced morphine analgesia compared with BALB mice. Furthermore, we found 100 nucleotide differences in the 5′ and 3′ noncoding regions of *Oprm1* gene between B6 and BALB mice, but the morphine-induced analgesia in B6 mice was not significantly different from that in BALB mice. Our results were consistent with the previous report showing that the ED_{50} value in the CXBK mice (more than 10 μg) for intracerebroventricular morphine in the tail-flick test was 20 to 30 times greater than those in B6 (0.5 μg) and BALB mice (0.6 μg), whereas the ED_{50} values for morphine and DAGO, another highly selective MOR agonist, did not significantly differ among B6 and BALB mice [32]. Considering the slight difference in morphine analgesic effects between B6 and BALB mice, we propose that the insertion of the CXBK-IAP element into the 3′ noncoding region of the *Oprm1* gene is mainly responsible for the reduced MOR-1 mRNA level and attenuated sensitivity to morphine in CXBK mice.

IAPs are retrovirus-like elements present in approximately 1000 copies per haploid genome in *Mus musculus* [33]. IAPs insert into the murine genome and sometimes change their genomic position. Consequently, the transposed IAP element affects the expression of the nearby gene by acting as a regulatory element for the gene or by initiating transcription of the adjacent gene from the IAP's LTRs [24]. There are some examples that an IAP insertion into the 3′ noncoding region of cytokine genes as well as oncogenes resulted in autocrine transformation [34,35], either by adding a transcriptional enhancer or by displacing the AUUUA motifs, which destabilize mRNAs. On the other hand, in the present study, the insertion of an IAP sequence within the 3′ noncoding region of the *Oprm1* gene appears to reduce the gene expression in CXBK mice. Thus, the added transcriptional enhancer or the disruption of the AUUUA motifs could not be the reason for the reduced MOR-1 transcript. One possible explanation for this decrease in MOR-1 mRNA expression is that the increase in the length of the 3′UTR by IAP insertion causes mRNA instability. Studies on the human alpha-globin gene have suggested that an increase in the length of the 3′UTR disrupted stability of the pre-mRNA and strongly influenced the level of the alpha-globin mRNA [36]. In CXBK mice, the long nucleotide insertion, irrespective of its sequence, might disrupt the stability of the MOR-1 mRNA. Another possibility is that the IAP insertion may separate the transcription factor elements in the 3′UTR, reduce the enhancing effects of these elements, and decrease MOR-1 mRNA expression.

Studies on various inbred strains of mice revealed significant strain differences in analgesic sensitivity to morphine [37–39]. Among a variety of mouse inbred strains, CXBK mice show a marked reduction in morphine-induced analgesia [14]. Thus, we anticipated that genetic differences in CXBK mice may be examples of genetic mechanisms underlying a wide range of opioid sensitivity. The present findings together with the previous findings in CXBK mice provide evidence for the involvement of the MOR-1 3′UTR in the regulation of MOR-1 expression, although further studies are necessary to elucidate whether the impairments of other factors are involved in the reduced morphine analgesia in CXBK mice, since it was not defined that the IAP insertion into the *Oprm1* gene was the only and direct cause in the low expression levels of MOR-1 mRNA and reduced morphine analgesia in CXBK mice. It is reasonable to consider that the human MOR-1 3′UTR also plays a crucial role in regulating MOR-1 expression and may be involved in individual differences in opioid sensitivity in humans. Actually, a large number of polymorphisms have been identified in the human *OPRM1* gene including the region corresponding to the 3′UTR [6,40]. Over 50 polymorphisms are localized especially in the 3′UTR of human *OPRM1* gene. If even one of the polymorphisms is located in the consensus sequences of regulatory protein binding sites such as AREs, the polymorphism may affect MOR-1 mRNA expression by causing a change in the binding of regulatory proteins to the mRNA or genomic DNA, and thus account for the individual differences in opioid sensitivity. Identifying the functional polymorphisms in the MOR-1 3′UTR may help to improve pain management for the individual patients.

Acknowledgements

We thank Junko Hasegawa and Keiko Matsuoka for their skilled technical assistance and animal care, respectively.

References

1 Mansour A, Khachaturian H, Lewis ME, Akil H, Watson SJ. Anatomy of CNS opioid receptors. *Trends Neurosci* 1988; **11**:308–314.

2 Uhl GR, Sora I, Wang Z. The mu opiate receptor as a candidate gene for pain: polymorphisms, variations in expression, nociception, and opiate responses. *Proc Natl Acad Sci U S A* 1996; **96**:7752–7755.

3 Kieffer BL, Gaveriaux-Ruff C. Exploring the opioid system by gene knockout. *Prog Neurobiol* 2002; **66**:285–306.

4 Matthes HW, Maldonado R, Simonin F, Valverde O, Slowe S, Kitchen I, *et al.* Loss of morphine-induced analgesia, reward effect and withdrawal symptoms in mice lacking the mu-opioid-receptor gene. *Nature* 1996; **383**:819–823.

5 Sora I, Takahashi N, Funada M, Ujike H, Revay RS, Donovan DM, *et al.* Opiate receptor knockout mice define mu receptor roles in endogenous nociceptive responses and morphine-induced analgesia. *Proc Natl Acad Sci U S A* 1997; **94**:1544–1549.

6 Ikeda K, Ide S, Han W, Hayashida M, Uhl GR, Sora I. How individual sensitivity to opiates can be predicted by gene analyses. *Trends Pharmacol Sci* 2005; **26**: 311–317.

7 Waldhoer M, Bartlett SE, Whistler JL. Opioid receptors. *Ann Rev Biochem* 2004; **73**:953–990.

8 Pan YX, Xu J, Mahurter L, Bolan E, Xu M, Pasternak GW. Generation of the mu opioid receptor (MOR-1) protein by three new splice variants of the Oprm gene. *Proc Natl Acad Sci U S A* 2001; **98**:14084–14089.

9 Min BH, Augustin LB, Felsheim RF, Fuchs JA, Loh HH. Genomic structure analysis of promoter sequence of a mouse mu opioid receptor gene. *Proc Natl Acad Sci U S A* 1994; **91**:9081–9085.

10 Kaufman DL, Keith DE Jr, Anton B, Tian J, Magendzo K, Newman D, *et al.* Characterization of the murine mu opioid receptor gene. *J Biol Chem* 1995; **270**:15877–15883.

11 Ikeda K, Kobayashi T, Ichikawa T, Kumanishi T, Niki H, Yano R. The untranslated region of (mu)-opioid receptor mRNA contributes to reduced opioid sensitivity in CXBK mice. *J Neurosci* 2001; **21**:1334–1339.

12 Ko JL, Minnerath SR, Loh HH. Dual promoters of mouse mu-opioid receptor gene. *Biochem Biophys Res Commun* 1997; **234**:351–357.

13 Liang Y, Carr LG. Transcription of the mouse mu-opioid receptor gene is regulated by two promoters. *Brain Res* 1997; **769**:372–374.

14 Han W, Ide S, Sora I, Yamamoto H, Ikeda K. A possible genetic mechanism underlying individual and interstrain differences in opioid actions: focus on the mu opioid receptor gene. *Ann N Y Acad Sci* 2004; **1025**:370–375.

15 Moskowitz AS, Goodman RR. Autoradiographic analysis of mu1, mu2, and delta opioid binding in the central nervous system of C57BL/6BY and CXBK (opioid receptor-deficient) mice. *Brain Res* 1985; **360**:108–116.

16 Ikeda K, Ichikawa T, Kobayashi T, Kumanishi T, Oike S, Yano R. Unique behavioural phenotypes of recombinant-inbred CXBK mice: partial deficiency of sensitivity to mu- and kappa-agonists. *Neurosci Res* 1999; **34**:149–155.

17 D'Amour F, Smith D. A method for determinating loss of pain sensation. *J Pharmacol Exp Ther* 1941; **72**:74–79.

18 Woolfe G, MacDonald A. The evaluation of the analgesic action of pethidine hydrochloride. *J Pharmacol Exp Ther* 1944; **80**:300–307.

19 Chen F, MacDonald CC, Wilusz J. Cleavage site determinants in the mammalian polyadenylation signal. *Nucleic Acids Res* 1995; **23**: 2614–2620.

20 Liang Y, Mestek A, Yu L, Carr LG. Cloning and characterization of the promoter region of the mouse mu opioid receptor gene. *Brain Res* 1995; **679**:82–88.

21 Beelman CA, Parker R. Degradation of mRNA in eukaryotes. *Cell* 1995; **81**:179–183.

22 Caput D, Beutler B, Hartog K, Thayer R, Brown-Shimer S, Cerami A. Identification of a common nucleotide sequence in the 3′-untranslated region of mRNA molecules specifying inflammatory mediators. *Proc Natl Acad Sci U S A* 1986; **83**:1670–1674.

23 Zhang T, Kruys V, Huez G, Gueydan C. AU-rich element-mediated translational control: complexity and multiple activities of trans-activating factors. *Biochem Soc Trans* 2002; **30**:952–958.

24 Kuff EL, Lueders KK. The intracisternal A-particle gene family: structure and functional aspects. *Adv Cancer Res* 1988; **51**:183–276.

25 Kuff EL, Smith LA, Lueders KK. Intracisternal A-particle genes in Mus musculus: a conserved family of retrovirus-like elements. *Mol Cell Biol* 1981; **1**:216–227.

26 Christy RJ, Brown AR, Gourlie BB, Huang RC. Nucleotide sequences of murine intracisternal A-particle gene LTRs have extensive variability within the R region. *Nucleic Acids Res* 1985; **13**:289–302.

27 Ide S, Han W, Kasai S, Hata H, Sora I, Ikeda K. Characterization of the 3′ untranslated region of the human mu opioid receptor (MOR-1) mRNA. *Gene* 2005; **364**:139–145.

28 Weiss IM, Liebhaber SA. Erythroid cell-specific determinants of alpha-globin mRNA stability. *Mol Cell Biol* 1994; **14**:8123–8132.

29 Wang X, Kiledjian M, Weiss IM, Liebhaber SA. Detection and characterization of a 3′ untranslated region ribonucleoprotein complex associated with human alpha-globin mRNA stability. *Mol Cell Biol* 1995; **15**:1769–1777.

30 Zöllner C, Johnson PS, Bei Wang J, Roy AJ Jr, Layton KM, Min Wu J, *et al.* Control of mu opioid receptor expression by modification of cDNA 5′- and 3′-noncoding regions. *Brain Res Mol Brain Res* 2000; **79**: 159–162.

31 Lee PW, Wu S, Lee YM. Differential expression of μ-opioid receptor gene in CXBK and B6 mice by Sp1. *Mol Pharmacol* 2004; **66**:1580–1584.

32 Vaught JL, Mathiasen JR, Raffa RB. Examination of the involvement of supraspinal and spinal mu and delta opioid receptors in analgesia using the mu receptor deficient CXBK mice. *J Pharmacol Exp Ther* 1988; **245**: 13–16.

33 Ono M, Cole MD, White AT, Huang RC. Sequence organization of cloned intracisternal A particle genes. *Cell* 1980; **21**:465–473.

34 Stocking C, Loliger C, Kawai M, Suciu S, Gough N, Ostertag W. Identification of genes involved in growth autonomy of hematopoietic cells by analysis of factor-independent mutants. *Cell* 1988; **53**:869–879.

35 Mayo MW, Wang XY, Algate PA, Arana GF, Hoyle PE, Steelman LS, *et al.* Synergy between AUUUA motif disruption and enhancer insertion results in autocrine transformation of interleukin-3-dependent hematopoietic cells. *Blood* 1995; **86**:3139–3150.

36 Provost PR, Tremblay Y. Length increase of the human alpha-globin 3′-untranslated region disrupts stability of the pre-mRNA but not that of the mature mRNA. *J Biol Chem* 2000; **275**:30248–30255.

37 Baran A, Shuster L, Eleftheriou BE, Bailey DW. Opiate receptors in mice: genetic differences. *Life Sci* 1975; **17**:633–640.

38 Pick CG, Cheng J, Paul D, Pasternak GW. Genetic influences in opioid analgesic sensitivity in mice. *Brain Res* 1991; **566**:295–298.

39 Mogil JS, Wilson SG, Bon K, Lee SE, Chung K, Raber P, *et al.* Heritability of nociception I: responses of 11 inbred mouse strains on 12 measures of nociception. *Pain* 1999; **80**:67–82.

40 Mayer P, Hollt V. Allelic and somatic variations in the endogenous opioid system of humans. *Pharmacol Ther* 2001; **91**:167–177.

Increased body weight in mice lacking mu-opioid receptors

Wenhua Han[a], Harumi Hata[a,b], Hiroki Imbe[c], Qing-Rong Liu[e], Yukio Takamatsu[a], Miwako Koizumi[d], Niall P. Murphy[d], Emiko Senba[c], George R. Uhl[e], Ichiro Sora[a,b] and Kazutaka Ikeda[a]

[a]Division of Psychobiology, Tokyo Institute of Psychiatry, Tokyo, [b]Department of Psychobiology, Tohoku University Graduate School of Medicine, Sendai, [c]Department of Anatomy and Neurobiology, Wakayama Medical University, Wakayama, [d]Neural Circuit Mechanisms Research Group, RIKEN Brain Science Institute, Wako, Japan and [e]Molecular Neurobiology Branch, NIDA-IRP, NIH, Baltimore, Maryland, USA

Correspondence and requests for reprints to Kazutaka Ikeda, Molecular Psychiatry Research, Tokyo Institute of Psychiatry, 2-1-8 Kamikitazawa, Setagaya-ku, Tokyo 156-8585, Japan
Tel: +81 3 3304 5701 ext. 508; fax: +81 3 3329 8035; e-mail: ikedak@prit.go.jp

Sponsorship: This work was supported by a research grant from MEXT of Japan (17025054), by grants from MHLW of Japan (H17-pharmaco-001, H16-iyaku-029, H15-kou-3-03) and by the Intramural Research Program of the National Institutes of Health – National Institute on Drug Abuse Intramural Research Program.

Received 15 March 2006; accepted 17 March 2006

Opioids have been suggested to affect feeding behaviour. To clarify the role of μ-opioid receptors in feeding, we measured several parameters relating to food intake in μ-opioid receptor knockout mice. Here, we show that the knockout mice had increased body weight in adulthood, although the intake amount of standard food was similar between the wild-type and knockout littermates. Serum markers for energy homeostasis were not significantly altered in the knockout mice. Hypothalamic neuropeptide Y mRNA, however, was higher in knockouts than in wild-type mice. Our results suggest that the up-regulated expression of neuropeptide Y mRNA might contribute to the increased weights of adult μ-opioid receptor knockout mice. *NeuroReport* 17:941–944 © 2006 Lippincott Williams & Wilkins.

Keywords: body weight, food intake, knockout, μ-opioid receptor, neuropeptide Y

Introduction

Increased body weight arises from imbalances between energy consumption and energy expenditure. Previous studies have revealed that several genetic factors contribute to weight gain. For example, mice lacking the *ob* gene that encodes leptin display profound hyperphagia and obesity [1]. Interestingly, the hyperphagia and obesity found in the leptin knockouts can be attenuated by adding knockouts of the neuropeptide Y (NPY) gene [2], which has been implicated in feeding behaviour through a number of lines of evidence [3].

Opioids can also play roles in regulating feeding behaviour and body weight [4]. Opioid antagonists decrease food intake and body weight [5,6], whereas opioid agonists increase them [7,8]. Further, these actions appear to occur only by central administration, as peripheral injection of opioid antagonists fails to suppress food intake [9]. The opioid peptides, including β-endorphin, enkephalins, and dynorphins, and the opioid receptors, μ, δ, and κ, are thus candidates to play roles in feeding and weight regulation.

Mu-opioid receptors (MOPs) are widely distributed in the central nervous system, and participate in modulating pain [10,11], addiction [12], and emotional responses [13]. MOP knockout (KO) mice [14,15] are viable and lack obvious impairments that would invalidate studies of food intake and weight gains. We now report assessments of parameters relating to food intake in MOP KO mice and their wild-type littermates, and observations that body weight and hypothalamic NPY mRNA are both increased in these KO mice.

Materials and methods

Animals

MOP KO mice and their wild-type littermates were produced by heterozygote–heterozygote mating of MOP KO mice with C57BL/6J genetic background, as previously described [16,17]. The mice were housed five per cage in an environment maintained at 22±2°C, a relative humidity of 55±5%, and with a 12-h light/12-h dark cycle (lights on 08:00–20:00 h) for a year. The mice had free access to a standard laboratory diet (CA-1; CLEA Japan Inc., Tokyo, Japan) *ad libitum* and water unless otherwise mentioned. All the experiments were approved by the Institutional Animal Care and Use Committee of Tokyo Institute of Psychiatry.

Body weight and food intake measurement

Body weight was measured once a week for a year. The data were analysed by a two-way mixed design analysis of variance (ANOVA) followed by post-hoc comparisons with the Scheffé test. For food intake measurement, 10- to 12-

week-old mice were housed individually for 4 days before the start of the experiment. The consumption of standard laboratory diet *ad libitum* and water was then measured for 5 consecutive days. The data were analysed by a Student's *t*-test.

Serum chemistry and hormone measurements

Mice were anaesthetized by an intraperitoneal pentobarbital sodium injection (50 mg/kg). Blood samples were collected through a carotid artery. Serum chemistry and hormone measurements were carried out by Ani Lytics (Gaithersburg, Maryland, USA). Beta-endonorphin was measured by using the Beta-endonorphin Assay Kit (Bachem Peninsula Laboratories Inc., Belmont, California, USA). The data were analysed by a Student's *t*-test.

Glucose tolerance test

Mice were fasted for at least 8 h and then given glucose (2 g/kg) by an intraperitoneal injection. Blood glucose levels in blood samples taken from a tail vein were measured using glucose strips (Miles Laboratories, Elkhart, Indiana, USA). The data were analysed by a two-way mixed-design ANOVA.

In-situ hybridization

Mice were anaesthetized with diethyl ether vapour, and the entire brain of each animal was rapidly excised and frozen between 24:00 and 11:30 h. Cryostat sections, 6 μm in thickness, were prepared from the frozen whole brains. NPY mRNA was detected by using a ^{35}S-labelled oligonucleotide probe. The sequence of the oligonucleotide was as follows: 5′-ctctgctggcgcgtcctcgcccggattgtccggcttggaggggta-3′. Pre-hybridization and hybridization were conducted as previously described [18].

Results

We measured the body weights of male wild-type and MOP KO mice every week for 1 year (n=20 for wild-type mice; n=20 for MOP KO mice; Fig. 1). A significant interaction was observed between effects of genotype and week [$F(46,1584)=1.834$; $P=0.0006$; two-way mixed-design ANOVA]. Post-hoc comparisons revealed that the body weights of the MOP KO mice were significantly greater than those of their wild-type littermates after 16 weeks of age. A similar difference in body weight between wild-type and MOP KO mice was also observed in female mice (data not shown).

To examine whether the increased body weight in adult MOP KO mice was caused by altered feeding behaviours, we tested intake of standard food pellets and water over a 5-day period. We used 14-week-old male mice (n=13 for wild-type mice; n=14 for MOP KO mice). No significant differences in food and water intake were noted between the two groups [$t(12)=1.154$, $P=0.27$ for food intake and $t(12)=1.003$, $P=0.34$ for water intake; Student's *t*-test; data not shown].

We also examined the levels of serum hormones and metabolites that can be related to total body fat and energy homeostasis: leptin, insulin, triiodothyronine, thyroxine, insulin-like growth factor 1, corticosterone, triglycerides, cholesterol, total protein, albumin, glucose, and β-endonorphin (n=6 for wild-type mice; n=6 for MOP KO mice; Table 1). No significant differences in the concentrations of any of these serum hormones or metabolites were found in comparisons between wild-type and MOP KO mice ($P>0.05$; Student's *t*-test). We also measured blood glucose concentrations following glucose injections (n=10 for wild-type mice; n=10 for MOP KO mice; Fig. 2). No significant interactions were observed between the effects of genotype and time after the glucose injections [$F(5,108)=0.236$; $P=0.94$; two-way mixed-design ANOVA]. MOP KO mice

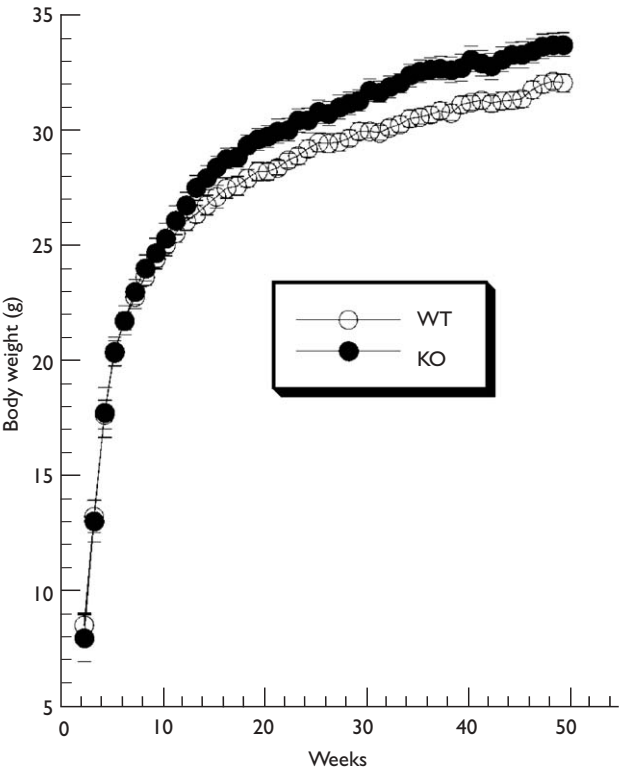

Fig. 1 One-year changes in body weight of μ-opioid receptor knockout (MOP KO) mice and their littermates. Growth curves for male wild-type (WT) mice and MOP KO (KO) mice (n=20 for wild-type mice and n=20 for MOP KO mice) are shown. The MOP KO mice displayed a significantly increased body weight compared with their littermates from postnatal week 16 to postnatal week 50. Data are means ± SEM.

Table 1 Serum hormone and metabolite levels in wild-type and MOP KO mice

	Wild-type mice	MOP KO mice
Leptin (ng/ml)	2.22 ± 0.55	3.74 ± 1.22
Insulin (ng/ml)	0.63 ± 0.07	0.63 ± 0.16
Triiodothyronine (T3) (ng/l)	813 ± 32.6	824 ± 82
Thyroxine (T4) (μg/l)	25.7 ± 2.6	25.5 ± 1.8
IGF-1 (ng/ml)	368.8 ± 5.7	359.5 ± 12.1
Corticosterone (mg/ml)	118.2 ± 16.8	135.7 ± 13.3
Triglycerides (ng/l)	868.3 ± 137	1141.7 ± 186
Cholesterol (mg/l)	655 ± 37.7	670 ± 48.1
Total protein (g/l)	45.2 ± 1.7	47.5 ± 0.6
Albumin (g/l)	31.3 ± 1.5	33.8 ± 0.4
Glucose (mg/l)	1825 ± 74	2043 ± 135
Beta-endorphin (pg/ml)	108.8 ± 24.3	114.3 ± 25.1

Blood was collected from 18- to 22-week-old mice (n=6). All values are means ± SEM. No significant difference was detected between wild-type and MOP KO mice ($P>0.05$). MOP, μ-opioid receptor; KO, knockout; IGF-1, insulin-like growth factor 1.

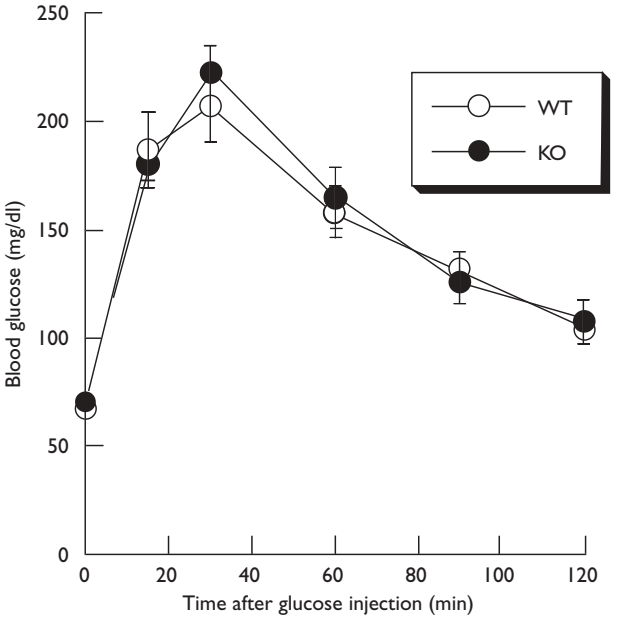

Fig. 2 Glucose tolerance test for wild-type (WT) and μ-opioid receptor knockout (MOP KO) (KO) mice (n=10 for wild-type mice and n=10 for MOP KO mice). No significant difference was detected between the genotypes. Data are means ± SEM.

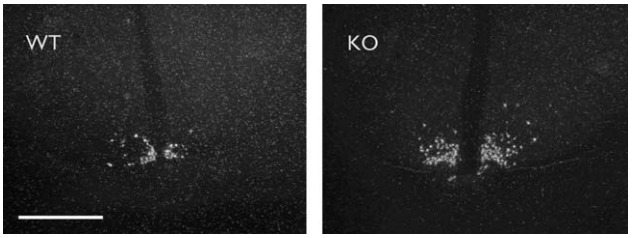

Fig. 3 Increased neuropeptide Y (NPY) mRNA expression in the hypothalamus of μ-opioid receptor knockout (MOP KO) mice. The level of NPY mRNA in the hypothalamus of wild-type (WT) and MOP KO (KO) mice was analysed by in-situ hybridization histochemistry. Scale bar=600 μm.

thus handled a glucose tolerance test as efficiently as the wild-type mice.

NPY, especially the NPY expressed in the hypothalamus, has been implicated in regulating food intake [3]. Thus, we examined the hypothalamic expression of NPY by in-situ hybridization histochemistry in KO mice (n=3) and wild-type mice (n=4). In the arcuate nucleus of the hypothalamus, a region known to play a role in the regulation of energy homeostasis [19], the expression of NPY mRNA was higher in MOP KO mice than in wild-type mice (Fig. 3). By using a DNA array, we found that the amount of NPY mRNA expressed in the whole brains of MOP KO mice was 2.2 times higher than that in the brains of wild-type animals.

Discussion

Pharmacological studies have suggested that MOP antagonists decrease appetite and body weight and that agonists increase them [5,7]. In the present study, we found that mice that lack the MOP gene display increased body weight compared with their wild-type littermates. The life-long disruption of MOP in these animals may thus engage compensatory mechanisms that could lead to the increased weight found in these animals. As we identified up-regulation of NPY mRNA in the arcuate nucleus of these KO mice and as several studies have implicated hypothalamic NPY in the regulation of food intake and body weight [20–23], we conclude that over-expression of NPY appears likely to represent one of the compensatory mechanisms that are likely to contribute to the increased weights of MOP KO mice.

Previously published data [24] suggest that an antagonist of MOP reduces NPY-induced feeding. This is in accordance with our data. In our study, although no significant difference was detected in daily food intake between the wild-type and MOP KO mice, we cannot exclude the possibility that feeding behaviours in MOP KO mice were changed and that such changes were related to the increased weight of the KO mice. During adulthood, the average body weights of MOP KO mice were higher than those of wild-type mice only by approximately 2 g (5%). The increased intake necessary to lead to this increased weight could well have been too small to be detected by our present approaches. Alternatively, a modest decline in the calories expended by these mice could also contribute to the observed results. While gross locomotor activity levels and the expression levels of other opioid receptors do not differ between wild-type and KO mice [25], it is again possible that more subtle differences in energy expenditures could have escaped detection by the methods used to characterize these KO animals in previous studies.

The present results suggest that long-term blockade of MOP may lead to over-expression of NPY and increased body weight. These observations open the possibility that chronic use of MOP antagonists might exacerbate obesity. Further long-term investigations on the antagonist effects of MOP on food intake are needed to evaluate better the risk of MOP antagonists as potential anti-obesity medications.

Conclusion

MOP KO mice displayed increased body weight and NPY mRNA expression in their adulthood compared with their wild-type littermates. The increased mRNA levels of NPY in the hypothalamus in MOP KO mice might have contributed to this increase in body weight.

Acknowledgements

We are grateful to Yurie Nakamoto for instruction on blood collection from mouse tails and Dr Keiko Matsuoka for animal care.

References

1. Zhang Y, Proenca R, Maffei M, Barone M, Leopold L, Friedman JM. Positional cloning of the mouse obese gene and its human homologue. *Nature* 1994; **372**:425–432.
2. Erickson JC, Hollopeter G, Palmiter RD. Attenuation of the obesity syndrome of ob/ob mice by the loss of neuropeptide Y. *Science* 1996; **274**:1704–1707.
3. Schwartz MW, Woods SC, Porte D Jr, Seeley RJ, Baskin DG. Central nervous system control of food intake. *Nature* 2000; **404**:661–671.
4. Glass MJ, Billington CJ, Levine AS. Opioids and food intake: distributed functional neural pathways? *Neuropeptides* 1999; **33**:360–368.

5. Levine AS, Grace M, Billington CJ, Zimmerman DM. Central administration of the opioid antagonist, LY255582, decreases short- and long-term food intake in rats. *Brain Res* 1991; **566**:193–197.
6. Cole JL, Leventhal L, Pasternak GW, Bowen WD, Bodnar RJ. Reductions in body weight following chronic central opioid receptor subtype antagonists during development of dietary obesity in rats. *Brain Res* 1995; **678**:168–176.
7. McCormack JF, Denbow DM. Ingestive responses to mu and delta opioid receptor agonists in the domestic fowl. *Br Poult Sci* 1989; **30**:327–340.
8. Grossman HC, Hadjimarkou MM, Silva RM, Giraudo SQ, Bodnar RJ. Interrelationships between mu opioid and melanocortin receptors in mediating food intake in rats. *Brain Res* 2003; **991**:240–244.
9. Marks-Kaufman R, Plager A, Kanarek RB. Central and peripheral contributions of endogenous opioid systems to nutrient selection in rats. *Psychopharmacology (Berlin)* 1985; **85**:414–418.
10. Porreca F, Burgess SE, Gardell LR, Vanderah TW, Malan TP Jr, Ossipov MH, *et al*. Inhibition of neuropathic pain by selective ablation of brainstem medullary cells expressing the mu-opioid receptor. *J Neurosci* 2001; **21**:5281–5288.
11. Sluka KA, Rohlwing JJ, Bussey RA, Eikenberry SA, Wilken JM. Chronic muscle pain induced by repeated acid injection is reversed by spinally administered mu- and delta-, but not kappa-, opioid receptor agonists. *J Pharmacol Exp Ther* 2002; **302**:1146–1150.
12. Contet C, Kieffer BL, Befort K. Mu opioid receptor: a gateway to drug addiction. *Curr Opin Neurobiol* 2004; **14**:370–378.
13. Moles A, Kieffer BL, D'Amato FR. Deficit in attachment behavior in mice lacking the mu-opioid receptor gene. *Science* 2004; **304**:1983–1986.
14. Matthes HW, Maldonado R, Simonin F, Valverde O, Slowe S, Kitchen I, *et al*. Loss of morphine-induced analgesia, reward effect and withdrawal symptoms in mice lacking the mu-opioid-receptor gene. *Nature* 1996; **383**:819–823.
15. Sora I, Takahashi N, Funada M, Ujike H, Revay RS, Donovan DM, *et al*. Opiate receptor knockout mice define mu receptor roles in endogenous nociceptive responses and morphine-induced analgesia. *Proc Natl Acad Sci USA* 1997; **94**:1544–1549.
16. Sora I, Elmer G, Funada M, Pieper J, Li XF, Hall FS, *et al*. Mu opiate receptor gene dose effects on different morphine actions: evidence for differential in vivo mu receptor reserve. *Neuropsychopharmacology* 2001; **25**:41–54.
17. Hall FS, Li XF, Goeb M, Roff R, Hoggatt H, Sora I, *et al*. Congenic C57BL/6 mu opiate receptor (MOR) knockout mice: baseline and opiate effects. *Genes Brain Behav* 2003; **2**:114–121.
18. Okamoto K, Imbe H, Morikawa Y, Itoh M, Sekimoto M, Nemoto K, *et al*. 5-HT2A receptor subtype in the peripheral branch of sensory fibers is involved in the potentiation of inflammatory pain in rats. *Pain* 2002; **99**:133–143.
19. Flier JS, Maratos-Flier E. Obesity and the hypothalamus: novel peptides for new pathways. *Cell* 1998; **92**:437–440.
20. Bugarith K, Dinh TT, Li AJ, Speth RC, Ritter S. Basomedial hypothalamic injections of neuropeptide Y conjugated to saporin selectively disrupt hypothalamic controls of food intake. *Endocrinology* 2005; **146**:1179–1191.
21. Kalra PS, Dube MG, Xu B, Kalra SP. Increased receptor sensitivity to neuropeptide Y in the hypothalamus may underlie transient hyperphagia and body weight gain. *Regul Pept* 1997; **72**:121–130.
22. Mashiko S, Ishihara A, Iwaasa H, Sano H, Oda Z, Ito J, *et al*. Characterization of neuropeptide Y (NPY) Y5 receptor-mediated obesity in mice: chronic intracerebroventricular infusion of D-Trp(34)NPY. *Endocrinology* 2003; **144**:1793–1801.
23. Ishihara A, Kanatani A, Okada M, Hidaka M, Tanaka T, Mashiko S, *et al*. Blockade of body weight gain and plasma corticosterone levels in Zucker fatty rats using an orally active neuropeptide Y Y1 antagonist. *Br J Pharmacol* 2002; **136**:341–346.
24. Dodo K, Izumi T, Ueda H, Bungo T. Response of neuropeptide Y-induced feeding to mu-, delta- and kappa-opioid receptor antagonists in the neonatal chick. *Neurosci Lett* 2005; **373**:85–88.
25. Sora I, Takahashi N, Funada M, Ujike H, Revay RS, Donovan DM, *et al*. Opiate receptor knockout mice define mu receptor roles in endogenous nociceptive responses and morphine-induced analgesia. *Proc Natl Acad Sci USA* 1997; **94**:1544–1549.

Available online at www.sciencedirect.com
ScienceDirect
Neuropharmacology 51 (2006) 651–658
NEURO PHARMACOLOGY
www.elsevier.com/locate/neuropharm

Mu opioid receptor-dependent and independent components in effects of tramadol

Soichiro Ide [a,b], Masabumi Minami [c], Kumatoshi Ishihara [b], George R. Uhl [d], Ichiro Sora [a,d,e], Kazutaka Ikeda [a,*]

[a] *Division of Psychobiology, Tokyo Institute of Psychiatry, 2-1-8 Kamikitazawa, Setagaya-ku, Tokyo 156-8585, Japan*
[b] *Laboratory of Neuropharmacology, Faculty of Pharmaceutical Sciences, Hiroshima International University, Kure 737-0112, Japan*
[c] *Department of Pharmacology, Graduate School of Pharmaceutical Sciences, Hokkaido University, Sapporo 060-0812, Japan*
[d] *Molecular Neurobiology, National Institute on Drug Abuse, Baltimore, MD 21224, USA*
[e] *Division of Psychobiology, Department of Neuroscience, Tohoku University Graduate School of Medicine, Sendai 980-8574, Japan*

Received 4 January 2006; received in revised form 20 April 2006; accepted 10 May 2006

Abstract

Tramadol is thought to induce analgesia via both opioid and non-opioid pathways, although the precise mechanisms remain to be elucidated. In this study, we investigated the roles of the μ-opioid receptor (MOP) in analgesic and rewarding effects of tramadol by using MOP knockout (KO) mice. Tramadol-induced antinociception, assessed by hot-plate and tail-flick tests, was significantly reduced in heterozygous and homozygous MOP-KO mice when compared with that in wild-type mice. Interestingly, however, tramadol retained its ability to induce significant antinociception in homozygous MOP-KO mice. The tramadol-induced antinociception remaining in homozygous MOP-KO mice was not significantly affected by methysergide, a serotonin receptor antagonist, but was partially blocked by yohimbine, an adrenaline α2 receptor antagonist, and both naloxone, a non-selective opioid receptor antagonist, and yohimbine. In addition, antinociceptive effects of an active tramadol metabolite M1 were abolished or remarkably reduced in MOP-KO mice. On the other hand, neither wild-type nor homozygous MOP-KO mice showed significant place preference for tramadol in a conditioned place preference test, although there were slight tendencies toward preference in wild-type mice and avoidance in homozygous MOP-KO mice. These results strongly support the idea suggested in the previous pharmacological studies that MOP and the adrenaline α2 receptor mediate most of the analgesic properties of tramadol.

Keywords: Opioid receptor; Knockout mice; Tramadol; Antinociception; Reward; Adrenaline

1. Introduction

Tramadol (1RS, 2RS)-2-[(dimethylamino)-methyl]-1-(3-methoxyphenyl)-cyclohexanol), a racemic mixture of 2 enantiomers, is one of the widely used weak opioid analgesics for step 2 pain management in WHO's pain ladder. (+)-Tramadol binds to μ-opioid receptors (MOPs) with low affinity and δ- or κ-opioid receptors with lower affinity (Hennies et al., 1988; Lee et al., 1993). Tramadol is mainly metabolized by *O*-demethylation (catalyzed by cytochrome P450 (CYP) 2D6 in human), and (+)-*O*-desmethyltramadol (M1) also binds to MOPs with relatively high affinity (Paar et al., 1997; Raffa et al., 1993). Furthermore, it has been also reported that (+)-tramadol inhibits neuronal reuptake of serotonin and (−)-tramadol inhibits neuronal reuptake of noradrenaline (Driessen and Reimann, 1992; Driessen et al., 1993; Raffa et al., 1992). Although the analgesic effects of tramadol are thought to result from the sum of these effects (Raffa et al., 1992), the detailed mechanisms have still not been completely clarified. Since both tramadol and its metabolites have analgesic properties, it is difficult to reveal the antinociceptive mechanisms of tramadol by conducting in vitro experiments only.

* Corresponding author. Tel.: +81 3 3304 5701; fax: +81 3 3329 8035.
E-mail address: ikedak@prit.go.jp (K. Ikeda).

0028-3908/$ - see front matter © 2006 Elsevier Ltd. All rights reserved.
doi:10.1016/j.neuropharm.2006.05.008

The rewarding effects of tramadol also remain to be elucidated. Some reports (Sprague et al., 2002; Yanagita, 1978) but not others (Miranda and Pinardi, 1998; Murano et al., 1978; Tzschentke et al., 2002) showed that tramadol has abuse potential. On the other hand, tramadol has also been shown to be a possible good agent for detoxification in cases of drug abuse (Tamaskar et al., 2003). Whether the drug has its own abuse potential or not is very important for its usage in the treatment of pain and drug abuse. Because the most selective ligands for a specific target possess little but significant affinity for others, the precise molecular mechanisms underlying the rewarding effects of tramadol have not been clearly delineated by traditional pharmacological studies.

Recent success in developing mice lacking the MOP gene has made it possible to reveal molecular mechanisms underlying opioid effects (Loh et al., 1998; Matthes et al., 1996; Sora et al., 1997b, 2001). Analgesic and rewarding effects of morphine are abolished in these knockout mice (Loh et al., 1998; Sora et al., 1997b, 2001). On the other hand, buprenorphine, a non-selective partial agonist of opioid receptors, has no analgesic effect but a significant rewarding effect in homozygous MOP knockout (KO) mice (Ide et al., 2004). These observations are especially interesting, as the distribution of δ- and κ-opioid receptors is nearly normal in MOP-KO mice (Loh et al., 1998; Matthes et al., 1996; Sora et al., 1997b). Thus, MOP-KO mice have afforded novel suggestions about the molecular mechanisms of opioid ligands.

We now report herein the results of investigations, using MOP-KO mice, on the molecular mechanisms underlying the antinociceptive and rewarding effects of tramadol. We found retention of thermal tramadol-mediated analgesia, which was partially sensitive to yohimbine, an adrenaline α2 receptor selective antagonist, but not sensitive to methysergide, a serotonin receptor antagonist, in homozygous MOP-KO mice. In addition, M1 antinociceptive effects were abolished or remarkably reduced in homozygous MOP-KO mice. On the other hand, neither wild-type nor homozygous MOP-KO mice showed significant rewarding effects of tramadol.

2. Methods

2.1. Animals

Wild-type, heterozygous, and homozygous MOP-KO mouse littermates from crosses of heterozygous/heterozygous MOP-KO mice on a C57BL/6J genetic background, as previously described (Sora et al., 2001), served as subjects. The experimental procedures and housing conditions were approved by the Institutional Animal Care and Use Committee, and all animals were cared for and treated humanely in accordance with our institutional animal experimentation guidelines. Naive adult (>10 weeks old) mice were housed in an animal facility maintained at 22 ± 2 °C and 55 ± 5% relative humidity under a 12 h/12 h light/dark cycle with lights on at 8:00 am and off at 8:00 pm. Food and water were available *ad libitum*.

2.2. Drugs

Tramadol hydrochloride and M1 hydrochloride were gifts from Nippon Shinyaku Co., Ltd (Kyoto, Japan). Naloxone hydrochloride, yohimbine hydrochloride and methysergide maleate were purchased from SIGMA Chemical Co. (St. Louis, MO).

2.3. Antinociceptive tests

Hot-plate testing was performed according to the method of Woolfe and MacDonald (1944) with slight modifications. A commercially available apparatus consisting of acrylic resin cage (20 × 25 × 25 cm: width × length × height) and a thermo-controlled aluminum plate (Model MK-350A, Muromachi Kikai Co., Tokyo, Japan) were used for this test. Mice were placed on a 52 ± 0.2 °C hot-plate, and latencies to paw licking were recorded with a cut-off time of 60 s. Tail-flick testing was carried out according to the method of D'Amour and Smith (1941) with slight modifications, by using a commercially available apparatus consisting of an irradiator for heat stimulation and a photosensor for detection of the tail-flick behavior (Model MK-330A, Muromachi Kikai Co., Tokyo, Japan). Mice were loosely wrapped in a felt towel, their tails were heated, and tail-flick latencies were automatically recorded with a cut-off time of 15 s. In the analyses of dose dependency, tramadol was administered in doses of 20, 20, 40 and 80 mg/kg, for cumulative doses of 20, 40, 80 and 160 mg/kg, respectively. Tail-flick and then hot-plate tests were conducted 20 min after each subcutaneous (s.c.) drug injection. Each injection was done just after the previous test. In the time course analyses, tail-flick and then hot-plate testing were conducted 0, 20, 40, 60 and 120 min after s.c. injection of tramadol, which was administered at a dose of 80 mg/kg, or after s.c. injection of M1, which was administered at a dose of 20 mg/kg. Naloxone (1.0 mg/kg s.c.), yohimbine (3.0 mg/kg s.c.) and methysergide (3.0 mg/kg s.c.) were administered 10 min before the injection of tramadol. The hot-plate and tail-flick responses of each mouse in the drug-induced antinociception were converted to percent of maximal possible effect (%MPE) according to the following formula:

$$\%\mathrm{MPE} = (\text{post drug latency} - \text{pre drug latency})/(\text{cut-off time} - \text{pre drug latency}) \times 100\%$$

2.4. Conditioned place preference (CPP) test

Conditioned place preference (CPP) testing was carried out according to the method of Hoffman and Beninger (1989) with some modifications. For this test we used a 2-compartment plexiglass chamber. One compartment (17.5 × 15 × 17.5 cm: width × length × height) was black with a smooth floor; and the other, of the same dimensions, was white with a textured floor. For pre- and post-conditioning test phases, a T-style division with double 6 × 6 cm openings allowed access to both compartments. During the conditioning phases the openings were eliminated to restrict mice to a single compartment. Locomotion and time spent in each compartment was recorded by using an animal activity-monitoring apparatus equipped with an infrared detector (Neuroscience Inc., Osaka, Japan). The compartment chamber was placed in a sound- and light-attenuated box under conditions of dim illumination (about 40 lux). Conditioned place preferences were assessed by a protocol consisting of 3 phases (preconditioning, conditioning, and test phases). On days 1 and 2, the mice were allowed to freely explore the 2 compartments through the openings for 900 s and become acclimated to the apparatus. On day 3 (preconditioning phase), the same trial was performed; and the time spent in each compartment was measured for 900 s. There was no significant difference between time spent in the black compartment with the smooth floor (489 ± 23 s, $n = 24$) and time spent in the white compartment with the textured floor (411 ± 23 s, $n = 24$), indicating that there was no preference before conditioning in the apparatus itself. We selected a counterbalancing protocol in order to nullify each mouse's initial preference, as previously discussed (Tzschentke, 1998). Biased mice that spent more than 80% of the time (i.e., 720 s) on one side on day 3 or more than 600 s on one side on day 2 and more than 600 s on the other side on day 3 were not used for further experiments. Conditioning was conducted once daily for 4 consecutive days (days 4–7). Mice were injected with either tramadol (80 mg/kg s.c.) or saline and immediately confined to the black or white compartment for 50 min on day

4. On day 5, the mice were injected with alternate saline or tramadol (80 mg/kg s.c.) and immediately confined to the opposite compartment for 50 min. On days 6 and 7, the same conditioning as on day 4 and day 5 was repeated. Assignment of the conditioned compartment was performed randomly and counterbalanced across subjects. During the test phase on day 8, the time spent in each compartment was measured for 900 s without drug injection. The CPP score was designated as the time spent in the drug-paired compartment on day 8 minus the time spent in the same compartment in the preconditioning phase on day 3. The scores were expressed as means ± the standard error of the mean (SEM).

2.5. Statistical analyses

In the analysis of differences among the genotypes, as there were no significant differences between male and female mice in the antinociceptive and reward effects of tramadol, we combined the data on males and females. The antinociceptive effects of tramadol were statistically evaluated by analysis of variance (ANOVA) followed by the Tukey–Kramer *post hoc* test. Time spent in the drug-paired compartment during pre- and post-conditioning phases of the CPP test were analyzed by within-group paired *t*-tests. Differences with $p < 0.05$ were considered significant.

3. Results

3.1. Antinociceptive effects

Dose-response relationships of tramadol antinociception were analyzed in wild-type, heterozygous, and homozygous MOP-KO mice. Tramadol induced significant increases in the %MPE in both hot-plate (Fig. 1A) and tail-flick (Fig. 1B) tests not only for wild-type [repeated measures ANOVA: $F(4,40) = 27.00, p < 0.0001$; $F(4,40) = 46.57, p < 0.0001$; respectively] and heterozygous MOP-KO mice [repeated measures ANOVA: $F(4,55) = 21.70, p < 0.0001$; $F(4,55) = 21.33, p < 0.0001$; respectively] but also for homozygous MOP-KO mice [repeated measures ANOVA: $F(4,60) = 20.10$, $p < 0.0001$; $F(4,60) = 27.01$, $p < 0.0001$; respectively]. However, antinociceptive effects of tramadol (%MPE) were significantly different among these genotypes of MOP-KO mice in both hot-plate and tail-flick tests [2-way mixed-design ANOVA: $F(2,31) = 18.79, p < 0.0001$; $F(2,31) = 43.06, p < 0.0001$; respectively]. Antinociceptive effects of tramadol (%MPE) in heterozygous and homozygous MOP-KO mice were significantly lower than those in wild-type mice in both hot-plate and tail-flick tests ($p < 0.05$, Tukey–Kramer *post hoc* test). We used 80 mg/kg s.c. tramadol for further analyses, because homozygous MOP-KO mice showed significant increment in the %MPE in both hot-plate and tail-flick tests at the dose ($p < 0.05$, Tukey–Kramer *post hoc* test).

Time course of tramadol antinociceptive effects were also analyzed in wild-type, heterozygous, and homozygous MOP-KO mice. A 3-way mixed-design ANOVA of antinociceptive effects (%MPE) and two within-subject factors (tramadol treatment and genotypes of mice) showed significant interactions in both hot-plate (Fig. 2A) and tail-flick (Fig. 2B) tests [$F(1,59) = 69.80$, $p < 0.0005$; $F(1,59) = 338.92$, $p < 0.0005$; respectively]. Tramadol (80 mg/kg s.c.) showed a significant increase in %MPE compared with saline injection in both hot-plate (Fig. 2A) and tail-flick (Fig. 2B) tests not only in wild-type [2-way mixed-design ANOVA: $F(1,18) = 34.23$, $p < 0.0001$; $F(1,18) = 400.29$, $p < 0.0001$; respectively] and heterozygous MOP-KO mice [2-way mixed-design ANOVA: $F(1,20) = 23.21$, $p < 0.0005$; $F(1,20) = 86.78$, $p < 0.0001$; respectively] but also in homozygous MOP-KO mice [2-way mixed-design ANOVA: $F(1,21) = 15.90$, $p < 0.001$; $F(1,21) = 21.83$, $p < 0.0005$; respectively]. The %MPE in all genotypes of mice showed significant increment by tramadol in hot-plate tests from 20 min to 60 min after the injection and in the tail-flick test from 20 to 120 min after the injection ($p < 0.05$; Tukey–Kramer *post hoc* test). However, antinociceptive effects of tramadol (%MPE) among the all genotypes of mice were significantly different in both hot-plate and tail-flick tests [2-way mixed-design ANOVA: $F(2,28) = 5.16$, $p < 0.05$; $F(2,28) = 36.73$, $p < 0.0001$; respectively], and further Tukey-Kramer *post hoc* test showed that the antinociceptive effects in heterozygous MOP-KO mice in the tail-flick test and homozygous MOP-KO mice in both hot-plate and tail-flick

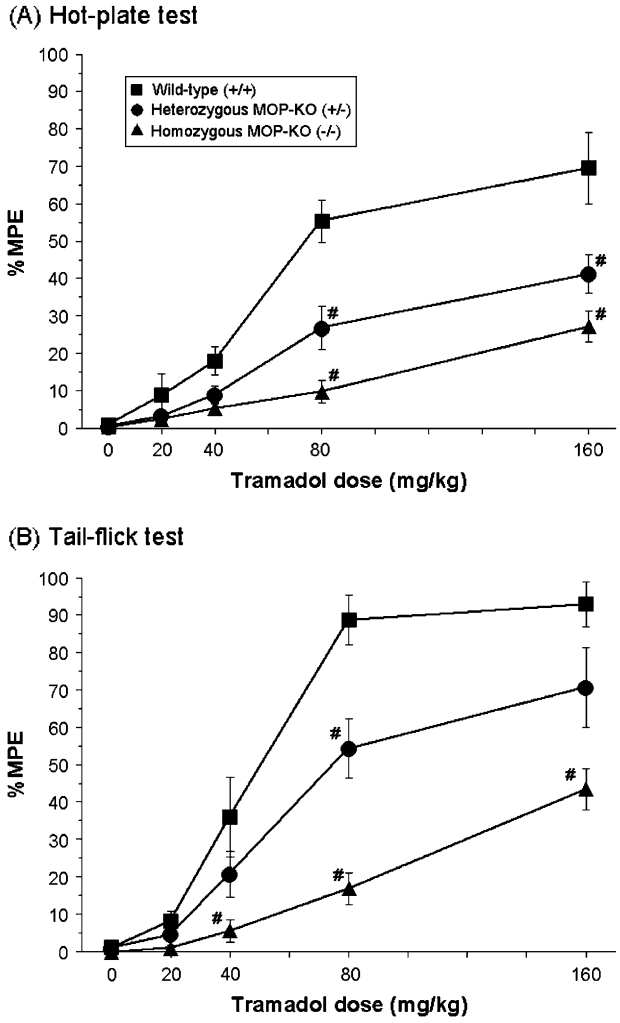

Fig. 1. Dose-dependent antinociceptive effects of tramadol in wild-type, heterozygous, and homozygous MOP-KO mice. Tramadol-induced alterations of %MPE in the hot-plate (A); and tail-flick (B) tests in wild-type (+/+, closed square, $n = 9$), heterozygous (+/−, closed circle, $n = 12$), and homozygous (−/−, closed triangle, $n = 13$) MOP-KO mice, under the cumulative dose-response paradigm. # indicates a significant difference ($p < 0.05$) from the corresponding value for wild-type mice. Data are presented as the mean ± S.E.M.

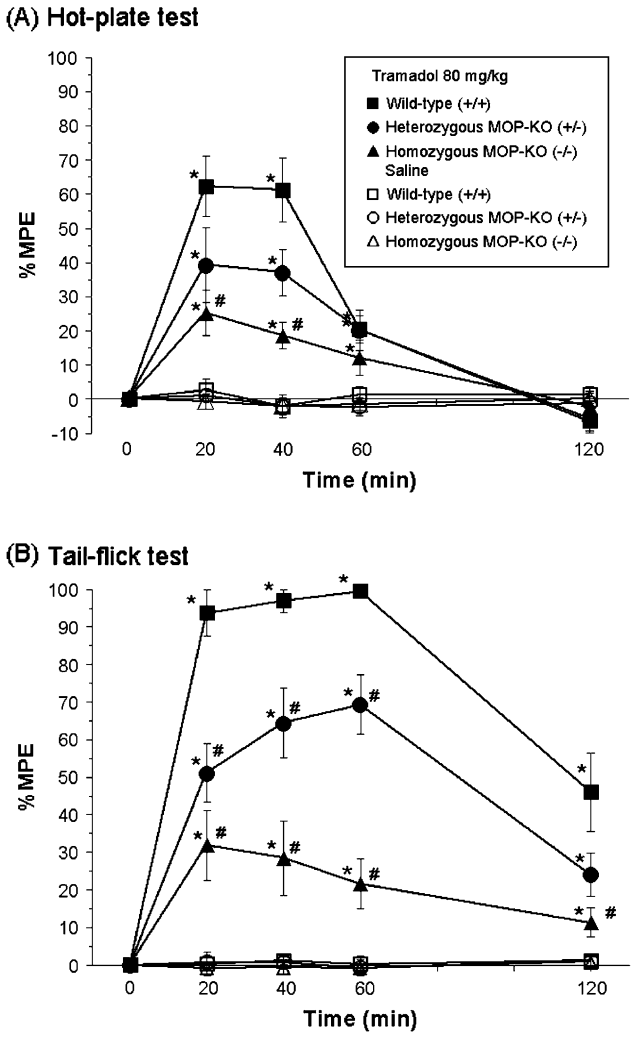

Fig. 2. Time course of tramadol induced antinociception in wild-type, heterozygous, and homozygous MOP-KO mice. Alterations of %MPE after tramadol (80 mg/kg s.c.) injection in the hot-plate (A); and tail-flick (B) tests in wild-type (+/+, closed square, $n = 11$), heterozygous (+/−, closed circle, $n = 10$), and homozygous (−/−, closed triangle, $n = 10$) MOP-KO mice. For the control, saline was treated in wild-type (+/+, open square, $n = 9$), heterozygous (+/−, open circle, $n = 12$), and homozygous (−/−, open triangle, $n = 13$) MOP-KO mice. # indicates a significant difference ($p < 0.05$) from the corresponding value for wild-type mice. * indicates a significant difference ($p < 0.05$) from the corresponding value for mice treated with saline. Data are presented as the mean ± S.E.M.

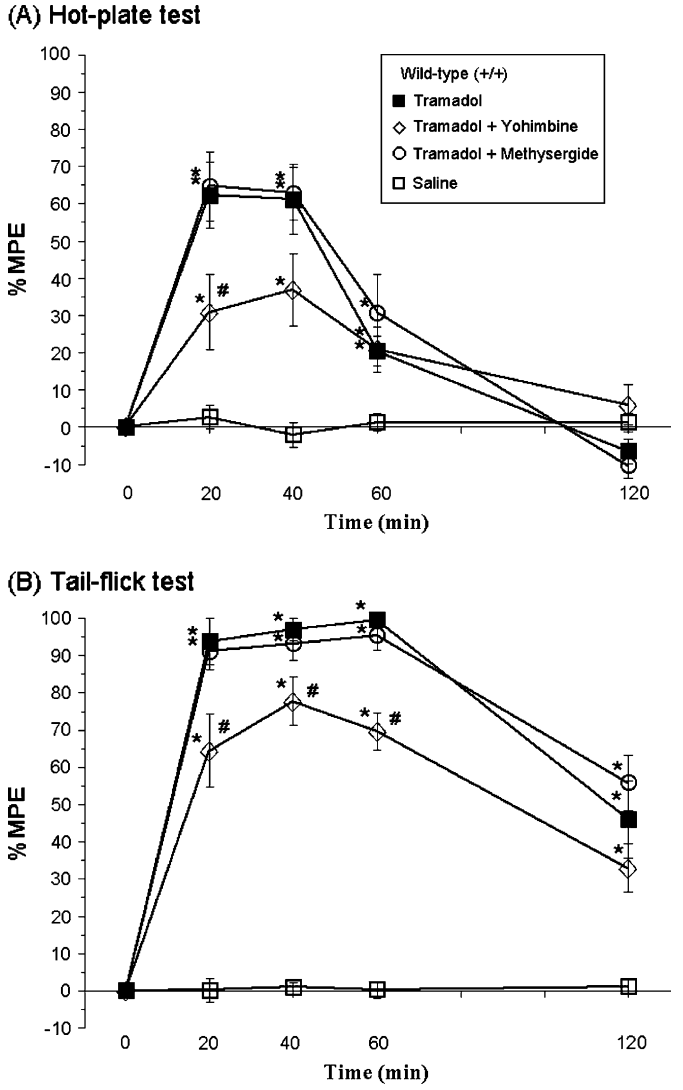

Fig. 3. Inhibitory effects of yohimbine and methysergide on tramadol-induced antinociceptive effects in wild-type mice. Time course of %MPE after saline injection (+/+, open square, $n = 9$), after tramadol (80 mg/kg s.c.) injection (closed square, $n = 11$), after tramadol injection with yohimbine (3 mg/kg s.c.) pretreatment (open diamond, $n = 11$) and after tramadol injection with methysergide (3 mg/kg s.c.) pretreatment (open circle, $n = 8$) in the hot-plate (A); and tail-flick (B) tests in wild-type mice. # indicates a significant difference ($p < 0.05$) from the corresponding value for tramadol alone injection. * indicates a significant difference ($p < 0.05$) from the corresponding value for saline injection. Data are presented as the mean ± S.E.M.

tests were significantly ($p < 0.05$) lower than those in wild-type mice.

Next, we tested the influence of yohimbine and methysergide on the antinociceptive effects of tramadol in wild-type mice. Mice were injected s.c. with 3.0 mg/kg of yohimbine or methysergide 10 min before the injection of tramadol and tested for their thermal nociceptive thresholds (Fig. 3). A 3-way mixed-design ANOVA of antinociceptive effects (%MPE) and two within-subject factors (tramadol treatment and yohimbine treatment) showed significant interactions in both hot-plate (Fig. 3A) and tail-flick (Fig. 3B) tests [$F(1,35) = 54.49$, $p < 0.0005$; $F(1,35) = 604.98$, $p < 0.0005$; respectively]. Although both tramadol alone and tramadol with yohimbine pretreatment induced significant %MPE increments compared with saline ($p < 0.05$; Tukey–Kramer *post hoc* test) [2-way repeated measures ANOVA: $F(2,28) = 14.45$, $p < 0.0001$; $F(2,28) = 142.66$, $p < 0.0001$; respectively], the yohimbine pretreatment significantly reduced the antinociceptive effects of tramadol in the tail-flick test ($p < 0.05$; Tukey–Kramer *post hoc* test). On the other hand, both tramadol alone and tramadol with methysergide pretreatment induced significant %MPE increments and there was no significant difference between them.

Further, we tested the influence of yohimbine, methysergide and naloxone (a non-selective opioid receptor antagonist) on the antinociceptive effects of tramadol in homozygous MOP-KO mice. Mice were injected s.c. with 3.0 mg/kg of

yohimbine, 3.0 mg/kg of methysergide, 1.0 mg/kg of naloxone, or a combination of yohimbine (3.0 mg/kg) and naloxone (1.0 mg/kg) 10 min before the injection of tramadol and tested for their thermal nociceptive thresholds (Fig. 4). A 5-way mixed-design ANOVA of antinociceptive effects (%MPE) and four within-subject factors (tramadol treatment, yohimbine treatment, methysergide treatment and naloxone treatment) showed significant interactions in both hot-plate (Fig. 4A) and tail-flick (Fig. 4B) tests [$F(1,70) = 9.84$, $p < 0.005$; $F(1,70) = 40.58$, $p < 0.0005$; respectively]. In the hot-plate test, tramadol alone but not tramadol with yohimbine pretreatment significantly increased the %MPE compared with saline in homozygous MOP-KO mice [2-way mixed-design ANOVA: $F(1,21) = 15.90$, $p < 0.001$; $F(1,23) = 2.34$, $p = 0.14$; respectively]. The pretreatment of yohimbine tended to decrease the %MPE of tramadol [2-way mixed-design ANOVA: $F(1,20) = 3.22$, $p = 0.09$]. Pretreatment with naloxone also showed tendency to reduce antinociceptive effects of tramadol, although tramadol significantly increased the %MPE even under the influence of naloxone when compared with saline in the hot-plate test [2-way mixed-design ANOVA: $F(1,23) = 18.11$, $p < 0.0005$]. Furthermore, pretreatment with both yohimbine and naloxone significantly decreased the %MPE of tramadol [2-way mixed-design ANOVA: $F(2,32) = 6.31$, $p < 0.005$], and no statistical difference was shown compared with saline treatment in the hot-plate test. In the tail-flick test, although tramadol with both yohimbine and naloxone pretreatment significantly increased the %MPE when compared with saline [2-way mixed-design ANOVA: $F(1,23) = 11.22$, $p < 0.005$; $F(1,23) = 24.34$, $p < 0.0001$, respectively], the pretreatment tended to reduce the %MPE when compared with tramadol alone. Furthermore, there was no significant difference between saline treatment and tramadol with both yohimbine and naloxone pretreatment. On the other hand, pretreatment with methysergide showed no influence on the %MPE of tramadol both in hot-plate and tail-flick tests.

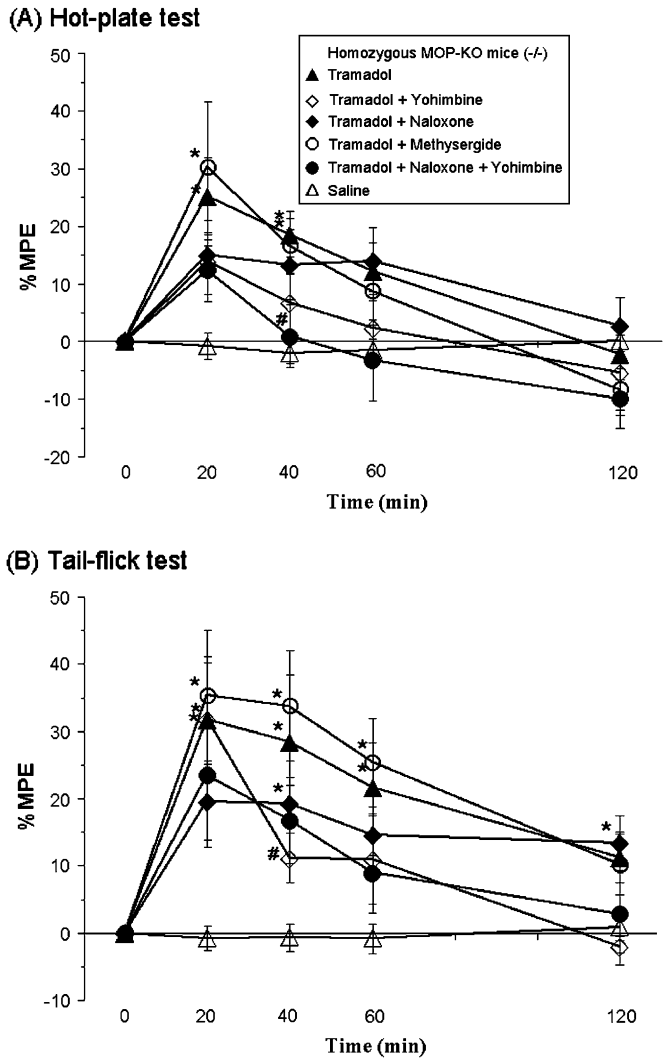

Fig. 4. Inhibitory effects of yohimbine, naloxone and methysergide on tramadol-induced antinociceptive effects in homozygous MOP-KO mice. Time course of %MPE after saline injection (open triangle, $n = 13$), after tramadol (80 mg/kg s.c.) injection (closed triangle, $n = 10$), after tramadol injection with yohimbine (3 mg/kg s.c.) pretreatment (closed diamond, $n = 12$), after tramadol injection with naloxone (1 mg/kg s.c.) pretreatment (open diamond, $n = 12$), after tramadol injection with methysergide (3 mg/kg s.c.) pretreatment (open circle, $n = 11$) and after tramadol injection with both yohimbine and naloxone pretreatment (closed circle, $n = 12$) in the hot-plate (A); and tail-flick (B) tests using homozygous MOP-KO mice. # indicates a significant difference ($p < 0.05$) from the corresponding value for tramadol alone injection in homozygous MOP-KO mice. * indicates a significant difference ($p < 0.05$) from the corresponding value for saline injection. Data are presented as the mean ± S.E.M.

We further tested the antinociceptive effects of M1, a main metabolite of tramadol, in wild-type and homozygous MOP-KO mice (Fig. 5). A 3-way mixed-design ANOVA of antinociceptive effects (%MPE) and two within-subject factors (M1 treatment and genotypes of mice) showed significant interactions in both hot-plate (Fig. 5A) and tail-flick (Fig. 5B) tests [$F(1,32) = 128.04$, $p < 0.0005$; $F(1,32) = 431.35$, $p < 0.0005$; respectively]. M1 (20 mg/kg s.c.) showed a significant increase in %MPE compared with saline injection in both hot-plate (Fig. 5A) and tail-flick (Fig. 5B) tests in wild-type [2-way mixed-design ANOVA: $F(1,14) = 134.75$, $p < 0.0001$; $F(1,14) = 507.80$, $p < 0.0001$; respectively]. On the other hand, M1 showed a significant increase in %MPE compared with saline injection only in the tail-flick test in homozygous MOP-KO mice [2-way mixed-design ANOVA: $F(1,18) = 14.26$, $p < 0.005$]. Antinociceptive effects of M1 between genotypes of mice were significantly different in both hot-plate and tail-flick tests [2-way mixed-design ANOVA: $F(1,12) = 106.82$, $p < 0.0001$; $F(1,12) = 255.69$, $p < 0.0001$; respectively], and further Tukey–Kramer *post hoc* test showed that the antinociceptive effects in homozygous MOP-KO mice in both hot-plate and tail-flick tests were significantly ($p < 0.05$) lower than those in wild-type mice.

3.2. Rewarding effects

Preferences for the places paired with 80 mg/kg tramadol s.c. were analyzed for wild-type and homozygous MOP-KO mice. Tramadol did not induce a significant increase in the time spent on the drug-paired side in either wild-type mice

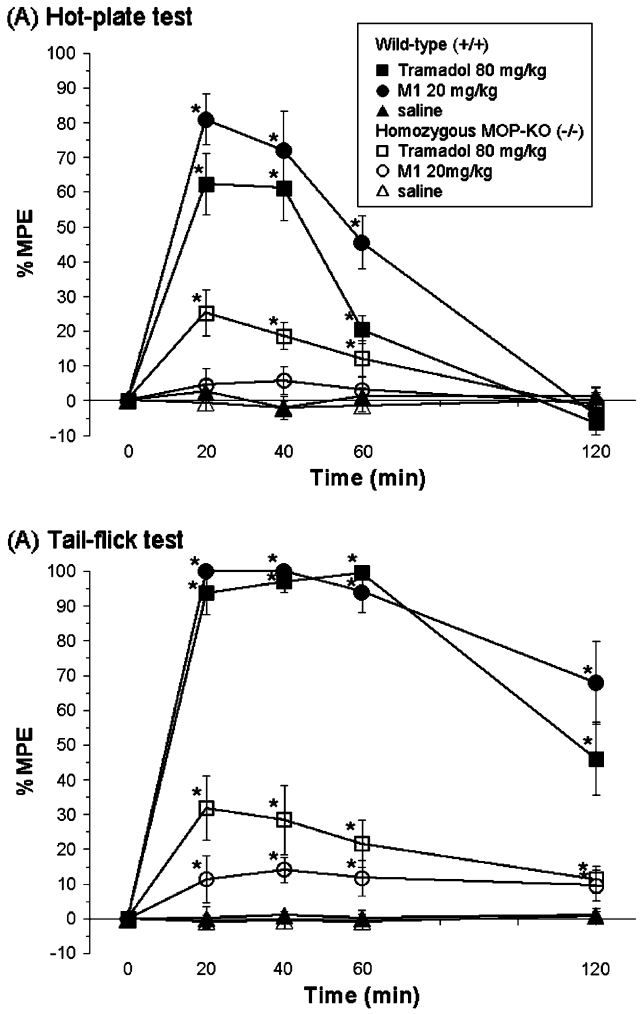

Fig. 5. Time course of tramadol and M1 metabolite induced antinociception in wild-type and homozygous MOP-KO mice. Alterations of %MPE after tramadol (80 mg/kg s.c.) injection and after M1 (20 mg/kg s.c.) injection in the hot-plate (A); and tail-flick (B) tests in wild-type (tramadol, closed square, $n = 11$; M1, closed circle, $n = 7$) and homozygous (tramadol, open square, $n = 10$; M1, open circle, $n = 7$) MOP-KO mice. For the control, saline was treated in wild-type (+/+, closed triangle, $n = 9$) and homozygous (−/−, open triangle, $n = 13$) MOP-KO mice. * indicates a significant difference ($p < 0.05$) from the corresponding value for mice treated with saline. Data are presented as the mean ± S.E.M.

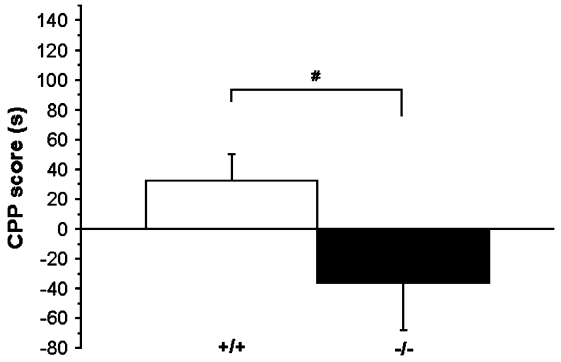

Fig. 6. Rewarding effects of tramadol in wild-type and homozygous MOP-KO mice. The CPP scores of wild-type (+/+, white column, $n = 12$) and homozygous (−/−, black column, $n = 12$) MOP-KO mice. # indicates a significant difference ($p < 0.05$) from the corresponding value for wild-type mice. Data are presented as the mean ± S.E.M.

or homozygous MOP-KO mice (CPP score = 32 ± 18 and −36 ± 26, respectively; Fig. 6). However, the paired *t*-test revealed a significant difference between these genotype groups. The CPP score for the tramadol-treated wild-type mice was significantly higher than that for the similarly treated homozygous MOP-KO ones ($p < 0.05$).

4. Discussion

The antinociceptive effects of tramadol were significantly reduced in heterozygous and homozygous MOP-KO mice compared with wild-type mice in both hot-plate and tail-flick tests. The decrease in the tramadol effect in either test was dependent on the copy number of the MOP gene. In addition, the antinociceptive effects of tramadol in homozygous MOP-KO mice still remained under the influence of naloxone, a non-selective opioid receptor antagonist. These results suggest that the MOP is the main opioid receptor involved in the tramadol-induced antinociceptive effects. This is consistent with previous reports. The antinociceptive effects of morphine, a MOP agonist with low affinity for δ- and κ-opioid receptors, are reduced in each of several strains of heterozygous MOP-KO mice and completely diminished in homozygous MOP-KO mice (Loh et al., 1998; Sora et al., 1997b, 2001). Also, the antinociceptive effects of DPDPE, a δ-opioid receptor-preferring ligand with modest affinity for the MOP, are reduced in MOP-KO mice (Matthes et al., 1998; Sora et al., 1997a). CXBK mice, which express MOPs at approximately half of the level of the progenitor strains C57BL/6 and BALB/c, show reduced analgesic effects of not only morphine but also of U50488H, a κ-selective agonist (Ikeda et al., 1999). Furthermore, antinociception by buprenorphine, a non-selective partial agonists for opioid receptors, is abolished in MOP-KO mice, although the rewarding effects of the drug remain (Ide et al., 2004). On the other hand, the antinociceptive effects of morphine are not altered in either mice lacking δ-opioid receptors (Zhu et al., 1999) or mice lacking κ-opioid receptors (Simonin et al., 1998). The present results together with these previous reports just cited suggest that MOPs among opioid receptors play a critical role in the thermal analgesia mediated by opioid receptors. MOP tolerance and inactivation and/or individual differences in MOP number are thus likely of importance in most of the variation in the degree of thermal analgesia induced by opioids.

In contrast to other opioids, tramadol showed antinociceptive effects in homozygous MOP-KO mice, and the effects still remained under the influence of naloxone. These results confirm the idea suggested in the previous pharmacological studies that tramadol is a unique opioid having both opioid and non-opioid properties. The present findings that the remaining effects of tramadol in MOP-KO mice were significantly reduced by pretreatment with yohimbine, an adrenaline α2 receptor antagonist, and that yohimbine also reduced the

antinociceptive effects of tramadol in wild-type mice, as previously reported (Desmeules et al., 1996; Driessen et al., 1993; Kayser et al., 1992), strongly suggest that tramadol induces analgesia via the noradrenaline nervous system, especially via adrenaline α2 receptors. One of possible mechanisms of tramadol antinociception via adrenaline α2 receptor may be an activation of the descending analgesic system that includes a noradrenergic pathway originating in the locus coeruleus and inhibits nociceptive responses at the level of the spinal cord. Furthermore, small antinociceptive effects of tramadol in the presence of both yohimbine and naloxone in MOP-KO mice suggest that thermal antinociceptive effects of tramadol are mainly caused by opioid receptors and adrenaline α2 receptors. On the other hand, although a serotonergic pathway is also included in the descending analgesic system, and tramadol inhibits neuronal reuptake of serotonin (Oliva et al., 2002; Rojas-Corrales et al., 2000), present results suggest that serotonin receptors are not significantly involved in tramadol-induced thermal antinociceptive effects. The inconsistency with other previous reports that the antinociceptive effects of tramadol is mediated by the serotonergic component (Oliva et al., 2002; Raffa et al., 1992) may be caused by differences in injection route, pain stimulus and/or mouse strains. Further analyses about serotonergic components in antinociceptive effects of tramadol will be required.

M1 treatment showed significant antinociceptive effects in wild-type mice in both hot-plate and tail-flick tests, but showed no and weak effects in homozygous MOP-KO mice in hot-plate test and tail-flick test, respectively. It has been reported that M1 is an only active metabolite among metabolites of tramadol, and (+)-M1 has high affinity for MOPs (Raffa et al., 1993). Presents results confirmed the idea that the antinociceptive effects of M1 is mainly caused by its MOP activations. On the other hand, the weak but significant remaining antinociceptive effects of M1 in homozygous MOP-KO mice shown in the tail-flick test also provide the evidence for existence of MOP-independent components in the mechanisms of M1 antinociceptive effects. Previous report showed that M1 also act as neuronal reuptake inhibitor of noradrenaline (Garrido et al., 2000), and that effects may cause the remaining antinociceptive effects of M1 in homozygous MOP-KO mice.

In the present study, tramadol (80 mg/kg) which produced significant antinociception even in the MOP-KO mice showed a slight tendency toward causing preference but no significant rewarding effects in wild-type mice in the CPP test. This result stands in sharp contrast to the significant rewarding effects found for other MOP agonists, such as morphine and buprenorphine, in the same paradigm of CPP test (Ide et al., 2004; Sora et al., 2001). Since the development of psychological dependence is one of the unwanted side effects of most opioid analgesics, tramadol may be a useful analgesic with low abuse potential. The results of the previous studies mentioned above (Miranda and Pinardi, 1998; Murano et al., 1978; Tzschentke et al., 2002) support this idea. On the other hand, tramadol showed slight tendency to cause aversion in homozygous MOP-KO mice, suggesting that the tramadol targets other than MOP are involved in this slight aversion. Since the CPP score for homozygous MOP-KO mice was significantly lower than that for wild-type mice, MOP activation by tramadol would be significantly involved in the tendency toward preference to tramadol but would fail to show significant preference because of the simultaneous slight aversion occurring via other pathways. Several reports have shown that not only opioid-responsive nerves but also adrenergic and serotonergic nerves are involved in the mechanisms of rewards. For example, the noradrenaline reuptake inhibitor desipramine produces conditioned place aversion (CPA) (Papp, 1989). Likewise, serotonin reuptake inhibitors, including citalopram, imipramine and amitryptiline (Papp, 1989), and the serotonin-releasing drug 5-methoxy-6-methyl-2-aminoindan (MMAI) (Marona-Lewicka et al., 1996) also produce CPA. The present results together with these previous findings suggest that MOPs mediate preference to tramadol, that other tramadol targets, probably norepinephrine and serotonin transporters, mediate aversion to tramadol, and that the combined activation of all tramadol targets leads to the loss of preference or aversion to tramadol.

Some reports have described opposing observations that tramadol possesses abuse potential (Sprague et al., 2002; Yanagita, 1978). As mentioned above, the CPP procedure without a counterbalancing protocol does not engender sufficient confidence, because it cannot nullify each mouse's initial preference, as previously discussed (Tzschentke, 1998). In our present study using the counterbalancing protocol for the CPP test, tramadol did not show significant rewarding effects, although it showed a slight tendency toward preference in wild-type mice. The discrepancy might be due to the differences in the experimental protocol. The present results together with all reports on tramadol rewards suggest that tramadol has little or low abuse potential when compared to other MOP agonists.

In conclusion, we demonstrated that the thermal antinociceptive effects of tramadol are mainly mediated by MOPs and adrenaline α2 receptors, but not significantly by serotonergic components. The present results also suggest that tramadol does not have rewarding or aversive effects, because MOP activation mediates rewarding effects while other tramadol targets simultaneously mediate aversive effects. Thus, the present results confirmed that tramadol is an opioid ligand that characteristically acts on not only opioid receptors but also other targets, and tramadol does not have rewarding effects in spite of its MOP-activating ability. Tramadol may be a unique useful analgesic with a low risk of substance dependence.

Acknowledgements

This study was supported by research grants from the Japanese Ministry of Health, Labour and Welfare (MHLW: H16-Iyaku-029, H17-pharmaco-001); the Japanese Ministry of Education, Culture, Sports, Science, and Technology (17025054); and the NIDA-IRP, NIH, DHSS. We thank

Yoko Hagino, Yukio Takamatsu, and Keiko Matsuoka for technical support and animal care.

References

D'Amour, F., Smith, D., 1941. A method for determining loss of pain sensation. J. Pharmacol. Exp. Ther. 72, 74–79.

Desmeules, J.A., Piguet, V., Collart, L., Dayer, P., 1996. Contribution of monoaminergic modulation to the analgesic effect of tramadol. Br. J. Clin. Pharmacol. 41, 7–12.

Driessen, B., Reimann, W., 1992. Interaction of the central analgesic, tramadol, with the uptake and release of 5-hydroxytryptamine in the rat brain in vitro. Br. J. Pharmacol. 105, 147–151.

Driessen, B., Reimann, W., Giertz, H., 1993. Effects of the central analgesic tramadol on the uptake and release of noradrenaline and dopamine in vitro. Br. J. Pharmacol. 108, 806–811.

Garrido, M.J., Valle, M., Campanero, M.A., Calvo, R., Troconiz, I.F., 2000. Modeling of the in vivo antinociceptive interaction between an opioid agonist, (+)-*O*-desmethyltramadol, and a monoamine reuptake inhibitor, (−)-*O*-desmethyltramadol, in rats. J. Pharmacol. Exp. Ther. 295, 352–359.

Hennies, H.H., Friderichs, E., Schneider, J., 1988. Receptor binding, analgesic and antitussive potency of tramadol and other selected opioids. Arzneimittelforschung 38, 877–880.

Hoffman, D.C., Beninger, R.J., 1989. Preferential stimulation of D1 or D2 receptors disrupts food-rewarded operant responding in rats. Pharmacol. Biochem. Behav. 34, 923–925.

Ide, S., Minami, M., Satoh, M., Uhl, G.R., Sora, I., Ikeda, K., 2004. Buprenorphine antinociception is abolished, but naloxone-sensitive reward is retained, in micro-opioid receptor knockout mice. Neuropsychopharmacology 29, 1656–1663.

Ikeda, K., Ichikawa, T., Kobayashi, T., Kumanishi, T., Oike, S., Yano, R., 1999. Unique behavioural phenotypes of recombinant-inbred CXBK mice: partial deficiency of sensitivity to mu- and kappa-agonists. Neurosci. Res. 34, 149–155.

Kayser, V., Besson, J.M., Guilbaud, G., 1992. Evidence for a noradrenergic component in the antinociceptive effect of the analgesic agent tramadol in an animal model of clinical pain, the arthritic rat. Eur. J. Pharmacol. 224, 83–88.

Lee, C.R., McTavish, D., Sorkin, E.M., 1993. Tramadol. A preliminary review of its pharmacodynamic and pharmacokinetic properties, and therapeutic potential in acute and chronic pain states. Drugs 46, 313–340.

Loh, H.H., Liu, H.C., Cavalli, A., Yang, W., Chen, Y.F., Wei, L.N., 1998. mu Opioid receptor knockout in mice: effects on ligand-induced analgesia and morphine lethality. Brain Res. Mol. Brain Res. 54, 321–326.

Marona-Lewicka, D., Rhee, G.S., Sprague, J.E., Nichols, D.E., 1996. Reinforcing effects of certain serotonin-releasing amphetamine derivatives. Pharmacol. Biochem. Behav. 53, 99–105.

Matthes, H.W., Maldonado, R., Simonin, F., Valverde, O., Slowe, S., Kitchen, I., Befort, K., Dierich, A., Le Meur, M., Dolle, P., Tzavara, E., Hanoune, J., Roques, B.P., Kieffer, B.L., 1996. Loss of morphine-induced analgesia, reward effect and withdrawal symptoms in mice lacking the mu-opioid-receptor gene. Nature 383, 819–823.

Matthes, H.W., Smadja, C., Valverde, O., Vonesch, J.L., Foutz, A.S., Boudinot, E., Denavit-Saubie, M., Severini, C., Negri, L., Roques, B.P., Maldonado, R., Kieffer, B.L., 1998. Activity of the delta-opioid receptor is partially reduced, whereas activity of the kappa-receptor is maintained in mice lacking the mu-receptor. J. Neurosci. 18, 7285–7295.

Miranda, H.F., Pinardi, G., 1998. Antinociception, tolerance, and physical dependence comparison between morphine and tramadol. Pharmacol. Biochem. Behav. 61, 357–360.

Murano, T., Yamamoto, H., Endo, N., Kudo, Y., Okada, N., Masuda, Y., Yano, I., 1978. Studies on dependence on tramadol in rats. Arzneimittelforschung 28, 152–158.

Oliva, P., Aurilio, C., Massimo, F., Grella, A., Maione, S., Grella, E., Scafuro, M., Rossi, F., Berrino, L., 2002. The antinociceptive effect of tramadol in the formalin test is mediated by the serotonergic component. Eur. J. Pharmacol. 445, 179–185.

Paar, W.D., Poche, S., Gerloff, J., Dengler, H.J., 1997. Polymorphic CYP2D6 mediates *O*-demethylation of the opioid analgesic tramadol. Eur. J. Clin. Pharmacol. 53, 235–239.

Papp, M., 1989. Differential effects of short-and long-term antidepressant treatments on the food-induced place preference conditioning in rats. Behav. Pharmacol. 1, 69–74.

Raffa, R.B., Friderichs, E., Reimann, W., Shank, R.P., Codd, E.E., Vaught, J.L., 1992. Opioid and non-opioid components independently contribute to the mechanism of action of tramadol, an 'atypical' opioid analgesic. J. Pharmacol. Exp. Ther. 260, 275–285.

Raffa, R.B., Friderichs, E., Reimann, W., Shank, R.P., Codd, E.E., Vaught, J.L., Jacoby, H.I., Selve, N., 1993. Complementary and synergistic antinociceptive interaction between the enantiomers of tramadol. J. Pharmacol. Exp. Ther. 267, 331–340.

Rojas-Corrales, M.O., Ortega-Alvaro, A., Gibert-Rahola, J., Roca-Vinardell, A., Mico, J.A., 2000. Pindolol, a beta-adrenoceptor blocker/5-hydroxytryptamine(1A/1B) antagonist, enhances the analgesic effect of tramadol. Pain 88, 119–124.

Simonin, F., Valverde, O., Smadja, C., Slowe, S., Kitchen, I., Dierich, A., Le Meur, M., Roques, B.P., Maldonado, R., Kieffer, B.L., 1998. Disruption of the kappa-opioid receptor gene in mice enhances sensitivity to chemical visceral pain, impairs pharmacological actions of the selective kappa-agonist U-50,488H and attenuates morphine withdrawal. Embo J. 17, 886–897.

Sora, I., Funada, M., Uhl, G.R., 1997a. The mu-opioid receptor is necessary for [D-Pen2,D-Pen5]enkephalin-induced analgesia. Eur. J. Pharmacol. 324, R1–R2.

Sora, I., Takahashi, N., Funada, M., Ujike, H., Revay, R.S., Donovan, D.M., Miner, L.L., Uhl, G.R., 1997b. Opiate receptor knockout mice define mu receptor roles in endogenous nociceptive responses and morphine-induced analgesia. Proc. Natl. Acad. Sci. U.S.A. 94, 1544–1549.

Sora, I., Elmer, G., Funada, M., Pieper, J., Li, X.F., Hall, F.S., Uhl, G.R., 2001. Mu opiate receptor gene dose effects on different morphine actions: evidence for differential in vivo mu receptor reserve. Neuropsychopharmacology 25, 41–54.

Sprague, J.E., Leifheit, M., Selken, J., Milks, M.M., Kinder, D.H., Nichols, D.E., 2002. In vivo microdialysis and conditioned place preference studies in rats are consistent with abuse potential of tramadol. Synapse 43, 118–121.

Tamaskar, R., Parran Jr., T.V., Heggi, A., Brateanu, A., Rabb, M., Yu, J., 2003. Tramadol versus buprenorphine for the treatment of opiate withdrawal: a retrospective cohort control study. J. Addict. Dis. 22, 5–12.

Tzschentke, T.M., 1998. Measuring reward with the conditioned place preference paradigm: a comprehensive review of drug effects, recent progress and new issues. Prog. Neurobiol. 56, 613–672.

Tzschentke, T.M., Bruckmann, W., Friderichs, E., 2002. Lack of sensitization during place conditioning in rats is consistent with the low abuse potential of tramadol. Neurosci. Lett. 329, 25–28.

Woolfe, G., MacDonald, A., 1944. The evaluation of the analgesic action of pethidine hydrochloride (demerol). J. Pharmacol. Exp. Ther. 80, 300–307.

Yanagita, T., 1978. Drug dependence potential of 1-(m-methoxyphenyl)-2-dimethylaminomethyl)-cyclohexan-1-ol hydrochloride (tramadol) tested in monkeys. Arzneimittelforschung 28, 158–163.

Zhu, Y., King, M.A., Schuller, A.G., Nitsche, J.F., Reidl, M., Elde, R.P., Unterwald, E., Pasternak, G.W., Pintar, J.E., 1999. Retention of supraspinal delta-like analgesia and loss of morphine tolerance in delta opioid receptor knockout mice. Neuron 24, 243–252.

Neuropsychopharmacology (2006) 31, 2132–2139

www.neuropsychopharmacology.org

Norepinephrine Transporter Blockade can Normalize the Prepulse Inhibition Deficits Found in Dopamine Transporter Knockout Mice

Motoyasu Yamashita[1], Setsu Fukushima[1], Hao-wei Shen[2], F Scott Hall[3], George R Uhl[3], Yohtaro Numachi[1], Hideaki Kobayashi[1] and Ichiro Sora*[1,2,3]

[1]Department of Psychobiology, Tohoku University Graduate School of Medicine, Sendai, Miyagi, Japan; [2]Department of Molecular Psychiatry, Tokyo Institute of Psychiatry, Tokyo, Japan; [3]Molecular Neurobiology Branch, Intramural Research Program, National Institute on Drug Abuse, NIH/DHHS, Baltimore, MD, USA

Dopamine transporter knockout (DAT KO) mice display deficits in sensorimotor gating that are manifested by reduced prepulse inhibition (PPI) of the acoustic startle reflex. Since PPI deficits may model some of the cognitive dysfunctions identified in certain neuropsychiatric patients, we have studied the effects of transporter blockers on PPI in wild-type and DAT KO mice. Treatments with High dose psychostimulants that block DAT as well as the norepinephrine (NET) and serotonin (SERT) transporters (60 mg/kg cocaine or methylphenidate) significantly impaired PPI in wild-type mice. By contrast, these treatments significantly ameliorated the PPI deficits observed in untreated DAT KO mice. In studies with more selective transport inhibitors, the selective NET inhibitor nisoxetine (10 or 30 mg/kg) also significantly reversed PPI deficits in DAT KO mice. By contrast, while the SERT inhibitor fluoxetine (30 mg/kg) normalized these PPI deficits in DAT KO mice, citalopram (30 or 100 mg/kg) failed to do so. The 'paradoxical' effects of cocaine and methylphenidate in DAT KO mice are thus likely to be mediated, at least in part by the ability of these drugs to block NET, although serotonin systems may also have some role. Together with recent microdialysis data, these results support the hypothesis that prefrontal cortical NET blockade and consequent enhancement of prefrontal cortical extracellular dopamine mediates the reversal of PPI deficits in DAT KO mice.

Neuropsychopharmacology (2006) **31,** 2132–2139. doi:10.1038/sj.npp.1301009; published online 11 January 2006

Keywords: dopamine transporter; norepinephrine transporter; serotonin transporter; knockout mice; prepulse inhibition; startle

INTRODUCTION

Microdialysis studies suggest that dopamine transporter knockout (DAT KO) mice exhibit striatal levels of extracellular dopamine (DA), under basal conditions, that are about 10 times higher than wild-type levels while prefrontal cortical levels are similar to those found in wild-type animals (Shen *et al*, 2004). DAT KO mice exhibit numerous behavioral alterations that can be linked to abnormal dopaminergic function that include hyperlocomotion and perseverative behaviors (Sora *et al*, 1998; Ralph *et al*, 2001). High doses of psychostimulant, monoamine transporter inhibitors, and/or monoamine releasers that produce marked motor stimulation in wild-type mice can produce paradoxical inhibitory effects on locomotor activity in DAT KO mice under some conditions (Gainetdinov *et al*, 1999). However, the effects of psychostimulants and transporter blockers on other tasks, including sensorimotor gating, have not been as thoroughly evaluated in DAT KO mice.

DAT KO mice display consistent deficits in an operational task of sensorimotor gating, prepulse inhibition of the acoustic startle reflex (PPI; Ralph *et al*, 2001; Barr *et al*, 2004). PPI refers to the reduction in the amplitude of the startle reflex that occurs when a brief, subthreshold stimulus immediately precedes a startle stimulus (Hoffman and Ison, 1980). PPI deficits are observed in several psychiatric disorders, especially schizophrenia, but also other disorders thought to disrupt cortico-striatal circuits, eg attention deficit hyperactivity disorder (ADHD) in the given conditions, (Braff *et al*, 2001; Swerdlow *et al*, 2001). This impairment of sensorimotor gating has been postulated to reflect at least some portion of the cognitive dysfunction observed in schizophrenia (Braff *et al*, 2001).

*Correspondence: Dr I Sora, Department of Psychobiology, Tohoku University Graduate School of Medicine, 1-1 Seiryo-machi, Sendai, Miyagi 980-8574, Japan, Tel: +81 22 717 7808, Fax: +81 22 717 7809, E-mail: isora@mail.tains.tohoku.ac.jp
Received 21 June 2005; revised 28 October 2005; accepted 8 November 2005
Online publication: 15 November 2005 at http://www.acnp.org/citations/Npp111505050378/default.pdf

Acute treatment with selective DA D_2 receptor antagonists (Ralph *et al*, 2001) or selective serotonin 5-HT_{2A} antagonists (Barr *et al*, 2004) can normalize PPI in DAT KO mice. The mechanisms by which these drugs restore PPI in DAT KO mice are likely to be mediated by direct actions on monoamine receptors. However, indirect effects that would result from monoamine transport inhibition (eg psychostimulants like cocaine or methylphenidate) on PPI in DAT KO mice is not known, but would be of substantial interest given the clinical effects of psychostimulants in schizophrenia (Laruelle and Abi-Dargham, 1999) and ADHD (Fone and Nutt, 2005). Thus, this paper determines whether psychostimulants could improve sensorimotor gating deficits reflecting cognitive dysfunctions in DAT KO mice, similar to the effects of such drugs on hyperlocomotion (Gainetdinov *et al*, 1999). Furthermore, this paper will determine which monoamine transporter might mediate such effects. Reuptake inhibitors have various degrees of selectivity for monoamine transporters, as well as other molecular targets, and thereby modulate extracellular monoamine levels in region-specific manners (Shen *et al*, 2004). We now report evaluation of PPI in DAT KO and wild-type mice and its modulation by the nonspecific monoamine transporter inhibitors cocaine and methylphenidate, the selective serotonin transporter (SERT) inhibitors fluoxetine and citalopram, and the selective norepinephrine transporter (NET) inhibitor nisoxetine.

Cocaine is a nonspecific transport inhibitor (ie, DAT, SERT, and NET inhibitor), although its binding affinity for NET is rather weak compared to nisoxetine (Paczkowski and Bryan-Lluka, 2002). Methylphenidate is also a nonspecific transport inhibitor, with a binding affinity for NET that is not much more than cocaine, and a binding affinity for SERT that is extremely weak (Gatley *et al*, 1996). Fluoxetine is a selective SERT inhibitor and the binding affinity for SERT differs little from citalopram. Although the binding affinity of fluoxetine at NET is very weak compared to nisoxetine, it presents about 30 times stronger binding affinity for the 5-HT_{2C} receptor than citalopram (Owens *et al*, 2001). Citalopram is also a selective SERT inhibitor, with a binding affinity for NET that is about 10 times weaker than that of fluoxetine (Owens *et al*, 2001). Nisoxetine is a selective NET inhibitor and shows very low binding affinity for SERT (Orjales *et al*, 2003).

MATERIALS AND METHODS

Subjects

Male DAT KO mice (Sora *et al*, 1998) were bred at the Animal Laboratory Institute of Tohoku University Graduate School of Medicine and maintained on a mixed genetic background combining C57BL/6 and 129Sv/J mouse strains. Offsprings from heterozygote crosses were weaned at 28 days postnatal and housed in groups of two to five (segregated by sex), in a temperature- and light-controlled colony (lights on at 0800 hours, lights off at 2000 hours), with food and water available *ad libitum*. Mice were genotyped using multiplex polymerase chain reaction methods on DNA extracted from tail biopsies, as previously described (Shen *et al*, 2004). Behavioral testing was conducted between 8 and 16 weeks of age. Separate cohorts of mice were used for different experiments. All animal experiments were performed in accordance with the Guidelines for the Care of Laboratory Animals of Tohoku University Graduate School of Medicine.

Drugs

Drugs were dissolved in 0.9% NaCl solution, and were administered intraperitoneally in a volume of 10 ml/kg. Cocaine HCl (COC) was supplied by Takeda Pharmaceutical Co., Japan. Methylphenidate HCl (MPO) was supplied by Novartis Pharma KK, Japan. Fluoxetine HCl (FLX), citalopram HBr (CTP), and nisoxetine HCl (NSX) were obtained from Sigma, Japan. No published studies have documented the effects of acute cocaine, methylphenidate, fluoxetine, citalopram, or nisoxetine on PPI in male mice. Hence, to determine dose ranges, we primarily consulted previous data on locomotor activity effects of these drugs in wild-type and DAT KO mice (Gainetdinov *et al*, 1999). Since effective doses may differ between locomotion and prepulse inhibition, preliminary studies were performed. Based on the preliminary results, effective doses of each drug (described below) or dose intervals were determined.

Apparatus

Startle chambers (SR-LAB, San Diego Instruments, San Diego, CA) were used to measure the startle response. Each chamber consisted of a nonrestrictive Plexiglas cylinder mounted on a frame inside a lighted, ventilated box ($35 \times 35 \times 47.5\,cm^3$). Movement within the cylinder was detected by piezoelectric accelerometers attached to the cylinder's bottom. Force detected by the accelerometer was converted into analog signals that were digitized and stored electronically. In all experiments, 65 readings were recorded at 1 ms intervals beginning at stimulus onset; the average amplitude was used to describe the acoustic startle response. A high-frequency loudspeaker inside the chamber, mounted above the cylinder, generated broadband background noise and acoustic stimuli, which were controlled by the SR-LAB software system and interface. Sound levels (dB (A) scale) and accelerometer sensitivity were calibrated routinely, as described previously (Dulawa *et al*, 1997; Geyer and Dulawa, 2003).

Experimental Procedure

Experiments were conducted using previously reported methods (eg Geyer and Dulawa, 2003). For acoustic startle experiments, mice were tested initially for baseline PPI and pseudo-randomly assigned to drug treatment groups based on these measurements. For the main experiments, mice were treated with vehicle (VEH) or drug 10 or 30 min before testing depending on the drug tested (see below). Experimental sessions consisted of a 5 min acclimatization periods with 65 dB broadband background noise followed by PPI sessions. Sessions consisted of five different trial types: no stimulus trials (nostim); startle pulse alone, 40 ms duration at 120 dB (p120); and three prepulse + pulse trials, 20 ms duration prepulse at 68 dB (pp3), 71dB (pp6), or 77dB (pp12), followed by a 40 ms duration startle stimulus at 120 dB after a 100 ms delay. The nostim trial consisted of

only background broadband noise. All test sessions started and concluded with six presentations of the p120 trial, while the remainder of the session consisted of 12 presentations of the p120 trial type, 10 presentations of the nostim, the pp3, pp6, and pp12 trial types, in a pseudorandom order, with varying intertrial intervals (mean 15 s, range 8–23 s). Each animal was tested on a PPI session for 21 min with a total of 64 trials.

Cocaine treatment. Male wild-type and DAT KO mice were used in a between-subjects dose design, with each subject receiving either saline (wild-type $n=10$, DAT KO $n=10$), cocaine 30 mg/kg (wild-type $n=11$, DAT KO $n=13$), or cocaine 60 mg/kg (wild-type $n=11$, DAT KO $n=10$) administered i.p. 10 min before testing.

Methylphenidate treatment. Male wild-type and DAT KO mice were used in a between-subjects dose design, with saline (wild-type $n=10$, DAT KO $n=9$), methylphenidate 30 mg/kg (wild-type $n=17$, DAT KO $n=10$), or methylphenidate 60 mg/kg (wild-type $n=11$, DAT KO $n=11$) administered i.p. 30 min before testing.

Fluoxetine treatment. Male wild-type and DAT KO mice were used in a between-subjects dose design. Saline (wild-type $n=10$, DAT KO $n=10$), fluoxetine 10 mg/kg (wild-type $n=14$, DAT KO $n=10$), or fluoxetine 30 mg/kg (wild-type $n=12$, DAT KO $n=10$) was administered i.p. 30 min before testing.

Citalopram treatment. Male wild-type and DAT KO mice were used in a between-subjects dose design. Saline (wild-type $n=10$, DAT KO $n=10$), citalopram 30 mg/kg (wild-type $n=10$, DAT KO $n=10$), or citalopram 100 mg/kg (wild-type $n=11$, DAT KO $n=10$) was administered i.p. 30 min before testing.

Nisoxetine treatment. Male wild-type and DAT KO mice were used in a between-subjects dose design. Saline (wild-type $n=12$, DAT KO $n=11$), nisoxetine 3 mg/kg (wild-type $n=13$, DAT KO $n=13$), nisoxetine 10 mg/kg (wild-type $n=12$, DAT KO $n=11$), or nisoxetine 30 mg/kg (wild-type $n=14$, DAT KO $n=11$) was administered i.p. 30 min before testing.

Data and Statistical Analysis

Prepulse inhibition was calculated as a percentage score for each prepulse intensity using the following equation: %PPI = 100–{(startle response for prepulse + pulse trials (pp3, pp6, or pp12))/(startle response for pulse alone trials (p120)) × 100}. The startle magnitude was calculated as the average of all pulse alone (p120) trials, excluding the first six and last six p120 trials in each session. Data were analyzed using the SPSS statistical package (SPSS for Windows, SPSS Inc., Tokyo, Japan). The effects of drug treatments on PPI and startle data were submitted to analysis of variance (ANOVA) with the between-subjects factors of drug treatment (DRUG) and GENOTYPE (wild-type *vs* DAT KO), and the within-subjects factor of prepulse intensity (INTENSITY). For brevity, main effects of prepulse intensity will not be discussed because they were always significant. Where ANOVA indicated significant effects of one or more factors, Tukey HSD tests of individual mean differences were conducted for *post hoc* analysis. The habituation of the startle response was analyzed by grouping the startle trials into four blocks (BLOCK): six pulse alone trials (p120) each, in order of presentation, and measuring the decrease of startle magnitude across BLOCK. Repeated ANOVAs always revealed significant main effects of BLOCK, indicating habituation of the startle response, but no significant DRUG × BLOCK and GENOTYPE × BLOCK interactions were found except a significant GENOTYPE × BLOCK interaction for fluoxetine treatment, which may reflect impairment of startle habituation in DAT KO mice (data not shown).

RESULTS

Overall Results

After saline treatment, significant PPI deficits were observed in DAT KO mice compared to wild-type mice in all experiments (Figures 1–5), findings consistent with prior reports (Ralph *et al*, 2001; Barr *et al*, 2004). Cocaine and methylphenidate (60 mg/kg) treatments significantly impaired PPI in wild-type mice. However, by contrast to these impairments observed in wild-type mice, these treatments normalized PPI deficits in DAT KO mice (Figures 1 and 2). Fluoxetine, citalopram, and nisoxetine treatments did not significantly alter PPI in wild-type mice (Figures 3–5). However, 10 and 30 mg/kg nisoxetine and 30 mg/kg fluoxetine treatments normalized PPI deficits in DAT KO mice (Figures 3 and 5), and 30 and 100 mg/kg citalopram treatment did not significantly alter PPI in DAT KO mice (Figure 4).

Effects of Cocaine on PPI and Acoustic Startle

ANOVA of baseline data revealed a significant GENOTYPE effect on PPI ($F(1,18)=27.97$; $p<0.001$); DAT KO mice displayed significantly reduced levels of PPI compared to

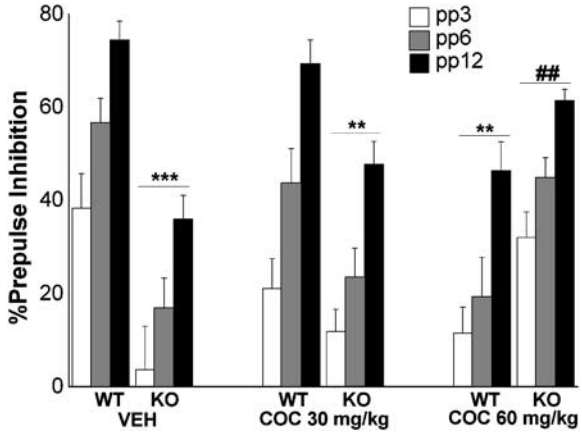

Figure 1 Prepulse inhibition (PPI) in wild-type mice (WT) and dopamine transporter knockout mice (KO) after administration of vehicle (VEH), 30 mg/kg cocaine (COC), or 60 mg/kg cocaine (COC); KO VEH displayed significantly reduced PPI compared with WT VEH. Although 60 mg/kg COC treatment significantly impaired PPI in WT VEH, it significantly reversed PPI deficits in KO VEH. %PPI values represent mean ± SEM. $^{**}p<0.01$, $^{***}p<0.001$ compared with WT VEH; $^{\#\#}p<0.01$ compared with KO VEH.

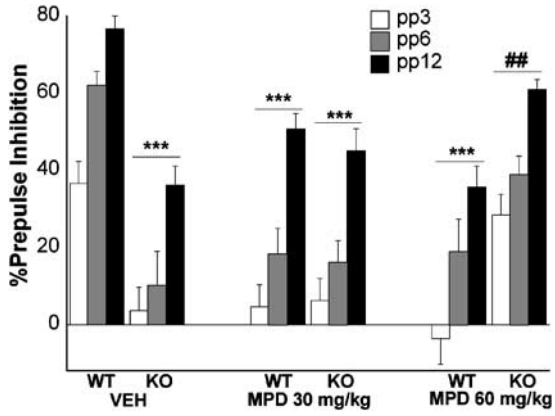

Figure 2 Prepulse inhibition (PPI) in wild-type mice (WT) and dopamine transporter knockout mice (KO) after administration of vehicle (VEH), 30 mg/kg methylphenidate (MPD), or 60 mg/kg methylphenidate (MPD); KO VEH displayed significantly reduced PPI compared with WT VEH. Although 30 mg/kg or 60 mg/kg MPD treatment significantly impaired PPI in WT VEH, 60 mg/kg MPD significantly reversed PPI deficits in KO VEH. %PPI values represent mean ± SEM. $^{***}p<0.001$ compared with WT VEH; $^{\#\#}p<0.01$ compared with KO VEH.

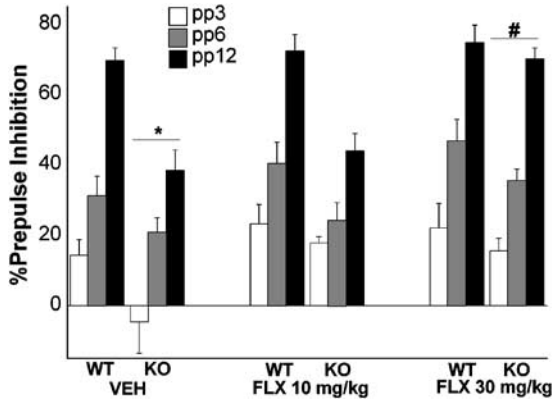

Figure 3 Prepulse inhibition (PPI) in wild-type mice (WT) and dopamine transporter knockout mice (KO) after administration of vehicle (VEH), 10 mg/kg fluoxetine (FLX), or 30 mg/kg fluoxetine (FLX); KO VEH displayed significantly reduced PPI compared with WT VEH. FLX (30 mg/kg) treatment significantly reversed PPI deficits in KO VEH without significantly affecting PPI in WT VEH. %PPI values represent mean ± SEM. $^{*}p<0.05$ compared with WT VEH; $^{\#}p<0.05$ compared with KO VEH.

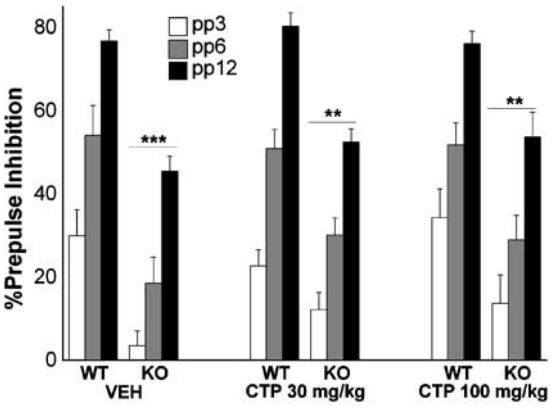

Figure 4 Prepulse inhibition (PPI) in wild-type mice (WT) and dopamine transporter knockout mice (KO) after administration of vehicle (VEH), 30 mg/kg citalopram (CTP), or 100 mg/kg citalopram (CTP); KO VEH displayed significantly reduced PPI compared with WT VEH. CTP (30 or 100 mg/kg) treatment did not significantly affect PPI in WT VEH or KO VEH. %PPI values represent mean ± SEM. $^{**}p<0.01$, $^{***}p<0.001$ compared with WT VEH.

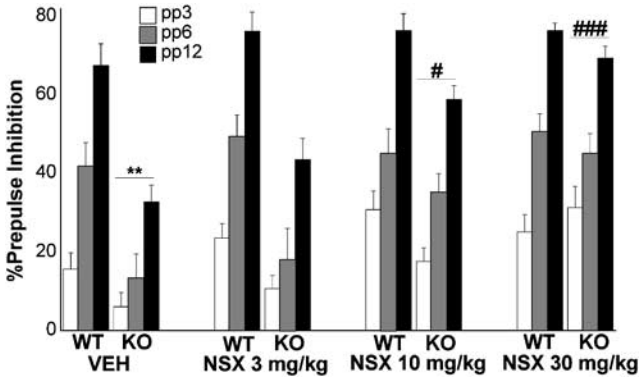

Figure 5 Prepulse inhibition (PPI) in wild-type mice (WT) and dopamine transporter knockout mice (KO) after administration of vehicle (VEH), 3 mg/kg nisoxetine (NSX), 10 mg/kg nisoxetine (NSX), or 30 mg/kg nisoxetine (NSX); KO VEH displayed significantly reduced PPI compared with WT VEH. NSX (10 or 30 mg/kg) treatment significantly reversed PPI deficits in KO VEH without significantly affecting PPI in WT VEH. %PPI values represent mean ± SEM. $^{**}p<0.01$ compared with WT VEH; $^{\#}p<0.05$, $^{\#\#\#}p<0.001$ compared with KO VEH.

wild-type mice after saline treatment (Figure 1). Cocaine (60 mg/kg), a nonspecific monoamine transport inhibitor, significantly reduced PPI in wild-type mice compared with saline treatment. Interestingly, cocaine (60 mg/kg) increased PPI in DAT KO mice compared to saline treatment (Figure 1). In addition to a significant effect of GENOTYPE ($F(1, 59) = 8.27$; $p<0.01$), the GENOTYPE × DRUG interaction term was also significant ($F(2, 59) = 17.49$; $p<0.001$), reflecting the decreased PPI after cocaine treatment in wild-type mice and the increased PPI after cocaine treatment in DAT KO mice. No other effects were statistically significant, including DRUG, GENOTYPE × INTENSITY, or DRUG × INTENSITY. *Post hoc* comparisons at each treated group are shown in Figure 1.

Startle reactivity was not significantly affected by either GENOTYPE or DRUG treatment (Table 1). There was also no significant GENOTYPE × DRUG interaction.

Effects of Methylphenidate on PPI and Acoustic Startle

ANOVA of baseline data revealed a significant GENOTYPE effect on PPI ($F(1, 17) = 42.51$; $p<0.001$); DAT KO mice displayed significantly reduced levels of PPI compared to wild-type mice after saline treatment (Figure 2). Methylphenidate (30 and 60 mg/kg), another non-specific monoaminergic transport inhibitor, reduced levels of PPI in wild-type mice compared to VEH treatment. By contrast, methylphenidate (60 mg/kg) significantly increased PPI in DAT KO mice when compared to VEH treatment (Figure 2). ANOVA displayed significant effects of DRUG ($F(2, 62) = 5.05$; $p<0.01$) and a DRUG × GENOTYPE interaction ($F(2, 62) = 25.10$; $p<0.01$). These statistically significant effects reflected the reduction of PPI by methylphenidate in wild-type mice and the increase of PPI by methylphenidate in DAT KO mice. There were no significant overall effects of GENOTYPE, GENOTYPE × INTENSITY,

Table 1 Effects of Drug Treatment on Acoustic Startle Reactivity

	Wild type	KO
Cocaine		
Vehicle	113.2±29.6	84.7±21.9
30 mg/kg	125.2±16.9	139.5±16.8
60 mg/kg	61.7±22.7	115.7±26.0
Methylphenidate		
Vehicle	106.7±29.0	89.0±23.0
30 mg/kg	104.5±19.3	95.0±16.2
60 mg/kg	58.2±11.0	84.0±16.0
*Fluoxetine**		
Vehicle	169.9±20.0	101.8±16.9
10 mg/kg	230.3±27.0	173.2±19.4
30 mg/kg	254.5±58.7	237.5±38.6
*Citalopram***		
Vehicle	116.2±12.2	95.5±18.7
30 mg/kg	254.3±35.3$^{\#}$	196.4±18.9
100 mg/kg	192.1±27.4	154.6±28.8
Nisoxetine		
Vehicle	147.7±31.3	125.1±28.5
3 mg/kg	133.7±14.5	115.4±18.5
10 mg/kg	138.8±14.4	132.8±23.1
30 mg/kg	139.9±23.7	105.0±10.8

Values (arbitrary units) represent mean startle magnitude±SEM. KO, dopamine transporter knockout mice.
*$p<0.05$, **$p<0.01$: there was a significant main effect of treatment on acoustic startle reactivity; $^{\#}p<0.01$, compared with wild-type vehicle.

or DRUG × INTENSITY. The results of *post hoc* comparisons for each treated-group are shown in Figure 2.

Startle reactivity was not significantly affected by GENOTYPE or DRUG treatment (Table 1), nor was there a significant DRUG × GENOTYPE interaction.

Effects of Fluoxetine on PPI and Acoustic Startle

ANOVA of baseline data revealed a significant GENOTYPE effect on PPI ($F(1,18)=10.53$; $p<0.01$); following saline treatment, DAT KO mice displayed significantly reduced levels of PPI compared to wild-type mice (Figure 3). Fluoxetine (30 mg/kg), a selective SERT inhibitor, increased PPI in DAT KO mice without significantly affecting PPI in wild-type mice (Figure 3). In the ANOVA, there were significant effects of DRUG ($F(2,60)=6.31$; $p<0.01$), GENOTYPE ($F(1,60)=17.19$; $p<0.001$), DRUG × INTENSITY ($F(4,120)=2.66$; $p<0.05$), and GENOTYPE × INTENSITY ($F(2,120)=3.73$; $p<0.05$), reflecting the increase in PPI only in DAT KO mice, but not in wild-type mice. There was no significant interaction between GENOTYPE and DRUG. The results of *post hoc* comparisons are shown in Figure 3.

There was no significant main effect of GENOTYPE on the magnitude of acoustic startle, but there was a significant main effect of DRUG ($F(2,60)=4.69$; $p<0.05$). Fluoxetine significantly increased the acoustic startle response independent of GENOTYPE (Table 1), as indicated by the main effect of DRUG in the absence of a significant DRUG × GENOTYPE interaction.

Effects of Citalopram on PPI and Acoustic Startle

ANOVA of baseline data revealed a significant GENOTYPE effect on PPI ($F(1,18)=27.97$; $p<0.001$); Once again, DAT KO mice displayed significantly reduced levels of PPI compared to wild-type mice after saline (Figure 4). Citalopram (30 and 100 mg/kg), a highly selective SERT inhibitor, did not significantly affect PPI in wild-type or DAT KO mice (Figure 4). Overall, there was a significant effect of GENOTYPE ($F(1,55)=50.39$; $p<0.001$) in the ANOVA, but none of the other factors were significantly different, including DRUG, DRUG × GENOTYPE, DRUG × INTENSITY, and GENOTYPE × INTENSITY. The results of *post hoc* comparisons are shown in Figure 4.

Although there was no significant main effect of GENOTYPE on the magnitude of the acoustic startle response, there was a significant main effect of DRUG ($F(2,55)=11.41$; $p<0.001$), but no significant GENOTYPE × DRUG interaction. Thus, the citalopram treatment significantly enhanced the acoustic startle response independent of GENOTYPE (Table 1).

Effects of Nisoxetine on PPI and Acoustic Startle

ANOVA of baseline data revealed a significant GENOTYPE effect on PPI ($F(1,21)=17.03$; $p<0.001$); as before, PPI was reduced in DAT KO mice after saline injection compared to wild-type mice (Figure 5). Nisoxetine (10 and 30 mg/kg), a selective NET inhibitor, significantly increased PPI in DAT KO mice without significantly affecting PPI in wild-type mice (Figure 5). In the ANOVA, there was a significant main effect of GENOTYPE ($F(1,89)=32.00$; $p<0.001$) and DRUG ($F(3,89)=8.96$; $p<0.001$), as well as a significant GENOTYPE × DRUG interaction ($F(3,89)=3.63$; $p<0.05$) reflecting this differential response to nisoxetine in DAT KO mice in the absence of any response in wild-type mice. The effects of GENOTYPE varied across prepulse intensities so that there was a significant GENOTYPE × INTENSITY interaction ($F(2,178)=12.70$; $p<0.001$). However, the effects of nisoxetine were consistent across prepulse intensities so there was no significant DRUG × INTENSITY interaction. The results of *post hoc* comparisons are shown in Figure 5.

The magnitude of the acoustic startle response was not affected by GENOTYPE or DRUG (Table 1). In the ANOVA, there was no significant effect of GENOTYPE or DRUG, nor was there a significant GENOTYPE × DRUG interaction.

DISCUSSION

The results from these experiments demonstrate that cocaine and methylphenidate ameliorate PPI deficits in DAT KO mice. As these mice lack DAT, one of the main pharmacological targets of these drugs, it is likely that

NET or SERT, the other main molecular targets of psychostimulants, mediate these residual effects. Current results are most consistent with the idea that the PPI-normalizing effects of these drugs are chiefly mediated via NET. Cocaine and methylphenidate share the ability to potently inhibit both NET and DAT, but since methylphenidate displays very lower affinity for SERT (Gatley *et al*, 1996), SERT blockade is not likely to mediate psychostimulant effects on PPI in DAT KO mice. Furthermore, the highly selective NET inhibitor nisoxetine, administered alone, also reversed the PPI deficits in DAT KO mice. By contrast, the highly selective SERT inhibitor citalopram failed to reverse these deficits, even at a high dose (100 mg/kg). There was significant amelioration of PPI deficits in DAT KO mice produced by the less selective SERT inhibitor fluoxetine. A comparison of these drugs is highly informative; although the affinity of fluoxetine and citalopram for SERT is not different (Owens *et al*, 2001), fluoxetine has about 10-fold higher affinity than citalopram for NET (Hughes and Stanford, 1996; Owens *et al*, 2001). Alternatively, fluoxetine has serotonin 5-HT_{2A} or 5-HT_{2C} receptor antagonistic effects that are not shared with citalopram (Koch *et al*, 2002) and could lead to the fluoxetine effects on the PPI deficits that we observe in DAT KO mice, as has been observed for 5-HT_{2A} antagonists (Barr *et al*, 2004).

The selective SERT inhibitors fluoxetine and citalopram significantly increased the acoustic startle response of C57BL/129Sv hybrid mice, independent of genotype. Although these increases are likely to be mediated through SERT blockade, no enhancement of acoustic startle response was previously observed in rats after SERT blockade (Martinez and Geyer, 1997; Pouzet *et al*, 2005), although decreased startle habituation has been reported in rats (Geyer and Tapson, 1988). Analyses of startle data after citalopram and fluoxetine revealed increased startle magnitude but no DRUG $\times$ BLOCK interactions indicating no effect on habituation. However, analyses of each block revealed significant effects of fluoxetine only in later blocks (from second to fourth block), but significant effects of citalopram throughout (data not shown). Thus, based on this analysis, citalopram might cause an alteration in general startle reactivity, but fluoxetine might affect startle habituation. Conceivably, these effects might be somewhat different from those in rats, given the substantial differences in startle and PPI indices that have been documented based on strain and species background (Ralph and Caine, 2005; Swerdlow *et al*, 2005). Serotonergic agents in mice exhibit strain differences in PPI, habituation, and startle reactivity (Dulawa and Geyer, 2000). The serotonin releaser methylene-dioxy-methamphetamine disrupts PPI in rats, but increases PPI in humans (Vollenweider *et al*, 1999; Liechti *et al*, 2001). Ayahuasca, containing 5-$HT_{2A/2C}$ agonistic compounds, has no effect on PPI, habituation, and startle reactivity in humans (Riba *et al*, 2002), although various serotonergic drugs affect PPI or startle habituation in rats (for a review, see Geyer *et al*, 1990; Geyer, 1998).

Methylphenidate and even more selective norepinephrine reuptake inhibitors can be clinically effective treatments for ADHD (Eiland and Guest, 2004). The superficial similarities of some phenotypes found in DAT KO mice to some of the motor symptoms of ADHD have suggested to some authors that DAT KO mice provide an animal model for this disorder. Indeed, these mice do display reductions in hyperlocomotion after treatment with psychostimulants under some conditions (Gainetdinov *et al*, 1999). Obviously, attentional and cognitive components of ADHD symptomatology may not be reflected by this model. It remains to be seen if PPI deficits induced by psychostimulants or dopaminergic overactivity (Wilkinson *et al*, 1994; Barr *et al*, 2004) reflect the sort of attentional deficits observed in ADHD. Nonetheless, it is interesting to note that selective serotonin reuptake inhibitors (SSRIs) are reported to be ineffective in ADHD (Findling, 1996), even though fluoxetine appears to reduce hyperactivity in DAT KO mice (Gainetdinov *et al*, 1999). In the present experiments, we found that the same class of drugs, selective noradrenaline reuptake inhibitors (NRIs), that has been recently shown to effectively treat ADHD symptoms (for a review, see Christman *et al*, 2004) can also normalize PPI function in DAT KO mice. Similarly, but in contrast to some previous observations (Gainetdinov *et al*, 1999), we have found that nisoxetine, an NRI, can reduce hyperactivity in DAT KO mice, while citalopram, an SSRI, does not (Fukushima and Sora, unpublished data). These results indicate that NET may be the critical molecular target for psychostimulant-induced normalization of PPI in this model.

Our recent microdialysis studies demonstrate enhanced DA levels in the prefrontal cortex (PFc), but not the nucleus accumbens (NAc), after systemic administration of cocaine (Shen *et al*, 2004) and methylphenidate (Shen and Sora, unpublished data) in DAT KO mice. By contrast, wild-type mice exhibit changes in both structures. Furthermore, systemic nisoxetine and fluoxetine administration in DAT KO mice enhances extracellular DA concentrations in PFc (Shen and Sora, unpublished data). Interestingly, systemic citalopram administration, which differs from fluoxetine in its effects on serotonin receptors and NET, did not have this effect (Shen and Sora, unpublished data). Atomoxetine, an NRI, can also increase PFc DA levels in rats, and it has been suggested that the atomoxetine-induced increase of catecholamines in PFc mediates the therapeutic effects of atomoxetine in ADHD (Bymaster *et al*, 2002).

Since DA has higher affinity for NET than for DAT (Eshleman *et al*, 1999) and PFc DAT densities are relatively low (Sesack *et al*, 1998) in comparison with PFc NET densities (Schroeter *et al*, 2000), PFc DA uptake may depend more significantly on NET (Carboni *et al*, 1990; Moron *et al*, 2002). In caudate putamen (CPu) and NAc, where DAT densities predominate, DA uptake is likely to depend primarily on DAT (Moron *et al*, 2002). Cocaine, methylphenidate, and nisoxetine, all NET blockers, could thus increase dopaminergic tone in PFc while leaving NAc DA levels virtually unchanged in DAT KO mice.

Effects of DAT KO on PPI are consistent with effects of excess synaptic DA produced in other ways, as assessed in other brain regions. For example, PPI is impaired by DA infusion into the NAc or anteromedial striatum (Swerdlow *et al*, 1992). On the other hand, DA in PFc appears to exert inhibitory control on NAc DA systems (Banks and Gratton, 1995). Depletion of prefrontal DA by 6-hydroxydopamine (6-OHDA), or infusion of D1 or D2 antagonists into the PFc, reduces PPI (Bubser and Koch, 1994; Ellenbroek *et al*, 1996). Reduced DA-mediated disinhibition of descending glutamatergic fibers could result in subcortical increases in

DA neurotransmission in the NAc (Swerdlow *et al*, 2001). Increased endogenous DA activity in PFc, resulting from inhibition of DA transport via NET, could possibly normalize PPI deficits caused by DA overactivity in NAc. Differences in the ratio between psychostimulant effects on DA uptake in PFc *vs* NAc in DAT KO mice compared to wild-type mice might underlie the profound differences in the effects of psychostimulants on PPI in these mice.

In conclusion, the normalization of the PPI deficits in DAT KO mice after administration of cocaine, methylphenidate, and nisoxetine are most likely to be mediated by NET inhibition. Since the affinities for NET binding were decreased in the order: nisoxetine $\gg$ methylphenidate $\geqslant$ cocaine (Gatley *et al*, 1996), the effective doses for PPI improvement in DAT KO mice may be consistent with their ability to inhibit NET. Microdialysis (Shen *et al*, 2004) and current results, taken together, suggest that enhanced PFc extracellular DA produced via NET blockade may mediate normalization of PPI in DAT KO mice under these circumstances. However, methylphenidate does require a high dose to ameliorate PPI deficits in DAT KO mice, compared to the clinically effective dose for the treatment of ADHD. The therapeutic mechanism of ADHD might not be explained solely by enhanced DA in PFc resulting from NET inhibition. Other mechanisms might be involved, such as the ability of methylphenidate to affect cognitive behavior through noradrenergic $\alpha 2$ adrenoceptors in the PFc (Arnsten and Dudley, 2005). Additionally, increases in PFc DA after cocaine are observed from after a 10 mg/kg dose (Shen *et al*, 2004), but cocaine requires 60 mg/kg to affect PPI in DAT KO mice. Thus, despite the substantial evidence given here supporting the role of NET in the mechanism of action of psychostimulants in the normalization of PPI deficits in DAT KO mice, it is not a complete explanation. The validity of DAT KO mice as a model of ADHD is limited by our understanding of the underlying biochemical basis of that disorder; thus, enhanced DA in PFc might only give a partial explanation for the therapeutic mechanisms of psychostimulants in ADHD. Nonetheless, NET blockers including methylphenidate and cocaine can normalize the PPI deficits in DAT KO mice, and, to the extent that DAT KO mice constitute an animal model of features of ADHD, such mechanisms could also underlie the therapeutic benefits of both psychostimulants and nonpsychostimulant NET blockers such as atomoxetine in ADHD.

ACKNOWLEDGEMENTS

We thank Ms Kayo Ohmi, Ms Harumi Hata, and Ms Maki Naka for their assistance. This study was supported by a Grant-in-Aid for Health Science Research, the Research on Psychiatric and Neurological Diseases from the Ministry of Health, Labor and Welfare of Japan; by Grants-in-Aid for Scientific Research (Nos. 15029204, 16015209, 17390315, 17022007), from the Ministry of Education, Culture, Sports, Science and Technology of Japan; and by the Mitsubishi Pharma Research Foundation.

REFERENCES

Arnsten AF, Dudley AG (2005). Methylphenidate improves prefrontal cortical cognitive function through alpha2 adrenoceptor and dopamine D1 receptor actions: relevance to therapeutic effects in attention deficit hyperactivity disorder. *Behav Brain Funct* **1**: 2.

Banks KE, Gratton A (1995). Possible involvement of medial prefrontal cortex in amphetamine-induced sensitization of mesolimbic dopamine function. *Eur J Pharmacol* **282**: 157–167.

Barr AM, Lehmann-Masten V, Paulus M, Gainetdinov RR, Caron MG, Geyer MA (2004). The selective serotonin-2A receptor antagonist M100907 reverses behavioral deficits in dopamine transporter knockout mice. *Neuropsychopharmacology* **29**: 221–228.

Braff DL, Geyer MA, Swerdlow NR (2001). Human studies of prepulse inhibition of startle: normal subjects, patient groups, and pharmacological studies. *Psychopharmacology (Berl)* **156**: 234–258.

Bubser M, Koch M (1994). Prepulse inhibition of the acoustic startle response of rats is reduced by 6-hydroxydopamine lesions of the medial prefrontal cortex. *Psychopharmacology (Berl)* **113**: 487–492.

Bymaster FP, Katner JS, Nelson DL, Hemrick-Luecke SK, Threlkeld PG, Heiligenstein JH *et al* (2002). Atomoxetine increases extracellular levels of norepinephrine and dopamine in prefrontal cortex of rat: a potential mechanism for efficacy in attention deficit/hyperactivity disorder. *Neuropsychopharmacology* **27**: 699–711.

Carboni E, Tanda GL, Frau R, Di Chiara G (1990). Blockade of the noradrenaline carrier increases extracellular dopamine concentrations in the prefrontal cortex: evidence that dopamine is taken up *in vivo* by noradrenergic terminals. *J Neurochem* **55**: 1067–1070.

Christman AK, Fermo JD, Markowitz JS (2004). Atomoxetine, a novel treatment for attention-deficit-hyperactivity disorder. *Pharmacotherapy* **24**: 1020–1036.

Dulawa SC, Geyer MA (2000). Effects of strain and serotonergic agents on prepulse inhibition and habituation in mice. *Neuropharmacology* **39**: 2170–2179.

Dulawa SC, Hen R, Scearce-Levie K, Geyer MA (1997). Serotonin1B receptor modulation of startle reactivity, habituation, and prepulse inhibition in wild-type and serotonin1B knockout mice. *Psychopharmacology (Berl)* **132**: 125–134.

Eiland LS, Guest AL (2004). Atomoxetine treatment of attention-deficit/hyperactivity disorder. *Ann Pharmacother* **38**: 86–90.

Ellenbroek BA, Budde S, Cools AR (1996). Prepulse inhibition and latent inhibition: the role of dopamine in the medial prefrontal cortex. *Neuroscience* **75**: 535–542.

Eshleman AJ, Carmolli M, Cumbay M, Martens CR, Neve KA, Janowsky A (1999). Characteristics of drug interactions with recombinant biogenic amine transporters expressed in the same cell type. *J Pharmacol Exp Ther* **289**: 877–885.

Findling RL (1996). Open-label treatment of comorbid depression and attentional disorders with co-administration of serotonin reuptake inhibitors and psychostimulants in children, adolescents, and adults: a case series. *J Child Adolesc Psychopharmacol* **6**: 165–175.

Fone KC, Nutt DJ (2005). Stimulants: use and abuse in the treatment of attention deficit hyperactivity disorder. *Curr Opin Pharmacol* **5**: 87–93.

Gainetdinov RR, Wetsel WC, Jones SR, Levin ED, Jaber M, Caron MG (1999). Role of serotonin in the paradoxical calming effect of psychostimulants on hyperactivity. *Science* **283**: 397–401.

Gatley SJ, Pan D, Chen R, Chaturvedi G, Ding YS (1996). Affinities of methylphenidate derivatives for dopamine, norepinephrine and serotonin transporters. *Life Sci* **58**: 231–239.

Geyer MA (1998). Behavioral studies of hallucinogenic drugs in animals: implications for schizophrenia research. *Pharmacopsychiatry* **31**(Suppl 2): 73–79.

Geyer MA, Dulawa SC (2003). Assessment of murine startle reactivity, prepulse inhibition, and habituation. In: Crawley J,

Gerfen C (eds). *Current Protocols in Neuroscience*. John Wiley & Sons Inc.: New Jersey. pp 8.17.1–8.17.15.

Geyer MA, Swerdlow NR, Mansbach RS, Braff DL (1990). Startle response models of sensorimotor gating and habituation deficits in schizophrenia. *Brain Res Bull* **25**: 485–498.

Geyer MA, Tapson GS (1988). Habituation of tactile startle is altered by drugs acting on serotonin-2 receptors. *Neuropsychopharmacology* **1**: 135–147.

Hoffman HS, Ison JR (1980). Reflex modification in the domain of startle: I. Some empirical findings and their implications for how the nervous system processes sensory input. *Psychol Rev* **87**: 175–189.

Hughes ZA, Stanford SC (1996). Increased noradrenaline efflux induced by local infusion of fluoxetine in the rat frontal cortex. *Eur J Pharmacol* **317**: 83–90.

Koch S, Perry KW, Nelson DL, Conway RG, Threlkeld PG, Bymaster FP (2002). *R*-fluoxetine increases extracellular DA, NE, as well as 5-HT in rat prefrontal cortex and hypothalamus: an *in vivo* microdialysis and receptor binding study. *Neuropsychopharmacology* **27**: 949–959.

Laruelle M, Abi-Dargham A (1999). Dopamine as the wind of the psychotic fire: new evidence from brain imaging studies. *J Psychopharmacol* **13**: 358–371.

Liechti ME, Geyer MA, Hell D, Vollenweider FX (2001). Effects of MDMA (ecstasy) on prepulse inhibition and habituation of startle in humans after pretreatment with citalopram, haloperidol, or ketanserin. *Neuropsychopharmacology* **24**: 240–252.

Martinez DL, Geyer MA (1997). Characterization of the disruptions of prepulse inhibition and habituation of startle induced by alpha-ethyltryptamine. *Neuropsychopharmacology* **16**: 246–255.

Moron JA, Brockington A, Wise RA, Rocha BA, Hope BT (2002). Dopamine uptake through the norepinephrine transporter in brain regions with low levels of the dopamine transporter: evidence from knock-out mouse lines. *J Neurosci* **22**: 389–395.

Orjales A, Mosquera R, Toledo A, Pumar MC, Garcia N, Cortizo L *et al* (2003). Syntheses and binding studies of new [(aryl)(aryloxy)methyl]piperidine derivatives and related compounds as potential antidepressant drugs with high affinity for serotonin (5-HT) and norepinephrine (NE) transporters. *J Med Chem* **46**: 5512–5532.

Owens MJ, Knight DL, Nemeroff CB (2001). Second-generation SSRIs: human monoamine transporter binding profile of escitalopram and *R*-fluoxetine. *Biol Psychiatry* **50**: 345–350.

Paczkowski FA, Bryan-Lluka LJ (2002). Amino acids involved in differences in the pharmacological profiles of the rat and human noradrenaline transporters. *Naunyn Schmiedebergs Arch Pharmacol* **365**: 312–317.

Pouzet B, Andersen MP, Hogg S (2005). Effects of acute treatment with antidepressant drugs on sensorimotor gating deficits in rats. *Psychopharmacology (Berl)* **178**: 9–16.

Ralph RJ, Caine SB (2005). Dopamine D1 and D2 agonist effects on prepulse inhibition and locomotion: comparison of Sprague–Dawley rats to Swiss–Webster, 129X1/SvJ, C57BL/6J, and DBA/2J mice. *J Pharmacol Exp Ther* **312**: 733–741.

Ralph RJ, Paulus MP, Fumagalli F, Caron MG, Geyer MA (2001). Prepulse inhibition deficits and perseverative motor patterns in dopamine transporter knock-out mice: differential effects of D1 and D2 receptor antagonists. *J Neurosci* **21**: 305–313.

Riba J, Rodriguez-Fornells A, Barbanoj MJ (2002). Effects of ayahuasca on sensory and sensorimotor gating in humans as measured by P50 suppression and prepulse inhibition of the startle reflex, respectively. *Psychopharmacology (Berl)* **165**: 18–28.

Schroeter S, Apparsundaram S, Wiley RG, Miner LH, Sesack SR, Blakely RD (2000). Immunolocalization of the cocaine- and antidepressant-sensitive l-norepinephrine transporter. *J Comp Neurol* **420**: 211–232.

Sesack SR, Hawrylak VA, Guido MA, Levey AI (1998). Cellular and subcellular localization of the dopamine transporter in rat cortex. *Adv Pharmacol* **42**: 171–174.

Shen HW, Hagino Y, Kobayashi H, Shinohara-Tanaka K, Ikeda K, Yamamoto H *et al* (2004). Regional differences in extracellular dopamine and serotonin assessed by *in vivo* microdialysis in mice lacking dopamine and/or serotonin transporters. *Neuropsychopharmacology* **29**: 1790–1799.

Sora I, Wichems C, Takahashi N, Li XF, Zeng Z, Revay R *et al* (1998). Cocaine reward models: conditioned place preference can be established in dopamine- and in serotonin-transporter knockout mice. *Proc Natl Acad Sci USA* **95**: 7699–7704.

Swerdlow NR, Caine SB, Geyer MA (1992). Regionally selective effects of intracerebral dopamine infusion on sensorimotor gating of the startle reflex in rats. *Psychopharmacology (Berl)* **108**: 189–195.

Swerdlow NR, Geyer MA, Braff DL (2001). Neural circuit regulation of prepulse inhibition of startle in the rat: current knowledge and future challenges. *Psychopharmacology (Berl)* **156**: 194–215.

Swerdlow NR, Kuczenski R, Goins JC, Crain SK, Ma LT, Bongiovanni MJ *et al* (2005). Neurochemical analysis of rat strain differences in the startle gating-disruptive effects of dopamine agonists. *Pharmacol Biochem Behav* **80**: 203–211.

Vollenweider FX, Remensberger S, Hell D, Geyer MA (1999). Opposite effects of 3, 4-methylenedioxymethamphetamine (MDMA) on sensorimotor gating in rats *versus* healthy humans. *Psychopharmacology (Berl)* **143**: 365–372.

Wilkinson LS, Killcross SS, Humby T, Hall FS, Geyer MA, Robbins TW (1994). Social isolation in the rat produces developmentally specific deficits in prepulse inhibition of the acoustic startle response without disrupting latent inhibition. *Neuropsychopharmacology* **10**: 61–72.

Neuroscience 144 (2007) 77–87

KNOCKOUT OF THE MU OPIOID RECEPTOR ENHANCES THE SURVIVAL OF ADULT-GENERATED HIPPOCAMPAL GRANULE CELL NEURONS

G. C. HARBURG,[a] F. S. HALL,[b] A. V. HARRIST,[c] I. SORA,[d] G. R. UHL[b] AND A. J. EISCH[a]*

[a]*Department of Psychiatry, University of Texas Southwestern Medical Center, 5323 Harry Hines Boulevard, Dallas, TX 75390-9070, USA*

[b]*Molecular Neurobiology Branch, NIDA-IRP, NIH/DHHS, Baltimore, MD, USA*

[c]*University of Pennsylvania School of Medicine, Philadelphia, PA, USA*

[d]*Tohoku University Graduate School of Medicine, Department of Neuroscience, Sendai, Japan*

Abstract—Recent evidence suggests that mu opioid receptors (MOR) are key regulators of hippocampal structure and function. For example, exogenous MOR agonists morphine and heroin negatively impact hippocampal function and decrease adult hippocampal neurogenesis. Here we explored the role of MOR in the birth and survival of hippocampal progenitor cells by examining adult neurogenesis in mice that lack MOR. Adult male mice lacking exon 1 of MOR were injected with the S phase marker bromodeoxyuridine (BrdU) and killed either 2 hours or 4 weeks later to evaluate proliferating and surviving BrdU-immunoreactive (IR) cells, respectively, in the adult hippocampal granule cell layer. Wild-type (WT), heterozygote, and homozygote mice did not differ in the number of BrdU-IR cells at a proliferation time point. However, 4 weeks after BrdU injection, heterozygote and homozygote mice had 57% and 54% more surviving BrdU-IR cells in the hippocampal granule cell layer as compared with WT mice. A decrease in apoptosis in the heterozygote and homozygote mice did not account for the difference in number of surviving BrdU-IR cells since there were no alterations in number of pyknotic, terminal deoxynucleotidyl transferase-mediated dUTP nick-end labeling (TUNEL)-positive, or activated caspase 3-IR cells compared with WT. In concordance with the increased numbers of granule cells maturing into neurons, heterozygote and homozygote mice had larger hippocampal granule cell layers and increased numbers of granule cells. These findings indicate that MOR may play a role in regulating progenitor cell survival and more generally encourage further exploration of how MOR activation can influence hippocampal structure and function.

*Corresponding author. Tel: +1-214-648-5549; fax: +1-214-645-9549.
E-mail address: amelia.eisch@utsouthwestern.edu (A. J. Eisch).

Abbreviations: ACh, acetylcholine; AChE, acetylcholinesterase; AC3, activated caspase 3; ANOVA, analysis of variance; BrdU, bromodeoxyuridine; GCL, granule cell layer; GFAP, glial fibrillary acidic protein; IHC, immunohistochemistry; IR, immunoreactive; KO, knockout; MOR, mu opioid receptor; NE, norepinephrine; PBS, phosphate-buffered saline; PCR, polymerase chain reaction; SGZ, subgranular zone; SVZ, subventricular zone; TUNEL, terminal deoxynucleotidyl transferase-mediated dUTP nick-end labeling; WT, wild-type.

Key words: mu, hippocampus, dentate gyrus, adult neurogenesis, BrdU, stereology.

The mu opioid receptor (MOR) is highly expressed in brain monoaminergic pathways, brainstem, and spinal cord, and has long been implicated in processes related to these brain regions, such as addiction, alertness, and nociception (Arvidsson et al., 1995; Mansour et al., 1995; Uhl et al., 1999; Kreek et al., 2005). However, recent evidence points to a more novel role for MOR: regulating hippocampal structure and function (Morris and Johnston, 1995; Martinez and Derrick, 1996; Terman et al., 2000; Kearns et al., 2001; Harrison et al., 2002; Guo et al., 2005; Vigano et al., 2005a,b). MOR is expressed on interneurons and primary cell types in all hippocampal regions (Meibach and Maayani, 1980; Arvidsson et al., 1995; Mansour et al., 1995; Svoboda et al., 1999; Drake and Milner, 2002), including in the granule cell layer (GCL) of the dentate gyrus. Hippocampal structure, physiology, and biochemistry are potently influenced by exogenous MOR agonists, like morphine and heroin, and by perturbation of the levels of endogenous agonists, like enkephalin and dynorphin (Morris and Johnston, 1995; Simmons and Chavkin, 1996; Chavkin, 2000). For example, chronic exposure to MOR agonists negatively impacts hippocampal function, defined here as hippocampal-dependent behaviors, while blockade of MOR and other opiate receptors enhances hippocampal function (Spain and Newsom, 1989, 1991). Supporting the role for MOR in hippocampal function, transgenic mice that lack MOR or endogenous MOR ligands have altered behavior in hippocampal-dependent tasks (Jamot et al., 2003; Jang et al., 2003; Nguyen et al., 2005; Sanders et al., 2005). These studies encourage more detailed exploration of how MOR regulates hippocampal structure and function.

In this regard, an intriguing property of the adult hippocampal dentate gyrus is its capability to generate new neurons throughout life (Eisch, 2002; Abrous et al., 2005). Neural progenitors located in and adjacent to the GCL proliferate, differentiate, and mature to become functional granule cell neurons (van Praag et al., 2002; Kempermann et al., 2004). All stages of hippocampal progenitor development—proliferation, differentiation, and survival—can be influenced by environmental and physiological stimuli (Cameron et al., 1998; Eisch, 2002; Abrous et al., 2005). For example, adult *in vivo* exposure to MOR agonists decreases the proliferation and survival of new neurons in the hippocampus (Eisch et al., 2000; Mandyam et al.,

0306-4522/07$30.00+0.00
doi:10.1016/j.neuroscience.2006.09.018

2004; Kahn et al., 2005; Eisch and Harburg, 2006). In order to examine the impact of loss of MOR on adult hippocampal neurogenesis, we examine the proliferation, differentiation, and survival of new neurons in the hippocampus of adult transgenic mice lacking exon 1 of MOR (Sora et al., 1997). We find that MOR knockout (KO) mice have normal proliferation and differentiation, but enhanced survival of new neurons and more granule cells. These results suggest a previously unappreciated role for MOR in the normal development of hippocampal granule cells.

EXPERIMENTAL PROCEDURES

Animals

Adult male mice with a deletion of exon 1 of MOR were created on a C57BL/6 and 129Sv mixed background as previously described (Sora et al., 1997). MOR KO mice were generated from heterozygote crosses to produce wild-type (WT), heterozygote, and homozygote littermates. WT, heterozygote KO and homozygote KO mice were genotyped by polymerase chain reaction (PCR) using two internal primers, one targeted at the NEO insertion in the KO construct and one targeted at the WT gene, and one external primer, which generated two products identifying the WT and KO genes. PCR using Tsg DNA polymerase (Lamda Biotech, St. Louis, MO, USA) was performed on tail DNA eluted after digestion overnight in Protease K. The forward primer (5′ CTG GAT GAG CTG TAA GAA TAG G 3′) and the WT primer (5′ CAG CCA ACA CAA TAT CAC ATT C 3′) produced a 550 bp band, while the forward primer and the NEO primer (5′ CGG ACA GGT CGG TCT TGA C 3′) produced an 800 bp band. PCR amplification products were separated by electrophoresis on 4% agarose gels and bands were visualized under UV illumination. The mice were housed at 24 °C with a 12-h light/dark cycle and *ad libitum* access to food and water, and all procedures were performed according to AAALAC guidelines in a vivarium at NIDA-IRP in Baltimore, MD, USA. All animal use procedures were performed in accordance with the U.S. National Institutes of Health Guide for the Care and Use of Laboratory Animals. Experiments were designed to minimize the number of animals used and their suffering.

Bromodeoxyuridine (BrdU) injections and tissue preparation

In order to assess levels of cell proliferation, differentiation, and survival of new cells in the dentate gyrus, mice were given one i.p. injection of BrdU (150 mg/kg; Boehringer Mannheim, Mannheim, Germany) dissolved in 0.9% saline and 0.007 N NaOH at 10 mg/ml as previously described (Mandyam et al., 2004). A total of 44 male mice were used for this study. To assess proliferation, 22 mice (WT=10, heterozygote=5, homozygote=7) were perfused 2 h after BrdU injection. To assess differentiation and survival 22 mice (WT=8, heterozygote=5, homozygote=9) were perfused 28 days after BrdU injection to allow time for BrdU cells born 4 weeks earlier to achieve their mature phenotype. All mice were anesthetized with chloral hydrate and perfused transcardially with cold 0.1 M phosphate-buffered saline (PBS) followed by 4% paraformaldehyde in 0.1 M PBS (pH 7.4) for 30 min at a rate of 7 ml/min. After perfusion, brains were removed and postfixed in 4% paraformaldehyde in 0.1 M PBS for at least 24 h at 4 °C. Brains were cryoprotected in 30% sucrose in 0.1 M PBS with 0.1% NaN_3 at 4 °C until sectioning. Thirty micrometer coronal sections were taken on a freezing microtome (Leica, Wetzlar, Germany). Nine serial sets of sections were collected through the entire hippocampus. Sections were stored in 0.1% NaN_3 in 1× PBS at 4 °C until processed for immunohistochemistry (IHC).

IHC and histology

Every ninth section of the hippocampus was mounted on glass slides (Fisher Superfrost/Plus, Hampton, NH, USA) and left to dry overnight prior to IHC. Slides were coded so the experimenter was blind to the genotype of the animal until completion of analysis. Sections used for IHC were pretreated as follows: DNA denaturation (0.01 M citric acid, pH 6.0, 95 °C, 10 min), membrane permeabilization (0.1% trypsin in 0.1 M Tris and 0.1% $CaCl_2$, 10 min), and acidification (2 M HCl in 1× PBS, 30 min). Primary antibody concentrations were as follows: rat anti-BrdU (Accurate, Westbury, NY, USA; 1:100), rabbit anti-activated caspase 3 (AC3; Cell Signaling Technology, Beverly, MA, USA; 1:500), rabbit anti-glial fibrillary acidic protein (GFAP; Dako, Carpinteria, CA, USA; 1:500), and mouse anti-NeuN (Chemicon, Temecula, CA, USA; 1:50). Single-labeling IHC for BrdU or AC3 was completed using the avidin–biotin/diaminobenzidine visualization method (Vector Laboratories, Pierce, Rockford, IL, USA) followed by counterstaining with Fast Red (Vector). Triple-labeling for BrdU, GFAP, and NeuN was performed by co-incubation in a primary cocktail overnight followed by co-incubation in a cocktail of the following fluorescent secondary antibodies (Jackson Immunoresearch, West Grove, PA, USA; anti-rat CY2 (1:200), anti-mouse CY3 (1:200), and anti-rabbit CY5, (1:500)), and completed by counterstaining with 4′, 6-diamidino-2-phenylindole (DAPI) (Roche, Basel, Switzerland; 1:5000). Apoptotic nuclei were detected using AC3-immunoreactivity as described above, presence of pyknotic cells in Fast Red-stained sections, or terminal deoxynucleotidyl transferase-mediated dUTP nick-end labeling (TUNEL). Before beginning the TUNEL procedure (DeadEnd Colorimetric TUNEL System; Promega, Madison, WI, USA), slide-mounted sections were pretreated with 0.1 M sodium citrate buffer, pH 6.0 at 95 °C for 5 min (Heine et al., 2004).

Quantification of immunoreactive (IR) and apoptotic cells

Cell birth, survival, and death were examined in the neurogenic region of the dentate gyrus. This region, referred to here as the GCL, was composed of the subgranular zone (SGZ; extending from the border of the GCL to three granule cell widths into the hilus) and the adjacent GCL (Kuhn et al., 1996; Kempermann et al., 1997; Donovan et al., 2006). Using modified stereology with the optical fractionator method (Eisch et al., 2000; Mouton, 2002), IR cells were quantified in the GCL along the longitudinal extent of the hippocampus (bregma −0.70 to −4.16,Franklin and Paxinos, 1997). Cell counts were performed at 400× and 1000× magnification with an Olympus BX-51 microscope (Olympus America Inc., Center Valley, PA, USA) while continually adjusting the focal plane through the depth of the section. Since counting of cells was conducted on every ninth section of the hippocampus, the number of counted cells in the region was multiplied by nine to obtain an estimate of the total number of cells per region. Cell birth and survival were determined by the number of BrdU-IR cells present in the GCL 2 h or 4 weeks after BrdU injection, respectively. To control for bioavailability of BrdU between genotypes, BrdU-IR cells within the medial habenula, putatively dividing mast cells (Zhuang et al., 1999), were also quantified (Mandyam et al., 2004; Donovan et al., 2006; Lagace et al., 2006). The habenula is non-neurogenic, unlike more commonly used control regions (e.g. subventricular zone (SVZ) (Ming and Song, 2005), corpus callosum (Dayer et al., 2005)), and its small volume and relative homogeneity allow appropriate stereologic analysis throughout its longitudinal axis. Cell death was assessed in GCL and hilus by quantification of AC3-IR, TUNEL-positive, or pyknotic cells (Eisch et al., 2000; Donovan et al., 2006) as previously described (Gould et al., 1990; Geloso et al., 2002; Heine et al., 2004).

Phenotypic analysis

In order to determine the differentiation of adult-generated GCL cells into either neurons or glia, triple-labeled sections from the 4-week group ($n=4$ animals of each genotype) were examined for co-localization of BrdU with NeuN or GFAP. At least 45 BrdU-IR cells in the GCL of each animal (WT 48±3, heterozygote 74±9, homozygote 66±6) were analyzed. All cells were optically sectioned in the Z plane using a confocal microscope (Zeiss Axiovert 200 and LSM510-META, Carl Zeiss, Oberkochen, Germany) with three laser lines (emission wavelengths 488, 543, and 633), multitrack scanning, and a section thickness of 0.45 μm. Orthogonal and rotational analysis in a 3D reconstruction program (Volocity, Improvision Inc., Lexington, MA, USA) confirmed co-localization.

Stereological estimation of structural volume and granule cell number

GCL volume and granule cell number were determined in 30 μm sections stained with Fast Red (Donovan et al., 2006). One section per 240 μm was analyzed spanning bregma −0.70 to −4.16 (Franklin and Paxinos, 1997) such that the entire longitudinal axis of the hippocampus was analyzed. Sections were coded so the experimenter was blind to the genotype of the animal until completion of analysis. All measurements were obtained using StereoInvestigator software (MBF Bioscience, Williston, VT, USA) and an Olympus BX51 microscope. Volumes were measured according to the Cavalieri principle (Gundersen and Jensen, 1987; West and Gundersen, 1990) using a 40× objective. The total number of granule cells was determined using optical disectors along with the optical fractionator method (West et al., 1991) and a 100×/NA 1.30 oil objective. The right GCL of each animal was analyzed for neuron number since there was no statistical difference between the right and left GCL volumes. Data are presented as right GCL neuron numbers only. A grid size of 125 μm×125 μm was superimposed over each section, and granule cells in fields within the GCL were counted in 15×15×6 μm sample volumes, with upper and lower guard volumes of 1 μm, resulting in an average of 160 sampling sites per GCL.

Statistical analyses and presentation

Data are represented as mean±S.E.M. Statistical analyses were performed using a multiple variable analysis of variance (ANOVA) followed by a Bonferroni post hoc test. For repeated measure variables (bregma), a repeated measures ANOVA was used to assess the effect of genotype on the number of BrdU-IR cells as specific bregma points, followed by a Bonferroni post hoc test. All statistical analysis was performed on a Macintosh computer using SPSS version 11.0.2. Statistical significance was defined as $P<0.05$. Images were imported into Photoshop version 7.0.1 (Adobe Systems Inc., San Jose, CA, USA) and the only adjustments made were via gamma in the Levels function.

RESULTS

Proliferation

Two hours after BrdU injection, BrdU-IR cells were evident in the SGZ and GCL of the hippocampus. As previously

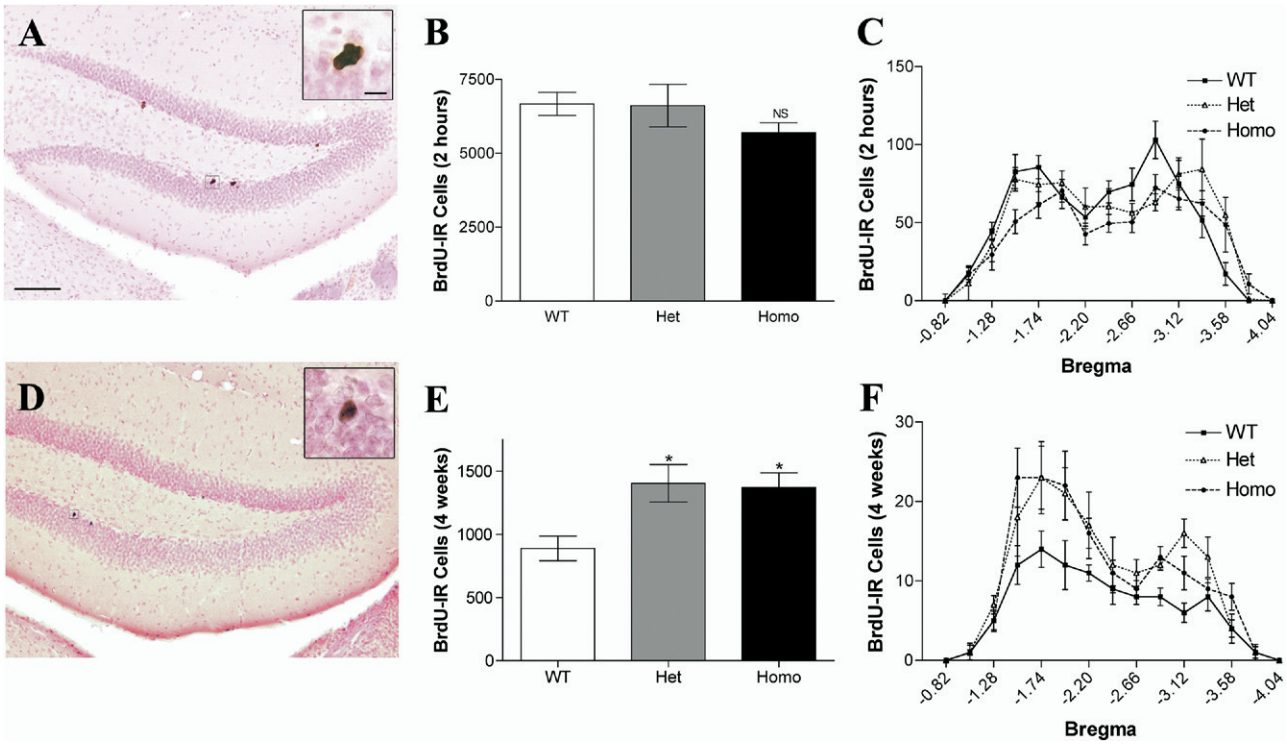

Fig. 1. MOR KO mice have increased cell survival without changes in proliferation. (A–C) Cell proliferation in the adult hippocampal GCL 2 h after BrdU administration. (A) BrdU-labeled cells in the SGZ of the dentate gyrus displayed a typical clustered appearance. Inset is a higher magnification image of a BrdU-IR cell cluster. Scale bar=100 μm. Inset scale bar=10 μm. (B) Homozygote MOR KO mice show a non-significant trend to decrease in cell proliferation in comparison to WT mice ($P=0.26$). (C) Distribution of BrdU-labeled cells along the anterior–posterior axis of the hippocampus. (D–E) Survival of new cells in the adult hippocampal GCL 4 weeks after BrdU administration. (D) BrdU-labeled cells in the SGZ of the dentate gyrus displayed a mature neuron phenotype. Inset is a higher magnification of a BrdU-IR cell. (E) Both heterozygote and homozygote animals show increased survival of newly born cells at 4 weeks in comparison to WT animals (* $P<0.05$). (F) Distribution of BrdU-labeled cells along the anterior–posterior axis of the hippocampus. Data for B, C, E, and F are presented as mean±S.E.M.

shown, proliferating cells were small, clustered, and irregularly shaped (Fig. 1). No differences were evident in the size, clustering, or shape of BrdU-IR cells across genotypes. Quantification of the total number of BrdU-IR cells showed no significant effect of genotype in the GCL (Fig. 1B; $F_{(2,19)}=1.430$, $P>0.05$) or the habenula (Fig. 1B; $F_{(2,19)}=0.478$, $P>0.05$), a region we use to assess bioavailability of BrdU (Mandyam et al., 2004; Donovan et al., 2006). The distribution of BrdU-IR cells in all groups differed significantly across the longitudinal axis of the GCL (Fig. 1C; $F_{(14,266)}=31.116$, $P<0.001$), with two peaks of BrdU-IR cells in the GCL at bregma −1.66 and bregma −3.2. There was also a significant interaction of bregma and genotype (Fig. 1C, $F_{(28,266)}=1.843$, $P<0.01$). However, post hoc analysis revealed no significant difference in cell number at any bregma value among the genotypes. Therefore, while a trend exists (Fig. 1B, 1C), the number of proliferating cells in the adult mouse GCL is unchanged in MOR KO mice.

Survival

Surviving cells in the hippocampus were assessed in mice injected with BrdU and killed 4 weeks later. Reflective of the maturation they undergo in the intervening 4 weeks, surviving BrdU-IR cells in the GCL were large, round, generally spotted or solid in staining, and rarely clustered (Fig. 1D). Quantification of BrdU-IR cells at this survival time point revealed a significant effect of genotype (Fig. 1E; $F_{(2,19)}=6.042$; $P<0.01$). Heterozygous and homozygous mice had significantly more BrdU-IR GCL cells in comparison to WT mice, with increases of 57% and 54% respectively (P's<0.05). There was no effect of genotype on the number of BrdU-IR cells in the habenula ($F_{(2,19)}=0.378$, $P>0.05$), indicating that the increased BrdU-IR cell number was selective for the hippocampus. There was not an interaction of bregma and genotype (Fig. 1F; $F_{(24,228)}=1.281$, $P>0.05$), suggesting that the increase in homozygous and heterozygous mice was spread across the hippocampus. These data show that while proliferation is unchanged in MOR KO mice, constitutive loss of or reduction in levels of MOR increases the number of surviving cells in the adult GCL.

Differentiation

Hippocampal progenitor cells can differentiate into several fates, including astrocytes or neurons (Reynolds and Weiss, 1992). To determine if loss or depletion of MOR influenced the fate of adult-generated hippocampal cells, we triple-labeled sections from mice given BrdU 4 weeks earlier with antibodies against glia (GFAP), neurons (NeuN), and BrdU. Confocal analysis showed that the majority of BrdU-IR cells in all three genotypes became neurons (Fig. 2; Table 1). There was no effect of genotype on the proportion of cells that became neurons ($F_{(2,11)}=1.349$, $P>0.05$), glia ($F_{(2,11)}=0.919$, $P>0.05$), or had an indeterminate fate ($F_{(2,11)}=0.616$, $P>0.05$). These data show that the increase in surviving BrdU-IR cells seen after loss or reduction of MOR (Fig. 1D–F) reflects an increase in adult hippocampal neurogenesis.

Cell death

Many adult-generated hippocampal neurons will die prior to incorporation into hippocampal circuitry (Dayer et al., 2003). Since we found that loss or reduction of MOR increases the survival of adult-generated neurons (Fig. 1D–F), we hypothesized that the increased survival was due to decreased cell death. To assess apoptosis, adjacent sets of sections were examined for the number of AC3-IR, TUNEL-positive, and pyknotic cells (Fig. 3). The majority of apoptotic cells were located within the SGZ region of the GCL, underscoring the high turnover of cells in this region (Thomaidou et al., 1997; Gould et al., 1999; Dayer et al., 2003; Heine et al., 2004). As noted previously (Geloso et al., 2002), the majority of AC3-IR cells were large, round cells, and many extended processes through the GCL (Fig. 3D). This morphology reflects AC3's early role in the apoptotic cascade (Faherty et al., 1999). TUNEL-positive (Fig. 3E) and pyknotic cells (Fig. 3F) were small and round, and processes were rare, emphasizing that these two methods of cell death detection capture cells in later stages of apoptosis (Faherty et al., 1999). Regardless of the method used to detect apoptosis, there was no significant effect of genotype (AC3, $F_{(2,19)}=0.984$, $P>0.05$; TUNEL, $F_{(2,12)}=0.055$, $P>0.05$, pyknosis, $F_{(2,12)}=1.166$, $P>0.05$). These data show that GCL cell death is not different between WT and MOR KO mice.

Stereological estimation of structural volume and granule cell number

Given that cell death was not different across genotypes (Fig. 3), the increased survival of newborn cells in the GCL of heterozygote and homozygote MOR KO mice (Fig. 1) would be expected to lead to an increased number of GCL cells. To address this possibility, we calculated the volume of the GCL and determined the number of granule cells using optical disectors along with the optical fractionator method (West and Andersen, 1980; Gundersen and Jensen, 1987; West and Gundersen, 1990). In regard to GCL volume, there was a significant effect of genotype ($F_{(2,18)}=5.833$; $P<0.05$; Table 2) with the GCL of MOR heterozygote and homozygote KO mice being 22% and 17% larger than WT littermates ($P<0.05$ in each case). This increase in GCL volume was specific to the hippocampus since a main effect of genotype was also seen in the hilus ($F_{(2,18)}=5.071$; $P<0.05$; heterozygote and homozygote 20% and 23% larger than WT), but no main effect of genotype was seen on the volume of the habenula, a region rich in MOR ($F_{(2,17)}=0.107$; $P>0.05$; Fig. 4A, Table 2). There was also a main effect of genotype on the number of neurons in the GCL ($F_{(2,17)}=11.06$; $P<0.001$) with heterozygote and homozygote possessing 30% ($P<0.05$) and 44% ($P<0.001$) more GCL neurons than WT (Fig. 4B, Table 3). Taken together these data show that enhanced survival of adult-generated neurons results in increased numbers of neurons in the GCL of adult mice lacking MOR.

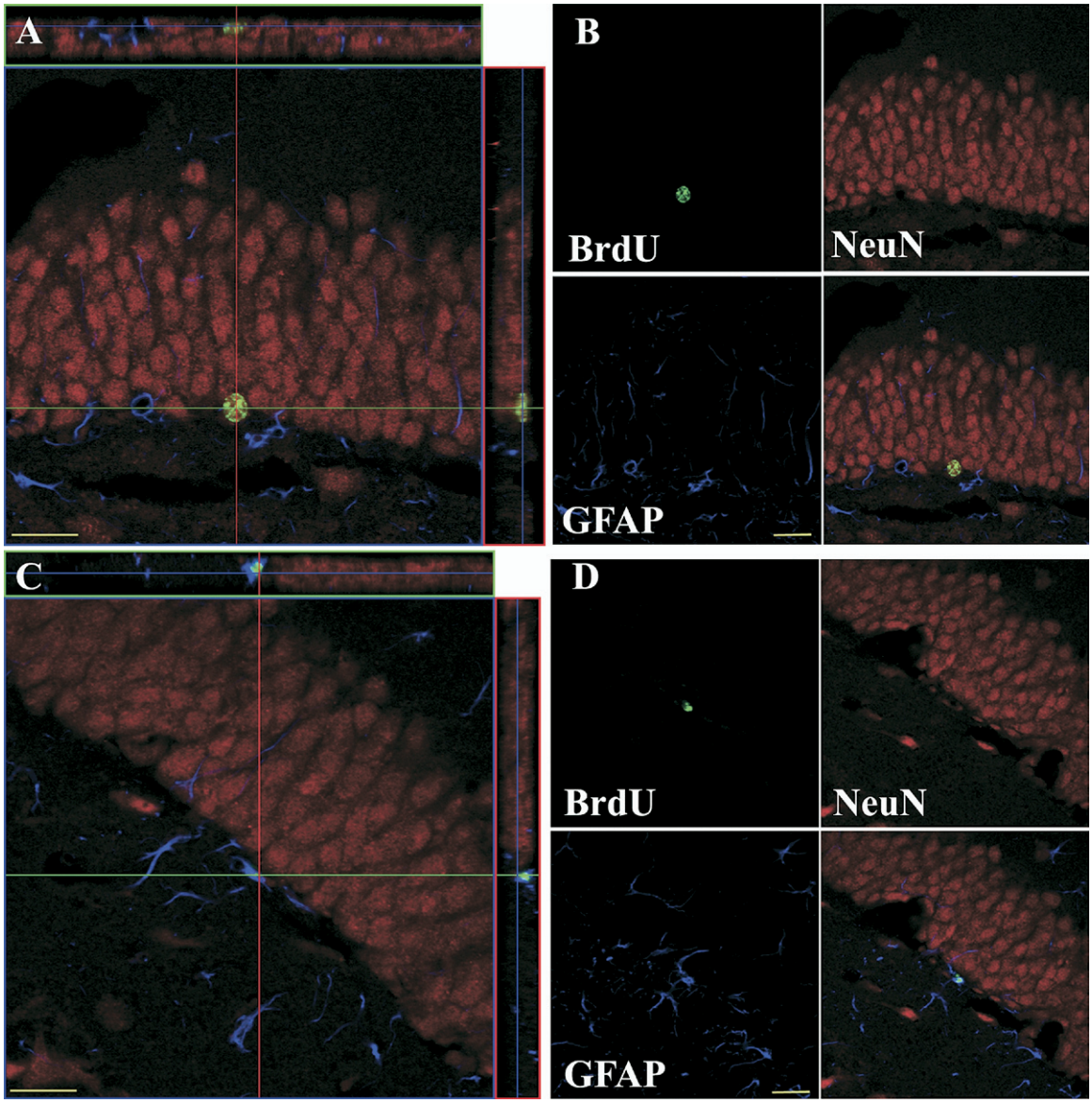

Fig. 2. Knockout of the μ opioid receptor does not alter cell fate during maturation. (A, B) Example of a BrdU-labeled cell with a neuronal phenotype. BrdU labeling (green) colocalizes with the neuronal marker, NeuN (red), but not a glial marker, GFAP (blue). (C, D) Example of a BrdU-labeled cell with a glial phenotype. BrdU labeling colocalizes with GFAP and not NeuN. Scale bars=20 μm. For interpretation of the references to color in this figure legend, the reader is referred to the Web version of this article.

DISCUSSION

These data show that heterozygote and homozygote MOR KO mice have enhanced adult hippocampal neurogenesis. This effect is due to an increase in the number of progenitor cells that survive, not to alteration in the number of proliferating GCL cells, and is independent of detectable changes in cell death. There is no influence of the MOR KO on cell fate determination since WT, heterozygote and homozygote mice all had equivalent proportions of surviving cells maturing into neurons. The impact of increased neurogenesis on the hippocampus is emphasized by the increased volume and neuron number in the GCL of the dentate gyrus in heterozygote and homozygote mice. These results indicate that MOR plays a role in regulating the survival of maturing neurons in adult hippocampal neurogenesis.

Table 1. Phenotype of BrdU-IR GCL cells

Genotype	% BrdU cells colocalizing with		
	NeuN	GFAP	Neither
WT	93.5 (±2.4)	1.7 (±1.2)	4.8 (±2.7)
Heterozygote	96.3 (±2.9)	0.6 (±0.6)	3.1 (±3.1)
Homozygote	98.6 (±0.5)	0.3 (±0.3)	1.1 (±0.4)

The majority of factors currently known to influence neurogenesis do so via influence on proliferating progen-

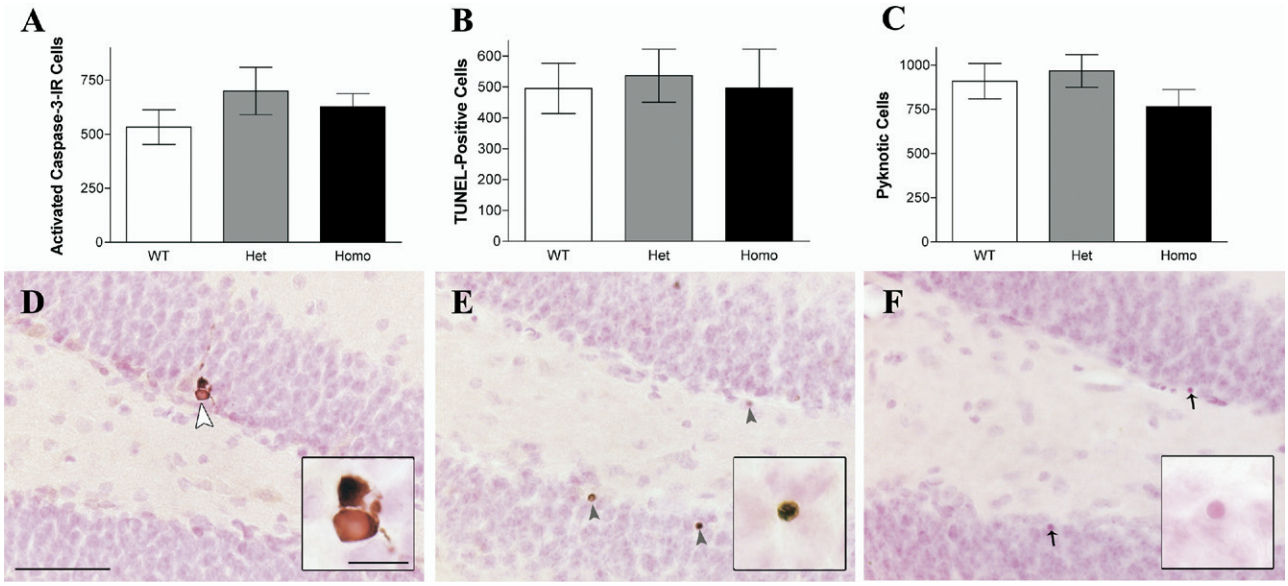

Fig. 3. Increased survival of neurons in MOR KO mice is not due to a detectable decrease in levels of apoptosis. Quantitative analysis of (A) activated caspase-3-IR cells, (B) TUNEL-positive cells, and (C) pyknotic cells in the GCL. Representative images of (D) activated caspase-3 cells (indicated by white arrowhead), (E) TUNEL-positive cells (indicated by gray arrowheads), and (F) pyknotic cells (indicated by black arrows) in the GCL. Data for A–C are presented as mean±S.E.M. Scale bar=50 μm. Inset scale bar=10 μm.

itor cells. Thus, it is of particular interest that deletion of MOR appears to confer a survival advantage to maturing neurons without altering the numbers of proliferating progenitor cells. These data add MOR to the limited list of factors that have a stronger effect on survival versus proliferation of new hippocampal neurons (Ambrogini et al., 2005; Rizk et al., 2006; Galea et al., 2006; Lichtenwalner et al., 2006). The data presented here suggest that MOR is critical to normal maturation of adult-generated granule cells. Studies are in progress to explore whether other aspects of progenitor cell development, e.g. establishment of the granule cell dendritic tree, are altered in MOR KO mice.

The increase in survival of maturing neurons in MOR KO mice occurs without the expected concurrent decrease in cell death, as three measures (AC3, TUNEL, pyknosis) were similar between WT and KO mice. While it is difficult to reconcile increased cell survival in the face of no decrease in cell death, two things give us confidence that MOR KO mice indeed do have enhanced cell survival. First, despite the lack of detectable changes in cell death levels, our finding of increased cell survival (Fig. 1) is supported by a concomitant increase in the number of GCL neurons (Fig. 4, Table 3). This emphasizes that more neurons appear to survive and likely integrate into the hippocampal circuitry in MOR KO mice. Second, available methods of cell death detection are hampered by the difficulty in catching the short window of time in which cells can be detected. Even those studies that show a correlation between cell birth and cell death show large differences between the number of proliferating cells and dying cells (Cameron and Gould, 1996; Cameron and McKay, 1999; Montaron et al., 1999; Biebl et al., 2000; Heine et al., 2004). This commonly-reported discrepancy between the number of proliferating progenitors and dying cells underscores the need for global technical advances in detection of cell death, as well as encourages more specific research into the relationship between these events as it relates to adult hippocampal neurogenesis.

It is interesting to note that heterozygote and homozygote MOR KO mice both have similar increases in cell survival in the GCL. While it is difficult to pinpoint the reason for the lack of a gene dosage effect, it is interesting to speculate if receptor density plays a role. MOR is expressed at low levels in the dentate gyrus (Arvidsson et al., 1995; Mansour et al., 1995; Drake and Milner, 2002), so a 50% reduction in MOR would have a significant impact on receptor density. *In vivo* studies have shown that MOR activity is highly dependent on receptor density (Pak et al., 1996; Law et al., 2000). Decreasing the number of func-

Table 2. Effect of genotype on size of brain regions

Genotype	GCL volume (mm^3)	% WT	Hilus volume (mm^3)	% WT	Habenula volume(mm^3)	% WT
WT	0.482 (±0.024)	100	0.494 (±0.032)	100	0.069 (±0.002)	100
Heterozygote	0.588 (±0.026)*	122	0.594 (±0.021)*	120	0.069 (±0.003)	100
Homozygote	0.565 (±0.016)*	117	0.608 (±0.003)*	123	0.067 (±0.003)	97

* $P<0.05$.

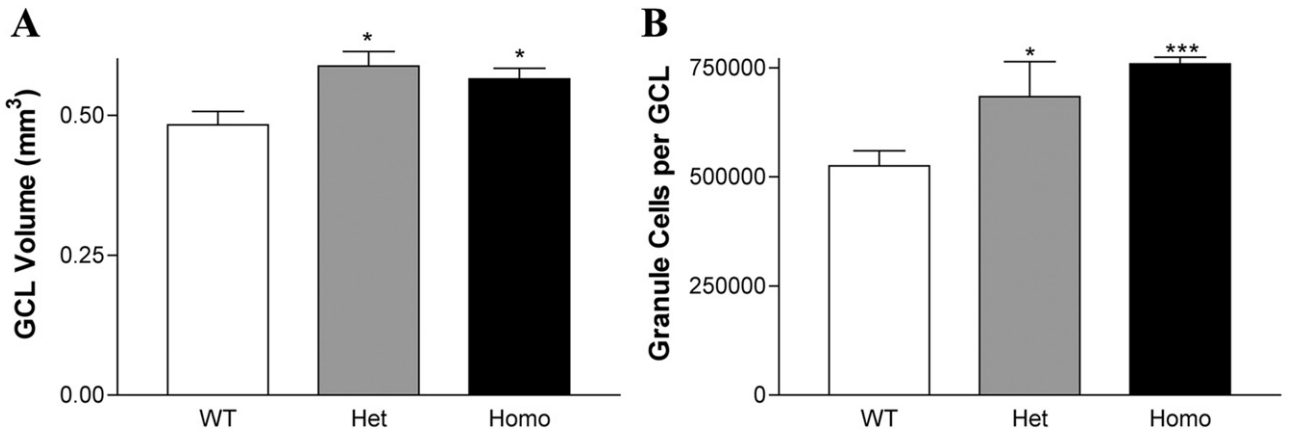

Fig. 4. MOR KO mice have larger GCLs and increased numbers of granule cells. (A) GCL volumes. (B) Number of granule cells per GCL as estimated by optical fractionator. (* $P<0.05$, *** $P<0.001$.) Data are presented as mean±S.E.M.

tional MOR receptors by treatment with irreversible MOR antagonists (β-CAN, β-FNA) results in a non-linear decrease in receptor function. This reduction in functional efficacy of the receptor/effector unit necessitates a greater percentage occupancy of receptors in order to generate a functional response (Pak et al., 1996). This work also suggests that secondary cascades initiated by MOR may be uniquely sensitive to MOR receptor density (Pak et al., 1996). Thus, loss of one copy of MOR could translate into greater than expected decrease in receptor function and downstream activity in the dentate gyrus, resulting in a phenotype similar to the homozygote. Future studies, beyond the scope of this paper, will explore the mechanism behind our heterozygote phenotype by focusing on the kinetics of MOR specifically in dentate gyrus neurons.

Possible mechanisms for MOR regulation of neurogenesis

Pharmacological evidence supports the hypothesis that MOR is a regulator of cell survival in the CNS. For example, pre- and postnatal exposure to the opioid antagonist naltrexone results in an increase in brain size (Zagon and McLaughlin, 1984, 1986a), while exposure to MOR agonists decreases brain size (Zagon and McLaughlin, 1977a,b; Ford and Rhines, 1979). Full exploration of the mechanism for MOR regulation of adult neurogenesis is outside the scope of the present study. However, several recent findings provide clues to how MOR regulates the survival of new neurons, and these deserve discussion. The most pressing question to be addressed is whether MOR impacts maturing neurons directly, indirectly, or both. Here we propose two different mechanisms—one direct, and one indirect—via which MOR could regulate neurogenesis.

Indirectly, MOR could regulate neurogenesis by altering the levels of pro-survival factors in the dentate gyrus. MOR activity has been shown to be involved in the regulation of a number of neurotransmitters in the hippocampus including acetylcholine (ACh, Lapchak et al., 1989; Kaplan et al., 2004), GABA (Drake and Milner, 1999, 2002; Akaishi et al., 2000), and norepinephrine (NE, Matsumoto et al., 1994). GABA modulates neurogenesis, but appears to do so by altering cell differentiation, not survival (Tozuka et al., 2005; Karten et al., 2006). Manipulations of ACh levels can alter both proliferation and survival (Cooper-Kuhn et al., 2004; Mohapel et al., 2005). However, a recent paper showed that chronic acetylcholinesterase (AChE) antagonist treatment results in increased cell survival in the SGZ without affecting cell proliferation or fate (Kotani et al., 2006). While it is intriguing to consider whether perturbations in cholinergic signaling contribute to the enhanced survival reported here, cholinergic receptor binding as well as AChE activity are both normal in MOR KO mice (Tien et al., 2004). Thus, it seems unlikely that alterations in the cholinergic system are the cause of increased cell survival in MOR KO mice. NE is perhaps a more likely candidate. Antagonism of the alpha2-adrenoceptor, which increases NE levels, enhances neurogenesis by specifically increasing survival of new neurons in the hippocampus independent of changes in cell proliferation or fate (Rizk et al., 2006). MOR agonists inhibit release of NE (Matsumoto et al., 1994) and ACh (Lapchak et al., 1989) in the rat

Table 3. Effect of genotype on GCL neuron number

Genotype	GCL volume (mm^3)	% WT	GCL neurons ($\times 10^6$)	% WT	Neuron density ($\times 10^5/mm^3$)
WT	0.482 (±0.024)	100	5.254 (±0.346)	100	10.90 (±0.490)
Heterozygote	0.588 (±0.026)*	122	6.840 (±0.798)*	130	12.00 (±1.222)
Homozygote	0.565 (±0.016)*	117	7.590 (±0.153)***	144	13.49 (±0.386)*

* $P<0.05$.
*** $P<0.001$.

hippocampus. Perhaps deletion of MOR results in increased levels of these neurotransmitters in the hippocampus, leading to the increase in survival of new neurons reported here. The mechanisms by which these neurotransmitters promote cell survival have not yet been elucidated, however it has been proposed that NE, and possibly ACh, promotes the survival of new neurons by increasing BDNF levels in the hippocampus (Rizk et al., 2006). Future experiments will address whether constitutive KO of MOR affects the levels of NE and BDNF in the hippocampus.

Alternatively, opioids could impact neurogenesis via direct activation of MOR. An *in vitro* study supports both the presence of MOR on hippocampal progenitors cells as well as the role of MOR in neuronal fate specification (Persson et al., 2003), and an *in vivo* study shows the presence of MOR on progenitors in another neurogenic region of the brain, the SVZ (Stiene-Martin et al., 2001). Furthermore, MOR may be expressed on a small population of cells of unknown identity in the dentate gyrus (Drake and Milner, 1999); these cells deserve further analysis for the possibility that they are progenitor cells. Studies are currently ongoing in our laboratory to establish if and when hippocampal progenitor cells and immature granule cells *in vivo* express MOR, and can thus directly respond to MOR agonists and antagonists. If these progenitor cells do express MOR, future studies could specifically KO MOR in progenitor cells or immature neurons (e.g. via viral knockdown (van Praag et al., 2002) or specific transgenic KO) to determine if direct activation of MOR in these cells is necessary for its regulatory effects on neurogenesis.

As with all constitutive KO mice, the possibility that the findings reported here are due to compensatory changes in the brain must also be considered. Potential adaptive alterations in the brains of MOR KO mice have previously been described (Hall and Uhl, 2006), including changes in the cholinergic system (discussed above), as well as changes in the dopaminergic and glutamatergic systems. In the hippocampus, MOR KO mice have been shown to have alterations in non-opioid receptor activities, including reduced dopamine D2 receptor binding (Matthies et al., 2000) and enhanced metabotropic glutamate receptor and somatostatin binding (Grecksch et al., 2004). One way to address whether the reported increase in cell survival is MOR-specific or due to compensatory changes is to examine the effects of chronic administration of an MOR antagonist. In line with our findings in the MOR KO mice, chronic naltrexone treatment in early postnatal rats increases hippocampal size and granule cell number (Zagon and McLaughlin, 1984, 1986b). *In vitro*, chronic exposure of progenitor cells to another opioid antagonist, naloxone, results in increased neurogenesis (Persson et al., 2003). However, we have found that pharmacological blockade of MOR via chronic treatment with a high dose of the opioid antagonist naltrexone in adult mice does not alter cell proliferation or survival in the SGZ (Harburg and Eisch, unpublished observations). This discrepancy with the MOR KO mice may be due to naltrexone's non-specificity since it acts on the delta and kappa opioid receptors as well (Raynor et al., 1994). This multiple opioid receptor antagonism could mask MOR-specific effects. Contradictory results have also been found with naltrexone's effects on cell proliferation in the SGZ (Persson et al., 2004; Galea et al., 2006), emphasizing the complexity of *in vivo* use of this compound, and the general challenges associated with attempts to mimic genetic manipulation with pharmacological blockade. Future studies will circumvent the natural confounds associated with constitutive KOs and the non-specificity of available MOR antagonists by studying the link between MOR and cell survival in a conditional MOR KO mouse.

Clearly, further studies are needed to elucidate whether the positive impact demonstrated here on adult neurogenesis is a result of the developmental expression of MOR on adult-generated neurons, an indirect effect such as via neurotransmitters, or perhaps a more global alteration in the hippocampal milieu that results in enhanced neurogenesis.

Implications of MOR regulation of neurogenesis on behavior

Increased neurogenesis can positively impact hippocampal function, resulting in enhanced hippocampal-dependent learning. Neurons produced by adult hippocampal neurogenesis integrate into the structure of the hippocampus, extending axons along the mossy fiber tract to CA3 (Stanfield and Trice, 1988; Hastings and Gould, 1999; Markakis and Gage, 1999; Overstreet et al., 2004; Wadiche et al., 2005). The new neurons also gain the electrophysiological properties of mature granule cells and respond appropriately to stimulus of the perforant pathway (van Praag et al., 2002) strengthening the position that these cells are functionally integrated into the synaptic circuitry of the hippocampus. Correlative evidence suggests neurogenesis can enhance hippocampal-dependent learning in rodents (Shors et al., 2001, 2002; Drapeau et al., 2003; Snyder et al., 2005). In line with this theory, heterozygote and homozygote exon 1 MOR KO mice perform better than WT littermates in the Morris water maze, a task of hippocampal-dependent memory (Meilandt et al., 2004) and have enhanced adult hippocampal neurogenesis (present data). Further exploration of adult neurogenesis and hippocampal-dependent memory in MOR KO mice is warranted given differences in key physiological measures and behavior among distinct transgenic MOR KO mice (Matthes et al., 1996; Sora et al., 1997; Kitanaka et al., 1998; Loh et al., 1998; Schuller et al., 1999; Matthies et al., 2000; Jamot et al., 2003; Jang et al., 2003; Meilandt et al., 2004; Hall and Uhl, 2006). Identification of the similarities and differences among these mice will be central to determination of the mechanism that underlies the enhanced neurogenesis reported here in MOR KO mice.

CONCLUSION

In summary, these findings implicate MOR as necessary for the survival of newly mature neurons in the hippocampus. We extrapolate that endogenous opioids may act to regulate numbers of surviving newly born neurons by bind-

ing to MOR to cause this suppression. Thus, opioids and opiates have the potential to negatively impact hippocampal-dependent learning and memory by decreasing neurogenesis.

Acknowledgments—Funding for this research was generously provided by NIH/NIDA R01 DA016765 (A.J.E.), NIDA T32 DA007290 (G.C.H.), and the NIDA Intramural Research Program (F.S.H. and G.R.U.).

REFERENCES

Abrous DN, Koehl M, Le Moal M (2005) Adult neurogenesis: from precursors to network and physiology. Physiol Rev 85:523–569.

Akaishi T, Saito H, Ito Y, Ishige K, Ikegaya Y (2000) Morphine augments excitatory synaptic transmission in the dentate gyrus through GABAergic disinhibition. Neurosci Res 38:357–363.

Ambrogini P, Cuppini R, Ferri P, Mancini C, Ciaroni S, Voci A, Gerdoni E, Gallo G (2005) Thyroid hormones affect neurogenesis in the dentate gyrus of adult rat. Neuroendocrinology 81:244–253.

Arvidsson U, Riedl M, Chakrabarti S, Lee JH, Nakano AH, Dado RJ, Loh HH, Law PY, Wessendorf MW, Elde R (1995) Distribution and targeting of a mu-opioid receptor (MOR1) in brain and spinal cord. J Neurosci 15:3328–3341.

Biebl M, Cooper CM, Winkler J, Kuhn HG (2000) Analysis of neurogenesis and programmed cell death reveals a self-renewing capacity in the adult rat brain. Neurosci Lett 291:17–20.

Cameron HA, Gould E (1996) Distinct populations of cells in the adult dentate gyrus undergo mitosis or apoptosis in response to adrenalectomy. J Comp Neurol 369:56–63.

Cameron HA, Hazel TG, McKay RD (1998) Regulation of neurogenesis by growth factors and neurotransmitters. J Neurobiol 36: 287–306.

Cameron HA, McKay RD (1999) Restoring production of hippocampal neurons in old age. Nat Neurosci 2:894–897.

Chavkin C (2000) Dynorphins are endogenous opioid peptides released from granule cells to act neurohumorly and inhibit excitatory neurotransmission in the hippocampus. Prog Brain Res 125: 363–367.

Cooper-Kuhn CM, Winkler J, Kuhn HG (2004) Decreased neurogenesis after cholinergic forebrain lesion in the adult rat. J Neurosci Res 77:155–165.

Dayer AG, Cleaver KM, Abouantoun T, Cameron HA (2005) New GABAergic interneurons in the adult neocortex and striatum are generated from different precursors. J Cell Biol 168:415–427.

Dayer AG, Ford AA, Cleaver KM, Yassaee M, Cameron HA (2003) Short-term and long-term survival of new neurons in the rat dentate gyrus. J Comp Neurol 460:563–572.

Donovan MH, Yazdani U, Norris RD, Games D, German DC, Eisch AJ (2006) Decreased adult hippocampal neurogenesis in the PDAPP mouse model of Alzheimer's disease. J Comp Neurol 495:70–83.

Drake CT, Milner TA (1999) Mu opioid receptors are in somatodendritic and axonal compartments of GABAergic neurons in rat hippocampal formation. Brain Res 849:203–215.

Drake CT, Milner TA (2002) Mu opioid receptors are in discrete hippocampal interneuron subpopulations. Hippocampus 12:119–136.

Drapeau E, Mayo W, Aurousseau C, Le Moal M, Piazza PV, Abrous DN (2003) Spatial memory performances of aged rats in the water maze predict levels of hippocampal neurogenesis. Proc Natl Acad Sci U S A 100:14385–14390.

Eisch AJ (2002) Adult neurogenesis: implications for psychiatry. Prog Brain Res 138:315–342.

Eisch AJ, Barrot M, Schad CA, Self DW, Nestler EJ (2000) Opiates inhibit neurogenesis in the adult rat hippocampus. Proc Natl Acad Sci U S A 97:7579–7584.

Eisch AJ, Harburg GC (2006) Opiates, psychostimulants, and adult hippocampal neurogenesis: Insights for addiction and stem cell biology. Hippocampus 16:271–286.

Faherty CJ, Xanthoudakis S, Smeyne RJ (1999) Caspase-3-dependent neuronal death in the hippocampus following kainic acid treatment. Brain Res Mol Brain Res 70:159–163.

Ford DH, Rhines RK (1979) Prenatal exposure to methadone HCL in relationship to body and brain growth in the rat. Acta Neurol Scand 59:248–262.

Franklin KBJ, Paxinos G (1997) The mouse brain in stereotaxic coordinates. San Diego: Academic Press.

Galea LA, Spritzer MD, Barker JM, Pawluski JL (2006) Gonadal hormone modulation of hippocampal neurogenesis in the adult. Hippocampus 16:225–232.

Geloso MC, Vercelli A, Corvino V, Repici M, Boca M, Haglid K, Zelano G, Michetti F (2002) Cyclooxygenase-2 and caspase 3 expression in trimethyltin-induced apoptosis in the mouse hippocampus. Exp Neurol 175:152–160.

Gould E, Beylin A, Tanapat P, Reeves A, Shors TJ (1999) Learning enhances adult neurogenesis in the hippocampal formation. Nat Neurosci 2:260–265.

Gould E, Woolley CS, McEwen BS (1990) Short-term glucocorticoid manipulations affect neuronal morphology and survival in the adult dentate gyrus. Neuroscience 37:367–375.

Grecksch G, Becker A, Schroeder H, Kraus J, Loh H, Hollt V (2004) Accelerated kindling development in mu-opioid receptor deficient mice. Naunyn Schmiedebergs Arch Pharmacol 369:287–293.

Gundersen HJ, Jensen EB (1987) The efficiency of systematic sampling in stereology and its prediction. J Microsc 147 (Pt 3): 229–263.

Guo M, Xu NJ, Li YT, Yang JY, Wu CF, Pei G (2005) Morphine modulates glutamate release in the hippocampal CA1 area in mice. Neurosci Lett 381:12–15.

Hall FS, Uhl GR (2006) Transgenic mouse studies reveal substantial roles for opioid receptors in the rewarding effects of several classes of addictive drugs. Curr Psychiatry Rev 2:27–37.

Harrison JM, Allen RG, Pellegrino MJ, Williams JT, Manzoni OJ (2002) Chronic morphine treatment alters endogenous opioid control of hippocampal mossy fiber synaptic transmission. J Neurophysiol 87:2464–2470.

Hastings NB, Gould E (1999) Rapid extension of axons into the CA3 region by adult-generated granule cells. J Comp Neurol 413: 146–154.

Heine VM, Maslam S, Joels M, Lucassen PJ (2004) Prominent decline of newborn cell proliferation, differentiation, and apoptosis in the aging dentate gyrus, in absence of an age-related hypothalamus-pituitary-adrenal axis activation. Neurobiol Aging 25:361–375.

Jamot L, Matthes HW, Simonin F, Kieffer BL, Roder JC (2003) Differential involvement of the mu and kappa opioid receptors in spatial learning. Genes Brain Behav 2:80–92.

Jang CG, Lee SY, Yoo JH, Yan JJ, Song DK, Loh HH, Ho IK (2003) Impaired water maze learning performance in mu-opioid receptor knockout mice. Brain Res Mol Brain Res 117:68–72.

Kahn L, Alonso G, Normand E, Manzoni OJ (2005) Repeated morphine treatment alters polysialylated neural cell adhesion molecule, glutamate decarboxylase-67 expression and cell proliferation in the adult rat hippocampus. Eur J Neurosci 21:493–500.

Kaplan TJ, Skyers PR, Tabori NE, Drake CT, Milner TA (2004) Ultrastructural evidence for mu-opioid modulation of cholinergic pathways in rat dentate gyrus. Brain Res 1019:28–38.

Karten YJ, Jones MA, Jeurling SI, Cameron HA (2006) GABAergic signaling in young granule cells in the adult rat and mouse dentate gyrus. Hippocampus 16:312–320.

Kearns IR, Morton RA, Bulters DO, Davies CH (2001) Opioid receptor regulation of muscarinic acetylcholine receptor-mediated synaptic responses in the hippocampus. Neuropharmacology 41:565–573.

Kempermann G, Kuhn HG, Gage FH (1997) More hippocampal neurons in adult mice living in an enriched environment. Nature 386: 493–495.

Kempermann G, Wiskott L, Gage FH (2004) Functional significance of adult neurogenesis. Curr Opin Neurobiol 14:186–191.

Kitanaka N, Sora I, Kinsey S, Zeng Z, Uhl GR (1998) No heroin or morphine 6beta-glucuronide analgesia in mu-opioid receptor knockout mice. Eur J Pharmacol 355:R1–R3.

Kotani S, Yamauchi T, Teramoto T, Ogura H (2006) Pharmacological evidence of cholinergic involvement in adult hippocampal neurogenesis in rats. Neuroscience 142:505–514.

Kreek MJ, Bart G, Lilly C, LaForge KS, Nielsen DA (2005) Pharmacogenetics and human molecular genetics of opiate and cocaine addictions and their treatments. Pharmacol Rev 57:1–26.

Kuhn HG, Dickinson-Anson H, Gage FH (1996) Neurogenesis in the dentate gyrus of the adult rat: age-related decrease of neuronal progenitor proliferation. J Neurosci 16:2027–2033.

Lagace DC, Yee JK, Bolanos CA, Eisch AJ (2006) Juvenile Administration of Methylphenidate Attenuates Adult Hippocampal Neurogenesis. Biol Psychiatry [Epub ahead of print], http://www.sciencedirect.com.

Lapchak PA, Araujo DM, Collier B (1989) Regulation of endogenous acetylcholine release from mammalian brain slices by opiate receptors: hippocampus, striatum and cerebral cortex of guinea-pig and rat. Neuroscience 31:313–325.

Law PY, Erickson LJ, El-Kouhen R, Dicker L, Solberg J, Wang W, Miller E, Burd AL, Loh HH (2000) Receptor density and recycling affect the rate of agonist-induced desensitization of mu-opioid receptor. Mol Pharmacol 58:388–398.

Lichtenwalner RJ, Forbes ME, Sonntag WE, Riddle DR (2006) Adult-onset deficiency in growth hormone and insulin-like growth factor-I decreases survival of dentate granule neurons: Insights into the regulation of adult hippocampal neurogenesis. J Neurosci Res 83:199–210.

Loh HH, Liu HC, Cavalli A, Yang W, Chen YF, Wei LN (1998) mu Opioid receptor knockout in mice: effects on ligand-induced analgesia and morphine lethality. Brain Res Mol Brain Res 54: 321–326.

Mandyam CD, Norris RD, Eisch AJ (2004) Chronic morphine induces premature mitosis of proliferating cells in the adult mouse subgranular zone. J Neurosci Res 76:783–794.

Mansour A, Fox CA, Burke S, Akil H, Watson SJ (1995) Immunohistochemical localization of the cloned mu opioid receptor in the rat CNS. J Chem Neuroanat 8:283–305.

Markakis EA, Gage FH (1999) Adult-generated neurons in the dentate gyrus send axonal projections to field CA3 and are surrounded by synaptic vesicles. J Comp Neurol 406:449–460.

Martinez JL Jr, Derrick BE (1996) Long-term potentiation and learning. Annu Rev Psychol 47:173–203.

Matsumoto M, Yoshioka M, Togashi H, Hirokami M, Tochihara M, Ikeda T, Smith CB, Saito H (1994) mu-Opioid receptors modulate noradrenaline release from the rat hippocampus as measured by brain microdialysis. Brain Res 636:1–8.

Matthes HW, Maldonado R, Simonin F, Valverde O, Slowe S, Kitchen I, Befort K, Dierich A, Le Meur M, Dolle P, Tzavara E, Hanoune J, Roques BP, Kieffer BL (1996) Loss of morphine-induced analgesia, reward effect and withdrawal symptoms in mice lacking the mu-opioid-receptor gene. Nature 383:819–823.

Matthies H, Schroeder H, Becker A, Loh H, Hollt V, Krug M (2000) Lack of expression of long-term potentiation in the dentate gyrus but not in the CA1 region of the hippocampus of mu-opioid receptor-deficient mice. Neuropharmacology 39:952–960.

Meibach RC, Maayani S (1980) Localization of naloxone-sensitive [3H]dihydromorphine binding sites within the hippocampus of the rat. Eur J Pharmacol 68:175–179.

Meilandt WJ, Villareal M, Hall FS, Sora I, Uhl GL, Martinez JL Jr (2004) The effects of beta-funaltrexamine on spatial learning and novel object recognition memory in exon 1 mu opioid receptor knockout mice. Proceedings of the Society for Neuroscience, San Diego, CA, 2004 Abstract Viewer and Itinerary Planner. Online, http://sfn.scholarone.com.

Ming GL, Song H (2005) Adult neurogenesis in the mammalian central nervous system. Annu Rev Neurosci 28:223–250.

Mohapel P, Leanza G, Kokaia M, Lindvall O (2005) Forebrain acetylcholine regulates adult hippocampal neurogenesis and learning. Neurobiol Aging 26:939–946.

Montaron MF, Petry KG, Rodriguez JJ, Marinelli M, Aurousseau C, Rougon G, Le Moal M, Abrous DN (1999) Adrenalectomy increases neurogenesis but not PSA-NCAM expression in aged dentate gyrus. Eur J Neurosci 11:1479–1485.

Morris BJ, Johnston HM (1995) A role for hippocampal opioids in long-term functional plasticity. Trends Neurosci 18:350–355.

Mouton PR (2002) Principles and practices of unbiased stereology: An introduction for bioscientists. Baltimore: Johns Hopkins University Press.

Nguyen XV, Masse J, Kumar A, Vijitruth R, Kulik C, Liu M, Choi DY, Foster TC, Usynin I, Bakalkin G, Bing G (2005) Prodynorphin knockout mice demonstrate diminished age-associated impairment in spatial water maze performance. Behav Brain Res 161:254–262.

Overstreet LS, Hentges ST, Bumaschny VF, de Souza FS, Smart JL, Santangelo AM, Low MJ, Westbrook GL, Rubinstein M (2004) A transgenic marker for newly born granule cells in dentate gyrus. J Neurosci 24:3251–3259.

Pak Y, Kouvelas A, Scheideler MA, Rasmussen J, O'Dowd BF, George SR (1996) Agonist-induced functional desensitization of the mu-opioid receptor is mediated by loss of membrane receptors rather than uncoupling from G protein. Mol Pharmacol 50: 1214–1222.

Persson AI, Naylor AS, Jonsdottir IH, Nyberg F, Eriksson PS, Thorlin T (2004) Differential regulation of hippocampal progenitor proliferation by opioid receptor antagonists in running and non-running spontaneously hypertensive rats. Eur J Neurosci 19:1847–1855.

Persson AI, Thorlin T, Bull C, Zarnegar P, Ekman R, Terenius L, Eriksson PS (2003) Mu- and delta-opioid receptor antagonists decrease proliferation and increase neurogenesis in cultures of rat adult hippocampal progenitors. Eur J Neurosci 17:1159–1172.

Raynor K, Kong H, Chen Y, Yasuda K, Yu L, Bell GI, Reisine T (1994) Pharmacological characterization of the cloned kappa-, delta-, and mu-opioid receptors. Mol Pharmacol 45:330–334.

Reynolds BA, Weiss S (1992) Generation of neurons and astrocytes from isolated cells of the adult mammalian central nervous system. Science 255:1707–1710.

Rizk P, Salazar J, Raisman-Vozari R, Marien M, Ruberg M, Colpaert F, Debeir T (2006) The alpha2-adrenoceptor antagonist dexefaroxan enhances hippocampal neurogenesis by increasing the survival and differentiation of new granule cells. Neuropsychopharmacology 31:1146–1157.

Sanders MJ, Kieffer BL, Fanselow MS (2005) Deletion of the mu opioid receptor results in impaired acquisition of Pavlovian context fear. Neurobiol Learn Mem 84:33–41.

Schuller AG, King MA, Zhang J, Bolan E, Pan YX, Morgan DJ, Chang A, Czick ME, Unterwald EM, Pasternak GW, Pintar JE (1999) Retention of heroin and morphine-6 beta-glucuronide analgesia in a new line of mice lacking exon 1 of MOR-1. Nat Neurosci 2: 151–156.

Shors TJ, Miesegaes G, Beylin A, Zhao M, Rydel T, Gould E (2001) Neurogenesis in the adult is involved in the formation of trace memories. Nature 410:372–376.

Shors TJ, Townsend DA, Zhao M, Kozorovitskiy Y, Gould E (2002) Neurogenesis may relate to some but not all types of hippocampal-dependent learning. Hippocampus 12:578–584.

Simmons ML, Chavkin C (1996) Endogenous opioid regulation of hippocampal function. Int Rev Neurobiol 39:145–196.

Snyder JS, Hong NS, McDonald RJ, Wojtowicz JM (2005) A role for adult neurogenesis in spatial long-term memory. Neuroscience 130:843–852.

Sora I, Takahashi N, Funada M, Ujike H, Revay RS, Donovan DM, Miner LL, Uhl GR (1997) Opiate receptor knockout mice define mu receptor roles in endogenous nociceptive responses and morphine-induced analgesia. Proc Natl Acad Sci U S A 94:1544–1549.

Spain JW, Newsom GC (1989) Chronic naltrexone enhances acquisition of the radial maze task in rats. Proc West Pharmacol Soc 32:141–142.

Spain JW, Newsom GC (1991) Chronic opioids impair acquisition of both radial maze and Y-maze choice escape. Psychopharmacology (Berl) 105:101–106.

Stanfield BB, Trice JE (1988) Evidence that granule cells generated in the dentate gyrus of adult rats extend axonal projections. Exp Brain Res 72:399–406.

Stiene-Martin A, Knapp PE, Martin K, Gurwell JA, Ryan S, Thornton SR, Smith FL, Hauser KF (2001) Opioid system diversity in developing neurons, astroglia, and oligodendroglia in the subventricular zone and striatum: impact on gliogenesis in vivo. Glia 36:78–88.

Svoboda KR, Adams CE, Lupica CR (1999) Opioid receptor subtype expression defines morphologically distinct classes of hippocampal interneurons. J Neurosci 19:85–95.

Terman GW, Drake CT, Simmons ML, Milner TA, Chavkin C (2000) Opioid modulation of recurrent excitation in the hippocampal dentate gyrus. J Neurosci 20:4379–4388.

Thomaidou D, Mione MC, Cavanagh JF, Parnavelas JG (1997) Apoptosis and its relation to the cell cycle in the developing cerebral cortex. J Neurosci 17:1075–1085.

Tien LT, Fan LW, Sogawa C, Ma T, Loh HH, Ho IK (2004) Changes in acetylcholinesterase activity and muscarinic receptor bindings in mu-opioid receptor knockout mice. Brain Res Mol Brain Res 126:38–44.

Tozuka Y, Fukuda S, Namba T, Seki T, Hisatsune T (2005) GABAergic excitation promotes neuronal differentiation in adult hippocampal progenitor cells. Neuron 47:803–815.

Uhl GR, Sora I, Wang Z (1999) The mu opiate receptor as a candidate gene for pain: polymorphisms, variations in expression, nociception, and opiate responses. Proc Natl Acad Sci U S A 96:7752–7755.

van Praag H, Schinder AF, Christie BR, Toni N, Palmer TD, Gage FH (2002) Functional neurogenesis in the adult hippocampus. Nature 415:1030–1034.

Vigano D, Rubino T, Parolaro D (2005a) Molecular and cellular basis of cannabinoid and opioid interactions. Pharmacol Biochem Behav 81:360–368.

Vigano D, Rubino T, Vaccani A, Bianchessi S, Marmorato P, Castiglioni C, Parolaro D (2005b) Molecular mechanisms involved in the asymmetric interaction between cannabinoid and opioid systems. Psychopharmacology (Berl) 182:527–536.

Wadiche LO, Bromberg DA, Bensen AL, Westbrook GL (2005) GABAergic signaling to newborn neurons in dentate gyrus. J Neurophysiol 94:4528–4532.

West MJ, Andersen AH (1980) An allometric study of the area dentata in the rat and mouse. Brain Res 2:317–348.

West MJ, Gundersen HJ (1990) Unbiased stereological estimation of the number of neurons in the human hippocampus. J Comp Neurol 296:1–22.

West MJ, Slomianka L, Gundersen HJ (1991) Unbiased stereological estimation of the total number of neurons in the subdivisions of the rat hippocampus using the optical fractionator. Anat Rec 231: 482–497.

Zagon IS, McLaughlin PJ (1977a) Effect of chronic maternal methadone exposure on perinatal development. Biol Neonate 31:271–282.

Zagon IS, McLaughlin PJ (1977b) Morphine and brain growth retardation in the rat. Pharmacology 15:276–282.

Zagon IS, McLaughlin PJ (1984) Naltrexone modulates body and brain development in rats: a role for endogenous opioid systems in growth. Life Sci 35:2057–2064.

Zagon IS, McLaughlin PJ (1986a) Opioid antagonist (naltrexone) modulation of cerebellar development: histological and morphometric studies. J Neurosci 6:1424–1432.

Zagon IS, McLaughlin PJ (1986b) Opioid antagonist-induced modulation of cerebral and hippocampal development: histological and morphometric studies. Brain Res 393:233–246.

Zhuang X, Silverman AJ, Silver R (1999) Distribution and local differentiation of mast cells in the parenchyma of the forebrain. J Comp Neurol 408:477–488.

(Accepted 5 September 2006)
(Available online 19 October 2006)

Psychopharmacology
DOI 10.1007/s00213-007-0749-4

ORIGINAL INVESTIGATION

Methamphetamine-induced locomotor activity and sensitization in dopamine transporter and vesicular monoamine transporter 2 double mutant mice

Setsu Fukushima · Haowei Shen · Harumi Hata · Arihisa Ohara · Kayo Ohmi · Kazutaka Ikeda · Yohtaro Numachi · Hideaki Kobayashi · F. Scott Hall · George R. Uhl · Ichiro Sora

Received: 6 September 2006 / Accepted: 19 February 2007

Abstract
Rationale The dopamine transporter (DAT) and the vesicular monoamine transporter 2 (VMAT2) play pivotal roles in the action of methamphetamine (MAP), including acute locomotor effects and behavioral sensitization. However, the relative impact of heterozygous DAT and VMAT2 knockouts (KOs) on the behavioral effects of MAP remains unknown.
Objectives To evaluate the roles of DAT and VMAT2 in MAP-induced locomotor behavior, we examined locomotor activity and sensitization in heterozygous DAT KO (DAT+/−), heterozygous VMAT2 KO (VMAT2+/−), double heterozygous DAT/VMAT2 KO (DAT+/−VMAT2+/−), and wild-type (WT) mice.
Results Acute 1 mg/kg MAP injection induced significant locomotor increases in WT and VMAT2+/− mice but not in DAT+/− and DAT+/−VMAT2+/− mice. Acute 2 mg/kg MAP significantly increased locomotor activity in all genotypes. Repeated 1 mg/kg MAP injections revealed a delayed and attenuated development of sensitization in DAT+/− and DAT +/−VMAT2+/− mice compared to WT mice and delayed development in VMAT2+/− mice. In repeated 2 mg/kg MAP injections, DAT+/− and DAT+/−VMAT2+/− mice showed delayed but not attenuated development of sensitization, while there was no difference in the onset of sensitization between VMAT2+/− and WT mice. In DAT+/−VMAT2+/− mice, all of MAP-induced behavioral responses were similar to those in DAT+/− but not VMAT2+/− mice.
Conclusions Heterozygous deletion of DAT attenuates the locomotor effects of MAP and may play larger role in behavioral responses to MAP compared to heterozygous deletion of VMAT2.

Keywords Sensitization · Dopamine transporter · Vesicular monoamine transporter 2 · Methamphetamine · Knockout mice · Locomotor activity · Heterozygote

S. Fukushima · H. Hata · A. Ohara · K. Ohmi · Y. Numachi · H. Kobayashi · I. Sora (✉)
Department of Biological Psychiatry,
Tohoku University Graduate School of Medicine,
1-1 Seiryo-machi,
Sendai 980-8574, Japan
e-mail: isora@mail.tains.tohoku.ac.jp

H. Shen · K. Ikeda · I. Sora
Division of Psychobiology, Tokyo Institute of Psychiatry,
Tokyo, Japan

F. S. Hall · G. R. Uhl · I. Sora
Molecular Neurobiology Branch,
National Institute on Drug Abuse-Intramural Research Program,
National Institutes of Health, DHHS,
Baltimore, MD, USA

Introduction

Methamphetamine (MAP) is a psychostimulant that induces enhanced arousal and euphoria acutely and psychosis and addiction chronically (Sato et al. 1992). The acute and chronic pharmacological consequences of MAP in human users have been observed in behavioral experiments in animals, including both hyperactivity and sensitization of locomotor responses (Segal and Schuckit 1983). Behavioral sensitization is a phenomenon whereby repeated intermittent exposure to MAP-like psychostimulant elicits a progressive enhancement of those responses, which persists for extended time periods after withdrawal from the drug and is easily reinstated by exposure to the drug or

psychosocial stress (Robinson and Becker 1986). This process closely resembles the course of the relapse in MAP-induced psychosis or schizophrenia, thus sensitization in animals has been suggested to model these psychoses (Sato et al. 1983). Behavioral sensitization is thought to be an early and enduring manifestation of neuronal plasticity associated with changes in mesolimbic dopamine neurotransmission (Kalivas et al. 1993; Kalivas and Stewart 1991). MAP induces dopamine release through exchange diffusion of plasma membrane dopamine transporter (DAT) (Seiden et al. 1993) and release of vesicular dopamine into the cytosol by acting on the vesicular monoamine transporter 2 (VMAT2) (Sulzer et al. 2005). The dopamine-releasing effect of MAP has been postulated to mediate its locomotor stimulant and rewarding effects (Pontieri et al. 1995; White and Kalivas 1998). Therefore, DAT and VMAT2 should play pivotal roles in the mechanisms underlying the actions of MAP.

DAT knockout (KO) mice and VMAT2 KO mice have been used to investigate the roles of DAT and VMAT2 in dopamine neurotransmission and pharmacological mechanisms underlying the actions of psychostimulants. Homozygous deletion of the DAT gene has been reported to produce a tenfold increase (Shen et al. 2004) or fivefold elevation (Jones et al. 1998a) of extracellular dopamine concentrations in the striatum measured by in vivo microdialysis, while heterozygous deletion of DAT was not found to significantly increase extracellular dopamine (Shen et al. 2004) or to produce a smaller twofold elevation (Jones et al. 1998a) of dopamine in the striatum. Homozygous DAT KO mice show growth retardation and hyperactivity, whereas heterozygous DAT KO mice did not show gross abnormalities in either development or baseline behavioral parameters (Giros et al. 1996; Sora et al. 1998). Habituated homozygous DAT KO mice do not show any significant cocaine-induced increase in locomotion (Giros et al. 1996; Mead et al. 2002; Sora et al. 1998; Uhl et al. 2002). However, when habituation is limited, cocaine and *d*-amphetamine can decrease locomotor activity in homozygous DAT KO mice (Gainetdinov et al. 1999). Consistent with the acute effects of psychostimulants, repeated *d*-amphetamine administration did not induce sensitization in homozygous DAT KO mice (Spielewoy et al. 2001).

Behavioral effects of psychostimulants on heterozygous DAT KO mice have been inconsistent and remain uncertain. Spielewoy et al. (2001) reported that acute and chronic *d*-amphetamine reduced locomotor activity in heterozygous DAT KO mice. Acute cocaine administration has been reported to increase locomotion in heterozygous DAT KO mice similar to wild-type (WT) mice (Giros et al. 1996; Sora et al. 1998), but Mead et al. (2002) reported that acute and chronic cocaine administration did not alter locomotion in heterozygous DAT KO mice.

As homozygous VMAT2 KO is lethal (Fon et al. 1997; Takahashi et al. 1997; Wang et al. 1997), only heterozygous VMAT2 KO mice are available for behavioral experiments. Heterozygous VMAT2 KO mice do not show gross abnormalities in development or baseline behavioral parameters (Takahashi et al. 1997). Acute amphetamine administration increased locomotor activity in heterozygous VMAT2 KO mice more than in WT mice (Takahashi et al. 1997; Uhl et al. 2000; Wang et al. 1997). Effects of chronic amphetamine or MAP administration on heterozygous VMAT2 KO mice have not yet been characterized. However, acute cocaine administration has also been shown to increase locomotor activity more in heterozygous VMAT2 KO mice than WT mice, although heterozygous VMAT2 KO mice did not apparently exhibit cocaine sensitization (Wang et al. 1997).

Thus, pharmacological responses of heterozygous DAT KO mice remain controversial, and characterization of heterozygous VMAT2 mice has been limited. Furthermore, the relative impact of VMAT2 and DAT KO on the behavioral effects of psychostimulants remains unknown. We therefore conducted studies to simultaneously examine the effects of these KOs alone and in combination. In this paper, we have directly compared behavioral responses of heterozygous DAT KO (DAT+/−), heterozygous VMAT2 KO (VMAT2+/−), combined heterozygous KO (DAT+/−VMAT+/−), and WT mice to acute and chronic MAP administration.

Materials and methods

Subjects

Individual DAT and VMAT2 KO strains used in this report have been described previously (Sora et al. 1998; Takahashi et al. 1997). All mice were bred at the Institute for Animal Experimentation, Tohoku University Graduate School of Medicine (Sendai, Japan). Mice lacking one copy of DAT and/or VMAT2 and WT littermate controls were obtained by heterozygote crosses that had been previously generated on 129Sv-C57BL/6J mixed genetic background. Genotypes of the KO mice were determined using polymerase chain reaction (PCR) with genomic DNA extracted from tail biopsies. Mice were weaned at 4 weeks of age and were group-housed (two to five per cage), segregated by sex, with food and water available ad libitum in a temperature- and light-controlled housing room (lights on at 0800 hours, lights off at 2000 hours). For locomotor testing, naïve 10–13-week-old male mice, weighing 20–35 g, were used. All experiments were conducted during the light phase of the cycle, between 9 A.M. and 5 P.M. All animal experiments were carried out according to the Guide for the Care and Use of

Laboratory Animals of Tohoku University. The experimental protocol was approved by the Animal Care and Use Committee, Tohoku University Graduate School of Medicine.

Drugs

For locomotor testing, methamphetamine hydrochloride (Dainippon-Sumitomo Pharmaceuticals, Osaka, JAPAN) dissolved in 0.9% sodium chloride (saline) was administered subcutaneously in a volume of 10 ml/kg.

Measurement of locomotor activity

Mice were placed individually in clear plastic cages (40×30×26 cm), and locomotor activity was measured in 5-min bins using digital counters with passive infrared sensors (Supermex system, Muromachi Kikai, Tokyo, Japan). In MAP-induced locomotor activity tests, the subjects were first habituated to the apparatus for 180 min and then injected with the drug or saline control subcutaneously. Locomotor activity was then assessed for 60 min post-injection. In the locomotor sensitization paradigm, mice were habituated to the test environment for 180 min and then injected with MAP (1 or 2 mg/kg) or saline subcutaneously, and locomotor activity was assessed for 60 min post-injection. This procedure was conducted eight times; sessions 1–7 were performed at 2-day intervals, and session 8 occurred 7 days after the last injection.

Statistical analysis

All data are presented as the mean±SEM. Multipoint measurements of locomotor activity in a novel environment were submitted to two-way mixed design analysis of variance (ANOVA), with time as the within-subjects factor and genotype as the between-subjects factor. MAP-induced locomotor sensitization data were submitted to two-way mixed design ANOVA, with genotype as the between-subjects factor and session as the within-subjects factor. For post hoc comparisons, Dunnett's t test was applied. Contrasted to all the above data, data from the acute MAP injection were not normally distributed. By this reason, only the acute administration data were submitted to Kruskal-Wallis test followed by Wilcoxon test with Bonferroni correction for each genotype in each drug dose. All data analyses were performed using the Statistical Package for the Social Sciences (SPSS, Tokyo, Japan).

Results

DAT/VMAT2 double heterozygous mice (DAT+/−VMAT2+/−), as well as DAT heterozygous (DAT+/−), VMAT2 heterozygous (VMAT2+/−), and WT mice did not exhibit any gross behavioral or anatomical differences. There was no difference in the rate of weight gain between the littermates of the four genotypes (data not shown).

Baseline locomotion

All mice (WT, DAT+/−, VMAT2+/−, and DAT+/−VMAT2+/−) showed the normal pattern of locomotor activity in a novel environment, with initially elevated levels that habituated to near-zero levels by the end of the period of testing (Fig. 1). There was no significant genotype effect on baseline locomotion among WT, DAT+/−, VMAT2+/−, and DAT+/−VMAT2+/− mice ($F_{3,\ 76}$=1.99, p>0.05).

Locomotor-stimulating effects of acute methamphetamine treatment

Analysis of the locomotor response to acute MAP treatment revealed a significant effect of dose in WT, DAT+/−, VMAT2+/−, and DAT+/−VMAT2+/− mice (WT: χ^2=16.65, p<0.001; DAT+/−: χ^2=13.37, p<0.01; VMAT2+/−: χ^2=10.77, p<0.01; DAT+/−VMAT2+/−: χ^2=7.45, p<0.05; Fig. 2). In post hoc comparisons, administration of 1 mg/kg MAP caused significant locomotor increases in WT and VMAT2+/− mice (p<0.01, compared to saline, respectively), but it produced no significant locomotor increases in genotypes with heterozygous deletion of DAT (DAT+/− and DAT+/−VMAT2+/− mice). Administration of 2 mg/kg MAP caused significant locomotor increase in all four genotypes: WT, DAT+/−, VMAT2, and DAT+/−VMAT2+/− (WT: p< 0.001; DAT+/−, VMAT2+/−, DAT+/−VMAT2+/−: p<0.01;

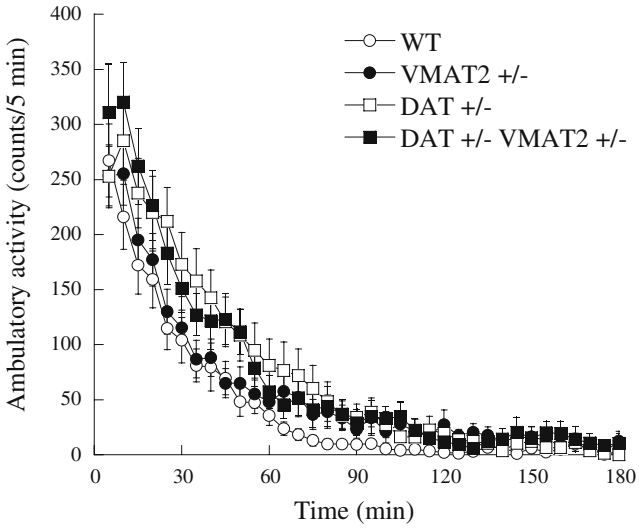

Fig. 1 Time course of locomotor activity to novelty environment in DAT and/or VMAT2 mutant mice. Time course of ambulatory activity (*beam breaks*) in WT, VMAT2+/−, DAT+/−, DAT+/−VMAT2+/− mice. Values represent mean±SEM. Number of mice (N)=19~20 per genotype

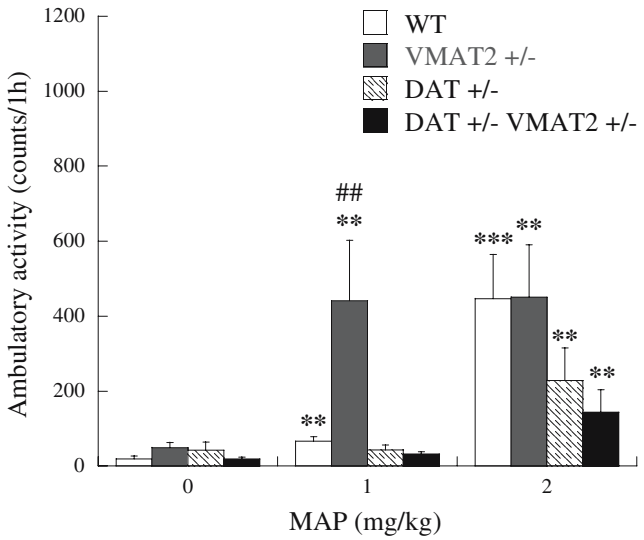

Fig. 2 Dose–response study of MAP-induced locomotor activity in mice with heterozygous deletion of the DAT and/or VMAT2 genes. Total ambulatory activity for 60 min after drug administration (saline or 1 or 2 mg/kg MAP s.c.) in WT, VMAT2+/−, DAT+/−, and DAT+/−VMAT2+/−mice. *Asterisk* Significant difference from saline treatment (**p<0.01, ***p<0.001, Wilcoxon test), *double number sign* significant difference from WT (p<0.01, Wilcoxon test). Values represent mean±SEM. N=12~20 per genotype

compared to saline, respectively). Treatment with 1 mg/kg MAP was significantly affected by genotype (χ^2=17.02, p<0.001), and when analyzed separately in post hoc comparisons, VMAT2+/− showed significantly greater increases in locomotor activity (p<0.01) compared to all other genotypes. However, after treatment with 2 mg/kg MAP, there was no significant overall effect of genotype.

Locomotor sensitization by repeated methamphetamine injections

Repeated saline injection produced no significant change in locomotor activity in any of the four genotypes: WT, DAT+/−, VMAT2+/−, and DAT+/−VMAT2+/− (Fig. 3a). Repeated 1 mg/kg MAP injections produced a significant increase in locomotor response (session $F_{7,\ 476}$=23.8, p<0.0001) that differed among genotypes as demonstrated by a significant genotype × session interaction ($F_{21,\ 476}$=3.36, p<0.001), reflecting an increase in locomotor activity over test sessions in some groups but not others. VMAT2+/− and WT mice exhibited substantial sensitization of the locomotor stimulant effects of MAP, although VMAT2+/− mice showed significant higher locomotor activity compared to WT in sessions 1 and 2 (p<0.01). By contrast, DAT+/− and DAT+/−VMAT2+/− mice showed lower locomotor responses over test sessions compared to WT mice (genotype × session: $F_{7,\ 252}$=8.09, p<0.001 for DAT+/−; $F_{7,245}$=4.27, p<0.05 for DAT+/−VMAT2+/−). In comparing locomotor activity among genotypes for each session, DAT+/− and DAT+/−VMAT2+/− mice had significantly lower locomotor activity compared to WT mice from sessions 5 to 8 (p<0.05). Thus, although DAT+/− and DAT+/−VMAT2+/− mice did show some sensitization, this was greatly reduced compared to WT mice. In individual post hoc ANOVA of each genotype, MAP significantly increased locomotor activity in WT mice from sessions 5 to 8 (p<0.05 compared to session 1), but in DAT+/−, VMAT2+/−, and DAT+/−VMAT2+/− mice, MAP-induced locomotor activity was enhanced compared to values in session 1 only after sessions 7 and 8 (p<0.05 compared to session 1). These data demonstrate a delayed and attenuated development of sensitization in DAT+/− and DAT+/−VMAT2+/− mice compared to WT mice and a slight delay in VMAT2+/− mice (Fig. 3b).

Repeated MAP injections with a higher dose (2 mg/kg) produced a significant increase in the locomotor response overall (session $F_{7,\ 336}$=11.02, p<0.0001) that differed between groups as demonstrated by a significant genotype × session interaction ($F_{21,\ 336}$=2.68, p<0.001), again representing differences in sensitization dependent upon genotype. DAT+/− and DAT+/−VMAT2+/− mice had reduced locomotor responses initially compared to WT mice but eventually reached the same levels of the activity by session 8, whereas VMAT 2+/− mice showed greater locomotor responses from sessions 4 to 6, which also stabilized at near-WT levels by session 7 (genotype × session: $F_{7,\ 147}$=3.84, p<0.01). Individual post hoc tests for each genotype indicated that MAP significantly increased locomotor activity at sessions 4, 7, and 8 (p<0.05, compared to session 1) in WT mice, at sessions 4, 5, and 6 (p<0.05, compared to session 1) in VMAT2+/− mice, at sessions 6 and 8 (p<0.05, compared to session 1) in DAT+/− mice, and at sessions 6, 7, and 8 (p<0.05, compared to session 1) in DAT+/−VMAT2+/− mice. As was observed after sensitization with the lower dose of MAP, the development of sensitization was delayed in DAT+/− and DAT+/−VMAT2+/− mice compared to WT mice after repeated injection of 2 mg/kg MAP. VMAT2+/− mice showed significantly higher locomotor responses in sessions 5 and 6 compared to WT mice (p<0.05), but this difference was not observed in later sessions (Fig. 3c).

Discussion

Our results suggest that the reduced DAT and VMAT2 expression have different effects on MAP-induced locomotor responses and the development of sensitization and, furthermore, that the reduced expression of the DAT gene has a greater influence on MAP-induced sensitization than the reduced expression of the VMAT2 gene.

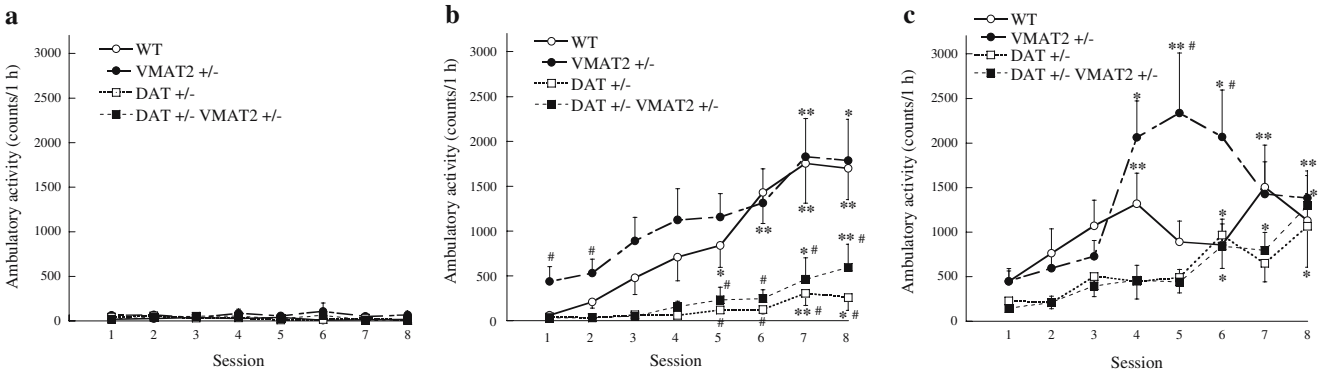

Fig. 3 **a**–**c** Sensitization of MAP-induced locomotor activity in mice with heterozygous deletion of the DAT and/or VMAT2 genes. Total ambulatory activity for 60 min of testing after saline (**a**), 1 mg/kg MAP (**b**), 2 mg/kg MAP (**c**) with 2-day intervals (sessions 1–7) and 1 week interval (session 8). Repeated administration of MAP in WT, VMAT2+/−, DAT+/−, and DAT+/−VMAT2+/−mice. *Asterisk* Significant difference from session 1 (*$p<0.05$, **$p<0.01$, Dunnett's *t* test), *number sign* significant difference from WT ($p<0.05$, Dunnett's *t* test). Values represent mean±SEM. $N=12\sim20$ per genotype

Acute administration of 1 mg/kg MAP did not increase locomotor activity in heterozygous DAT KO mice, while a higher dose of MAP (2 mg/kg) did induce a significant increase in locomotor activity in those mice compared to saline controls, but the magnitude of this increase was a half of that observed in WT mice. These data indicate a rightward shift in the dose–response curve for MAP in heterozygous DAT KO mice. Reports have suggested that DAT blockers suppress amphetamine-mediated dopamine release (Baumann et al. 2002; Sulzer et al. 1995; Villemagne et al. 1999) and that the dopamine-releasing action of amphetamines is dependent on DAT expression (Eshleman et al. 1994; Giros et al. 1996; Jones et al. 1998b). DAT expression in heterozygous DAT KO mice is reduced by half compared to WT mice (Sora et al. 1998, 2001). Thus, the decreased response of heterozygous DAT KO mice to acute MAP administration might reflect attenuation of MAP-induced dopamine release due to reduced DAT expression. Alternatively, changes in other aspects of dopamine neurotransmission in heterozygous DAT KO mice might underlie the decreased response to MAP administration in these mice. Of importance in considering these possibilities are previous in vivo microdialysis data demonstrating that heterozygous deletion of the DAT gene did not alter basal extracellular dopamine in the striatum or nucleus accumbens of mutant mice (Shen et al. 2004). While tissue dopamine concentrations and dopamine D2 receptor expression in the striatum were not reported to be altered in heterozygous DAT KO mice compared to WT mice (Sora et al. 2001), other studies have reported changes in dopaminergic function in heterozygous DAT KO mice. Using other methods in heterozygous DAT KO mice, in vivo quantitative microdialysis has demonstrated that heterozygous deletion of DAT induces a twofold elevation of basal extracellular dopamine level in the striatum (Jones et al. 1998a), while electrically stimulated dopamine release and the dopamine clearance rate constant are reduced by half compared to WT mice (Giros et al. 1996; Jones et al. 1998a), and tissue dopamine concentrations and tyrosine hydroxylase levels in the striatum were reported to be decreased (Jones et al. 1998a). In addition, dopamine D1 and D2 receptor mRNA levels are down-regulated in the basal ganglia of heterozygous DAT KO mice (Giros et al. 1996). Given the conflicting and apparently opposing changes in various indices of dopamine neurotransmission, the mechanism of the reduced behavioral responses of heterozygous DAT KO mice to MAP administration cannot be determined absolutely, although it appears likely that reduced DAT expression itself may be the main mechanism.

In contrast to the effects of heterozygous DAT KO, it is interesting to note that 1 mg/kg MAP administration had greater effects on locomotor activity in heterozygous VMAT2 KO mice than in WT mice. These effects with MAP are consistent with previous findings that heterozygous deletion of VMAT2 increased the locomotor-stimulating effects of *d*-amphetamine (Takahashi et al. 1997; Wang et al. 1997). Single 2 mg/kg MAP administration also increased locomotion of heterozygous VMAT2 KO mice, but the magnitude of the increase was equivalent to the increase observed in WT mice, indicating that VMAT2 KO induces a leftward shift in the dose–response curve. Previous in vivo microdialysis data have demonstrated that basal and *d*-amphetamine-induced extracellular dopamine in the striatum is reduced in heterozygous VMAT2 KO mice (Wang et al. 1997). In addition, amphetamine-induced dopamine release from midbrain cell cultures from heterozygous VMAT2 KO mice was reduced (Fon et al. 1997). In these mutant mice, striatal dopamine D1 and D2 receptor mRNA and overall receptor binding were not altered (Takahashi et al. 1997; Wang et al. 1997). Wang et al. (1997)

suggested that functional changes in dopamine receptors may underlie the hypersensitivity to the low dose of MAP in heterozygous VMAT2 KO mice. Alternatively, serotonin and norepinephrine neurotransmissions that are also affected by heterozygous VMAT2 gene deletion may have some role in the increased sensitivity to MAP in heterozygous VMAT2 KO mice.

In mice with combined heterozygous KO of DAT and VMAT2, 1 mg/kg MAP did not induce hyperlocomotion. The behavioral patterns of the DAT/VMAT2 double KO mice were the same as heterozygous DAT KO mice. Heterozygous VMAT2 KO mice have been reported to have normal levels (Gainetdinov et al. 1998) or slight (16%) reductions (Takahashi et al. 1997) in the number of striatal DAT binding sites, and the dopamine uptake function of DAT in heterozygous VMAT2 KO mice was not different from WT mice (Gainetdinov et al. 1998). Nonetheless, baseline and *d*-amphetamine-induced extracellular dopamine in the striatum is reduced in heterozygous VMAT2 KO mice (Wang et al. 1997). Thus, in mice with double heterozygous KO of DAT and VMAT2, reduction in released dopamine in the synaptic cleft due to half deletion of VMAT2, concurrent with the decrease in reuptake due to half deletion of DAT, might prevent some alterations in dopamine function that would otherwise occur from either KO alone. At the same time, the MAP-induced elevation of extracellular dopamine in the striatum may be more greatly affected by combined deletion of VMAT2 and DAT than that observed by VMAT2 alone. In transgenic mice with 95% reduced expression of the VMAT2 (KA1 VMAT2 mutant), amphetamine-induced dopamine release of striatal slices was reduced compared to WT mice, and the DAT inhibitor GBR12935 further attenuated the dopamine release (Patel et al. 2003), suggesting a synergy of effects on MAP-induced dopamine release by reduction in both DAT and VMAT2 expressions. However, the finding that single-MAP treatment in mice with double heterozygous deletion of DAT and VMAT2 produced almost the same effect as in heterozygous DAT KO mice indicates that half deletion of DAT is the dominant factor determining the locomotor-stimulating effect of single MAP treatment compared to the effect of half deletion of VMAT2.

Repeated administration of 1 mg/kg MAP sensitized locomotor responses in heterozygous DAT KO mice. However, the magnitude of increase in locomotor activity was lower, and the development of sensitization was delayed compared to WT mice. Lasting locomotor inhibitory responses and delayed sensitization in heterozygous DAT KO mice could be attributed to the initial poor locomotor response that was observed after acute MAP treatment of these mice. Interestingly, the dose of MAP that did not induce locomotor responses after the first treatment led to sensitization after repeated treatments. Spielewoy et al. (2001) reported that heterozygous DAT KO mice showed hypolocomotor activity after administration of 1 mg/kg *d*-amphetamine but not after higher doses up to 10 mg/kg and furthermore that the effect of *d*-amphetamine was enhanced after repeated exposures to the drug. Contrary to the effect of *d*-amphetamine on heterozygous DAT KO mice, the current study found that administration of MAP did not induce a hypolocomotor effect in heterozygous DAT KO mice. One possibility that might explain this discrepancy is that Spielewoy et al. (2001) used mice backcrossed for 12 generations on a C57BL/6 background, whereas we used mice on a mixed 129Sv/C57B6 background. Genetic background of mice is an important factor that may affect the consequences of gene deletion (Schlussman et al. 1998; Zhang et al. 2001). Another factor that may have an impact upon studies is the amount of habituation to the environment before drug injection. In the study of Spielewoy et al. (2001), mice were placed in the activity boxes immediately after injection, whereas mice were habituated in the test box for 3 h, and basal activity was largely, although not completely, equalized in our study. The degree of habituation has long been known to influence the effect of psychostimulants on locomotor activity (Dews and Wenger 1977; Robbins 1977). After repeated administration of higher doses (2 mg/kg) MAP, we observed that both the onset of the establishment of sensitization and the magnitude of sensitization were accelerated compared to 1 mg/kg MAP injections in heterozygous DAT KO mice as well as in WT mice. This result may reflect dose-dependent increase in MAP-induced extracellular dopamine levels in heterozygous DAT KO mice.

In the 1 mg/kg MAP sensitization experiment, development of sensitization in heterozygous VMAT2 KO mice was delayed. Although MAP-induced dopamine release was reduced in heterozygous VMAT2 mice (Fon et al. 1997; Wang et al. 1997), they had a greater initial locomotor response to 1 mg/kg MAP administration, suggesting that a greater behavioral response to first MAP administration does not necessarily accelerate the development of sensitization, and released dopamine levels may play more dominant role in the development of sensitization. Alternatively, hyperactivity after single MAP treatment may induce some tolerance in locomotor responses to initial MAP injections in heterozygous VMAT2 mice. In 2 mg/kg MAP sensitization experiments, there was no difference in heterozygous VMAT2 mice in the onset of sensitization compared to WT mice, indicating that half deletion of VMAT2 has some effect on the development of MAP sensitization but is not sufficient to completely eliminate it.

In double heterozygous DAT/VMAT2 KO mice, repeated administration of either 1 mg/kg or 2 mg/kg MAP

induced sensitization. The magnitude of the locomotor response and latency to the onset of sensitization were similar to what was observed in heterozygous DAT KO mice but not heterozygous VMAT2 KO mice, suggesting that the half deletion of DAT is more crucial in determining the magnitude of locomotor responses in chronic MAP administration and latency to the establishment of sensitization than the half deletion of VMAT2.

In conclusion, behavioral effects of both acute and chronic MAP administration were suppressed in heterozygous DAT KO mice, whether or not it was combined with heterozygous VMAT2 KO. Contrary to the effect observed in heterozygous DAT KO mice, acute MAP administration produced greater locomotor responses in heterozygous VMAT2 KO mice. While repeated 1 mg/kg MAP administration induced sensitization to an equivalent extent in heterozygous VMAT2 KO and WT mice, the latency until the establishment of behavioral sensitization was delayed in the mutant mice. In response to repeated 2 mg/kg MAP injections, there was no difference in the onset of sensitization between heterozygous VMAT2 KO and WT mice. These findings indicate that the half deletion of DAT plays a major role in both acute and chronic behavioral responses to MAP, while the effect of the half deletion of VMAT2 is less prominent. These findings lead us to hypothesize that DAT variants may have more profound effects than VMAT2 variants on the clinically important consequences of acute and chronic MAP abuse in humans.

Acknowledgment We thank Maki Naka for technical assistance. This study was supported in part by the Intramural Research Program of the NIH, NIDA (USA), Grant-in-Aid for Health and Labor Science Research (Research on Psychiatric and Neurological Diseases, Research on Pharmaceutical and Medical Safety) from the Ministry of Health, Labor and Welfare of Japan; by Grants-in-Aid for Scientific Research (B), Scientific Research on Priority Areas-System study on higher-order brain functions and Research on Pathomechanisms of Brain Disorders-, Core Research for Evolutional Science and Technology (CREST), from the Ministry of Education, Culture, Sports, Science and Technology of Japan (No. 17390315, 17022007, 18023007); and by the Mitsubishi Pharma Research Foundation.

References

Baumann MH, Ayestas MA, Sharpe LG, Lewis DB, Rice KC, Rothman RB (2002) Persistent antagonism of methamphetamine-induced dopamine release in rats pretreated with GBR12909 decanoate. J Pharmacol Exp Ther 301:1190–1197

Dews PB, Wenger WG (1977) Rate-dependency of the behavioral effects of amphetamine. In: Thompson T, Dews PB (eds) Advances in behavioral pharmacology. Academic, New York, pp 167–227

Eshleman AJ, Henningsen RA, Neve KA, Janowsky A (1994) Release of dopamine via the human transporter. Mol Pharmacol 45:312–316

Fon EA, Pothos EN, Sun BC, Killeen N, Sulzer D, Edwards RH (1997) Vesicular transport regulates monoamine storage and release but is not essential for amphetamine action. Neuron 19:1271–1283

Gainetdinov RR, Fumagalli F, Wang YM, Jones SR, Levey AI, Miller GW, Caron MG (1998) Increased MPTP neurotoxicity in vesicular monoamine transporter 2 heterozygote knockout mice. J Neurochem 70:1973–1978

Gainetdinov RR, Wetsel WC, Jones SR, Levin ED, Jaber M, Caron MG (1999) Role of serotonin in the paradoxical calming effect of psychostimulants on hyperactivity. Science 283:397–401

Giros B, Jaber M, Jones SR, Wightman RM, Caron MG (1996) Hyperlocomotion and indifference to cocaine and amphetamine in mice lacking the dopamine transporter. Nature 379:606–612

Jones SR, Gainetdinov RR, Jaber M, Giros B, Wightman RM, Caron MG (1998a) Profound neuronal plasticity in response to inactivation of the dopamine transporter. Proc Natl Acad Sci U S A 95:4029–4034

Jones SR, Gainetdinov RR, Wightman RM, Caron MG (1998b) Mechanisms of amphetamine action revealed in mice lacking the dopamine transporter. J Neurosci 18:1979–1986

Kalivas PW, Stewart J (1991) Dopamine transmission in the initiation and expression of drug-and stress-induced sensitization of motor activity. Brain Res Brain Res Rev 16:223–244

Kalivas PW, Sorg BA, Hooks MS (1993) The pharmacology and neural circuitry of sensitization to psychostimulants. Behav Pharmacol 4:315–334

Mead AN, Rocha BA, Donovan DM, Katz JL (2002) Intravenous cocaine induced-activity and behavioural sensitization in norepinephrine-, but not dopamine-transporter knockout mice. Eur J Neurosci 16:514–520

Patel J, Mooslehner KA, Chan PM, Emson PC, Stamford JA (2003) Presynaptic control of striatal dopamine neurotransmission in adult vesicular monoamine transporter 2 (VMAT2) mutant mice. J Neurochem 85:898–910

Pontieri FE, Tanda G, Di Chiara G (1995) Intravenous cocaine, morphine, and amphetamine preferentially increase extracellular dopamine in the "shell" as compared with the "core" of the rat nucleus accumbens. Proc Natl Acad Sci U S A 92:12304–12308

Robbins TW (1977) A critique of the methods available for the measurement of spontaneous motor activity. In: Iverson LL, Synder SH (eds) Handbook of psychopharmacology. Plenum, New York, pp 37–82

Robinson TE, Becker JB (1986) Enduring changes in brain and behavior produced by chronic amphetamine administration: a review and evaluation of animal models of amphetamine psychosis. Brain Res 396:157–198

Sato M, Chen CC, Akiyama K, Otsuki S (1983) Acute exacerbation of paranoid psychotic state after long-term abstinence in patients with previous methamphetamine psychosis. Biol Psychiatry 18:429–440

Sato M, Numachi Y, Hamamura T (1992) Relapse of paranoid psychotic state in methamphetamine model of schizophrenia. Schizophr Bull 18:115–122

Schlussman SD, Ho A, Zhou Y, Curtis AE, Kreek MJ (1998) Effects of "binge" pattern cocaine on stereotypy and locomotor activity in C57BL/6J and 129/J mice. Pharmacol Biochem Behav 60:593–599

Segal DS, Schuckit MA (1983) Animal models of stimulant-induced psychosis. In: Grees I (ed) Stimulants: neurochemical, behavioral and clinical perspectives. Reven, New York, pp 131–167

Seiden LS, Sabol KE, Ricaurte GA (1993) Amphetamine: effects on catecholamine systems and behavior. Annu Rev Pharmacol Toxicol 33:639–677

Shen HW, Hagino Y, Kobayashi H, Shinohara-Tanaka K, Ikeda K, Yamamoto H, Yamamoto T, Lesch KP, Murphy DL, Hall FS, Uhl GR, Sora I (2004) Regional differences in extracellular dopamine and serotonin assessed by in vivo microdialysis in mice lacking dopamine and/or serotonin transporters. Neuropsychopharmacology 29:1790–1799

Sora I, Wichems C, Takahashi N, Li XF, Zeng Z, Revay R, Lesch KP, Murphy DL, Uhl GR (1998) Cocaine reward models: conditioned

place preference can be established in dopamine-and in serotonin-transporter knockout mice. Proc Natl Acad Sci U S A 95:7699–7704

Sora I, Hall FS, Andrews AM, Itokawa M, Li XF, Wei HB, Wichems C, Lesch KP, Murphy DL, Uhl GR (2001) Molecular mechanisms of cocaine reward: combined dopamine and serotonin transporter knockouts eliminate cocaine place preference. Proc Natl Acad Sci U S A 98:5300–5305

Spielewoy C, Biala G, Roubert C, Hamon M, Betancur C, Giros B (2001) Hypolocomotor effects of acute and daily d-amphetamine in mice lacking the dopamine transporter. Psychopharmacology (Berl) 159:2–9

Sulzer D, Chen TK, Lau YY, Kristensen H, Rayport S, Ewing A (1995) Amphetamine redistributes dopamine from synaptic vesicles to the cytosol and promotes reverse transport. J Neurosci 15:4102–4108

Sulzer D, Sonders MS, Poulsen NW, Galli A (2005) Mechanisms of neurotransmitter release by amphetamines: a review. Prog Neurobiol 75:406–433

Takahashi N, Miner LL, Sora I, Ujike H, Revay RS, Kostic V, Jackson-Lewis V, Przedborski S, Uhl GR (1997) VMAT2 knockout mice: heterozygotes display reduced amphetamine-conditioned reward, enhanced amphetamine locomotion, and enhanced MPTP toxicity. Proc Natl Acad Sci U S A 94:9938–9943

Uhl GR, Li S, Takahashi N, Itokawa K, Lin Z, Hazama M, Sora I (2000) The VMAT2 gene in mice and humans: amphetamine responses, locomotion, cardiac arrhythmias, aging, and vulnerability to dopaminergic toxins. FASEB J 14:2459–2465

Uhl GR, Hall FS, Sora I (2002) Cocaine, reward, movement and monoamine transporters. Mol Psychiatry 7:21–26

Villemagne VL, Wong DF, Yokoi F, Stephane M, Rice KC, Matecka D, Clough DJ, Dannals RF, Rothman RB (1999) GBR12909 attenuates amphetamine-induced striatal dopamine release as measured by [(11)C]raclopride continuous infusion PET scans. Synapse 33:268–273

Wang YM, Gainetdinov RR, Fumagalli F, Xu F, Jones SR, Bock CB, Miller GW, Wightman RM, Caron MG (1997) Knockout of the vesicular monoamine transporter 2 gene results in neonatal death and supersensitivity to cocaine and amphetamine. Neuron 19:1285–1296

White FJ, Kalivas PW (1998) Neuroadaptations involved in amphetamine and cocaine addiction. Drug Alcohol Depend 51:141–153

Zhang Y, Schlussman SD, Ho A, Kreek MJ (2001) Effect of acute binge cocaine on levels of extracellular dopamine in the caudate putamen and nucleus accumbens in male C57BL/6J and 129/J mice. Brain Res 923:172–177

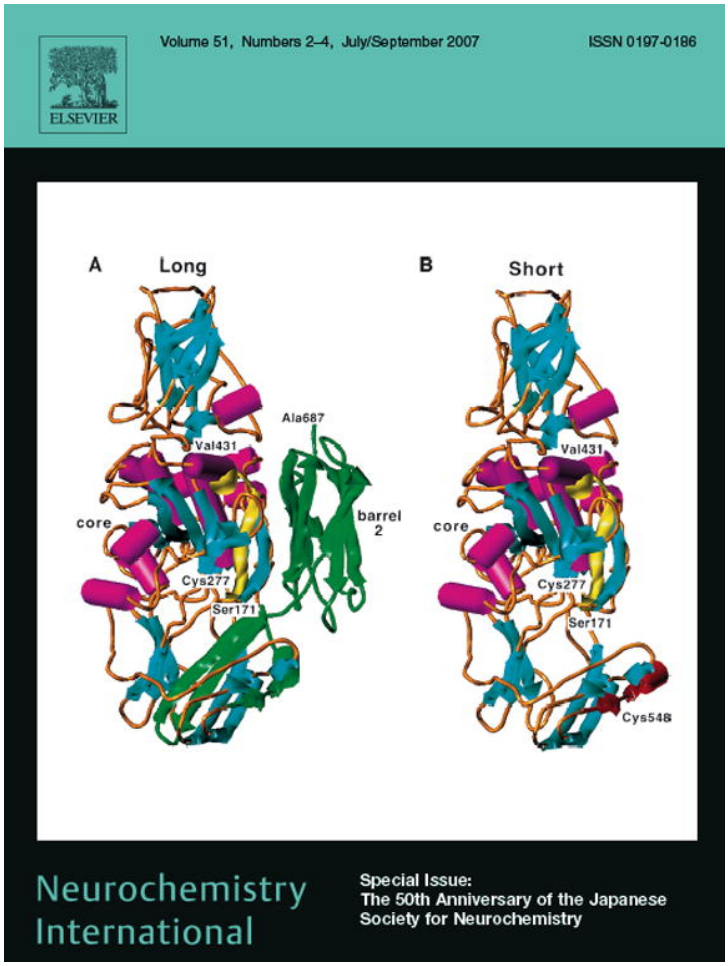

Available online at www.sciencedirect.com
ScienceDirect
Neurochemistry International 51 (2007) 237–244
NEUROCHEMISTRY International
www.elsevier.com/locate/neuint

Genetic deletion of vesicular monoamine transporter-2 (VMAT2) reduces dopamine transporter activity in mesencephalic neurons in primary culture

Hideko Yamamoto [a,*], Etsuko Kamegaya [a], Yoko Hagino [a], Kazuhide Imai [b], Akihiro Fujikawa [c], Kohei Tamura [a,d], Tomoyuki Enokiya [d], Toshifumi Yamamoto [a,d], Takao Takeshima [e], Hisashi Koga [b], George R. Uhl [f], Kazutaka Ikeda [a], Ichiro Sora [g]

[a] *Division of Psychobiol., Tokyo Institute of Psychiatry, 2-1-8 Kamikitazawa, Setagaya-ku, Tokyo 156-8585, Japan*
[b] *Department of Human Genome Technology, Kazusa DNA Research Institute, Chiba, Japan*
[c] *Division of Molecular Neurobiology, National Institute for Basic Biology, Okazaki, Japan*
[d] *Molecular Recognition, Yokohama City University, Yokohama, Japan*
[e] *Neurology, Institute of Neurological Sciences, Tottori University, Faculty of Medicine, Tottori, Japan*
[f] *Molecular Neurobiology Branch, NIDA, NIH, Baltimore, USA*
[g] *Department of Psychobiology, Tohoku University, School of Medicine, Sendai, Japan*

Received 31 March 2007; received in revised form 8 June 2007; accepted 16 June 2007
Available online 29 June 2007

Abstract

Our aim was to investigate whether a defect in vesicular monoamine transporter-2 (VMAT2) activities would affect dopaminergic cell functions or not. We examined mesencephalon dopaminergic cultures prepared from VMAT2 wild-type, heterozygous or homozygous knockout (KO) 14-day-old mouse fetuses to determine the number of tyrosine hydroxylase (TH)-positive cells and dopamine transporter activity. The number of TH-positive cells remained unchanged in the VMAT2-KO cultures. Of interest, the dopamine transporter activity in the homozygous cells was significantly decreased, but not in the heterozygous cells, suggesting that complete deletion of VMAT2 inhibited dopamine transporter function. Furthermore, dopamine transporter activity was prominently decreased in the synaptosomal fraction of neonatal homozygous VMAT2-KO mice compared with that of wild-type/heterozygous VMAT2-KO ones, indicating that VMAT2 activity might be one of the factors regulating dopamine transporter activities. To test this possibility, we used reserpine, a VMAT2 inhibitor. Reserpine (1 μM) decreased dopamine transporter activity (approx. 50%) in wild-type and heterozygous VMAT2-KO cultures but not in homozygous ones, indicating that blockade of VMAT2 activity reduced dopamine transporter activity. To investigate possible mechanisms underlying the decreased dopamine transporter activity in VMAT2-KO mice, we measured dopamine transporter activities after 24–48 h exposure of primary cultures of mesencephalic neurons to dopamine receptor antagonists, PKC inhibitor, PI_3K inhibitor, and L-DOPA. Among these drugs, L-DOPA slightly reduced the dopamine transporter activities of all genotypes, but the other drugs could not. Since the ratios of reduction in dopamine transporter activity of each genotype treated with L-DOPA were similar, substrate inhibition of dopamine transporters was not the main mechanism underlying the reduced dopamine transporter activity due to genetic deletion of VMAT2. Our results demonstrate that genetic deletion of VMAT2 did not induce immediate cell death but did markedly inhibit dopamine transporter activity.

Keywords: VMAT2-KO; DAT; Primary brain stem culture; mKIAA gene

1. Introduction

Dysfunction of dopamine (DA) neurons has been implicated in several neurodegenerative and neuropsychiatric disorders, including Parkinson's disease, addiction, bipolar disorder, and depression. DA neurons in the substantia nigra (SN) degenerate in Parkinson's disease, whilst ventral tegmental area (VTA) DA neurons are thought to be involved in addiction and mood disorders. The magnitude and duration of dopaminergic signaling are defined by the amount of DA released, the sensitivity of the DA receptors, and the efficiency of DA clearance.

* Corresponding author. Tel.: +81 3 3304 5701; fax: +81 3 3329 8035.
E-mail address: yamahide@prit.go.jp (H. Yamamoto).

0197-0186/$ – see front matter © 2007 Elsevier Ltd. All rights reserved.
doi:10.1016/j.neuint.2007.06.022

Vesicular release of DA is dependent on vesicular monoamine transporter-2 (VMAT2) activities of DA neurons in the CNS. VMAT2 is expressed on the monoaminergic secretory vesicles in the CNS (Erickson et al., 1992; Erickson and Eiden, 1993) and is responsible for packaging DA, noradrenalin, serotonin, and histamine in the neuronal cytoplasm into synaptic vesicles (Johnson, 1988; Henry et al., 1994; Liu et al., 1992; Erickson et al., 1992). VMAT2-knockout (KO) mice completely lacking VMAT2 survive less than a few days after birth (Fon et al., 1997; Takahashi et al., 1997; Wang et al., 1997), whereas mice that express approx. 5% of the normal VMAT2 level are viable into adulthood (Mooslehner et al., 2001). The brains of VMAT2-KO mice show extremely low contents of catecholamines including serotonin, noradrenalin, and DA (Fon et al., 1997). Lack of VMAT2 causes depletion of DA in synaptic vesicles, and cytoplasmic DA is immediately metabolized by monoamine oxidase.

In heterozygous VMAT2-KO mice, the administration of the MPP^+ precursor *N*-methyl-4-phenyl-1,2,3,6-tetrahydropyridine produces more than twice the DA cell loss found in wild-type mice treated with the precursor (Takahashi et al., 1997). Also, VMAT2 has been implicated in effecting methamphetamine-induced DA deficits. Methamphetamine-induced dopaminergic neurotoxicity is increased in the striatum of VMAT2-KO mice compared with that in wild-type mice, as revealed by a more consistent DA and metabolite depletion and a greater decrease in DA transporter (DAT) expression (Fumagalli et al., 1999). The DAT is largely responsible for regulating DA clearance (Giros et al., 1996) and is a main target of amphetamines.

Of interest, morphometric analysis of cultured midbrain DA neurons from wild-type and VMAT2-KO mice has revealed that the ultrastructure of DA terminals and synaptic vesicles in the neurons from VMAT2-KO mice is indistinguishable from that of those in wild-type cultures (Croft et al., 2005). Also, VMAT2-KO does not influence the total number of synaptic vesicles or their ability to cycle (Croft et al., 2005). These studies using VMAT2-KO mice have yielded an abundance of valuable information; however, aside from the neurotoxicity caused by genetic deletion of VMAT2, the effects of this deletion on dopaminergic cell functions are not clear.

Here, we investigated dopaminergic neurons more precisely by using midbrain cultures derived from fetuses of wild-type and VMAT2-KO (heterozygous and homozygous) mice. We found that DAT activity was reduced by genetic deletion or pharmacological blockade of VMAT2. In addition, the results of cDNA array experiments showed a difference in the gene expression profile between wild-type and VMAT2-KO mice.

2. Materials and methods

2.1. Animals and genotype

Timed pregnant heterozygous VMAT2-KO mice that had been mated with male heterozygous VMAT2-KO mice (Takahashi et al., 1997) were used. The experimental procedures and housing conditions were approved by our Institutional Animal Care and Use Committee, and all animals were cared for and treated humanely in accordance with our institutional guidelines on animal experimentation. VMAT2 genotypic status was assessed by PCR using primers (5′-GTG CCC AGT TTA TGT AGC ATT G-3′), (5′-TTG AGT CGG ATG TCT TCA TCC T-3′), and neomycin resistant gene (neo) primer (5′-TCG ACG TTG TCA CTG AAG CGG-3′), yielding a 0.4-kb fragment in wild-type alleless and a 0.9-kb neo fragment in KO alleles after amplification performed in a 20 μl volume containing 50 ng of genomic DNA, 400 μM dNTPs, 400 pM concentration of each primer, 2.5 mM $MgCl_2$, 1 × PCR buffer, and 0.05 U of LA Taq polymerase (PCR reagents by TAKARA BIO Inc, Shiga, Japan). Fragments were amplified by initial denaturation at 94 °C (5 min), followed by 35 cycles at 94 °C (60 s), 57 °C (60 s), and 72 °C (60 s).

2.2. Culture of mesencephalic dopaminergic neurons

The preparation of primary cultures of mesencephalic cells was as described previously (Shimoda et al., 1992), with a few modifications. In brief, timed-pregnant heterozygous VMAT2-KO mice were anesthetized with diethyl ether. On the 14th gestational day (E 14), the fetal heads were removed and collected in cold DMEM. Subsequently, the brainstems were isolated under a dissecting microscope; and the rest of the brain tissue was frozen until genotyping could be performed. Each brainstem in culture medium was immediately triturated by using a 1000-μl volume pipette, and the dispersed cells were diluted with culture medium and plated in poly-L-lysine-coated 96-well tissue culture dishes (BD Sciences, Franklin Lakes, NJ, USA) or poly-D-lysine-coated 8-well culture slide (Becton Dickinson Labware, Bedford, MA, USA). The culture medium was composed of 90% DMEM supplemented with 10% fetal bovine serum, 10 μg/ml insulin, 0.1 mg/ml human apotransferrin, 100 μM putrescine, 1 mM sodium pyruvate, and 10 nM progesterone. Two days after plating, the medium was changed to serum-free culture medium. Serum-free culture medium of the above composition was supplemented with 1 mg/ml bovine serum albumin, 1 nM 3,3′,5-triiodo-L-thyronine, 1 μg/ml aprotinin, and 30 nM selenium in place of the 10% fetal bovine serum (Yamamoto et al., 1995). At 4 or 5 days *in vitro* (DIV), the cells were treated with drugs; and then at 6 DIV the cells were used for analysis.

2.3. Synaptosomal [^{3}H]DA uptake

Neonatal mouse pups were killed by decapitation, and their brains were removed. The hemispheres (cerebrum, hippocampus, and striatum) of each mouse were dissected on ice and homogenized with 1.5 ml of ice-cold 10 mM phosphate buffer, pH 7.4, containing 0.32 M sucrose and 1 mM EGTA. Each homogenate was linked to VMAT2 genotypic status assessed by PCR as described above. Uptake of [^{3}H]DA was determined according to a modification of a method described by Boja et al. (1992). First, the homogenate was centrifuged (800 × *g* for 12 min; 4 °C). The resulting supernatant (S_1) was then centrifuged (20,000 × *g* for 25 min; 4 °C), and the pellet (P_2) resuspended in ice-cold modified Kreb's buffer. Assays were conducted in modified Kreb's buffer (in mM: NaCl, 126; KCl, 4.8; $CaCl_2$, 1.3; sodium phosphate, 16; $MgSO_4$, 1.4; dextrose, 11; ascorbic acid, 1; pH 7.4). Each assay tube contained synaptosomal tissue and 0.1 mM pargyline. Nonspecific values were determined in the presence of 10 μM GBR12909, a specific DAT inhibitor. After preincubation of assay tubes for 10 min at 37 °C, assays were initiated by the addition of [^{3}H]DA (0.3 nM final concentration). Samples were incubated at 37 °C for 3 min and then filtered through Whatman GF/B filters soaked previously in 0.05% polyethylenimine. The filters were washed rapidly three times with ice-cold PBS by using an Inotech Cell Harvester (Wohlen, Switzerland). Radioactivity trapped in the filters was counted with a liquid scintillation counter.

2.4. Uptake of [^{3}H]DA into the cultured cells

Mesencephalic cells that had been cultured for 6 DIV were washed twice with DMEM, and then the cells were incubated with 4 nM [^{3}H]DA (with or without different test drugs) at 37 °C for 4 min. Uptake was then terminated by washing the cells three times in ice-cold DMEM. Radioactivity in the cells was extracted into 100% EtOH for 60 min. Non-specific uptake was determined in the presence of GBR12909 (10 μM).

2.5. Immunostaining

The cells were washed twice with cold PBS, and then fixed with 4% paraformadehyde in 10 mM phosphate buffer (pH 7.2) for 30 min at room temperature (r.t.). The dishes were washed twice in PBS and stored at 4 °C. The immunostaining procedure was started with a 20-min incubation in PBS containing 0.01% Triton X-100 followed by a 5-min incubation with 3% H_2O_2 at room temperature. Then the cells were blocked by incubation for 2 h in PBS containing 5% normal goat serum, 1% bovine serum albumin, and 0.3% Triton X-100. For tyrosine hydroxylase (TH) immunostaining to identify dopaminergic neurons, the cells were incubated overnight at 4 °C with rabbit polyclonal anti-TH affinity-purified antibody (Chemicon Int., Temecula, CA) at a dilution of 1:250 in PBS containing 1% goat serum, 1% RIA grade BSA, and 0.3% Triton X-100. Sequential 60-min incubations with biotinylated anti-rabbit secondary antibody (0.5%; Vector Laboratories, Minneapolis, MN) and peroxidase-conjugated avidin–biotin complex (ABC; Vector Laboratories) were subsequently performed. TH immunoreactivity was developed with a chromogen containing 0.05% 3,3′-diaminobenzidine, 2.5% nickel sulfate, and 0.005% H_2O_2. For cell counting, an investigator blinded to the treatment history counted the number of TH-positive cells in the cultures.

2.6. Western blotting

Proteins in the SDS sample buffer containing β-mercaptoethanol were heated at 95 °C for 3 min, resolved by 10–20% gradient SDS-PAGE, and transferred to PVDF membranes. DAT protein was detected with rat anti-DAT as the primary antibody (Chemicon Int., Temecula, CA) diluted 1:10,000 and horseradish peroxidase-conjugated anti-rat antibody (diluted 1:50,000) as the secondary antibody by using a SuperSignal WestDura extended duration substrate Western blotting detection system (Pierce Biotech., Rockford, IL).

2.7. Microarray analysis

mRNA was extracted from primary cultures of mesencephalic cells by using a messenger RNA Isolation Kit (Stratagene, LaJolla, CA). Radiolabeled cDNA probes were prepared from 1.0 μg of heat-denatured (70 °C, 10 min) poly A^+ RNA or 0.1 μg Tet1-polyA^+ RNA in the presence of random nonamer, dATP, dTTP, dGTP, [^{33}P]dCTP, Superscript II reverse transcriptase, and RNase inhibitor at 43 °C for 1 h (Yamamoto et al., 2005). Subsequently, the RNA in the reaction mixture was decomposed by incubation with RNase H and RNase A at 37 °C for 10 min. The labeled cDNAs were purified with a QIAquick PCR Purification Kit (Qiagen Inc. Valencia, CA, USA) and quantified by using a liquid scintillation counter. Approximately 1700 mKIAA clones and 63 well-characterized non-mKIAA cDNAs were each blotted onto a nylon membrane. In brief, mKIAA cDNA plasmids were amplified by using a TempliPhi DNA amplification kit (GE Healthcare UK Ltd Amersham Place, Little Chalfont, England) and then spotted onto a nylon membrane (Biodyne Plus; Pall, East Hills, NY) attached to a slide glass by using a GeneTac RA1 microarrayer (Genomic Solutions, Ann Arbor, MI; Yamakawa et al., 2004). To reduce the false-positive rate, we used three membranes per each labeled DNA probe prepared from an mRNA sample. Array membranes were prehybridized for 1 h at 68 °C in 0.4 ml of PerfectHyb (TOYOBO Co., Osaka, Japan) hybridization buffer for each membrane. Purified labeled DNA probes together with 50 μg Mouse Cot-1 DNA, 2 μg poly dA, and 1/100 (counts/counts of labeled DNAs) Tet1 were heat-denatured (100 °C for 5 min). After prehybridization, the membranes were hybridized with the mixture of these labeled cDNA probes overnight at 68 °C in a 10-ml vial in a rotating hybridization oven. Membranes were washed at 68 °C with 2 × SSC/1% SDS twice for 15 min each time and then at 68 °C with 0.1 × SSC/1% SDS twice for 30 min each time. They were subsequently dried and exposed to an IP plate (Fuji Film, BAS-IP SR 0813) for 2–3 days. Image acquisition and quantification were performed with an FLA-8000 (Fuji Photo, Tokyo, Japan). The calculation of the gene expression level and the statistical analysis of the data were performed by using the Phoretix™ array system (Nonlinear Dynamics Ltd, Newcastle upon Tyne, UK).

2.8. Real-time quantitative PCR (qRT-PCR)

The following primers were designed by using Lasergene (DNASTAR, Inc., Madison, WI) and used for qRT-PCR:

DAT	Forward	5′-ATC AAC CCA CCG CAG ACA CCA GT-3′
DAT	Reverse	5′-GGC ATC CCG GCA ATA ACC AT-3′
mKIAA0739	Forward	5′-CGAGCTGAGTCTGGCCCCGTTCTT-3′
mKIAA0739	Reverse	5′-ACTGGCGCCTGGCTGCTGGTATGT-3′
Synaptogyrin 3	Forward	5′-GGTCCTTCCTGTGGTTCGTA-3′
Synaptogyrin 3	Reverse	5′-GAAGAAGCTGAAAGCGATGG-3′
GAPDH	Forward	5′-CTG ACG TGC CGC CTG GAG AAA C-3′
GAPDH	Reverse	5′-CCC GGC ATC GAA GGT GGA AGA GT-3′

The PCR products obtained with the primer sets were electrophoresed on a 4% agarose gel and detected as a single band of the expected molecular size.

qRT-PCR was performed by using the pooled mRNA, the gene-specific primers, and a cybergreen fluorescence-based assay kit (SYBR Green RT-PCR kit; TAKARA BIO Inc., Shiga, Japan) according to the manufacturer's instructions. Briefly, the pooled mRNAs isolated from wild-type or VMAT2-KO cultures were reverse-transcribed by using random nonamer for priming. The first-strand cDNAs from the pooled mRNAs were used as templates in a 25-μl PCR reaction mixture containing 400 nM primers and SYBR Green PCR Master Mix. Forty-five cycles of PCR were performed by using an Applied Biosystems 7300 Real Time PCR System (Applied Biosystems, UK). The primers and probe for beta actin were purchased from Applied Biosystems as a part of TaqMan® Gene Expression Assays (Yamamoto et al., 2005).

Levels of all PCR products were calculated from absolute quantification assays and normalized with respect to GAPDH transcript levels, since the GAPDH mRNA level was unchanged in our cDNA array analysis.

3. Results

[^{3}H]DA uptake by the cells in primary culture was characterized first. Uptake of [^{3}H]DA into cultures of each VMAT2 genotype by DAT was potently inhibited by the DAT-selective blocker GBR 12909 at a concentration of 2 or 10 μM, but not by a noradrenalin transporter (NET) inhibitor desipramine (0.5 μM), serotonin transporter (SERT) inhibitors fluoxetine (1 μM) and clomipramine (10 μM) (Fig. 1). These

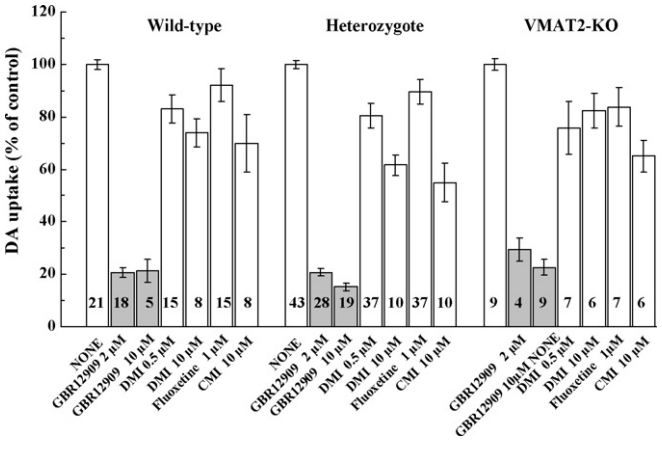

Fig. 1. Pharmacological profile of dopamine uptake into mesencephalon cells derived from fetal wild-type and VMAT2-KO mice. Values are presented as means ± S.E.M. The number in the bottom part of each column indicates the number of cultures used. DMI, desipramine; CMI, clomipramine.

results indicate that [^{3}H]DA uptake into the primary cultures was mediated by mainly DATs, irrespective of the VMAT2 genotype. For the data presented in Fig. 1, there was a large disparity between the numbers of cultures used for each group. As is apparent, there were fewer cultures from the homozygous KO mice, the reason being that sometimes we found a dead fetus in the uterus, suggesting that homozygous KO mice might be gradually lost during the course of gestation.

Representative photomicrographs of DA neurons in primary mesencephalic cultures at 6 DIV are shown in Fig. 2. Under our culture conditions, each culture from wild-type or heterozygous or homozygous VMAT2-KO mice contained normally shaped TH-immunoreactive (THir) neurons with extensive processes. The numbers of THir cells in the mesencephalic cultures derived from both heterozygotes and homozygotes were similar to the number found for their wild-type littermates. Therefore, the viability of dopaminergic cells was not immediately affected by genomic VMAT2 deletion (Fig. 3).

Next, we investigated the effect of genomic VMAT2 deletion on the DAT activity of the various genotypes. Of interest, DAT activity in the mesencephalic cultures derived from the homozygous VMAT2-KO mice was markedly reduced compared with that in the wild-type cultures; whereas that in the heterozygous VMAT2 cultures was not different from that in the wild-type cultures (Fig. 3).

Furthermore, using the synaptosomal fraction from neonatal mice (on the day of birth), we measured [^{3}H]DA uptake. When [^{3}H]DA uptake into the synaptosomes from the wild-type mice was set as 100%, the [^{3}H]DA uptake into the synaptosomes from heterozygous and homozygous KO mice was 92.9 ± 7.6 (4) and 15.0 ± 2.7 (4), respectively ($p < 0.01$, between heterozygous and homozygous KO mice by Student's t-test).

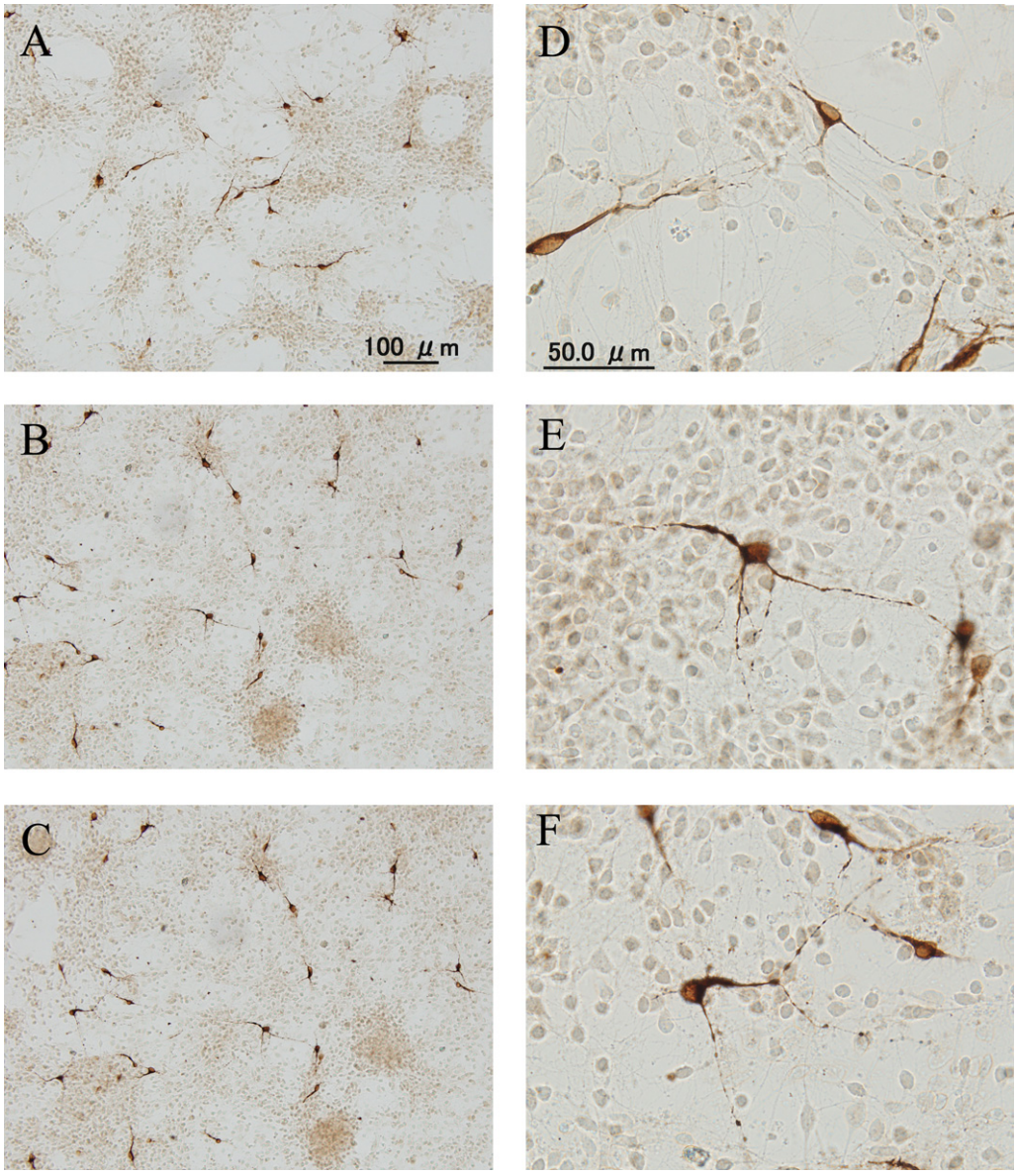

Fig. 2. Photomicrographs showing examples of TH-immunoreactive neurons in primary mesencephalic cultures derived from wild-type (A, D), heterozygous VMAT2-KO (B, E), and homozygous VMAT-KO (C, F) mice. (A)–(C) represent low magnification and (D)–(F) represent high magnification of TH-immunoreactive neurons. No major morphological differences were observed, as previously reported by Fon et al. (1997).

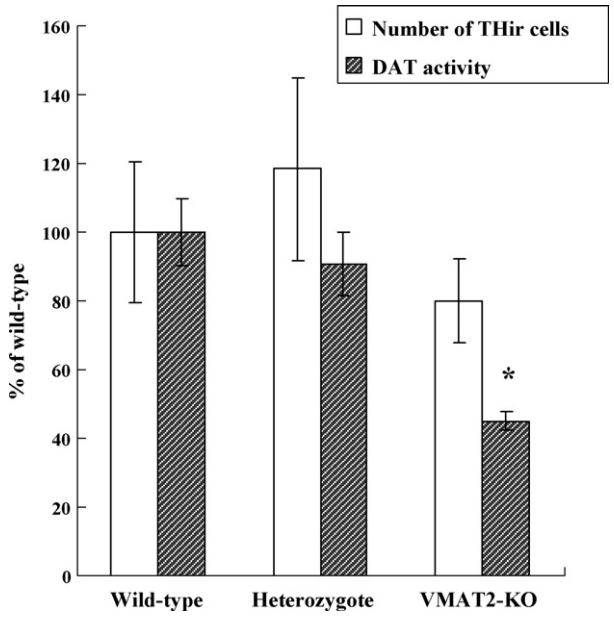

Fig. 3. Quantification of number of TH-immunoreactive cells and DAT activities in primary cultures derived from wild-type and VMAT2-KO mice. The number of TH-immunoreactive cells remained unchanged among all genotypes. DAT activity in the homozygous VMAT-KO cells was significantly decreased ($^{*}p < 0.05$.), but not in the heterozygous ones (Student's *t*-test). Data are expressed as a percentage of the wild-type values. Values are means ± S.E.M. S.E.M. of five to six independent experiments.

Thus, the DAT activity of the homozygous VMAT2-KO mouse was apparently decreased compared with that of wild-type/heterozygous KO mice.

Further, total DAT protein was compared among the genotypes by Western blot analysis after normalization of protein loading (20 μg protein/well). The total content of immunoreactive DAT was apparently not different in the primary cultures derived from wild-type, heterozygous VMAT2-KO and homozygous VMAT2-KO mice (% of wild control: 100 ± 9.3 ($n = 11$), 109.8 ± 3.8 ($n = 10$) and 102.5 ± 10.7 ($n = 5$), respectively). These results demonstrate that complete deletion of VMAT2 could not induce the loss of DA-synthesizing neurons.

Reserpine does not inhibit [^{3}H]DA uptake into SK-N-MC cells expressing human DAT but not VMAT2 (Metzger et al., 2002). In the present study, reserpine treatment at a concentration of 1 μM interestingly decreased DAT activity in wild-type and heterozygous VMAT2-KO cultures. In contrast, the drug did not decrease DAT activity in the homozygous VMAT2-KO ones ($p < 0.001$ versus wild-type; Table 1). These results suggest that reserpine decreased DAT activity via VMAT2 inhibition.

Inhibitors of PKC and PI_3K did not affect DAT activities in cultures of any genotype (Table 1). On the other hand, treatment with an excess amount of L-DOPA (100 μM) for 48 h slightly reduced DAT activity, though not significantly different among these cultures ($p = 0.70$, ANOVA). After L-DOPA (100 μM) treatment for 48 h, the number of TH-immunoreactive cells was almost equal to that of saline-treated cells among these cultures from wild-type, heterozygous VMAT2-KO, and homozygous VMAT2-KO mice (% of saline-treated control: 92.1, 109.9, and 101.8, respectively). When we treated these cultures with a higher concentration of L-DOPA (500 μM), however, almost all cells died 48 h after the treatment.

To explore factors affected by VMAT2-KO, we performed cDNA array analysis on homozygous VMAT2-KO and its wild-type littermates. In this study, pooled mRNA from 5 culture dishes was used, with cells in each dish having been derived from an individual fetal brain stem. In the customized cDNA microarray analysis, hybridization signals in the KO samples were reduced to less than 0.7-fold of the wild type for 12 out of the 1700 mKIAA genes and enhanced more than 1.3-fold for 19 out of the 1700. Although the half of these genes was not

Table 1
Effect of various agents on DAT-mediated [^{3}H]DA uptake

Treatment	Wild-type		Heterozygote		VMAT2-KO	
	% of saline	Control	% of saline	Control	% of saline	Control
Catecholamine depleter						
Reserpine 1 μM	59.5 ± 7.8	(4)	54.1 ± 1.6	(3)	109.3 ± 6.7	(4)*
DA receptor antagonist						
SCH23390 1 μM	108.9 ± 13	(4)	91.3 ± 4.2	(10)	111.0 ± 5.9	(3)
Sulpiride 10 μM	94.0 ± 11	(6)	95.9 ± 14	(5)	105.5 ± 18.6	(4)
PKC inhibitor						
Calphostin 0.1 μM	105 ± 1.2	(6)	103.2 ± 9.3	(8)	117.1 ± 20.6	(5)
PI_3K inhibitor						
Wortmannin 10 nM	111.6 ± 9.7	(6)	115.5 ± 4.1	(8)	113.3 ± 22.2	(5)
DA precursor						
L-DOPA 100 μM	76.5 ± 8.9	(3)	67.2 ± 9.1	(3)	76.9 ± 9.3	(3)

Cultures were treated with each drug for 1 h except L-DOPA for 48 h.
Values are presented as means ± S.E.M.
Number of cultures used is given in parentheses except L-DOPA.
Number of independent experiments used is given in parentheses in L-DOPA treatments.
Statistical analyses were performed using one-way ANOVA with pairwise comparison by Bonferroni method.
* $p < 0.001$.

Table 2
Down-regulated gene expressions in homozygous VMAT2-KO mice

GenBank accession	mKIAA No.	Description	cDNA array KO/wild (%)	qRT-PCR KO/wild (%)
AK173014	mKIAA0739	NBC-3	73.8 ± 5.7	80.1 ± 1.6
NM 010020	–	DAT	75.8 ± 10.9	93.0 ± 5.9
NM 011522	–	Synaptogyrin 3	n.d.	62.4 ± 3.5

NBC-3, sodium bicarbonate cotransporter isoform 3; n.d., not determined.
The values represent the means of more than five determinations ± S.E.M.
The data from the cDNA array and qRT-PCR analysis was normalized to the GAPDH transcript level.

annotated yet, stress proteins (neurodegeneration associated protein 1 and heat shock 70 kDa protein 5 binding protein 1), cytoskeleton proteins (actin, dendrin, protocadherin 21, collagen type VIII and palladin) and mKIAA 0739 (sodium bicarbonate cotransporter isoform 3, NBC-3) were extracted by cDNA array analysis. Gene expression of glyceraldehyde-3-phosphate dehydrogenase (GAPDH) was not changed by VMAT2 deletion (94.5% of wild-type cultures).

Next, we performed qRT-PCR analysis using the same mRNA used for cDNA array. NBC-3 might be involved in the regulation of DAT function. Although the reduction in gene expression of NBC-3 was confirmed by qRT-PCR analysis, reduced ratio of gene expression was smaller than that by the cDNA analysis (Table 2).

Gene expressions of DAT in the VMAT2-KO cultures were not significantly different from those for wild-type mice by cDNA array and qRT-PCR analyses (Table 2).

Synaptogyrin represent a major constituent of synaptic vesicles. Since cDNA of synaptogyrin 3 was not included in our cDNA array, we only performed qRT-PCR analysis of gene expression of synaptogyrin 3. Its expression was potently reduced in homozygousVMAT2-KO cultures (Table 2). The statistical significance was not determined, since these analyses were done using pooled mRNA samples for multiple measurements. The data from the cDNA array and qRT-PCR analysis in Table 2 was normalized to the GAPDH transcript level. Other cDNA array data significantly changed were presented as Table 3.

4. Discussion

Up to now, several studies on heterozygous VMAT2-KO mice have been already reported; and quite a few studies have been done on homozygotes. This study demonstrated that the dopaminergic neurons lacking VMAT2 showed a marked decrease in DAT activity. The complete deletion of VMAT2 did not accelerate dopaminergic cell death in *in vitro* cultures for at least 2 weeks, even though the homozygous mice have poor postnatal viability.

Our experiments, including cDNA array, qRT-PCR and immunoblotting, showed that the gene expression and immunoreactivity of DAT in the VMAT2-KO cultures were not significantly different from those for wild-type mice. Therefore, the marked reduction in DAT activity in the homozygous VMAT2-KO cultures was not likely due to decreased DAT biosynthesis. DAT protein levels can reliably serve as a viability marker of DA terminals, as previously suggested (Wilson et al., 1996; Miller et al., 1997; Gainetdinov

Table 3
Significantly changed gene expressions in homozygous VMAT2-KO mice by using the cDNA array

GenBank accession	mKIAA No.	Description	KO/Wild (%)
AB093302	mKIAA1842	T-cell activation kelch repeat protein	62.6
AK122475	mKIAA1244	DNA segment, Chr 10, Brigham & Women's Genetics 1379 expressed	63.6
AK129075	mKIAA0173	tubulin tyrosine ligase-like family, member 4	73.2
AF317839	mKIAA1355	immunoglobulin superfamily, member 9	74.6
AK129052	mKIAA0090	RIKEN cDNA C230096C10 gene	77.6
BC031652	mKIAA1331	SUMO/sentrin specific peptidase 2	78.2
AK129059	mKIAA0127	SERTA domain containing 2	79.3
AK131123	mFLJ00062	histone deacetylase 7A	79.5
AK173132	mKIAA1208	N-acetylglucosamine-1-phosphate transferase, alpha and beta subunits	121.5
AF090190	mKIAA0591	kinesin family member 1B	122.3
AK129304	mKIAA1171	TBC1 domain family, member 24	125.8
AK129113	mKIAA0297	RIKEN cDNA 4930573I19 gene	130.6
AK122470	mKIAA1219	RIKEN cDNA B230339M05 gene	131.2
AK129168	mKIAA0593	N-terminal truncated TRAP240	132.9
AK122289	mKIAA0463	plexin A2	133.2
AB093213	mKIAA0184	DIP2 disco-interacting protein 2 homolog A (*Drosophila*)	134.1
AK052203	mKIAA0469	kelch-like 21 (*Drosophila*)	135.8
		GAPDH	94.5

Data not normalized to the GAPDH transcript level are presented as percentages of wild-type. The cDNA array data were analyzed by using Student's *t*-test.

et al., 1998). However, DAT activity was not correlated with the cell viability of the dopaminergic neurons lacking the VMAT2 molecule.

The regulation of surface DAT expression in neurons may be far more complex than once thought. Mortensen and Amara (2003) precisely summarized the factors involved in DAT activity. They mentioned that presynaptic DA receptors are poised to regulate the activity of the DAT acutely through their actions on intracellular signaling systems. However, in the present study, there were no changes in the DAT activity in our cultures when D1 and D2 antagonists blocking presynaptic DA receptors were added to the cultures.

As another possibility, re-distribution of DAT from the synaptosomal membrane to intracellular subfractions might have occurred in the VMAT2-KO cells, since dynamic regulation of DAT function is known to occur in several ways. One major pathway for the regulation is the sequestration of DAT by second messenger systems. Earlier an immunofluorescence confocal microscopy study demonstrated that an observable functional consequence of PKC activation with respect to [^{3}H]DA uptake was the rapid sequestration/internalization of DAT protein from the cell surface and that an increase in DA uptake occurred following PKC/PKA inhibition, being a consequence of the recruitment of internalized or intracellular transporters to the plasma membrane (Pristupa et al., 1998). In that process, phorbol ester-mediated PKC activation accelerates DAT endocytosis and attenuates transporter recycling in a manner sensitive to DAT expression levels (Loder and Melikian, 2003). So we used the PKC inhibitor calphostin to investigate whether its inhibition of PKC in the VMAT2-KO cultures could restore the DAT activity or not. However, the inhibition of PKC did not increase DA uptake into VMAT2-KO cells, thus indicating that the reduced DAT activity in them was not due to the accelerated internalization of DAT from the plasma membrane by a PKC-activated pathway.

We added insulin to the medium of our primary cultures for the purpose of increasing cell viability. One known effect of insulin is the activation of PI_3K. However, the addition of the PI_3K inhibitor wortmannin to the medium did not affect DA uptake in the cultures. Therefore, it is unlikely that the reduced activity of DAT in the homozygous VMAT2-KO mice was due to the cell surface redistribution of DAT by a stimulated PI_3K pathway.

The most discriminative drug to detect differences in the DA uptake between wild-type cells and homozygous VMAT2-KO cells was reserpine. In the present study, reserpine treatment at a concentration of 1 μM decreased DAT activities in wild-type and heterozygousVMAT2-KO cultures approx. 50%, whereas the drug failed to reduce DAT activity in homozygousVMAT2-KO ones. These results are in good agreement with the report by Metzger et al. (2002) that reserpine transiently alters DAT function in a noncompetitive, indirect manner in the presence of VMAT2, though reserpine, at concentrations ranging from 0.01 to 10 μM, is without effect on DAT activity in the absence of VMAT2 (Metzger et al., 2002). Our results suggest that lack of VMAT2 activity by genetic or pharmacological manipulation could result in the marked decrease in DAT activity possibly through a similar mechanism. If complete deletion of VMAT2 results in an increased concentration of intracellular DA, it might induce a substrate inhibition of DAT. However, the brains of VMAT2-KO mice show extremely low contents of catecholamines including serotonin, noradrenalin, and DA (Fon et al., 1997), indicating that complete deletion of VMAT2 reduces the content of catecholamines. To assess substrate inhibition of DAT in those cultures, we performed the experiment of increasing intracellular DA by the addition of an excess amount of L-DOPA, a precursor of DA. All three genotypes showed comparable reductions (approx. 25%) in DAT activities when treated with excess L-DOPA. The inhibitory effect on DAT via substrate inhibition and that by genetic deletion of VMAT2 were additive. Furthermore, DAT activity was markedly reduced by using the P2 (synaptosomal) fraction from newborn homozygous VMAT2-KO mice even in the absence of endogenous DA. This finding means that the phenomenon of reduced DAT activity in VMAT2-KO cultures was due to a mechanism different than substrate inhibition.

From the cDNA array and qRT-PCR results, we found that the gene expression of a sodium-bicarbonate cotransporter isoform 3 (NBC-3) was reduced (cDNA array, approx. 30%; qRT-PCR, approx. 20%) in the homozygous VMAT2-KO cultures. NBC-3 is highly expressed in the brain and spinal column; and its mRNA and protein are present in the cortex, brainstem-diencephalon, and cerebellum (Schmitt et al., 2000). The NBC carries sodium with bicarbonate into or out of the cell in an electrogenic mode (Romero et al., 1997) and maintains the extracellular pH properly. Intracellular and extracellular pH also modulates DAT activity. However, the reduction in gene expression of NBC-3 was not as large as that in DAT activity in the homozygous VMAT2-KO cultures.

Synaptogyrin represent a major constituent of synaptic vesicles. In the present study, the reduced gene expression of synaptogyrin 3 is well consistent with the reduced DAT activities in the homozygous VMAT2-KO cultures. However, further studies are necessary.

In conclusion, our data demonstrate that complete deletion of VMAT2 induced a marked decrease in DAT activity, probably through a mechanism similar to that operating during reserpine treatment. The reduction of DAT activity was also observed in the synaptosomal fractions of neonatal homozygous VMAT2-KO mice, suggesting the possibility that the VMAT2 could be an essential molecule to make DAT operate more efficiently.

Acknowledgements

This work was supported by grants from the MEXT (17025054) and MHLW (H17-Pharmaco-001, H16-Iyaku-029, 18A-3 for Nervous and Mental Disorders) in Japan. We are grateful to Drs. Makoto Arai, Makoto Honda, and Masanari Itokawa for their helpful instructions regarding the RT-PCR experiments and to Dr. Haruhiko Akiyama for his worthwhile recommendation.

References

Boja, J.W., McNeill, R.M., Lewin, A.H., Abraham, P., Carroll, F.I., Kuhar, M.J., 1992. Selective dopamine transporter inhibition by cocaine analogs. Neuroreport 3, 984–986.

Croft, B.G., Fortin, G.D., Corera, A.T., Edwards, R.H., Beaudet, A., Trudeau, L.E., Fon, E.A., 2005. Normal biogenesis and cycling of empty synaptic vesicles in dopamine neurons of vesicular monoamine transporter 2 knockout mice. Mol. Biol. Cell. 16, 306–315.

Erickson, J.D., Eiden, L.E., Hoffman, B.J., 1992. Expression cloning of a reserpine-sensitive vesicular monoamine transporter. Proc. Natl. Acad. Sci. U.S.A. 89, 10993–10997.

Erickson, J.D., Eiden, L.E., 1993. Functional identification and molecular cloning of a human brain vesicle monoamine transporter. J. Neurochem. 61, 2314–2317.

Fon, E.A., Pothos, E.N., Sun, B.C., Killeen, N., Sulzer, D., Edwards, R.H., 1997. Vesicular transport regulates monoamine storage and release but is not essential for amphetamine action. Neuron 19, 1271–1283.

Fumagalli, F., Gainetdinov, R.R., Wang, Y.M., Valenzano, K.J., Miller, G.W., Caron, M.G., 1999. Increased methamphetamine neurotoxicity in heterozygous vesicular monoamine transporter 2 knock-out mice. J. Neurosci. 19, 2424–2431.

Gainetdinov, R.R., Fumagalli, F., Wang, Y.M., Jones, S.R., Levey, A.I., Miller, G.W., Caron, M.G., 1998. Increased MPTP neurotoxicity in vesicular monoamine transporter knockout mice. J. Neurochem. 70, 1973–1978.

Giros, B., Jaber, M., Jones, S.R., Wightman, R.M., Caron, M.G., 1996. Hyperlocomotion and indifference to cocaine and amphetamine in mice lacking the dopamine transporter. Nature 379, 606–612.

Henry, J.-P., Botton, D., Sagne, C., Isambert, M.-F., Desnos, C., Blanchard, V., Raisman-Vozari, R., Krejci, E., Massoulie, J., Gasnier, B., 1994. Biochemistry and molecular biology of the vesicular monoamine transporter from chromaffin granules. J. Exp. Biol. 196, 251–262.

Johnson, R.G., 1988. Accumulation of biological amines into chromaffin granules: a model for hormone and neurotransmitter transport. Physiol. Rev. 68, 232–307.

Liu, Y., Peter, D., Roghani, A., Schuldiner, S., Prive', G.G., Eisenberg, D., Brecha, N., Edwards, R.H., 1992. A cDNA that suppresses MPP^+ toxicity encodes a vesicular amine transporter. Cell 70, 539–551.

Loder, M.K., Melikian, H.E., 2003. The dopamine transporter constitutively internalizes and recycles in a protein kinase C-regulated manner in stably transfected PC12 cell lines. J. Biol. Chem. 278, 22168–22174.

Metzger, R.R., Brown, J.M., Sandoval, V., Rau, K.S., Elwan, M.A., Miller, G.W., Hanson, G.R., Fleckenstein, A.E., 2002. Inhibitory effect of reserpine on dopamine transporter function. Eur. J. Pharmacol. 456, 39–43.

Miller, G.W., Staley, J.K., Heilman, C.J., Perez, J.T., Mash, D.C., Rye, D.B., Levey, A.I., 1997. Immunochemical analysis of dopamine transporter protein in Parkinson's disease. Ann. Neurol. 41, 530–539.

Mooslehner, K.A., Chan, P.M., Xu, W., Liu, L., Smadja, C., Humby, T., Allen, N.D., Wilkinson, L.S., Emson, P.C., 2001. Mice with very low expression of the vesicular monoamine transporter 2 gene survive into adulthood: potential mouse model for parkinsonism. Mol. Cell. Biol. 21, 5321–5331.

Mortensen, O.V., Amara, S.G., 2003. Dynamic regulation of the dopamine transporter. Eur. J. Pharmacol. 479, 159–170.

Pristupa, Z.B., McConkey, F., Liu, F., Man, H.Y., Lee, F.J., Wang, Y.T., Niznik, H.B., 1998. Protein kinase-mediated bidirectional trafficking and functional regulation of the human dopamine transporter. Synapse 30, 79–87.

Romero, M.F., Hediger, M.A., Boulpaep, E.L., Boron, W.F., 1997. Expression cloning and characterization of a renal electrogenic Na^+/HCO_3^- cotransporter. Nature 387, 409–413.

Schmitt, B.M., Berger, U.V., Douglas, R.M., Bevensee, M.O., Hediger, M.A., Haddad, G.G., Boron, W.F., 2000. Na/HCO_3 cotransporters in rat brain: expression in glia, neurons, and choroid plexus. J. Neurosci. 20, 6839–6848.

Shimoda, K., Sauvt, Y., Marini, A., Schwartz, J.P., Commissiong, J.W., 1992. A high percentage yield of tyrosine hydroxylase-positive cells from rat E 14 mesencephalic cell culture. Brain Res. 586, 19–33.

Takahashi, N., Miner, L.L., Sora, I., Ujike, H., Revay, R.S., Kostic, V., Jackson-Lewis, V., Przedborski, S., Uhl, G.R., 1997. VMAT2 knockout mice: heterozygotes display reduced amphetamine-conditioned reward, enhanced amphetamine locomotion, and enhanced MPTP toxicity. Proc. Natl. Acad. Sci. U.S.A. 94, 9938–9943.

Wang, Y.M., Gainetdinov, R.R., Fumagalli, F., Xu, F., Jones, S.R., Bock, C.B., Miller, G.W., Wightman, R.M., Caron, M.G., 1997. Knockout of the vesicular monoamine transporter 2 gene results in neonatal death and supersensitivity to cocaine and amphetamine. Neuron 19, 1285–1296.

Wilson, J.M., Levey, A.I., Rajput, A., Ang, L., Guttman, M., Shannak, K., Niznik, H., Hornykiewicz, O., Pifl, C., Kish, S., 1996. Differential changes in neurochemical markers of striatal dopamine nerve terminals in idiopathic Parkinson's disease. Neurology 47, 718–726.

Yamakawa, H., Yokoyama, S., Hiran, T., Kitamura, H., Ohara, O., 2004. A simple and robust method for preparation of cDNA nylon microarrays. DNA Res. 11, 353–360.

Yamamoto, H., Yamamoto, T., Sagi, N., Klenerova, V., Goji, K., Kawai, N., Baba, A., Takamori, E., Moroji, T., 1995. Sigma ligands indirectly modulate the NMDA receptor-ion channel complex on intact neuronal cells via sigma 1 site. J. Neurosci. 15, 731–736.

Yamamoto, H., Imai, K., Takamatsu, Y., Kamegaya, E., Kishida, M., Hagino, Y., Hara, Y., Shimada, K., Yamamoto, T., Sora, I., Koga, H., Ikeda, K., 2005. Methamphetamine modulation of gene expression in the brain: analysis using customized cDNA microarray system with the mouse homologues of KIAA genes. Brain Res. Mol. Brain Res. 137, 40–46.

Available online at www.sciencedirect.com
ScienceDirect
European Journal of Pharmacology 572 (2007) 120–128
www.elsevier.com/locate/ejphar

Methamphetamine-induced hyperthermia and lethal toxicity: Role of the dopamine and serotonin transporters

Yohtaro Numachi [a], Arihisa Ohara [a], Motoyasu Yamashita [a], Setsu Fukushima [a], Hideaki Kobayashi [a], Harumi Hata [a], Hidekazu Watanabe [a], F. Scott Hall [b], Klaus-Peter Lesch [c], Dennis L. Murphy [d], George R. Uhl [b], Ichiro Sora [a,b,*]

[a] *Department of Biological Psychiatry, Tohoku University Graduate School of Medicine, Japan*
[b] *Molecular Neurobiology Branch, National Institute on Drug Abuse, Division of Intramural Research, USA*
[c] *Department of Psychiatry, University of Wurzburg, Germany*
[d] *Laboratory of Clinical Science, National Institute of Mental Health, Division of Intramural Research Programs, USA*

Received 1 February 2007; received in revised form 4 June 2007; accepted 7 June 2007
Available online 27 June 2007

Abstract

We examined the hyperthermic and lethal toxic effects of methamphetamine in dopamine transporter (DAT) and/or serotonin transporter (SERT) knockout (KO) mice. Methamphetamine (45 mg/kg) caused significant hyperthermia even in the mice with a single DAT gene copy and no SERT copies ($DAT^{+/-}$ $SERT^{-/-}$ mice). Mice with no DAT copies and a single SERT gene copy ($DAT^{-/-}$ $SERT^{+/-}$ mice) showed significant but reduced hyperthermia when compared to wild-type mice after methamphetamine. Surprisingly, DAT/SERT double KO mice exhibited a paradoxical hypothermia after methamphetamine. These results demonstrate that methamphetamine exerts a hyperthermic effect via DAT, or via SERT, in the absence of DAT. The selective norepinephrine transporter blocker (20 mg/kg nisoxetine) caused hyperthermia in DAT/SERT double KO mice, suggesting that the norepinephrine system is not responsible for methamphetamine-induced paradoxical hypothermia in the double KO mice. DAT gene deletion in mice strikingly increased LD_{50} of methamphetamine by 1.7–1.8 times that of wild-type mice, suggesting that the lethal toxic effect of methamphetamine is mainly dependent on DAT. Moreover, dissociation between hyperthermic and lethal toxic effects of methamphetamine in DAT single KO mice and DAT/SERT double KO mice suggest that hyperthermia is not a prerequisite for methamphetamine-induced lethality. Methamphetamine (45 mg/kg) significantly increased mRNA of interleukin-1β, which is the major endogenous pyrogen, in the hypothalamus of wild-type mice but not in DAT/SERT double KO mice, which provides a partial mechanism of methamphetamine-induced paradoxical hypothermia. These results suggest that DAT and SERT are key molecules for hyperthermic and lethal toxic effects of methamphetamine.

Keywords: Monoamine; Norepinephrine; Paradoxical hypothermia; Interleukin-1β; Transgenic knockout mouse

1. Introduction

Methamphetamine is abused worldwide for its potent stimulant and euphoric effects (Sato et al., 1992; Hanson et al., 2004). Methamphetamine abuse causes serious health hazards including irreversible neuronal degeneration, seizures, hyperthermia and death in human and experimental animals (Davidson et al., 2001; Kita et al., 2003; Chan et al., 1997). Among these side effects, methamphetamine produces hyperthermia and/or dopaminergic neurotoxicity in most species, although differences in age (Imam and Ali, 2001), sex (Wagner et al., 1993), ambient temperature (Ali et al., 1994; Miller and O'Callaghan, 2003; Namiki et al., 2005), dosing, and route of administration (Davidson et al., 2001) can influence these effects. Clinical reports and animal studies indicate that lethality by methamphetamine closely correlates with hyperthermia, which may be the primary cause of death (Bowyer et al., 1994; Davidson et al., 2001; Namiki et al., 2005). Methamphetamine enters the terminals/neuron via the monoamine transporters (dopamine transporter: DAT, serotonin transporter: SERT, or

* Corresponding author. Department of Biological Psychiatry, Tohoku University Graduate School of Medicine 1-1 Seiryo-machi, Sendai, 980-8574, Japan. Tel.: +81 22 717 7808; fax: +81 22 717 7809.
E-mail address: isora@mail.tains.tohoku.ac.jp (I. Sora).

0014-2999/$ - see front matter © 2007 Elsevier B.V. All rights reserved.
doi:10.1016/j.ejphar.2007.06.022

norepinephrine transporter: NET), displaces both vesicular and intracellular monoamines and facilitates release of monoamines into the extraneuronal space by synaptic transport in the monoamine transporters (Seiden et al., 1993). Animal studies suggest that dopamine receptor activation is crucial for methamphetamine-induced hyperthermia (Funahashi et al., 1990; Albers and Sonsalla, 1995; Kuperman et al., 1997; Canini and Bourdon, 1998; He et al., 2004; Broening et al., 2005) and lethality (Davis et al., 1978; Uchima et al., 1983; Derlet et al., 1990; Bronstein and Hong, 1995). There has also been an assumption that the hyperthermia that follows methamphetamine administration is serotonin receptor-mediated (Green et al., 2003). According to these reports, we hypothesized that DAT and/or SERT mediated monoamine increase would have important roles for methamphetamine-induced hyperthermia, but the precise mechanism of the hyperthermia remains to be elucidated. In the present study, we examined hyperthermic and lethal toxic effects of methamphetamine in DAT, SERT and DAT/SERT double knockout (KO) mice to elucidate the role of these two transporters in methamphetamine-induced hyperthermia and lethality. Because methamphetamine caused paradoxical hypothermia in DAT/SERT double KO mice, we also studied the effects of selective SERT blocker (fluoxetine) and selective NET blocker (nisoxetine) on body temperature of DAT, SERT and DAT/SERT double KO mice.

Another proposed mechanism of methamphetamine-induced hyperthermia is that methamphetamine may increase hypothalamic concentrations of interleukin-1β, commonly known as the major endogenous pyrogen (Schobitz et al., 1994; Tringali et al., 1998; Leon, 2002). Interleukin-1β produces hyperthermia when introduced into the rat brain (Dascombe, et al., 1989). Methamphetamine caused a marked induction of hypothalamic interleukin-1β mRNA in mice (Halladay et al., 2003) and rats (Yamaguchi et al., 1991). Interleukin-1 receptor antagonists reduce the hyperthermic and lethal effects of methamphetamine in rats (Bowyer et al., 1994). Therefore, interleukin-1β could contribute to the hyperthermic and lethal effects of methamphetamine. To examine potential mechanisms mediated the paradoxical effects of methamphetamine on body temperature reported here in DAT/SERT double KO mice, we compared brain expression of interleukin-1β mRNA after methamphetamine in wild-type and DAT/SERT double KO mice.

2. Materials and methods

2.1. Subjects

Male and female DAT/SERT double KO mice weighing 15–35 g (see Bengel et al., 1998; Sora et al., 1998; Sora et al., 2001 for a full description) were used in these experiments. The effects of methamphetamine on temperature and lethality were studied in all nine potential genotypes ($DAT^{+/+}$ $SERT^{+/+}$, $DAT^{+/-}$ $SERT^{+/+}$, $DAT^{-/-}$ $SERT^{+/+}$, $DAT^{+/+}$ $SERT^{+/-}$, $DAT^{+/-}$ $SERT^{+/-}$, $DAT^{-/-}$ $SERT^{+/-}$, $DAT^{+/+}$ $SERT^{-/-}$, $DAT^{+/-}$ $SERT^{-/-}$ and $DAT^{-/-}$ $SERT^{-/-}$). All mice were bred at the Institute for Animal Experimentation in Tohoku University Graduate School of Medicine (Sendai, Japan), which met all Japanese federal government requirements for animal care and use. The genetic background of these mice was a combination of C57BL/6J and 129Sv/J strains. For all experiments, wild-type, DAT and/or SERT KO mice pups were weaned at 28 days of age and were housed in groups of two to five, segregated by sex, in a temperature and light-controlled colony (lights on at 0800 h, lights off at 2000 h), with food and water available ad libitum. The mice were genotyped by multiplex PCR from genomic DNA extracted from tail tissue. All experiments were conducted with the approval of the Animal Ethics Committee at Tohoku University Graduate School of Medicine.

2.2. Body temperature measurements and lethal toxicity

All experiments were conducted at 2–3 PM in a room maintained at 20–24 °C using male and female mice of 20–30 weeks of age for each genotype. Nine genotypes of DAT/SERT KO mice received intraperitoneal injection with methamphetamine hydrochloride (45 mg/kg, 0.9% saline solution, Dainippon Pharmaceuticals, Osaka, JAPAN). Wild-type, DAT single KO, SERT single KO, and DAT/SERT double KO mice received intraperitoneal injections of fluoxetine hydrochloride (20 mg/kg, saline solution, Sigma-Aldrich Inc., St. Louis, MO, USA), or nisoxetine hydrochloride (20 mg/kg, saline solution, Sigma-Aldrich Inc., St. Louis, MO, USA). Mice were removed from their home cages, weighed, injected with the drugs, and returned to home cages in a group of 2–3 mice/cage. A digital thermometer (BAT-10; Physitemp Instruments Inc., Clifton, NJ, USA) and rectal probe for mice (RET-3, Physitemp Instruments Inc., Clifton, NJ, USA) were used to measure the body temperature of mice. The probe was inserted 2 cm into the rectum. In the present study, body temperature was measured just before (0 min) and after the injection of the drugs at 15, 30, 45 and 60 min. For lethal toxicity, 9 genotypes of DAT/SERT KO mice were removed from their home cages, weighed, injected with methamphetamine (15–150 mg/kg, saline solution), and returned to home cages in a group of 2–3 mice/cage. In preliminary tests, we found that deaths occurred within 1 h after drug injection, and most mice that were alive 1 h after the injections survived. Therefore, we measured the body temperature of mice until 1 h after methamphetamine injection and calculated lethal toxicity of methamphetamine as a percent lethality at the end of this period.

2.3. Determination of murine interleukin-1β mRNA by relative RT-PCR

Wild-type and DAT/SERT double KO mice received intraperitoneal injections of methamphetamine (saline solution, 45 mg/kg) or saline solution. One hour after the injection, mice were sacrificed by cervical dislocation. Following previously published methods (Halladay et al., 2003) the hypothalamus, nucleus caudatus, nucleus accumbens and frontal cortex were dissected on ice, and the samples were stored at −80 °C until later analysis. Total RNA was extracted using the RNeasy Mini Kit (QIAGEN, Valencia, CA, USA) for cDNA synthesis with Thermoscript RT-PCR System (Invitrogen, Carlsbad, CA, USA), to quantify relative expression of IL-1β mRNA with Gene Specific Relative RT-PCR Kits (Ambion, Austin, TX, USA) with QuantumRNA 18S Internal Standards (Ambion, Austin, TX, USA). For cDNA synthesis,

approximately 0.5 μg total RNA was first denatured at 65 °C for 5 min in a 12 μl reaction containing 2 μl 10 mM dNTP mix and 1 μl 50 μM Oligo $(dT)_{20}$ and was placed on ice. After addition of 8 μl cDNA synthesis mix containing 4 μl 5× cDNA Synthesis Buffer, 1 μl 0.1 M dithiothreitol, 1 μl RNAseOUT™ (40 U/μl) and 1 μl Thermoscript™ Reverse Transcriptase (15 U/μl), the RNA was reverse-transcribed at 50 °C for 60 min, denatured at 85 °C for 5 min, and finally cooled at 4 °C. After addition of 1 μl *E. coli* RNAse H (2 U/μl), cDNA synthesis reaction was incubated at 37 °C for 20 min, diluted in 79 μl Tris–EDTA solution (10 mM Tris–HCl and 1 mM EDTA, pH 8.0), and stored at −20 °C until PCR.

PCR amplification of interleukin-1β and 18 S cDNA was then conducted in a same tube. A 15 μl PCR reaction was established containing 1.2 μl 2.5 mM dNTP mix, 0.075 μl TaKaRa Ex Taq® (5 U/μl, TAKARA BIO Inc., Otsu, JAPAN), 1.5 μl 10× Ex Taq Buffer (2 mM Mg^{2+} final), 1% DMSO, 0.3 μl Mouse IL-1β Relative RT-PCR primers (5 μM mix of forward and reverse primers), 0.3 μl mix (1:9) of 5 μM 18S PCR competimers and 5 μM 18S PCR primer pair (Ambion, Austin, TX, USA), and 3.75 μl cDNA solution. Thermocycling involved an initial 3 min denaturation step at 94 °C, and followed by 40 cycles of 94 °C for 0.5 min, 65 °C for 0.5 min, and 72 °C for 0.5 min. PCR products were separated by 1.2 % agarose gel electrophoresis, stained with ethidium bromide and visualized by UV trans-illuminator (TDM-20, UVP Inc., Upland, CA, USA) and gel documentation system (GelPrint 2000i, Genomic Solutions Inc., Ann Arbor, MI, USA), with product size determined using a 100 bp DNA ladder (New England Biolabs, Inc, Beverly, MA, USA). ImageJ (Version 1.24, http://rsb.info.nih.gov/ij/), a public domain image analysis program, was used for densitometric analysis to calculate ratios for cDNA of interleukin-1β/cDNA of 18S rRNA.

2.4. Data analysis and statistical tests

All data analysis and statistical tests were performed using SPSS statistical package (SPSS Inc., Tokyo, JAPAN), unless otherwise stated. Data from the body temperature experiments and relative RT-PCR experiments for interleukin-1β mRNA are presented as mean±S.E.M., and were submitted to analysis of variance (ANOVA). For post hoc comparisons, Dunnett's test was used for effects of methamphetamine, fluoxetine or nisoxetine on body temperature, Tukey's HSD test was used for effects of genotype on body temperature of methamphetamine-treated DAT/SERT KO mice and for effects of methamphetamine on the expression of interleukin-1β mRNA in the mice brain,

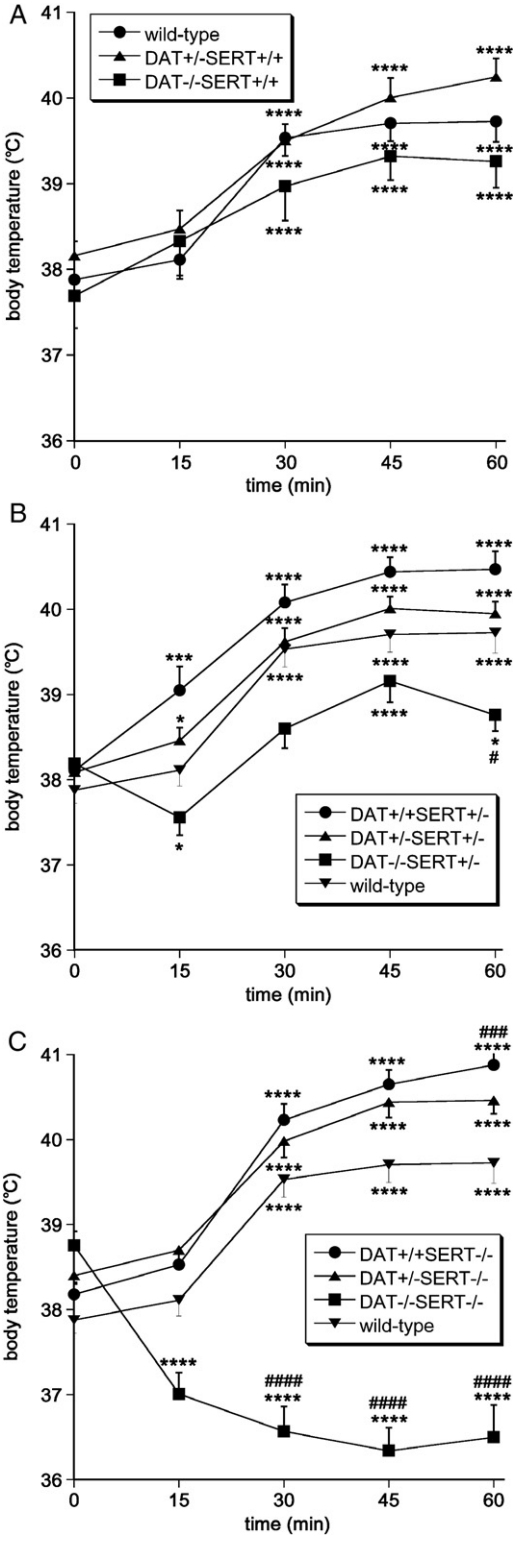

Fig. 1. A. Time course of body temperature of mice after intraperitoneal injection of methamphetamine (45 mg/kg). This dose of methamphetamine caused significant hyperthermia even in the mice lacking DAT. ****$P<0.001$ compared to 0 min (Dunnett's test). Values represent mean±S.E.M., $n=10$–12 mice per genotype. B. Time course of body temperature of mice after intraperitoneal injection of methamphetamine (45 mg/kg). Methamphetamine caused significant hyperthermia in $DAT^{+/+}$ $SERT^{+/-}$ and $DAT^{+/-}$ $SERT^{+/-}$ mice, but in $DAT^{-/-}$ $SERT^{+/-}$ mice, methamphetamine caused transient hypothermia followed by hyperthermia. *$P<0.05$; ***$P<0.005$; and ****$P<0.001$ compared to 0 min (Dunnett's test). $^{\#}P<0.05$ compared to wild-type (Tukey's HSD test). Values represent mean±S.E.M., $n=14$–39 mice per genotype. C. Time course of body temperature of mice after intraperitoneal injection of methamphetamine (45 mg/kg). Methamphetamine caused significant hyperthermia in $DAT^{+/+}$ $SERT^{-/-}$ and $DAT^{+/-}$ $SERT^{-/-}$ mice, but in $DAT^{-/-}$ $SERT^{-/-}$ mice, methamphetamine caused paradoxical hypothermia, revealed by significantly lower body temperature compared to 0 min as well as wild-type mice. Compared to wild-type mice, $DAT^{+/+}$ $SERT^{-/-}$ mice showed more severe hyperthermia 60 min after the injection. ****$P<0.001$ compared to 0 min (Dunnett's test). $^{\#\#\#}P<0.005$; and $^{\#\#\#\#}P<0.001$, compared to wild-type (Tukey's HSD test). Values represent mean±S.E.M., $n=7$–22 mice per genotype.

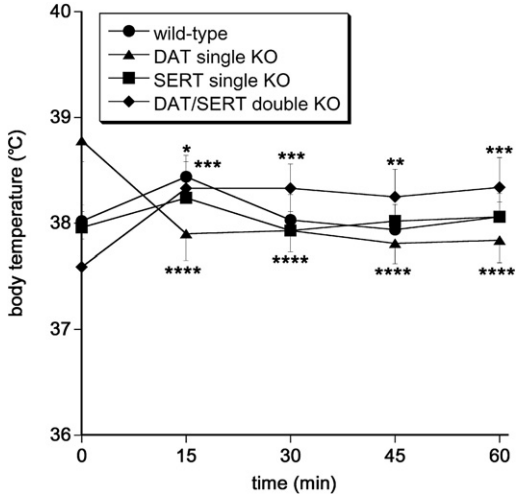

Fig. 2. Time course of body temperature of mice after intraperitoneal injection of fluoxetine (20 mg/kg). Fluoxetine caused transient but significant hyperthermia in wild-type mice at 15 min after injection compared to 0 min, significant hyperthermia in DAT/SERT double KO mice from 15 to 60 min after injection compared to 0 min, and significant hypothermia in DAT single KO mice from 15 to 60 min after injection compared to 0 min, respectively. *$P<0.05$; **$P<0.01$; ***$P<0.005$; and ****$P<0.001$ compared to 0 min (Dunnett's test). Values represent mean±S.E.M., $n=12$–15 mice per genotype.

respectively. Differences in percent lethality at each dose of methamphetamine between wild-type mice and the other 8 genotypes of DAT/SERT KO mice were compared using the χ^2 test. We also calculated LD_{50} value and its 95% confidence interval for methamphetamine in 9 genotypes of DAT/SERT KO mice by probit analysis (LC50MV5; http://www.vector.co.jp/soft/dl/win95/edu/se125220.html). The criterion of statistical significance was $P<0.05$.

3. Results

3.1. Body temperature by methamphetamine, fluoxetine or nisoxetine

In the 9 genotypes of DAT/SERT KO mice, there were no significant differences in basal body temperature. Following methamphetamine administration, there was a significant genotype effect on body temperature ($F(8,157=16.725$, $P<0.001$) and significant genotype×time interaction for changes of body temperature ($F(32,628=10.792$, $P<0.001$). Methamphetamine significantly increased body temperature of mice with any DAT genotype and both wild-type copies of the SERT gene (wild-type, $DAT^{+/-}$ $SERT^{+/+}$, and $DAT^{-/-}$ $SERT^{+/+}$), and also for mice with full or single copies of the wild-type DAT gene with homozygous SERT KO ($DAT^{+/+}$ $SERT^{-/-}$ and $DAT^{+/-}$ $SERT^{-/-}$), from 30 to 60 min after injection compared to 0 min (Fig. 1A and C). Methamphetamine also caused significant hyperthermia in SERT single heterozygous KO mice ($DAT^{+/+}$ $SERT^{+/-}$) and DAT/SERT double heterozygous KO mice ($DAT^{+/-}$ $SERT^{+/-}$) from 15 to 60 min after injection compared to 0 min (Fig. 1B). However, in the mice with no DAT copies and a single SERT gene copy ($DAT^{-/-}$ $SERT^{+/-}$) methamphetamine caused significant hypothermia 15 min after injection followed by significant hyperthermia from 45 to 60 min after injection compared to 0 min (Fig. 1B). Surprisingly, DAT/SERT double KO mice showed significant hypothermia after methamphetamine for the entire test period from 15 to 60 min after injection compared to 0 min and showed significantly lower body temperature from 30 to 60 min after injection compared to wild-type mice (Fig. 1C). The magnitude of the hyperthermic effect also varied across genotypes. Mice with no DAT copies and a single SERT gene copy ($DAT^{-/-}$ $SERT^{+/-}$) had significantly lower body temperature after methamphetamine compared to wild-type mice (Fig. 1B) while SERT single KO mice showed significantly higher body temperature at 60 min after injection compared to wild-type (Fig. 1C).

Because methamphetamine is a potent blocker of all three monoamine transporters, methamphetamine-induced paradoxical hypothermia in DAT/SERT double KO mice might be mediated by an effect of methamphetamine on the norepinephrine transporter. Therefore, we investigated the effects of a potent blocker of SERT (fluoxetine) as well as potent blocker of NET (nisoxetine) in wild-type, DAT single KO mice, SERT single KO mice, and DAT/SERT double KO mice. Following fluoxetine administration, a significant genotype×time interaction was observed for changes in body temperature ($F(12,200=6.293$, $P<0.001$). Fluoxetine caused transient but significant hyperthermia in wild-type mice 15 min after injection compared to 0 min, which returned to baseline in subsequent time periods. This hyperthermic effect was prolonged in DAT/SERT double KO mice so that significant hyperthermia was observed from 15 to 60 min after injection compared to 0 min. In sharp contrast to these effects, a significant hypothermia was observed in DAT single KO mice from 15 to 60 min after injection compared to 0 min, respectively (Fig. 2). Following nisoxetine administration, there was a significant genotype effect on body temperature ($F(3,38=5.690$, $P<0.005$) and significant genotype×time interaction for changes in body temperature ($F(12,152=6.367$, $P<0.001$). Nisoxetine caused significant

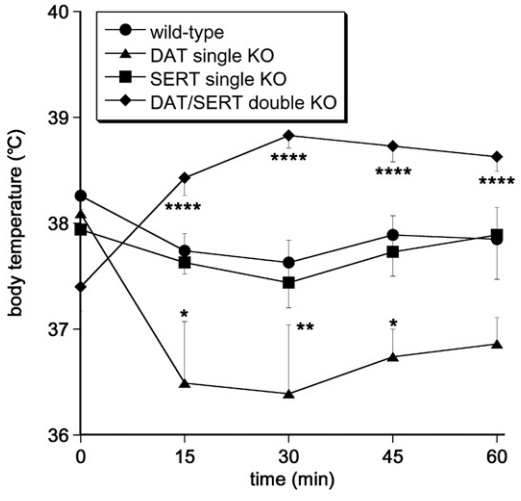

Fig. 3. Time course of body temperature of mice after intraperitoneal injection of nisoxetine (20 mg/kg). Nisoxetine caused significant hypothermia in DAT single KO mice from 15 to 45 min after injection compared to 0 min, and significant hyperthermia in DAT/SERT double KO mice from 15 to 60 min after injection compared to 0 min, respectively. *$P<0.05$; **$P<0.01$; and ****$P<0.001$ compared to 0 min (Dunnett's test). Values represent mean±S.E.M., $n=7$–12 mice per genotype.

Table 1
Comparison of percent lethality and LD_{50} of methamphetamine in 9 genotypes of DAT/SERT KO mice

Genotype	Percent lethality by each dose of methamphetamine (%)						LD_{50} (mg/kg)
	Dose of methamphetamine (mg/kg)						
	15	45	75	90	110	150	
$DAT^{+/+}$ $SERT^{+/+}$	5.0 (1/20)	24.0 (6/25)	38.1 (8/21)	57.1 (12/21)	100 (21/21)	N.A.	67.8 (55.5–81.8)
$DAT^{+/-}$ $SERT^{+/+}$	0 (0/21)	26.7 (8/30)	31.8 (7/22)	58.3 (14/24)	84.0 (21/25)	95.5 (21/22)	73.3 (62.6–83.7)
$DAT^{-/-}$ $SERT^{+/+}$	0 (0/9)	9.1 (1/11)	0 (0/16)[b]	14.3 (3/21)[b]	45.5 (5/11)[c]	100 (11/11)	112.6 (101.1–132.5)
$DAT^{+/+}$ $SERT^{+/-}$	N.A.	6.7 (1/15)	25.0 (4/16)	83.3 (5/6)	100 (3/3)	N.A.	80.5 (69.1–103.1)
$DAT^{+/-}$ $SERT^{+/-}$	N.A.	13.3 (6/45)	19.0 (4/21)	56.3 (9/16)	93.8 (15/16)	100 (1/1)	81.0 (71.4–95.6)
$DAT^{-/-}$ $SERT^{+/-}$	N.A.	0 (0/18)[a]	11.8 (2/17)	0 (0/3)	N.A.	N.A.	N.A.
$DAT^{+/+}$ $SERT^{-/-}$	N.A.	9.5 (2/21)	28.6 (6/21)	76.2 (16/21)	95.0 (19/20)	95.5 (21/22)	76.5 (67.9–84.5)
$DAT^{+/-}$ $SERT^{-/-}$	N.A.	4.3 (1/23)	19.0 (4/21)	64.0 (16/25)	81.0 (17/21)[a]	94.7 (36/38)	86.0 (77.6–94.0)
$DAT^{-/-}$ $SERT^{-/-}$	N.A.	0 (0/7)	0 (0/9)[a]	10.0 (1/10)[a]	20.0 (2/10)[c]	100 (5/5)	119.6 (108.4–141.7)

Values represent percent lethality at each dose of methamphetamine or LD_{50}. In parentheses, number of dead mice/number of mice treated at each dose of methamphetamine is shown after percent lethality, and 95% confidence interval is shown after LD_{50}. For $DAT^{-/-}$ $SERT^{+/-}$ mice data was not sufficient to calculate LD_{50}. [a]$P<0.05$; [b]$P<0.01$; and [c]$P<0.001$ compared to wild-type mice (χ^2 test), N.A.: not applicable.

hypothermia in DAT single KO mice from 15 to 45 min after injection compared to 0 min, and significant hyperthermia in DAT/SERT double KO mice from 15 to 60 min after injection compared to 0 min, respectively (Fig. 3).

3.2. Lethal toxicity of methamphetamine

Table 1 shows percent lethality and LD_{50} for methamphetamine in all 9 genotypes of DAT/SERT KO mice. In double wild-type

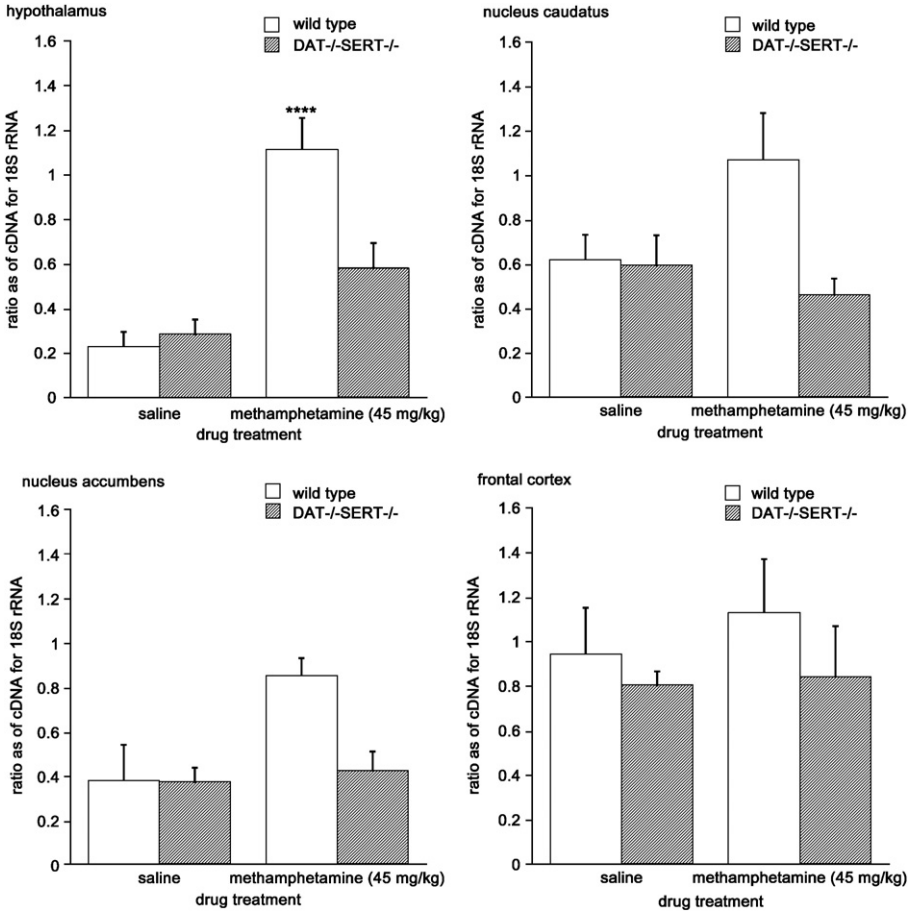

Fig. 4. Relative expression of interleukin-1β mRNA in the hypothalamus (a), nucleus caudatus (b), nucleus accumbens (c) and frontal cortex (d) of wild-type mice and DAT/SERT double KO mice after administration of saline or 45 mg/kg methamphetamine (saline solution). Methamphetamine significantly increased hypothalamic interleukin-1β mRNA by 5 times only in wild-type mice, compared to saline control. ****$P<0.001$ compared to saline treated mice of same genotype (Tukey's HSD test). Values represent mean±S.E.M., $n=4$–7 mice per group.

mice ($DAT^{+/+}$ $SERT^{+/+}$), the LD_{50} for methamphetamine was estimated to be 67.8 mg/kg (95% confidence interval 55.5–81.8 mg/kg). The LD_{50} was calculated for 7 of the other 8 genotypes, but we were unable to calculate the LD_{50} in $DAT^{-/-}$ $SERT^{+/-}$ mice because the percent lethality was substantially reduced. Full deletion of the DAT gene, or partial or full deletion of the SERT gene, increased the LD_{50} for methamphetamine compared to wild-type mice. DAT single KO mice and DAT/SERT double KO mice showed a significantly lower percent lethality against 75, 90, and 110 mg/kg methamphetamine compared to wild-type mice. These 2 genotypes of mice showed the first and second highest LD_{50} values examined for methamphetamine (112.6 mg/kg for DAT single KO mice, 119.6 mg/kg for DAT/SERT double KO mice, respectively), which were 1.7–1.8 times that observed in wild-type mice. Mice with no DAT copies and a single SERT gene copy ($DAT^{-/-}$ $SERT^{+/-}$) also showed significantly lower percent lethality against 45 mg/kg methamphetamine, suggesting that full deletion of DAT gene is protective factor against lethal toxicity of methamphetamine.

3.3. Effects of methamphetamine on the expression of interleukin-1β mRNA in the mice brain

In the hypothalamus there was a significant effect of methamphetamine on the relative expression of interleukin-1β mRNA ($F(1,17=24.666$, $P<0.001$). There was also a significant methamphetamine × genotype interaction ($F(1,17=6.154$, $P<0.05$), reflecting genotype-dependent effects of methamphetamine on hypothalamic interleukin-1β mRNA. Compared to saline control, methamphetamine significantly increased hypothalamic interleukin-1β mRNA by 5 times in wild-type mice, but not in DAT/SERT double KO mice (Fig. 4). In the nucleus caudatus, nucleus accumbens and frontal cortex, there were no significant effects of methamphetamine on interleukin-1β mRNA expression, nor were there any significant methamphetamine × genotype interactions (Fig. 4).

4. Discussion

These results demonstrate that methamphetamine (45 mg/kg) can exert a hyperthermic effect via DAT or via SERT in the absence of DAT. This conclusion is supported by the following observations: (1) the hyperthermic effect of methamphetamine was intact in DAT single KO mice; (2) the hyperthermic effect of methamphetamine was weakened in the mice with no DAT copies and a single SERT gene copy ($DAT^{-/-}$ $SERT^{+/-}$), which showed transient hypothermia at 15 min after methamphetamine injection, followed by hyperthermia which was reduced compared to wild-type mice at 60 min after methamphetamine injection; and (3) no hyperthermia was observed in DAT/SERT double KO mice, which instead exhibited a paradoxical hypothermia after methamphetamine administration. Fumagalli et al. (1998) used a lower dose of methamphetamine (30 mg/kg compared to 45 mg/kg in the present study) and reported that wild-type (C57BL/129SvJ background) and DAT heterozygous mice showed hyperthermia at 1 h after single injection of methamphetamine, but DAT single KO mice did not. In accordance with these results, in initial studies we administered 30 mg/kg methamphetamine to DAT single KO mice but observed no significant changes in body temperature from 0 to 60 min after treatment (data not shown). Subsequently we increased the dose of methamphetamine to 45 mg/kg, as presented here. This dose was the lowest enough to exert its hyperthermic effect even in the absence of DAT and caused not so high lethal toxicity. This was why we used only one dose in the hyperthermia and interleukin-1β experiments.

In the present study, methamphetamine (45 mg/kg) increased the body temperature (1.8 °C increment from 37.9 °C to 39.7 °C over the course of the experiment) of 20–30 week old female and male wild-type mice. There were no significant differences between female and male wild-type mice in the elevation of body temperature by methamphetamine (data not shown). Elevation of body temperature by methamphetamine was comparable to a previous study (Fumagalli et al., 1998) that used three-month-old male mice of a similar genetic background to ours (C57BL/129SvJ background) and 30 mg/kg of methamphetamine. Therefore, the differences in hyperthermic and lethal toxic effects of methamphetamine in DAT/SERT KO mice are likely to be attributed to deletion of DAT and/or SERT genes, and are not confounded with any of these other factors.

The hyperthermic effect of methamphetamine was intact in the mice with a single DAT gene copy and no SERT copies ($DAT^{+/-}$ $SERT^{-/-}$) but reduced in mice with no DAT copies and a single SERT gene copy ($DAT^{-/-}$ $SERT^{+/-}$), suggesting that half-normal expression of DAT (without SERT expression) was enough for methamphetamine to raise body temperature of mice, but half-normal expression of SERT (without DAT) was not. Therefore, the contribution of DAT to the hyperthermic effect of methamphetamine seems to be much larger than the contribution of SERT, although SERT possibly compensates to maintain the hyperthermic effect of methamphetamine in the absence of DAT. Intriguingly, the current results for hyperthermia produced by methamphetamine in DAT/SERT KO mice appear similar to our previous studies of cocaine-induced place preference (Sora et al., 2001; Murphy et al., 2003) as well as our recent microdialysis data on cocaine-induced extracellular dopamine concentrations in caudate putamen (Shen et al., 2004) in these mice. Both the mice with no DAT copies and a single SERT gene copy and DAT/SERT double KO mice failed to exhibit rewarding effects of cocaine (Sora et al., 2001) or increases in extracellular dopamine concentrations in the caudate putamen after cocaine (Shen et al., 2004). Although several mechanisms might underlie these findings, these data are consistent with the hypothesis that the absence of cognate DAT might allow dopamine to be accumulated by SERT (and/or NET), allowing cocaine to act at these targets to affect extracellular DA levels (Shen et al., 2004).

Methamphetamine caused unexpected and paradoxical hypothermia in DAT/SERT double KO mice. Since there has not been any report that DAT and/or SERT gene deletion could affect drug metabolism, it seems to be unlikely that this paradoxical hypothermia in DAT/SERT double KO mice was due to differences in the metabolism of methamphetamine. One possible explanation for this could be that methamphetamine could act on NET in DAT/SERT double KO mice to cause hypothermia, but this hypothesis was not supported by other data, as nisoxetine

caused significant hyperthermia in DAT/SERT double KO mice. Nisoxetine did not affect the body temperature in wild-type mice, so nisoxetine-induced hyperthermia in DAT/SERT double KO mice must have resulted from interactions between the effect of nisoxetine and neuroadaptations to chronic DAT and/or SERT loss in DAT/SERT double KO mice (Sora et al., 2001). Fluoxetine, the selective SERT blocker, has a weak binding potency for NET (Owens et al., 2001; Orjales et al., 2003), and also caused hyperthermia in DAT/SERT double KO mice supporting the idea that NET blockade in DAT/SERT double KO mice could lead to hyperthermia. In any case the current data showed that the norepinephrine system is not responsible for methamphetamine-induced paradoxical hypothermia in DAT/SERT double KO mice.

In contrast to the observations in combined DAT/SERT double KO mice both fluoxetine and nisoxetine caused hypothermia in DAT single KO mice but did not affect the body temperature of SERT single KO mice. As in DAT/SERT double KO mice, DAT single KO mice and SERT single KO mice show neuroadaptive changes in both postsynaptic receptors, and presynaptic neurotransmitter levels (Sora et al., 2001). Our results reflect complex interactions between actions of fluoxetine or nisoxetine and neurochemical backgrounds of DAT KO, SERT KO, and DAT/SERT double KO mice. We have previously found evidence for adaptations that affect responses to selective monoamine transporter blockers in DAT KO mice (Hall et al., 2002).

Previous animal studies suggest that dopamine receptor activation is crucial for amphetamine- or methamphetamine-induced lethality (Davis et al., 1978; Uchima et al., 1983; Derlet et al., 1990; Bronstein and Hong, 1995). These results suggest that lethal effects of amphetamines are closely related to their indirect agonistic effects on the dopaminergic terminals/neurons via DAT, which displaces both vesicular and intracellular dopamine and facilitates release of dopamine into the extraneuronal space by synaptic transport (Seiden et al., 1993). In our experiments, full deletion of DAT and full or partial deletion of SERT increased methamphetamine LD_{50} compared to wild-type mice, suggesting that both DAT and SERT have a role in the lethal toxicity of methamphetamine. Especially in DAT single KO mice and DAT/SERT double KO mice, DAT deletion strikingly increased the LD_{50} for methamphetamine to 1.7–1.8 times that observed in wild-type mice. Moreover, mice with DAT deletion (DAT single KO mice, $DAT^{-/-}$ $SERT^{+/-}$, and DAT/SERT double KO mice) all showed significantly lower percent lethality against methamphetamine (45 mg/kg in $DAT^{-/-}$ $SERT^{+/-}$, 75, 90, and 110 mg/kg in DAT single KO mice and DAT/SERT double KO mice) compared to wild-type mice, indicating a major role of DAT in the lethal toxicity produced by methamphetamine. On the other hand, addition of SERT deletion slightly increased LD_{50}. However, these small but consistent differences produced by SERT deletion were not statistically significant, so the lethal toxic effect of methamphetamine is mainly dependent on DAT.

In comparing the results of the temperature and lethality studies across the DAT/SERT genotypes, it is obvious that hyperthermia is not a prerequisite for methamphetamine-induced lethality. Previous clinical and animal studies suggest that hyperthermia is the primary cause of death by methamphetamine (Bowyer et al., 1994; Davidson et al., 2001; Namiki et al., 2005). But in our experiments, there was a dissociation between hyperthermic and lethal toxic effects of methamphetamine in DAT single KO mice and DAT/SERT double KO mice. The former mice showed hyperthermia and the latter showed hypothermia by methamphetamine, respectively, but both showed markedly elevated LD_{50} values for methamphetamine compared to wild-type mice. So, contrary to the previous conceptions of the causes of methamphetamine-induced toxicity, methamphetamine-induced hyperthermia does not appear to be the mediator of lethal toxicity produced by methamphetamine.

Yamaguchi et al. (1991) reported that 2–15 mg/kg methamphetamine caused a marked induction of interleukin-1β mRNA exclusively in the hypothalamus of rats which peaked at 1 h after administration. Halladay et al. (2003) reported that 8 mg/kg methamphetamine increased hypothalamic expression of interleukin-1β mRNA in BALB/c mice at 2 h after administration. Bowyer et al. (1994) reported that interleukin-1 receptor antagonist reduced maximal body temperature by methamphetamine in rats. We also observed that methamphetamine significantly increased hypothalamic interleukin-1β mRNA in wild-type mice, but not in DAT/SERT double KO mice, that fail to exhibit methamphetamine-induced hyperthermia. Since interleukin-1β is known to be the major endogenous pyrogen (Dascombe et al., 1989; Schobitz et al., 1994; Tringali et al., 1998; Leon, 2002), our finding can provide a partial explanation of the mechanism of methamphetamine-induced paradoxical hypothermia in DAT/SERT double KO mice: methamphetamine did not increase hypothalamic interleukin-1β mRNA in the mice, and thus could not raise their body temperature. But as to the methamphetamine-induced decrease in body temperature observed in DAT/SERT double KO mice, the precise mechanism remains unknown. We also examined methamphetamine-induced interleukin-1β mRNA in the nucleus accumbens, nucleus caudatus and frontal cortex, which were not involved in temperature regulation (Leon, 2002) since methamphetamine significantly increased TNF-α mRNA, another endogenous pyrogen, in the nucleus accumbens and caudatus but not in the frontal cortex of mice (Nakajima et al., 2004). But we did not find any significant changes in these brain regions.

In conclusion, these studies have demonstrated that the hyperthermic effect of methamphetamine is dependent on DAT, and in the absence of DAT, on SERT. Furthermore, combined deletion of both the DAT and SERT genes in mice resulted in a paradoxical hypothermia produced by methamphetamine. Although the noradrenergic system does not appear to be responsible for methamphetamine-induced paradoxical hypothermia in DAT/SERT double KO mice, a partial explanation of this mechanism is that methamphetamine failed to increase hypothalamic interleukin-1β mRNA in DAT/SERT double KO mice. Although DAT and SERT were shown here to be involved in both the effects of methamphetamine on temperature as well as methamphetamine lethal toxicity, the mechanisms are nonetheless different; DAT single KO mice exhibited hyperthermia but greatly reduced methamphetamine lethality, and the lethality was no different from DAT/SERT double KO mice that had hypothermic responses to methamphetamine. Thus, although the lethal toxic effect of methamphetamine is mainly dependent on

DAT, with some contribution from SERT, hyperthermia is not prerequisite for methamphetamine-induced lethality.

Acknowledgements

We thank Ms. Kayo Ohmi and Ms. Maki Naka for their assistance. This study was supported in part by Grant-in-Aid for Health and Labor Science Research (Research on Pharmaceutical and Medical Safety) from the Ministry of Health, Labor and Welfare of Japan; by Grants-in-Aid for Scientific Research (B), Scientific Research on Priority Areas — System study on higher-order brain functions and Research on Pathomechanisms of Brain Disorders, Core Research for Evolutional Science and Technology (CREST), from the Ministry of Education, Culture, Sports, Science and Technology of Japan (No. 17390315, 17022007, 18023007); and by the Mitsubishi Pharma Research Foundation. This study was also supported in part by intramural funding from the National Institute on Drug Abuse, NIH/DHHS (USA).

References

Albers, D.S., Sonsalla, P.K., 1995. Methamphetamine-induced hyperthermia and dopaminergic neurotoxicity in mice: pharmacological profile of protective and nonprotective agents. J. Pharmacol. Exp. Ther. 275, 1104–1114.

Ali, S.F., Newport, G.D., Holson, R.R., Slikker Jr., W., Bowyer, J.F., 1994. Low environmental temperatures or pharmacologic agents that produce hypothermia decrease methamphetamine neurotoxicity in mice. Brain Res. 658, 33–38.

Bengel, D., Murphy, D.L., Andrews, A.M., Wichems, C.H., Feltner, D., Heils, A., Mossner, R., Westphal, H., Lesch, K.P., 1998. Altered brain serotonin homeostasis and locomotor insensitivity to 3, 4-methylenedioxymethamphetamine ("Ecstasy") in serotonin transporter-deficient mice. Mol. Pharmacol. 53, 649–655.

Bowyer, J.F., Davies, D.L., Schmued, L., Broening, H.W., Newport, G.D., Slikker Jr., W., Holson, R.R., 1994. Further studies of the role of hyperthermia in methamphetamine neurotoxicity. J. Pharmacol. Exp. Ther. 268, 1571–1580.

Broening, H.W., Morford, L.L., Vorhees, C.V., 2005. Interactions of dopamine D1 and D2 receptor antagonists with D-methamphetamine-induced hyperthermia and striatal dopamine and serotonin reductions. Synapse 56, 84–93.

Bronstein, D.M., Hong, J.S., 1995. Effects of sulpiride and SCH 23390 on methamphetamine-induced changes in body temperature and lethality. J. Pharmacol. Exp. Ther. 274, 943–950.

Canini, F., Bourdon, L., 1998. Dopamine involvement in thermoregulatory responses to heat in rats. Neurosci. Lett. 241, 91–94.

Chan, T.C., Evans, S.D., Clark, R.F., 1997. Drug-induced hyperthermia. Crit. Care Clin. 13, 785–808.

Dascombe, M.J., Rothwell, N.J., Sagay, B.O., Stock, M.J., 1989. Pyrogenic and thermogenic effects of interleukin 1 beta in the rat. Am. J. Physiol. 256, E7–E11.

Davidson, C., Gow, A.J., Lee, T.H., Ellinwood, E.H., 2001. Methamphetamine neurotoxicity: necrotic and apoptotic mechanisms and relevance to human abuse and treatment. Brain Res. Brain Res. Rev. 36, 1–22.

Davis, W.M., Hatoum, H.T., Waters, I.W., 1978. Interactions of catecholaminergic receptor blockers with lethal doses of amphetamine or substituted amphetamines in mice. Res. Commun. Chem. Pathol. Pharmacol. 21, 27–36.

Derlet, R.W., Albertson, T.E., Rice, P., 1990. Antagonism of cocaine, amphetamine, and methamphetamine toxicity. Pharmacol. Biochem. Behav. 36, 745–749.

Fumagalli, F., Gainetdinov, R.R., Valenzano, K.J., Caron, M.G., 1998. Role of dopamine transporter in methamphetamine-induced neurotoxicity: evidence from mice lacking the transporter. J. Neurosci. 18, 4861–4869.

Funahashi, M., Kohda, H., Hori, O., Hayashida, H., Kimura, H., 1990. Potentiating effect of morphine upon D-methamphetamine-induced hyperthermia in mice. Effects of naloxone and haloperidol. Pharmacol. Biochem. Behav. 36, 345–350.

Green, A.R., Mechan, A.O., Elliott, J.M., O'Shea, E., Colado, M.I., 2003. The pharmacology and clinical pharmacology of 3,4-methylenedioxymethamphetamine (MDMA, "ecstasy"). Pharmacol. Rev. 55, 463–508.

Hall, F.S., Li, X.F., Sora, I., Xu, F., Caron, M., Lesch, K.P., Murphy, D.L., Uhl, G.R., 2002. Cocaine mechanisms: enhanced cocaine, fluoxetine and nisoxetine place preferences following monoamine transporter deletions. Neuroscience 115, 153–161.

Halladay, A.K., Kusnecov, A., Michna, L., Kita, T., Hara, C., Wagner, G.C., 2003. Relationship between methamphetamine-induced dopamine release, hyperthermia, self-injurious behaviour and long term dopamine depletion in BALB/c and C57BL/6 mice. Pharmacol. Toxicol. 93, 33–41.

Hanson, G.R., Rau, K.S., Fleckenstein, A.E., 2004. The methamphetamine experience: a NIDA partnership. Neuropharmacology 47 (Suppl 1), 92–100.

He, J., Xu, H., Yang, Y., Zhang, X., Li, X.M., 2004. Neuroprotective effects of olanzapine on methamphetamine-induced neurotoxicity are associated with an inhibition of hyperthermia and prevention of Bcl-2 decrease in rats. Brain Res. 1018, 186–192.

Imam, S.Z., Ali, S.F., 2001. Aging increases the susceptibility to methamphetamine-induced dopaminergic neurotoxicity in rats: correlation with peroxynitrite production and hyperthermia. J. Neurochem. 78, 952–959.

Kita, T., Wagner, G.C., Nakashima, T., 2003. Current research on methamphetamine-induced neurotoxicity: animal models of monoamine disruption. J. Pharmacol. Sci. 92, 178–195.

Kuperman, D.I., Freyaldenhoven, T.E., Schmued, L.C., Ali, S.F., 1997. Methamphetamine-induced hyperthermia in mice: examination of dopamine depletion and heat-shock protein induction. Brain Res. 771, 221–227.

Leon, L.R., 2002. Invited review: cytokine regulation of fever: studies using gene knockout mice. J. Appl. Physiol. 92, 2648–2655.

Miller, D.B., O'Callaghan, J.P., 2003. Elevated environmental temperature and methamphetamine neurotoxicity. Environ. Res. 92, 48–53.

Murphy, D.L., Uhl, G.R., Holmes, A., Ren-Patterson, R., Hall, F.S., Sora, I., Detera-Wadleigh, S., Lesch, K.P., 2003. Experimental gene interaction studies with SERT mutant mice as models for human polygenic and epistatic traits and disorders. Genes Brain Behav. 2, 350–364.

Nakajima, A., Yamada, K., Nagai, T., Uchiyama, T., Miyamoto, Y., Mamiya, T., He, J., Nitta, A., Mizuno, M., Tran, M.H., Seto, A., Yoshimura, M., Kitaichi, K., Hasegawa, T., Saito, K., Yamada, Y., Seishima, M., Sekikawa, K., Kim, H.C., Nabeshima, T., 2004. Role of tumor necrosis factor-alpha in methamphetamine-induced drug dependence and neurotoxicity. J. Neurosci. 24, 2212–2225.

Namiki, M., Mori, T., Sawaguchi, T., Ito, S., Suzuki, T., 2005. Underlying mechanism of combined effect of methamphetamine and morphine on lethality in mice and therapeutic potential of cooling. J. Pharmacol. Sci. 99, 168–176.

Orjales, A., Mosquera, R., Toledo, A., Pumar, M.C., Garcia, N., Cortizo, L., Labeaga, L., Innerarity, A., 2003. Syntheses and binding studies of new [(aryl)(aryloxy)methyl]piperidine derivatives and related compounds as potential antidepressant drugs with high affinity for serotonin (5-HT) and norepinephrine (NE) transporters. J. Med. Chem. 46, 5512–5532.

Owens, M.J., Knight, D.L., Nemeroff, C.B., 2001. Second-generation SSRIs: human monoamine transporter binding profile of escitalopram and *R*-fluoxetine. Biol. Psychiatry 50, 345–350.

Sato, M., Numachi, Y., Hamamura, T., 1992. Relapse of paranoid psychotic state in methamphetamine model of schizophrenia. Schizophr. Bull. 18, 115–122.

Schobitz, B., De Kloet, E.R., Holsboer, F., 1994. Gene expression and function of interleukin 1, interleukin 6 and tumor necrosis factor in the brain. Prog. Neurobiol. 44, 397–432.

Seiden, L.S., Sabol, K.E., Ricaurte, G.A., 1993. Amphetamine: effects on catecholamine systems and behavior. Annu. Rev. Pharmacol. Toxicol. 33, 639–677.

Shen, H.W., Hagino, Y., Kobayashi, H., Shinohara-Tanaka, K., Ikeda, K., Yamamoto, H., Yamamoto, T., Lesch, K.P., Murphy, D.L., Hall, F.S., Uhl, G.R., Sora, I., 2004. Regional differences in extracellular dopamine and serotonin assessed by in vivo microdialysis in mice lacking dopamine and/or serotonin transporters. Neuropsychopharmacology 29, 1790–1799.

Sora, I., Hall, F.S., Andrews, A.M., Itokawa, M., Li, X.F., Wei, H.B., Wichems, C., Lesch, K.P., Murphy, D.L., Uhl, G.R., 2001. Molecular mechanisms of cocaine reward: combined dopamine and serotonin transporter knockouts eliminate cocaine place preference. Proc. Natl. Acad. Sci. U. S. A. 98, 5300–5305.

Sora, I., Wichems, C., Takahashi, N., Li, X.F., Zeng, Z., Revay, R., Lesch, K.P., Murphy, D.L., Uhl, G.R., 1998. Cocaine reward models: conditioned place preference can be established in dopamine- and in serotonin-transporter knockout mice. Proc. Natl. Acad. Sci. U. S. A. 95, 7699–7704.

Tringali, G., Dello Russo, C., Preziosi, P., Navarra, P., 1998. Hypothalamic interleukin-1 in physiology and pathology. Toxicol. Lett. 102–103, 295–299.

Uchima, E., Ogura, Y., Hiraga, Y., Shikata, I., 1983. Relationship between methamphetamine toxicity and catecholamine levels in heart and brain of mice. Nippon Hoigaku Zasshi 37, 198–208.

Wagner, G.C., Tekirian, T.L., Cheo, C.T., 1993. Sexual differences in sensitivity to methamphetamine toxicity. J. Neural Transm. Gen. Sect. 93, 67–70.

Yamaguchi, T., Kuraishi, Y., Minami, M., Nakai, S., Hirai, Y., Satoh, M., 1991. Methamphetamine-induced expression of interleukin-1 beta mRNA in the rat hypothalamus. Neurosci. Lett. 128, 90–92.

Mu (μ) Opioid Receptor Regulation of Ethanol-Induced Dopamine Response in the Ventral Striatum: Evidence of Genotype Specific Sexual Dimorphic Epistasis

Martin O. Job, Amanda Tang, F. Scott Hall, Ichiro Sora, George R. Uhl, Susan E. Bergeson, and Rueben A. Gonzales

Background: Ethanol stimulates the dopaminergic mesoaccumbal pathway, which is thought to play a role in ethanol reinforcement. Mu (μ)-opioid (MOP) receptors modulate accumbal dopamine activity, but it is not clear whether MOP receptors are involved in the mechanism of ethanol-stimulated accumbal dopamine release.

Methods: We investigated the role that MOP receptors play in ethanol (2.0 g/kg)-stimulated accumbal dopamine release by using MOP receptor knockout mice (C57BL/6J-129SvEv and congenic C57BL/6J genotypes) along with blockade of MOP receptors with a μ1 selective antagonist (naloxonazine).

Results: Both gene deletion and pharmacological antagonism of the MOP receptor decreased ethanol-stimulated accumbal dopamine release compared with controls with female mice showing a larger effect in the C57BL/6J-129SvEv genotype. However, both male and female mice showed reduced ethanol-stimulated dopamine release in the congenic MOP receptor knockout mice (C57BL/6J). No differences in the time course of dialysate ethanol concentration were found in any of the experiments.

Conclusions: The data demonstrate the existence of a novel interaction between genotype and sex in the regulation of ethanol-stimulated mesolimbic dopamine release by the MOP receptor. This implies that a more complete understanding of the epistatic influences on the MOP receptor and mesolimbic dopamine function may provide more effective pharmacotherapeutic interventions in the treatment of alcoholism.

Key Words: Dopamine, genotype, knockout mice, microdialysis, nucleus accumbens, sexual dimorphism

The mesoaccumbal dopaminergic pathway is proposed to play a role in mediating the reinforcing properties of ethanol (Doyon et al 2003; Imperato and Di Chiara 1986; Melendez et al 2002; Weiss et al 1993), although the precise mechanisms by which this occurs are unclear at present. Several subtypes of opioid receptors are known to modulate dopamine activity in the nucleus accumbens (NAcc) (Borg and Taylor 1997; Spanagel et al 1992; Yoshida et al 1999), and these receptors are potential targets for altering ethanol-reinforced behavior. The nonselective opioid receptor antagonists naltrexone and nalmefene reduce alcohol drinking behavior in both humans and in animal models (Gonzales and Weiss 1998; Kornet et al 1991; Mason et al 1999; Volpicelli et al 1992), but the subtypes of opioid receptors that mediate these effects are not yet clear.

Ethanol activation of the mesolimbic dopamine system may, in part, be mediated by stimulating the release of β-endorphin or other endogenous opioid peptides (Gianoulakis 1990; Marinelli et al 2003; Olive et al 2001). β-endorphin activates both delta and mu opioid receptors (MOPr) that are located either in the ventral tegmental area or the NAcc to alter accumbal dopamine release (Dilts and Kalivas 1990; Houghten et al 1984; Mansour et al 1987; Svingos et al 1999). Consistent with this data, naltrexone reduced the accumbal dopamine release associated with ethanol self-administration (Gonzales and Weiss 1998). The MOPr has been implicated by data showing that systemic administration of naloxonazine, a long-lasting mu1 antagonist, inhibits ethanol-stimulated accumbal dopamine release in rats (Tanda and Di Chiara 1998). However, naloxonazine may also act on receptors other than mu1 (Dray and Nunan 1984; Ling et al 1986), so the role of the MOPr in regulation of ethanol-stimulated dopamine release is still uncertain. Oslin et al (2003) recently reported that a functional polymorphism of the human gene that codes for the MOPr is associated with the clinical response to naltrexone in treating alcohol dependence. Therefore, clarifying the role of the MOPr in neurochemical mechanisms that may contribute to ethanol reinforcement may lead to improvements in pharmacotherapy for treatment of alcohol dependence.

A decrease in both ethanol self-administration and/or conditioned place preference has been shown in three MOPr knockout mouse models, further suggesting a key role for the MOPr in ethanol reward and reinforcement (Becker et al 2002; Hall et al 2001; Roberts et al 2000). In this study, we investigated the role of the MOPr in ethanol stimulation of mesolimbic dopamine activity using both null mutants and pharmacological blockade. The importance of sex influences in neuroscience studies is well known (Cahill 2006), and several sex differences in opioid responsiveness have been detected (Baamonde et al 1989; Bartok and Craft, 1997; Cicero et al 1996; Cicero et al 2000). We therefore included both sexes in our studies and tested a secondary hypothesis that MOPr-mediated alcohol responsiveness included sexually dimorphic influences.

From the Division of Pharmacology (MOJ, AT, RAG), College of Pharmacy, and the Waggoner Center for Alcohol and Addiction Research and Sections of Neurobiology and Molecular Genetics and Microbiology (SEB), University of Texas, Austin, Texas; Molecular Neurobiology Branch (FSH, IS, GRU), National Institute on Drug Abuse, Intramural Research Program, National Institute of Health, Baltimore, Maryland; AT is currently affiliated with Lexicon Genetics Inc., The Woodlands, Texas; IS is currently affiliated with the Department of Psychobiology (IS), Tohoku University Graduate School of Medicine, Sendai, Japan.

Address reprint requests to Rueben A. Gonzales, Ph.D., University of Texas at Austin, PHAR-Pharmacology, 1 University Station A1915, Austin, Texas 78712-0125; E-mail: rgonzales@mail.utexas.edu.

Received August 2, 2006; revised November 13, 2006; accepted November 14, 2006.

0006-3223/07/$32.00
doi:10.1016/j.biopsych.2006.11.016

Methods and Materials

Subjects

Mice (male and female, 4–16 months old, 21–38 g) were obtained from the National Institute on Drug Abuse (NIDA, Baltimore, Maryland) or bred at the University of Texas at Austin. The mice were housed in a humidity and temperature controlled room with a 12:12-hour light/dark cycle (lights on 7 am), and animals had free access to food and water. All animal experiments were conducted under protocols approved by the Institutional Animal Care and Use Committee at the University of Texas, following National Institute of Heath (NIH) and United States Department of Agriculture (USDA) guidelines and regulations.

Heterozygous MOPr knockout mice were derived from the colony originally developed by Sora et al (1997) at NIDA. Two colonies of MOPr knockout mice were established by nonsibling heterozygous breeding at the Animal Resources Center at the University of Texas at Austin. The first colony was on a mixed genetic background (C57BL/6J-129SvEv; 1:1) that had been maintained for approximately 30 generations, and breeding pairs were transferred to the University of Texas. The inbreeding coefficient as described by Falconer and Mackay (1996) was calculated at .926 indicating that by the 30^{th} generation, 89% of the C57BL/6J-129SvEv genome was homozygous with a certainty of less than 11% possible segregation of B6 and 129 alleles. The second colony was from a congenic line created at NIDA in which the mixed background knockout mice were backcrossed for 10 generations onto the C57BL/6J strain. The C57BL/6J model was chosen for the backcross because these mice are well known to have high levels of drinking relative to other inbred strains (Belknap et al 1993).

Genotyping

Genotyping was determined by polymerase chain reaction of tissue extracts. Details are provided in Supplement 1 online.

Surgery, Recovery, and Handling

Surgical preparation of the mice for microdialysis was conducted as previously described (Tang et al 2003). We anesthetized the mice with 2.5% Avertin (2,2,2-tribromoethanol; .016 ml/g) or isoflurane (2%). The stainless steel guide cannula (8 mm long, .8 mm 20–21 gauge; Small Parts Inc., Miami Lakes, Florida) was positioned above the right NAcc (anterior (AP) +1.5–1.7, lateral (LAT) +.8, ventral (DV) −2.0–2.5 from bregma; Paxinos and Franklin 2001) and secured with a skull screw and dental cement. An obturator was placed into the guide cannula to prevent blockage. After the surgery, each animal was singly housed and given at least 4 days for recovery. During recovery, each mouse was injected daily with .1 ml saline for at least 3 days immediately before the microdialysis experiment in order to habituate the mouse to the intraperitoneal (IP) injection.

Microdialysis

Dialysis probes with 1 mm active dialyzing area were constructed as previously described (Tang et al 2003). A probe was inserted into the guide cannula under halothane or isoflurane anesthesia (2.0% in air, flow rate at 2.0 liter/min) the night before the experiment, and the mouse was placed in a dialysis chamber. The probe was perfused with artificial cerebrospinal fluid (ACSF: 145 mM NaCl, 2.8 mM KCl, 1.2 mM $CaCl_2$, 1.2 mM $MgCl_2$, .25 mM ascorbic acid, and 5.4 mM D-glucose) at .2 μl/min overnight. The flow rate was increased to 1.0 μl/min the next morning, and after one hour, sample collection (15-17 min intervals) commenced. After the collection of four basal samples, we injected each animal with either saline or 2.0 g/kg ethanol (15% w/v, in saline). Sample collection continued for 3–4 hours. Calcium-dependency (percent decrease in dopamine concentration obtained during perfusion with calcium-free ACSF from regular ACSF) was determined by perfusing calcium-free ACSF for one hour at the end of the experiment. Dialysate samples were handled and analyzed by gas chromatography (for ethanol) and high performance liquid chromatography with electrochemical detection (for dopamine) as described in Tang et al (2003) and Doyon et al (2003). The detection limit for dopamine was 2 fmol.

Experimental Design

The first experiment used wildtype and MOPr knockout mice with a mixed genetic background (C57BL/6J − 129SvEv) to investigate the effect of the MOPr on ethanol-evoked (2.0 g/kg, IP) dopamine release in the ventral striatum. This dose was chosen because we and others previously showed that it reliably stimulates dopamine release (Olive et al 2000; Tang et al 2003). In addition, doses of ethanol in this range produce conditioned place preference in a variety of mouse strains indicating that this route and dose induce ethanol reward (Boyce-Rustay and Risinger 2003; Cunningham et al 1996; Nocjar et al 1999). The second experiment used mixed background wildtype animals to determine the effect of pharmacological antagonism of the mu1 opioid receptor with naloxonazine on the dopamine response stimulated by ethanol. Mice were pretreated with saline or naloxonazine (15 mg/kg, IP) 19 – 20 hours prior to microdialysis sampling. The third experiment was similar to the first except that the mice used were from the congenic line with a C57BL/6J background. Sex was an independent variable in the first three experiments. In addition, we performed a separate control experiment to examine the potential effect of saline injection on dopamine release in wildtype and MOPr knockout mice (congenic line).

Histology

After each experiment the mouse was given an intraperitoneal injection of chloral hydrate (60 mg/mouse) or pentobarbital (500 mg/kg) and was perfused intracardially with a 10% (v/v) formalin solution. Analysis of probe placement was carried out as previously described (Tang et al 2003).

Data Analysis

Statistical significance was determined using a random block analysis of variance (ANOVA) with two between-subject variables (genotype or pretreatment and sex) and one within-subject variable (time before and after the injection). The basal response was defined as the dopamine level in the last two samples prior to the ethanol injection. ANOVA was used to determine the differences in the dialysate ethanol peak concentration and the rate of decline between either the genotypes or the pretreatments across sexes. The rate of decline was calculated as the slope of the linear part of the time-concentration curve. The criterion for the type I error was set to $p < .05$. Simple effect tests with Bonferroni correction factors were used to distinguish the influence of one variable on another variable when a significant interaction was detected. During the HPLC analysis there were a few samples lost due to technical reasons (either unidentified contaminants co-eluting with dopamine or the recorder was off-scale during dopamine elution) and these were estimated by averaging the dopamine responses before and after the missing point for statistical analysis. The degrees of freedom were corrected for each ANOVA based on the number of estimated points in each specific data set. Overall there were six missing

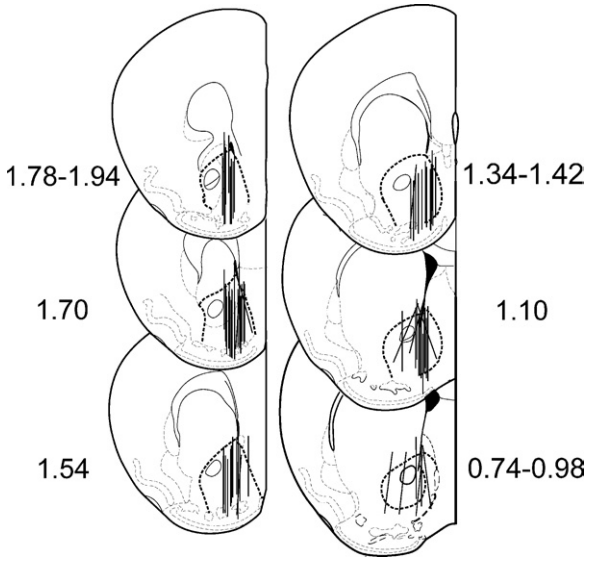

Figure 1. Microdialysis probe placements in the ventral striatum in MOPr knockout mice and their wildtype controls. Numbers on either side of the figure represent the position of the slice (in millimeters) relative to bregma. The border of the NAcc is highlighted with a heavy dashed line. Drawings were from Paxinos and Franklin (2001). MOPr, mu opioid receptors; NAcc, nucleus accumbens.

points in the knockout experiment with the mixed background, three missing points in the naloxonazine experiment, and one missing point in the congenic experiment. Values are reported as mean ± SEM.

Results

Histological Analysis and Ca^{2+}-Dependence of Dopamine Release

The microdialysis probe placements are shown in Figure 1. They were distributed either in the medial NAcc and passed through both the shell and core regions, or exclusively in the shell. The calcium-dependency, a functional measure of the physiological state of the dopamine nerve terminals during microdialysis sampling, was determined for all the animals used in the study. The criterion for acceptable calcium-dependency was the attainment of at least a 40% decrease in dialysate dopamine concentrations during the calcium-free ACSF perfusion compared with regular ACSF perfusion. Mean calcium-dependency for all groups was between 47–84%.

Effect of MOPr Knockout on Ethanol-Evoked Dopamine Release in the Ventral Striatum: Mixed Background

The increase in dialysate dopamine concentration stimulated by 2.0 g/kg ethanol (IP) was dependent on the MOPr and sex with female knockouts showing a greater reduction in the ethanol stimulation compared with males (Figure 2A, 2B). ANOVA on dialysate dopamine concentration revealed a significant three-way interaction, sex × genotype × time ($F(8, 218) = 2.9$, $p < .05$). Simple effects tests for the female mice revealed that deletion of the MOPr virtually abolished ethanol-stimulated dopamine release ($F(8, 218) = 5.7$, $p < .05$, for the genotype × time interaction). In control mice the maximal response was observed at the first point after the injection ($F(1, 218) = 79$, $p < .05$; simple effects within the female wildtype group), and the dopamine concentration was significantly elevated for 102 min compared with basal levels. In contrast, ethanol did not significantly stimulate dopamine release in the female knockout mice. Instead, there was a gradual decrease in accumbal dopamine levels relative to basal that was significant at 85 min after the injection ($F(1, 218) > 10.9$, $p < .05$; simple effects within the female knockout group).

In male mice the effect of the null mutation of the MOPr was more subtle than in the females (Figure 2B). The peak ethanol stimulated dopamine response was similar in both the knockout and wildtype mice, but the knockout mice showed a more rapid return to baseline compared with the controls ($F(8, 218) = 2.84$, $p < .05$).

Basal dopamine levels were lower in the female knockout mice compared with the other groups ($F(1, 28) = 5.10$, $p < .05$ for the sex × genotype interaction, see caption Figure 2). Although the low basal level in female knockout mice tends to magnify changes in dopamine after ethanol injection when expressed as percentage of basal, this cannot account for the significant three-way interaction (sex × genotype × time) found in the ethanol-induced accumbal dopamine response because this group had the least response to ethanol.

Dialysate ethanol concentrations were maximal in the first sample, and this was followed by a linear decline in ethanol concentrations (Figure 2C, 2D). Neither sex nor genotype significantly affected peak concentration of ethanol ($F(1, 21) = 1.12$, $p > .05$) or the rate of decline ($F(1, 21) = .01$, $p > .05$).

Effect of Pharmacological Blockade of the mu1 Receptor on Ethanol-Evoked Dopamine Release in the Ventral Striatum: Mixed Background

Antagonism of the mu1 receptor with naloxonazine (15 mg/kg, IP) caused a sex dependent attenuation of the ethanol-

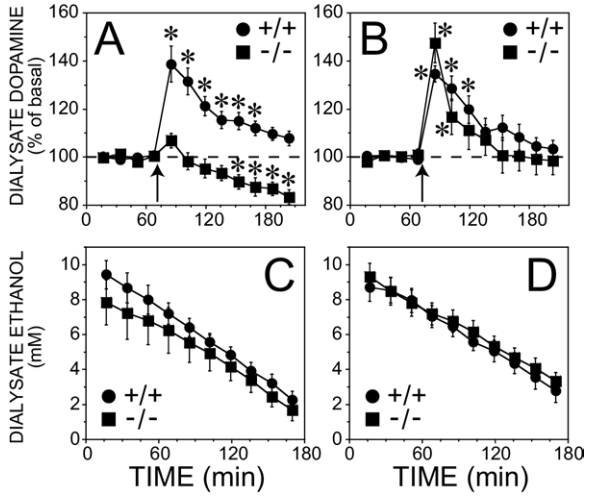

Figure 2. Dopamine response and dialysate ethanol in the ventral striatum after intraperitoneal administration of ethanol (2 g/kg) in MOPr knockout mice on a mixed genetic background (C57BL/6J-129SvEv) and their wildtype controls. **(A)** Female mice. The basal dopamine concentrations were 1.1 ± .2 nM and .4 ± .1 nM for wildtype and knockout groups, respectively ($n = 8$). **(B)** Male mice. The basal dopamine concentrations were 1.3 ± .1 nM and 1.7 ± .3 nM for wildtype and knockout groups, respectively ($n = 8$). The arrow indicates when the ethanol injection was given. *indicates significant different from basal dopamine concentration by simple effects post hoc analysis ($p < .05$) after a significant three-way interaction in the overall ANOVA. The ethanol content in samples taken after the injection is shown in **(C)** female mice and **(D)** male mice. Note that the x-axis starts at the point of the ethanol injection which is different from that shown in panels A and B. MOPr, mu opioid receptors; NAcc, nucleus accumbens; ANOVA, analysis of variance.

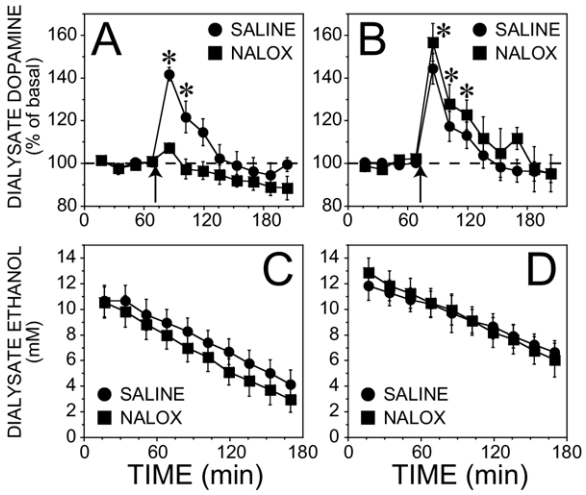

Figure 3. Effect of naloxonazine on ethanol-stimulated (2 g/kg, IP) dialysate dopamine and ethanol concentrations in the ventral striatum in wildtype mice with a mixed genetic background (C57BL/6J-129SvEv). Naloxonazine (NALOX) (15 mg/kg), IP, or saline was given 19–20 hours prior to the experiment. **(A)** Female mice. The basal dopamine concentrations were 1.7 ± .4 nM and 1.9 ± .6 nM for saline and naloxonazine groups, respectively ($n = 7$). **(B)** Male mice. The basal dopamine concentrations were 1.1 ± .2 nM ($n = 6$) and .8 ± .1 nM ($n = 5$) for saline and naloxonazine groups, respectively. The arrow indicates when the ethanol injection was given. *Significantly different from basal dopamine concentration by simple effects post hoc analysis ($p < .05$) after a significant three-way interaction in the overall ANOVA. The ethanol content in samples taken after the injection is shown in **(C)** female mice and **(D)** male mice. Note that the x-axis starts at the point of the ethanol injection which is different from that shown in panels A and B. ANOVA, analysis of variance; IP, intraperitoneally.

stimulated dopamine response similar to our findings with the MOPr knockout mice (Figure 3A, 3B; $p < .05$ for the sex × pretreatment × time interaction by ANOVA, $F(8, 165) = 2.3$). Naloxonazine pretreatment abolished the stimulation of dialysate dopamine concentrations in response to the 2.0 g/kg ethanol challenge in the females ($F(8, 165) = 2.9$, $p < .05$). In males ethanol produced a similar increase in dialysate dopamine concentrations in the naloxonazine and saline groups ($F(8, 165) = .39$, $p > .05$ for the interaction between pretreatment and time).

Basal concentrations of dopamine were not significantly affected by naloxonazine, and male and female mice also had similar basal values ($F(1, 21) = 2.19$, $p > .05$). Neither blockade of the mu1 receptor nor sex affected the time course of dialysate ethanol concentrations in terms of peak concentration ($F(1, 15) = .36$, $p > .05$) and the rate of decline (Figure 3C, 3D; $F(1, 15) = .01$, $p > .05$).

Effect of MOPr Knockout on Ethanol-Evoked Dopamine Release in the Ventral Striatum: Congenic C57BL/6J Background

Deletion of the MOPr gene strongly inhibited the dopamine response due to ethanol administration in mice that were backcrossed onto the C57BL/6J strain (Figure 4A, 4B, $F(8, 160) = 9.4$, $p < .05$, genotype by time interaction in the overall ANOVA). Although ANOVA revealed that the effect of genotype was significantly different between males and females ($F(8, 160) = 2.3$, $p < .05$), the MOPr knockout in both sexes clearly showed a dramatic reduction in the stimulation of dopamine release immediately after the injection. Instead, the sex-dependence of the effect of MOPr deletion was due to a difference between males and females in the delayed reduction of dialysate dopamine concentrations below basal levels after the ethanol injection. Specifically, for both the male and female wildtype mice, the maximal dopamine response occurred immediately after the injection ($F(1, 160) > 40.1$, $p < .05$; simple effects test within the group). In contrast, in the male and female knockout mice, no changes were observed immediately after the ethanol injection. However, there was a slowly developing decrease in accumbal dopamine levels relative to basal that reached significance 45 min after the injection in the females ($F(1, 160) = 9.3$, $p < .05$; simple effects test within the knockouts), and 2 hr after the injection in males ($F(1,160) = 9.1$, $p < .05$).

Basal dopamine concentrations were not affected by the deletion of the MOPr knockout in the congenic strain in either males or females ($F(1, 19) = 4.28$, $p > .05$ for the interaction between genotype and sex). Additionally, peak dialysate ethanol concentrations ($F(1,20) = 3.11$, $p > .05$) and the rate of decline in ethanol concentration (Figure 4C, 4D, $F(1,20) = .03$, $p > .05$) were not different among the groups.

Effect of MOPr Knockout on Dopamine Release in the Ventral Striatum after Saline Injection: Congenic C57BL/6J Background

To determine whether the stimulation of dialysate dopamine concentrations may be affected by the IP injection procedure, we performed a separate experiment using the congenic strain of MOPr knockouts and their wildtype controls. Basal concentrations of dopamine were 2.0 ± .5 ($n = 6$), 1.2 ± .4 ($n = 4$), 1.8 ± .6 ($n = 6$), and 1.8 ± .5 nM ($n = 4$) for the male wildtype, male knockout, female wildtype, and female knockout mice, respectively. Saline injection did not significantly alter dialysate dopa-

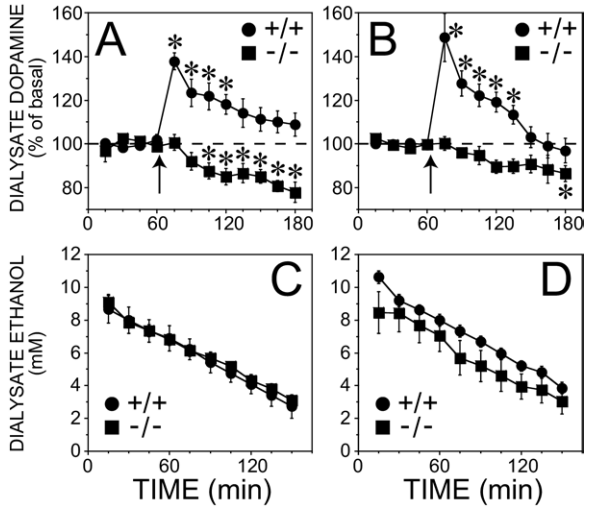

Figure 4. Dopamine response and dialysate ethanol in the ventral striatum after intraperitoneal administration of ethanol (2 g/kg) in MOPr knockout mice and their wildtype controls with a C57BL/6J background. Dialysate samples were collected every 15 min. **(A)** Female mice. The basal dopamine concentrations were .7 ± .1 nM ($n = 5$) and .7 ± .2 nM ($n = 7$) for wildtype and knockout groups, respectively. **(B)** Male mice. The basal dopamine concentrations were .9 ± .1 nM ($n = 6$) and 1.1 ± .3 nM ($n = 6$) for wildtype and knockout groups, respectively. The arrow indicates when the ethanol injection was given. *Significantly different from basal values by simple effects post hoc analyses ($p < .05$) after a significant three-way interaction overall ANOVA. The ethanol content in samples taken after the injection is shown in **(C)** female mice and **(D)** male mice. Note that the x-axis starts at the point of the ethanol injection which is different from that shown in panels A and B. MOPr, mu opioid receptors; ANOVA, analysis of variance.

mine concentrations compared with basal concentrations in any of the groups (no effect of genotype × time, sex × time, or genotype × sex × time, $F(4, 64) < 1.4$, $p > .05$, ANOVA). In addition, neither the MOPr knockout nor sex significantly affected basal dopamine concentrations ($F(1, 16) < .8$, $p > .05$, ANOVA for main effects and interaction).

Discussion

Our study is the first to report diminished ethanol-stimulated dopamine release in any MOPr knockout model. A secondary finding from the present study is the novel interaction between sex and genotype in the MOPr-dependence of ethanol-stimulated mesolimbic dopamine release. Female, but not male, 129SvEv-C57BL/6J mice were found to require the MOPr for the expression of the neurochemical response to ethanol. Similar results were observed following pharmacological blockade of the mu1 receptor. In contrast, both male and female C57BL/6J mice required the MOPr for the ethanol-stimulated dopamine response. Previous work in rats has shown that the mu1 receptor is involved in ethanol-stimulated accumbal dopamine release (Tanda and Di Chiara 1998), but our study is the first to show that this mechanism is influenced by sex and genotype. Together, the results strongly support the hypothesis that activation of MOPr is a necessary step, under specific conditions, in the mesoaccumbal dopamine pathway that is activated by ethanol. This pathway is likely to mediate, at least in part, the reinforcing or rewarding properties of ethanol. The variation in the mechanism of the effect of ethanol on mesolimbic dopamine activity has important implications for understanding the development of alcohol abuse as well as for its treatment.

Our conclusion that the MOPr regulates ethanol-stimulated dopamine release in a sex and genotype dependent manner rests primarily on the results with the 129SvEv-C57BL/6J mice. On the basis of the breeding strategy used to maintain this model, the level of gene fixation is approximately 90%. Because we are the first to report this epistatic interaction between the MOPr and mesolimbic dopamine function, it is not known whether this interaction occurs in MOPr knockout mice generated by other investigators (Loh et al 1998; Matthes et al 1996; Schuller et al 1999; Tian et al 1997). However, one previous study using the same MOP knockout strain as the present experiments also reported a sexual dimorphism in ethanol reward (Hall et al 2001). The correspondence between our neurochemical data and the previous behavioral studies further strengthens the idea that the MOPr mediation of mesolimbic dopamine activity contributes to the expression of the rewarding and reinforcing properties of ethanol. Taken together, these findings suggest that the influence of sex should be included in future studies of the interaction between the MOPr and ethanol.

A large body of evidence from behavioral and clinical studies has suggested that ethanol reward is influenced by endogenous opioid peptide dependent mechanisms (for review see Gianoulakis 2001). However, there is a controversy regarding the opioid receptor subtypes that mediate these effects of ethanol. Both MOP and delta opioid receptor antagonists decrease ethanol consumption (Honkanen et al 1996; Hyytia 1993; Krishnan-Sarin et al 1995; Krishnan-Sarin et al 1998; Le et al 1993), but clinical studies that investigate the effectiveness of opioid receptor antagonists for reducing relapse in alcoholism have mainly utilized nonselective antagonists (Mason et al 1999; Volpicelli et al 1992). Furthermore, the clinical efficacy of naltrexone, the most widely studied opioid receptor antagonist used for treatment of alcohol dependence, is low and inconsistent according to some authors (Kranzler and Van Kirk 2001). However, meta-analyses have demonstrated significant effects of naltrexone on relapse rate (Bouza et al 2004). It has been suggested that genetic contributions to therapeutic response may underlie the somewhat disappointing effects of opiate antagonists in broader populations of alcoholics, but that specific, genetically distinct, subpopulations might exhibit better responses to naltrexone (Edenberg and Kranzler 2005). One possible explanation for the variability in clinical responses may be that there is underlying variability of the alcoholic population in the possible mechanisms that contribute to the rewarding and reinforcing properties of ethanol in the first place. This may include the regulation by opioid versus nonopioid mechanisms of actions of ethanol on the mesoaccumbal dopamine system.

Our finding that genotype dependent epistasis influences the mechanism by which the MOPr regulates the mesolimbic dopamine system has important implications for the pharmacological treatment of alcoholism. First, alterations in MOPr function through functional polymorphisms may affect the role of mesolimbic dopamine in ethanol reward. Alcohol dependent patients who possess a functional polymorphism in the MOPr gene have been shown to have lower rates of relapse in response to naltrexone (Oslin et al 2003). These results are consistent with the findings that individuals with the polymorphism report enhanced positive feelings after ethanol administration (Ray and Hutchison 2004). Taken together, the results support the idea that genetic variation in the MOPr system, or in systems that interact with the MOPr, may influence the rewarding and reinforcing properties of ethanol. This implies that genetic variability in the MOPr system will also influence the ability of MOPr antagonists to reduce these effects. It is unclear whether the MOPr regulation of ethanol-stimulated dopamine release in the ventral striatum plays a role in human alcohol addiction, but our results suggest that genetic null variants of the MOPr could influence the vulnerability to ethanol addiction. It should be noted, however, that a null mutation in the MOPr gene will likely produce a much larger decrease in MOPr signaling compared with the Asn40Asp polymorphism that has been studied in human alcoholism.

Second, our finding that sex is an important factor that interacts with genotype in the modulation of ethanol-stimulated dopamine release by the MOPr suggests that sexual dimorphism may exist for the clinical response to MOPr antagonists used for the treatment of alcoholism. Recent reports suggest a sexually dimorphic response to naltrexone in the treatment of alcoholism (Garbutt et al 2005; Kiefer et al 2005), further pointing to the potential significance of the present findings. Our results imply that a more complete understanding of the influence of sex and genotype on ethanol responses may eventually lead to more effective pharmacological treatments for alcoholism.

The mechanisms that underlie MOPr regulation of ethanol-stimulated accumbal dopaminergic transmission are not clear. However, several lines of evidence show 1) the existence of endogenous opioid peptides in the VTA (Greenwell et al 2002; Khachaturian et al 1983), 2) that ethanol increases the release of a variety of endogenous opioid peptides from brain tissue in vitro and in vivo (Gianoulakis 1990; Olive et al 2001), and 3) the stimulation of VTA dopamine neuron firing rate by activation of MOPr on GABA interneurons in the VTA (Johnson and North 1992). Our studies specifically implicate the MOPr as a regulator of the stimulation of VTA dopamine neurons by ethanol, but the present

studies do not allow us to make conclusions regarding the anatomical sites of action of the MOPr that mediate these effects.

Ethanol concentrations in NAcc dialysates were monitored concurrently with the dopamine concentrations. No differences in the ethanol peak concentration and the rate of decline were observed in either the gene deletion or antagonist experiments. This confirms that the decrease in ethanol-stimulated accumbal dopamine we observed is the result of dysfunction of central mechanisms mediated by MOP receptors and potential epistatic interactions rather than an effect on ethanol pharmacokinetics. In agreement with our previous findings in C57BL/6 mice (Tang et al 2003), we confirmed that the stimulation of dopamine release by ethanol administration is not due to the IP injection procedure. The results from our saline control experiments suggest that the ethanol-evoked dopamine response in the ventral striatum was due to a central pharmacological effect rather than a stress related phenomenon in the congenic MOPr knockouts of either sex. Therefore, we believe it is unlikely that the attenuation of ethanol-stimulated dopamine response in the female 129SvEv-C57BL/6J MOPr knockouts is due to an attenuation of the response due to the injection alone, although we cannot totally exclude this possibility.

Another interesting finding from our study is that females, but not males, from the 129SvEv-C57BL/6J MOPr knockout mice exhibited an apparent decrease in basal dopamine concentration, an effect not found in the naloxonazine experiment. This suggests that the apparent decrease in basal dopamine was due to developmental or compensatory mechanisms due to the lifelong deletion of the MOPr and not specifically due to MOPr mediated mechanisms. Male MOPr null mutants on a C57BL/6 background were previously reported to have decreased dopamine uptake and reduced dopamine release (Chefer et al 2003) compared with wildtype controls, but females were not studied. It is possible that similar mechanisms occur in the female 129SvEv-C57BL/6J mice in the present study, and this could contribute to the apparent reduction in basal dopamine we observed.

Several pharmacological effects of morphine previously have been shown to differ between males and females, for example, antinociception (Baamonde et al 1989; Bartok and Craft 1997; Cicero et al 1996) and reinforcement (Cicero et al 2000). In addition, an interaction between sex and genotype in MOPr mediated analgesia has previously been reported (Kest et al 1999). Furthermore, sex differences in behavior have been reported in null mutant mice on a mixed genetic background (Hall et al 2001; Walther et al 2000). We now report an interaction between sex and genotype in the role of the MOPr in neurochemical effects of ethanol. The mechanism of the sex dependence of the various phenotypes cited above, including our data, is unclear at present. For our studies it is apparent that the 129SvEv strain contributes the gene(s) that is/are responsible for the epistatic interaction(s) we observed since there was no difference in the C57BL/6J congenic strain. Additional genetic studies are needed to determine the specific gene or genes that produce the sexual dimorphism of the MOPr response that we observed. In particular, it would be useful to replicate these experiments using the MOPr knockout backcrossed onto the 129SvEv strain. However, this model is not yet available.

A small but significant decrease in accumbal dopamine release occurred approximately 60-120 min after ethanol administration in the MOPr knockouts, but not in the naloxonazine experiment. This delayed inhibitory response in the MOPr knockouts may reflect the activation of kappa opioid (KOP) receptors in the NAcc by dynorphin-like peptide release produced by ethanol (Marinelli et al 2006), which would reduce dopamine release (Spanagel et al 1992). This effect would not be observed in wildtype mice because of the predominant effect of MOPr-mediated stimulation of dopamine release. Alternatively, the small delayed reduction in dopamine could reflect a general baseline drift that could be due, in part, to circadian variation. We think this is unlikely because it did not occur in every experiment, and we did not previously observe this phenomenon in C57BL/6 mice (Tang et al 2003). Furthermore, this is supported by previously published data that showed minimal variation of accumbal extracellular dopamine during the light cycle (Paulson and Robinson 1994). The lack of delayed inhibition of dopamine release produced after ethanol administration in naloxonazine-pretreated mice suggests that dysfunction of the MOPr system at the gene level or at the receptor level may unmask the inhibitory tone to varying degrees.

The precise role that ethanol-stimulated dopamine release plays in the rewarding or reinforcing effects of ethanol is not completely clear at present. Accumbal dopamine signals may contribute to ethanol reward (Weiss et al 1993), incentive-salience of ethanol (Robinson and Berridge 1993), or reward prediction (Schultz et al 1997). In the present study the mice were ethanol naive, so the incentive and rewarding properties of ethanol were not established. Regardless of the role or roles that dopamine plays in the development and maintenance of ethanol reinforcement, our data suggests that the MOPr may be part of the neurochemical mechanisms that contribute to the behavioral consequences of ethanol administration, at least in specific populations.

In summary, our data demonstrate a novel interaction between genotype and sex in MOPr mediation of the stimulation of mesolimbic dopamine activity by ethanol. This interaction was not due to compensatory mechanisms in the MOPr knockout mice because it was observed after pharmacological blockade by naloxonazine. The results suggest that both sex and genotype specific epistasis are major factors that determine the role of the MOPr in mechanisms that contribute to ethanol reinforcement. Our results may help explain some of the variation in the effectiveness of MOPr antagonists in the treatment of alcohol dependence.

This work was supported by grants AA11852 and AA13486 from the National Institute on Alcohol Abuse and Alcoholism (NIAAA), the Texas Commission on Alcohol and Drug Abuse, and by intramural funding at the National Institute on Drug Abuse, National Institute of Health (NIH)/Department of Health and Human Services (DHHS) (GRU, FSH, IS). Martin Job and Amanda Tang were supported by a training grant T32 AA07471 from NIAAA and fellowships from the Waggoner Center for Alcohol and Addiction Research. We thank Judith A. Randall for excellent technical assistance, and Julie Wu, Julie Owen, and Christina Schier for assistance with genotyping.

Both MOJ and AT should be considered first authors based on their respective contributions.

Supplementary material cited in this article is available online.

Baamonde AI, Hidalgo A, Andres-Trelles F (1989): Sex-related differences in the effects of morphine and stress on visceral pain. *Neuropharmacology* 28:967–970.

Bartok RE, Craft RM (1997): Sex differences in opioid antinociception. *J Pharmacol Exp Ther* 282:769–778.

Becker A, Grecksch G, Kraus J, Loh HH, Schroeder H, Hollt V (2002): Rewarding effects of ethanol and cocaine in mu opioid receptor-deficient mice. *Naunyn Schmiedebergs Arch Pharmacol* 365:296–302.

Belknap JK, Crabbe JC, and Young ER (1993): Voluntary consumption of ethanol in 15 inbred mouse strains. *Psychopharmacology (Berl)* 112:503–510.

Borg PJ, Taylor DA (1997): Involvement of mu- and delta-opioid receptors in the effects of systemic and locally perfused morphine on extracellular levels of dopamine, DOPAC and HVA in the nucleus accumbens of the halothane-anaesthetized rat. *Naunyn Schmiedebergs Arch Pharmacol* 355:582–588.

Bouza C, Angeles M, Munoz A, Amate JM (2004): Efficacy and safety of naltrexone and acamprosate in the treatment of alcohol dependence: a systematic review. *Addiction* 99:811–828.

Boyce-Rustay JM, Risinger FO (2003): Dopamine D3 receptor knockout mice and the motivational effects of ethanol. *Pharmacol Biochem Behav* 75: 373–379.

Cahill L (2006): Why sex matters for neuroscience. *Nat Rev Neurosci* 7:477–484.

Chefer VI, Kieffer BL, Shippenberg TS (2003): Basal and morphine-evoked dopaminergic neurotransmission in the nucleus accumbens of MOR- and DOR-knockout mice. *Eur J Neurosci* 18:1915–1922.

Cicero TJ, Nock B, Meyer ER (1996): Gender-related differences in the antinociceptive properties of morphine. *J Pharmacol Exp Ther* 279:767–773.

Cicero TJ, Ennis T, Ogden J, Meyer ER (2000): Gender differences in the reinforcing properties of morphine. *Pharmacol Biochem Behav* 65:91–96.

Cunningham CL, Okorn DM, Howard CE (1996): Ethanol-induced conditioned place preference and activation in 15 inbred mouse strains. *Alcohol Clin Exp Res* 20:59A.

Dilts RP, Kalivas PW (1990): Autoradiographic localization of delta opioid receptors within the mesocorticolimbic dopamine system using radioiodinated [2-D- penicillamine, 5-D-penicillamine]enkephalin (125I-DPDPE). *Synapse* 6:121–132.

Doyon WM, York JL, Diaz LM, Samson HH, Czachowski CL, Gonzales RA (2003): Dopamine activity in the nucleus accumbens during consummatory phases of oral ethanol self-administration. *Alcohol Clin Exp Res* 27: 1573–1582.

Dray A, Nunan L (1984): Evidence that naloxonazine produces prolonged antagonism of central delta opioid receptor activity in vivo. *Brain Res* 323:123–127.

Edenberg HJ, Kranzler HR (2005): The contribution of genetics to addiction therapy approaches. *Pharmacol Ther* 108:86–93.

Falconer DS, Mackay TFC (1996): *Introduction to Quantitative Genetics*, 4th edition. Essex, England, Longman.

Garbutt JC, Kranzler HR, O'Malley SS, Gastfriend DR, Pettinati HM, Silverman BL, et al (2005): Efficacy and tolerability of long-acting injectable naltrexone for alcohol dependence: a randomized controlled trial. *JAMA* 293: 1617–1625.

Gianoulakis C (1990): Characterization of the effects of acute ethanol administration on the release of beta-endorphin peptides by the rat hypothalamus. *Eur J Pharmacol* 180:21–29.

Gianoulakis C (2001): Influence of the endogenous opioid system on high alcohol consumption and genetic predisposition to alcoholism. *J Psychiatry Neurosci* 26:304–318.

Gonzales RA, Weiss F (1998): Suppression of ethanol-reinforced behavior by naltrexone is associated with attenuation of the ethanol-induced increase in dialysate dopamine levels in the nucleus accumbens. *J Neurosci* 18:10663–10671.

Greenwell TN, Zangen A, Martin-Schild S, Wise RA, Zadina JE (2002): Endomorphin-1 and −2 immunoreactive cells in the hypothalamus are labeled by fluoro-gold injections to the ventral tegmental area. *J Comp Neurol* 454:320–328.

Hall FS, Sora I, Uhl GR (2001): Ethanol consumption and reward are decreased in mu-opiate receptor knockout mice. *Psychopharmacology (Berl)* 154:43–49.

Honkanen A, Vilamo L, Wegelius K, Sarviharju M, Hyytia P, Korpi ER (1996): Alcohol drinking is reduced by a mu 1- but not by a delta-opioid receptor antagonist in alcohol-preferring rats. *Eur J Pharmacol* 304:7–13.

Houghten RA, Johnson N, Pasternak GW (1984): [3H]-beta-endorphin binding in rat brain. *J Neurosci* 4:2460–2465.

Hyytia P (1993): Involvement of mu-opioid receptors in alcohol drinking by alcohol-preferring AA rats. *Pharmacol Biochem Behav* 45:697–701.

Imperato A, Di Chiara G (1986): Preferential stimulation of dopamine release in the nucleus accumbens of freely moving rats by ethanol. *J Pharmacol Exp Ther* 239:219–228.

Johnson SW, North RA (1992): Opioids excite dopamine neurons by hyperpolarization of local interneurons. *J Neurosci* 12:483–488.

Kest B, Wilson SG, Mogil JS (1999): Sex differences in supraspinal morphine analgesia are dependent on genotype. *J Pharmacol Exp Ther* 289:1370–1375.

Khachaturian H, Lewis ME, Watson SJ (1983): Enkephalin systems in diencephalon and brainstem of the rat. *J Comp Neurol* 220:310–320.

Kiefer F, Jahn H, Wiedemann K (2005): A neuroendocrinological hypothesis on gender effects of naltrexone in relapse prevention treatment. *Pharmacopsychiatry* 38:184–186.

Kornet M, Goosen C, Van Ree JM (1991): Effect of naltrexone on alcohol consumption during chronic alcohol drinking and after a period of imposed abstinence in free-choice drinking rhesus monkeys. *Psychopharmacology (Berl)* 104:367–376.

Kranzler HR, Van Kirk J (2001): Efficacy of naltrexone and acamprosate for alcoholism treatment: a meta-analysis. *Alcohol Clin Exp Res* 25:1335–1341.

Krishnan-Sarin S, Jing SL, Kurtz DL, Zweifel M, Portoghese PS, Li TK, Froehlich JC (1995): The delta opioid receptor antagonist naltrindole attenuates both alcohol and saccharin intake in rats selectively bred for alcohol preference. *Psychopharmacology (Berl)* 120:177–185.

Krishnan-Sarin S, Wand GS, Li XW, Portoghese PS, Froehlich JC (1998): Effect of mu opioid receptor blockade on alcohol intake in rats bred for high alcohol drinking. *Pharmacol Biochem Behav* 59:627–635.

Le AD, Poulos CX, Quan B, Chow S (1993): The effects of selective blockade of delta and mu opiate receptors on ethanol consumption by C57BL/6 mice in a restricted access paradigm. *Brain Res* 630:330–332.

Ling GS, Simantov R, Clark JA, Pasternak GW (1986): Naloxonazine actions in vivo. *Eur J Pharmacol* 129:33–38.

Loh HH, Liu HC, Cavalli A, Yang W, Chen YF, Wei LN (1998): mu Opioid receptor knockout in mice: effects on ligand-induced analgesia and morphine lethality. *Brain Res Mol Brain Res* 54:321–326.

Mansour A, Khachaturian H, Lewis ME, Akil H, Watson SJ (1987): Autoradiographic differentiation of mu, delta, and kappa opioid receptors in the rat forebrain and midbrain. *J Neurosci* 7:2445–2464.

Marinelli PW, Lam M, Bai L, Quirion R, Gianoulakis C (2006): A microdialysis profile of dynorphin A (1-8) release in the rat nucleus accumbens following alcohol administration. *Alcohol Clin Exp Res* 30:982–990.

Marinelli PW, Quirion R, Gianoulakis C (2003): A microdialysis profile of beta-endorphin and catecholamines in the rat nucleus accumbens following alcohol administration. *Psychopharmacology (Berl)* 169:60–67.

Mason BJ, Salvato FR, Williams LD, Ritvo EC, Cutler RB (1999): A double-blind, placebo-controlled study of oral nalmefene for alcohol dependence. *Arch Gen Psychiatry* 56:719–724.

Matthes HW, Maldonado R, Simonin F, Valverde O, Slowe S, Kitchen I, et al (1996): Loss of morphine-induced analgesia, reward effect and withdrawal symptoms in mice lacking the mu-opioid-receptor gene. *Nature* 383:819–823.

Melendez RI, Rodd-Henricks ZA, Engleman EA, Li TK, McBride WJ, Murphy JM (2002): Microdialysis of dopamine in the nucleus accumbens of alcohol-preferring (P) rats during anticipation and operant self-administration of ethanol. *Alcohol Clin Exp Res* 26:318–325.

Nocjar C, Middaugh LD, Tavernetti M (1999): Ethanol consumption and place-preference conditioning in the alcohol-preferring C57BL/6 mouse: relationship with motor activity patterns. *Alcohol Clin Exp Res* 23:683–692.

Olive MF, Koenig HN, Nannini MA, Hodge CW (2001): Stimulation of endorphin neurotransmission in the nucleus accumbens by ethanol, cocaine, and amphetamine. *J Neurosci* 21:RC184(1–5).

Olive MF, Mehmert KK, Messing RO, Hodge CW (2000): Reduced operant ethanol self-administration and in vivo mesolimbic dopamine responses to ethanol in PKCepsilon-deficient mice. *Eur J Neurosci* 12:4131–4140.

Oslin DW, Berrettini W, Kranzler HR, Pettinati H, Gelernter J, Volpicelli JR, O'Brien CP (2003): A functional polymorphism of the mu-opioid receptor gene is associated with naltrexone response in alcohol-dependent patients. *Neuropsychopharmacology* 28:1546–1552.

Paulson PE, Robinson TE (1994): Relationship between circadian changes in spontaneous motor activity and dorsal versus ventral striatal dopamine neurotransmission assessed with on-line microdialysis. *Behav Neurosci* 108:624–635.

Paxinos G, Franklin KBJ (2001): The mouse brain in stereotaxic coordinates. San Diego, CA: Academic Press.

Ray LA, Hutchison KE (2004): A polymorphism of the mu-opioid receptor gene (OPRM1) and sensitivity to the effects of alcohol in humans. *Alcohol Clin Exp Res* 28:1789–1795.

Roberts AJ, McDonald JS, Heyser CJ, Kieffer BL, Matthes HW, Koob GF, Gold LH (2000): mu-Opioid receptor knockout mice do not self-administer alcohol. *J Pharmacol Exp Ther* 293:1002–1008.

Robinson TE, Berridge KC (1993): The neural basis of drug craving: an incentive-sensitization theory of addiction. *Brain Res Brain Res Rev* 18:247–291.

Schuller AG, King MA, Zhang J, Bolan E, Pan YX, Morgan DJ, et al (1999): Retention of heroin and morphine-6 beta-glucuronide analgesia in a new line of mice lacking exon 1 of MOR-1. *Nat Neurosci* 2:151–156.

Schultz W, Dayan P, Montague PR (1997): A neural substrate of prediction and reward. *Science* 275:1593–1599.

Sora I, Takahashi N, Funada M, Ujike H, Revay RS, Donovan DM, et al (1997): Opiate receptor knockout mice define mu receptor roles in endogenous nociceptive responses and morphine-induced analgesia. *Proc Natl Acad Sci U S A* 94:1544–1549.

Spanagel R, Herz A, Shippenberg TS (1992): Opposing tonically active endogenous opioid systems modulate the mesolimbic dopaminergic pathway. *Proc Natl Acad Sci U S A* 89:2046–2050.

Svingos AL, Clarke CL, Pickel VM (1999): Localization of the delta-opioid receptor and dopamine transporter in the nucleus accumbens shell: implications for opiate and psychostimulant cross-sensitization. *Synapse* 34:1–10.

Tanda G, Di Chiara G (1998): A dopamine-mu1 opioid link in the rat ventral tegmentum shared by palatable food (Fonzies) and nonpsychostimulant drugs of abuse. *Eur J Neurosci* 10:1179–1187.

Tang A, George MA, Randall JA, Gonzales RA (2003): Ethanol increases extracellular dopamine concentration in the ventral striatum in C57BL/6 mice. *Alcohol Clin Exp Res* 27:1083–1089.

Tian M, Broxmeyer HE, Fan Y, Lai Z, Zhang S, Aronica S, et al (1997): Altered hematopoiesis, behavior, and sexual function in mu opioid receptor-deficient mice. *J Exp Med* 185:1517–1522.

Volpicelli JR, Alterman AI, Hayashida M, O'Brien CP (1992): Naltrexone in the treatment of alcohol dependence. *Arch Gen Psychiatry* 49:876–880.

Walther T, Voigt JP, Fink H, Bader M (2000): Sex specific behavioural alterations in Mas-deficient mice. *Behav Brain Res* 107:105–109.

Weiss F, Lorang MT, Bloom FE, Koob GF (1993): Oral alcohol self-administration stimulates dopamine release in the rat nucleus accumbens: genetic and motivational determinants. *J Pharmacol Exp Ther* 267: 250–258.

Yoshida Y, Koide S, Hirose N, Takada K, Tomiyama K, Koshikawa N, Cools AR (1999): Fentanyl increases dopamine release in rat nucleus accumbens: involvement of mesolimbic mu- and delta-2-opioid receptors. *Neuroscience* 92:1357–1365.

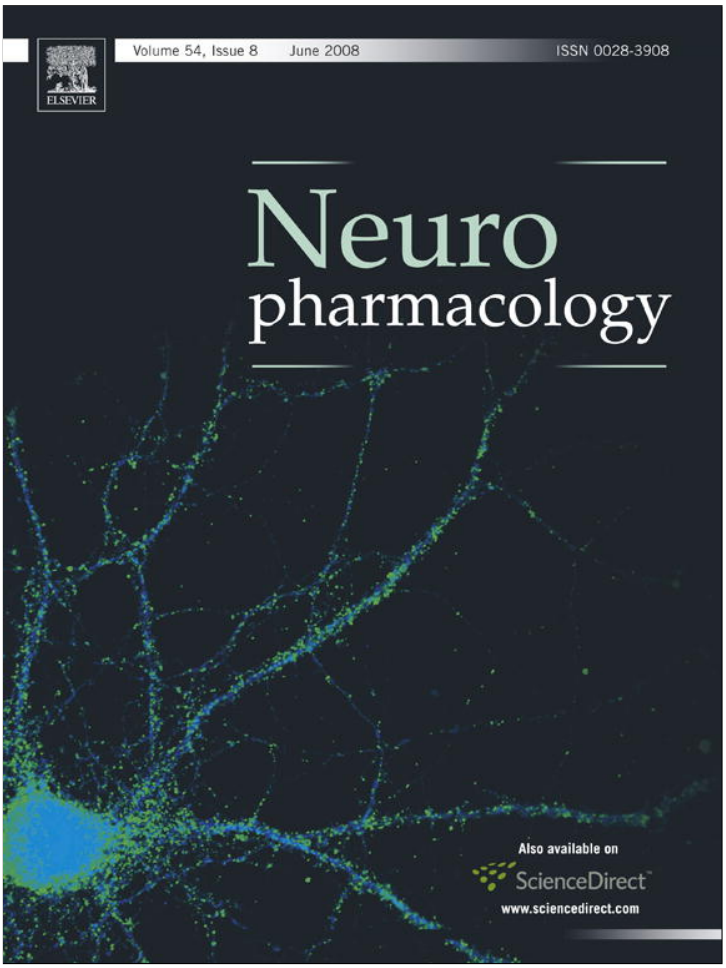

Neuropharmacology 54 (2008) 1182–1188

Contents lists available at ScienceDirect

Neuropharmacology

journal homepage: www.elsevier.com/locate/neuropharm

Abolished thermal and mechanical antinociception but retained visceral chemical antinociception induced by butorphanol in μ-opioid receptor knockout mice

Soichiro Ide [a,b], Masabumi Minami [c], Kumatoshi Ishihara [b], George R. Uhl [d], Masamichi Satoh [e], Ichiro Sora [a,d,f], Kazutaka Ikeda [a,*]

[a] Division of Psychobiology, Tokyo Institute of Psychiatry, 2-1-8 Kamikitazawa, Setagaya-ku, Tokyo 156-8585, Japan
[b] Laboratory of Neuropharmacology, Faculty of Pharmaceutical Sciences, Hiroshima International University, Kure 737-0112, Japan
[c] Department of Pharmacology, Graduate School of Pharmaceutical Sciences, Hokkaido University, Sapporo 060-0812, Japan
[d] Molecular Neurobiology, National Institute on Drug Abuse, Baltimore, MD 21224, USA
[e] Department of Pharmacy, Yasuda Women's University, Hiroshima 731-0153, Japan
[f] Department of Biological Psychiatry, Tohoku University Graduate School of Medicine, Sendai 980-8574, Japan

ARTICLE INFO

Article history:
Received 28 November 2007
Received in revised form 25 February 2008
Accepted 19 March 2008

Keywords:
Opioid receptor
Knockout mice
Butorphanol
Antinociception

ABSTRACT

Butorphanol is hypothesized to induce analgesia via opioid pathways, although the precise mechanisms for its effects remain unknown. In this study, we investigated the role of the μ-opioid receptor (MOP) in thermal, mechanical, and visceral chemical antinociception induced by butorphanol using MOP knockout (KO) mice. Butorphanol-induced thermal antinociception, assessed by the hot-plate and tail-flick tests, was significantly reduced in heterozygous and abolished in homozygous MOP-KO mice compared with wildtype mice. The results obtained from our butorphanol-induced mechanical antinociception experiments, assessed by the Randall–Selitto test, were similar to the results obtained from the thermal antinociception experiments in these mice. Interestingly, however, butorphanol retained its ability to induce significant visceral chemical antinociception, assessed by the writhing test, in homozygous MOP-KO mice. The butorphanol-induced visceral chemical antinociception that was retained in homozygous MOP-KO mice was completely blocked by pretreatment with nor-binaltorphimine, a κ-opioid receptor (KOP) antagonist. In vitro binding and cyclic adenosine monophosphate assays also showed that butorphanol possessed higher affinity for KOPs and MOPs than for δ-opioid receptors. These results molecular pharmacologically confirmed previous studies implicating MOPs, and partially KOPs, in mediating butorphanol-induced analgesia.

1. Introduction

Butorphanol (17-cyclobutylmethyl-3,14-dihydroxymorphinan) tartrate, known by the trade name Stadol, is a widely used synthetic opioid analgesic used for Step 2 pain management in the World Health Organization's pain ladder. Butorphanol binds μ-, δ-, and κ-opioid receptors (MOP, DOP, and KOP) in rat brain membranes with high affinity (Chang et al., 1981) and acts as a partial agonist. Several reports have indicated that the effects of butorphanol are mediated via its agonistic action at the MOP. Butorphanol exhibited cross-tolerance with morphine in rats (Picker et al., 1990). Butorphanol also has been reported to act as a MOP partial agonist in the antinociceptive effects assessed in the tail-flick test in mice (Garner et al., 1997), in the warm-water tail withdrawal assay in rhesus monkeys (Butelman et al., 1995), and in responses to shock titration in squirrel monkeys (Dykstra, 1990). In addition, the involvement of the KOP in the antinociceptive effects of butorphanol in responses to shock titration in squirrel monkeys and in tail-flick and writhing tests in rats has been reported (Dykstra, 1990; Feng et al., 1994). Although these previous studies suggest that butorphanol acts both as a MOP partial agonist and a KOP partial agonist, several contradictory results remain. Nor-binaltorphimine (nor-BNI), a selective KOP antagonist, precipitated withdrawal in butorphanol-dependent rats. Pretreatment with nor-BNI inhibited the development of butorphanol dependence, and β-funaltrexamine, a MOP-selective antagonist, was less effective than nor-BNI at precipitating withdrawal in butorphanol-dependent rats (Jaw et al., 1993a,b). These reports suggest that KOPs have a more significant

* Corresponding author. Tel.: +81 3 3304 5701; fax: +81 3 3329 8035.
E-mail address: ikedak@prit.go.jp (K. Ikeda).

0028-3908/$ – see front matter © 2008 Elsevier Ltd. All rights reserved.
doi:10.1016/j.neuropharm.2008.03.008

role than MOPs in mediating physical dependence on butorphanol. In contrast, the degree of dependence caused by chronic butorphanol administration into the lateral cerebral ventricle is decreased by β-funaltrexamine treatment in rats (Oh et al., 1992). Furthermore, the most selective ligands for a specific subtype of opioid receptors (i.e. β-funaltrexamine for MOP, naltrindole for DOP, and nor-BNI for KOP) possess certain affinities for other subtypes (Newman et al., 2002). Thus, the precise molecular mechanisms underlying the antinociceptive effects of butorphanol have not been clearly delineated by traditional pharmacological studies that only used selective ligands.

Recent success in developing mice lacking the MOP gene has made possible the discovery of molecular mechanisms underlying opioid effects (Loh et al., 1998; Matthes et al., 1996; Sora et al., 1997b, 2001). Both the analgesic effects of morphine in the tail-flick and hot-plate tests and the rewarding effects of morphine in self-administration tests are abolished in MOP knockout (KO) mice (Loh et al., 1998; Sora et al., 1997b, 2001). Buprenorphine, a non-selective opioid receptor partial agonist, has no analgesic effect in the tail-flick and hot-plate tests but a significant rewarding effect in the conditioned place preference tests in homozygous MOP-KO mice (Ide et al., 2004). These observations are especially interesting because the distributions of DOP and KOP are not apparently altered in MOP-KO mice (Loh et al., 1998; Matthes et al., 1996; Sora et al., 1997b). Using MOP-KO mice in tail-flick and hot-plate tests, the antinociceptive effects of tramadol, an analgesic possessing both opioid and non-opioid activity, were shown to be mediated mainly by MOPs and adrenergic α_2 receptors (Ide et al., 2006). Although several compensatory changes might occur in KO animals, they have potential utility in investigating in vivo roles of specific proteins. Thus, the use of MOP-KO mice has provided novel theories on the molecular mechanisms underlying the effects of opioid ligands. The present study investigated the molecular mechanisms underlying the antinociceptive effects of butorphanol using MOP-KO mice and human MOP, DOP, and KOP cDNA.

2. Methods

2.1. Animals

The present study used wildtype, heterozygous, and homozygous MOP-KO mouse littermates from heterozygous/heterozygous MOP-KO crosses on a C57BL/6J genetic background (backcrossed at least 10 generations) as previously described (Sora et al., 2001). The experimental procedures and housing conditions were approved by the Institutional Animal Care and Use Committee, and all animal care and treatment were in accordance with our institutional animal experimentation guidelines. Naive adult (>10 weeks old) male and female mice were group housed in an animal facility maintained at 22 ± 2 °C and 55 ± 5% relative humidity under a 12 h/12 h light/dark cycle with lights on at 8:00 am and off at 8:00 pm. Food and water were available ad libitum.

2.2. Drugs

Butorphanol tartrate and nor-BNI dihydrochloride were purchased from Sigma Chemical Co. (St. Louis, MO). For in vitro assays, [D-Ala^2,*N*-MePhe^4,Gly-ol^5]enkephalin (DAMGO), a MOP-selective agonist, and [D-Pen^2,D-Pen^5]enkephalin (DPDPE), a DOP agonist, were purchased from Peninsula Laboratories Ltd. (Merseyside, UK). (+)-(5α,7α,8β)-*N*-methyl-*N*-[7-(1-pyrrolidinyl)-1-oxaspiro[4,5]dec-8-yl]benzeneacetamide (U69593), a KOP-selective agonist, was a gift from Upjohn (Kalamazoo, MI). Compounds [tyrosyl-3,5-^{3}H(N)]DAMGO (50.5 Ci/mmol), [phenyl-3,4-^{3}H]U69593 (47.5 Ci/mmol), and [tyrosyl-2,6-^{3}H(N)]DPDPE (33.0 Ci/mmol) were purchased from DuPont-New England Nuclear (Boston, MA).

2.3. Antinociceptive tests

Thermal antinociception was evaluated using the hot-plate and tail-flick tests. Hot-plate testing was performed according to the method of Woolfe and MacDonald (1944) with slight modifications. A commercially available apparatus consisting of an acrylic resin cage (20 × 25 × 25 cm: width × length × height) and a temperature-controlled aluminum plate (Model MK-350A, Muromachi Kikai Co., Tokyo, Japan) were used for this test. Mice were placed on a 52 ± 0.2 °C hot-plate, and latencies to hind-paw-lick or jump were recorded. We selected a relatively lower temperature (52 °C) to examine the mild thermal antinociceptive effects of opioid partial agonists (Ide et al., 2004). The cut-off time was 60 s. Tail-flick testing was carried out according to the method of D'Amour and Smith (1941) with slight modifications using a commercially available apparatus consisting of an irradiator for heat stimulation and a photosensor for detection of tail-flick behavior (Model MK-330A, Muromachi Kikai Co., Tokyo, Japan). Mice were loosely wrapped in a felt towel. Their tails were heated, and tail-flick latencies were automatically recorded. The cut-off time was 15 s. Mechanical antinociception was evaluated using the hind-paw pressure test according to the method of Randall and Selitto (1957) with slight modifications using a commercially available apparatus (Pressure Analgesy-Meter, Model MK-201D, Muromachi Kikai Co., Tokyo, Japan). Mice were loosely wrapped in a felt towel. Their hind paws were gradually pressed, and hind-paw drawing or struggle latencies were automatically recorded. The cut-off pressure was 250 mmHg. The drug injection volume was 10 ml/kg.

In the time-course analyses, the tail-flick, hot-plate, and hind-paw pressure tests were conducted before and 5, 10, 20, 40, 60, 120, and 180 min after subcutaneous (s.c.) injection of butorphanol (3.0 mg/kg). In the dose–response analyses, butorphanol was administered at doses of 0.3, 0.7, 2.0, and 7.0 mg/kg (s.c.), for cumulative doses of 0.3, 1.0, 3.0, and 10 mg/kg, respectively. Tail-flick, hot-plate, and hind-paw pressure tests were conducted 20 min after each drug injection. Drug injections occurred immediately after the previous test.

The hot-plate, tail-flick, and hind-paw pressure responses of each mouse in the drug-induced antinociception tests were converted to percentage of maximal possible effect (%MPE) according to the following formula:

$$\%\mathrm{MPE} = (\text{postdrug latency} - \text{predrug latency})/(\text{cut-off time or pressure} - \text{predrug latency}) \times 100\%$$

Visceral chemical antinociception was evaluated using the writhing test (Collier et al., 1968). Acetic acid (0.6% v/v, 10 ml/kg) was injected intraperitoneally (i.p.), and the mouse was placed in a large plastic cage. The intensity of nociceptive behavior was quantified by counting the total number of writhes occurring between 0 and 15 min after acetic acid injection. The writhing response consists of a contraction of the abdominal muscles. Nociception was expressed as writhing scores during the 15 min period. Butorphanol (3.0 mg/kg, s.c.) or saline was administered 10 min before acetic acid injection. nor-BNI (5.0 mg/kg, s.c.) was administered 24 h before butorphanol injection.

2.4. Stable expression of human opioid receptors in Chinese hamster ovary cells

Chinese hamster ovary (CHO) cell lines stabling expressing human μ-, δ-, and κ-opioid receptors (MOP/CHO, DOP/CHO, and KOP/CHO, respectively) were established as previously described (Ide et al., 2004). K_d values of [^{3}H]DAMGO to MOP, [^{3}H]DPDPE to DOP, and [^{3}H]U69593 to KOP were 1.7 ± 0.3 nM (n = 4), 2.2 ± 0.2 nM (n = 4), and 2.5 ± 0.2 nM (n = 3), respectively. B_{max} estimates of receptor densities in these cell lines were 2300 ± 160, 3000 ± 270, and 5000 ± 450 fmol/mg protein, respectively.

2.5. Radioligand binding assay

Binding assays were performed as previously described (Katsumata et al., 1995) with slight modifications. Expressing cells were harvested after 65 h in culture, homogenized in 50 mM Tris buffer (pH 7.4) containing 10 mM $MgCl_2$ and 1 mM EDTA, pelleted by centrifugation for 20 min at 30 000g, and resuspended in the same buffer. For saturation binding assays, cell membrane suspensions were incubated for 60 min at 25 °C with various concentrations of [^{3}H]DAMGO for human MOP, [^{3}H]DPDPE for human DOP, or [^{3}H]U69593 for human KOP. Nonspecific binding was determined in the presence of 10 mM unlabeled ligands. For competitive binding assays, the cell membrane suspensions were incubated for 60 min at 25 °C with 2 nM [^{3}H]DAMGO for human MOP, 2 nM [^{3}H]DPDPE for human DOP, or 3 nM [^{3}H]U69593 for human KOP in the presence of various concentrations of ligands. After incubation for 60 min, membrane suspensions were rapidly filtrated, and the radioactivity on each filter was then measured by liquid scintillation counting. K_d values of the radiolabeled ligands were obtained by Scatchard analysis of the data from the saturation binding assay. For the competitive binding assay, non-linear regression analysis using a one-competitionmodel (GraphPad Prism, GraphPad, San Diego, CA) was conducted to estimate the inhibitory concentration at 50% (IC_{50}). K_i values were calculated from IC_{50} values obtained from the competitive binding assay in accordance with the equation $K_i = IC_{50}/(1 + [\text{radiolabeled ligand}]/K_d)$, where IC_{50} is the concentration of unlabeled ligand producing 50% inhibition of the specific binding of radiolabeled ligand. The binding assay results are presented as mean ± S.E.M. of 11–15 independent experiments.

2.6. cAMP assay

3′,5′-Cyclic adenosine monophosphate (cAMP) assays were performed as previously described (Katsumata et al., 1995) with slight modifications. Briefly, 10^5 cells were placed into each well of a 24-well plate, grown for 24 h, washed, and incubated with 0.45 ml HEPES-buffered saline containing 1 mM 3-isobutyl-1-methylxanthine for 10 min at 37 °C. Next, the cells were stimulated for 10 min by the addition of 50 ml HEPES-buffered saline containing 100 mM forskolin and 1 mM

3-isobutyl-1-methylxanthine in the presence or absence of various concentrations of opioid ligands and then disrupted by adding 0.5 ml ice-cold 10% trichloroacetic acid to each well. Concentrations of cAMP were measured by radioimmunoassay (Amersham, Buckinghamshire, UK). cAMP accumulation is presented as a fraction of the control value obtained without the addition of opiates. Inhibition curves were generated by a computer-generated non-linear least-squares fit using GraphPad Prism (GraphPad, San Diego, CA). IC_{50} values were calculated as the concentration of ligand producing 50% of maximal inhibition of cAMP accumulation. IC_{50} values and the maximal inhibitory effects (I_{max}) in the cAMP assays are presented as mean ± S.E.M. of 3–5 independent experiments, each performed in triplicate.

2.7. Statistical analyses

The time-courses of butorphanol effects were statistically analyzed by one-way, repeated-measures analysis of variance (ANOVA) followed by the Tukey–Kramer post hoc test. The dose–response functions of the antinociceptive effects of butorphanol in wildtype, heterozygous, and homozygous MOP-KO mice were statistically evaluated by two-way, mixed-design ANOVA and one-way, repeated-measures ANOVA followed by the Tukey–Kramer post hoc test. The visceral chemical antinociceptive effects of butorphanol were analyzed by one-way factorial ANOVA followed by the Tukey–Kramer post hoc test. Differences with $p < 0.05$ were considered statistically significant. In the analysis of differences among genotypes, no significant differences were observed between male and female mice in the antinociceptive effects of butorphanol (although the antinociceptive effects of butorphanol were slightly greater in male mice than in female mice), thus male and female data were combined.

3. Results

3.1. Antinociceptive effects

First, the time-courses of the thermal antinociceptive effects of butorphanol were analyzed in wildtype mice (Fig. 1a, b). The thermal antinociceptive effects of butorphanol (3 mg/kg, s.c.) were expressed early (<5 min), reached peak effects approximately Twenty minutes after injection, and were long-lasting (>3 h) in both the hot-plate (Fig. 1a) and tail-flick (Fig. 1b) tests. Butorphanol showed a significant increase in %MPE in both the hot-plate and tail-flick tests in wildtype mice [one-way, repeated-measures ANOVA: $F_{(7,56)} = 2.27$, $p = 0.042$; $F_{(7,56)} = 9.63$, $p < 0.0001$, respectively]. Post hoc analysis revealed that the thermal antinociceptive effects of butorphanol were significant at all examined time-points in the tail-flick test and 20–180 min after butorphanol injection in the hot-plate test. Second, the thermal antinociceptive dose–response relationships of butorphanol were analyzed in wildtype, heterozygous, and homozygous MOP-KO mice (Fig. 1c, d). Butorphanol dose-dependently showed thermal antinociceptive effects in both wildtype and heterozygous MOP-KO mice, but not in homozygous MOP-KO mice. Two-way, mixed-design ANOVA revealed that the antinociceptive effects of butorphanol (%MPE) were significantly different among these genotypes in both the hot-plate test [significant difference between genotypes, $F_{(2,29)} = 8.99$, $p < 0.001$; no significant genotype × dose interaction, $F_{(8,116)} = 1.75$, $p = 0.095$; Fig. 1c] and tail-flick test [significant difference between genotypes, $F_{(2,29)} = 28.71$, $p < 0.0001$; significant genotype × dose interaction, $F_{(8,116)} = 9.08$, $p < 0.0001$; Fig. 1d]. The antinociceptive effects of butorphanol (%MPE) in heterozygous and homozygous MOP-KO mice were significantly lower than in wildtype mice, both in the hot-plate and tail-flick tests ($p < 0.05$, Tukey–Kramer post hoc test). One-way, repeated-measures ANOVA revealed that butorphanol-induced significant increases in %MPE in both the hot-plate [$F_{(4,50)} = 3.40$, $p < 0.05$] and tail-flick tests [$F_{(4,50)} = 17.69$, $p < 0.0001$]

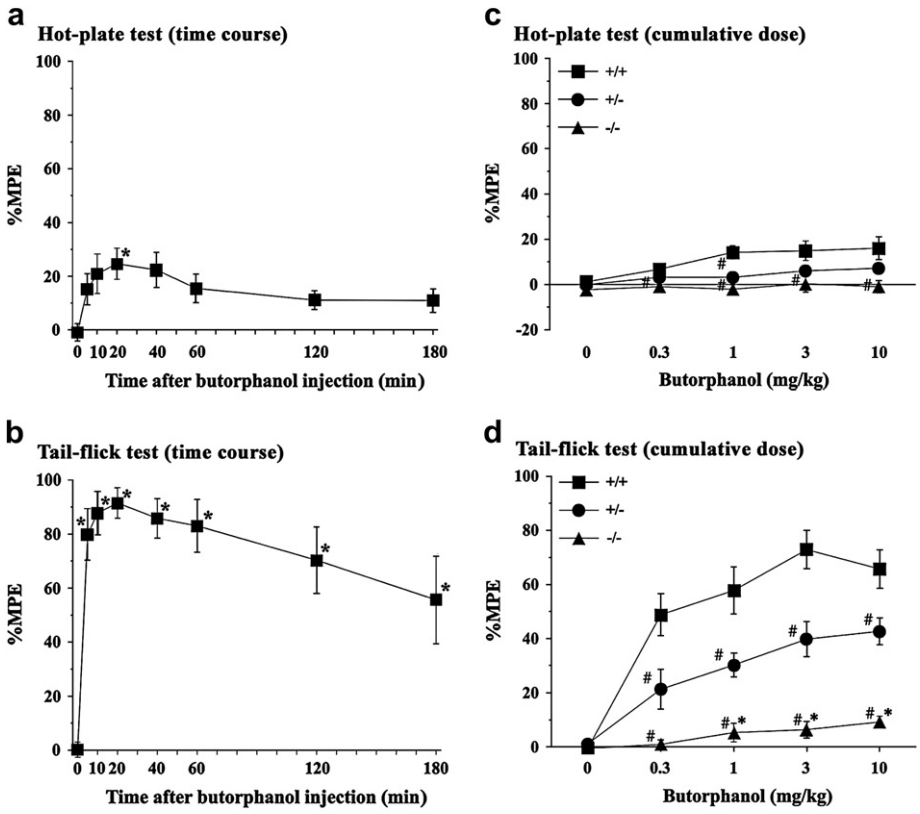

Fig. 1. Thermal antinociceptive effects of butorphanol in wildtype, heterozygous, and homozygous MOP-KO mice. (a, b) Butorphanol (3 mg/kg, s.c.)-induced alterations of %MPE in the hot-plate (a) and tail-flick (b) tests in wildtype mice [$n = 8$ (male, 4; female, 4)] under the time-course paradigm. $^{*}p < 0.05$, Significantly different from pre-injection (0 min). (c, d) Butorphanol-induced alterations of %MPE in the hot-plate (c) and tail-flick (d) tests in wildtype [+/+, closed square, $n = 11$ (male, 6; female, 5)], heterozygous [+/−, closed circle, $n = 12$ (male, 7; female, 5)], and homozygous [−/−, closed triangle, $n = 9$ (male, 6; female, 3)] MOP-KO mice under the cumulative dose–response paradigm. $^{\#}p < 0.05$, Significantly different from wildtype mice; $^{*}p < 0.05$, significantly different from heterozygous MOP-KO mice. Data are expressed as mean ± S.E.M.

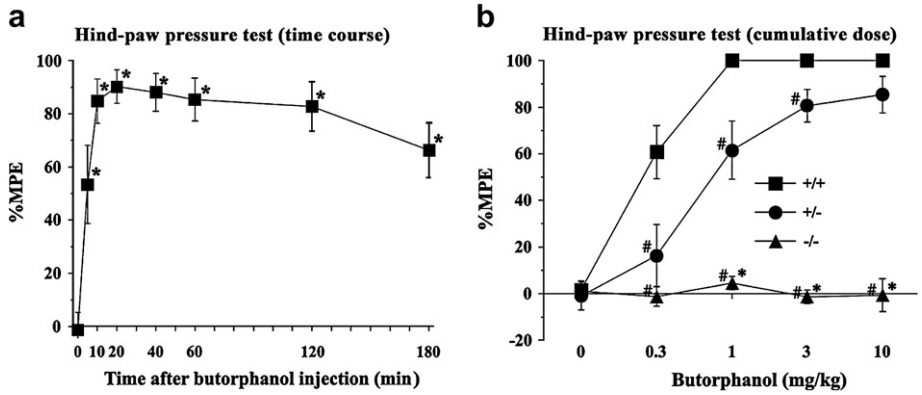

Fig. 2. Mechanical antinociceptive effects of butorphanol in wildtype, heterozygous, and homozygous MOP-KO mice. (a) Butorphanol (3 mg/kg, s.c.)-induced alterations of %MPE in the hind-paw pressure test in wildtype mice [$n = 8$ (male, 4; female, 4)] under the time-course paradigm. $^{*}p < 0.05$, Significantly different from pre-injection (0 min). (b) Butorphanol-induced alterations of %MPE in the hind-paw pressure test in wildtype [+/+, closed square, $n = 10$ (male, 4; female, 6)], heterozygous [+/−, closed circle, $n = 12$ (male, 7; female, 5)], and homozygous [−/−, closed triangle, $n = 11$ (male, 5; female, 6)] MOP-KO mice under the cumulative dose–response paradigm. $^{\#}p < 0.05$, Significantly different from wildtype mice; $^{*}p < 0.05$, significantly different from heterozygous MOP-KO mice. Data are expressed as mean ± S.E.M.

in wildtype mice. By contrast, butorphanol-induced significant increases in %MPE only in the tail-flick test in heterozygous MOP-KO mice [$F_{(4,40)} = 2.77$, $p < 0.05$] and failed to significantly change %MPE in either the hot-plate or tail-flick test in homozygous MOP-KO mice at cumulative doses up to 10 mg/kg (Fig. 1c, d).

Next, the time-course of the mechanical antinociceptive effects of butorphanol was analyzed in wildtype mice. Similar to the thermal antinociceptive effects, the mechanical antinociceptive effects of butorphanol (3 mg/kg, s.c.) were expressed early (<5 min), reached peak effects approximately 20 min after injection, and were long-lasting (>3 h) in the hind-paw pressure test (Fig. 2a). Butorphanol showed a significant increase in %MPE in the hind-paw pressure test in wildtype mice [one-way, repeated-measures ANOVA: $F_{(7,56)} = 11.35$, $p < 0.0001$]. Post hoc analysis revealed that the mechanical antinociceptive effects of butorphanol were significant at all examined time-points (5–180 min after butorphanol injection). The mechanical antinociceptive effects of butorphanol also were analyzed in wildtype, heterozygous, and homozygous MOP-KO mice (Fig. 2b). Butorphanol showed dose-dependent mechanical antinociceptive effects in both wildtype and heterozygous MOP-KO mice, but not in homozygous MOP-KO mice. Two-way, mixed-design ANOVA revealed that the antinociceptive effects of butorphanol (%MPE) were significantly different between genotypes in the hind-paw pressure test [significant difference between genotypes, $F_{(2,30)} = 66.05$, $p < 0.0001$; significant genotype × dose interaction, $F_{(8,120)} = 14.67$, $p < 0.0001$]. The antinociceptive effects of butorphanol (%MPE) in heterozygous and homozygous MOP-KO mice were significantly lower than in wildtype mice in the hind-paw pressure test ($p < 0.05$, Tukey–Kramer post hoc test). One-way, repeated-measures ANOVA revealed that butorphanol-induced significant increases in %MPE in the hind-paw pressure test in both wildtype mice [$F_{(4,45)} = 64.88$, $p < 0.0001$] and heterozygous MOP-KO mice [$F_{(4,55)} = 15.82$, $p < 0.0001$]. By contrast, butorphanol failed to significantly change %MPE in the hind-paw pressure test in homozygous MOP-KO mice at cumulative doses up to 10 mg/kg (Fig. 2b).

The visceral chemical antinociceptive effects of butorphanol (3 mg/kg, s.c.) were analyzed in wildtype, heterozygous, and homozygous MOP-KO mice. The 3 mg/kg butorphanol dose was chosen because it induced almost maximal antinociceptive effects in wildtype mice in the hot-plate, tail-flick, and hind-paw pressure tests (Figs. 1 and 2). Interestingly, butorphanol-induced chemical antinociceptive effects not only in wildtype and heterozygous MOP-KO mice, but also in homozygous MOP-KO mice. One-way factorial ANOVA revealed that butorphanol-induced significant decreases in writhing (Fig. 3) in wildtype mice [$F_{(1,14)} = 265.0$, $p < 0.0001$], in heterozygous MOP-KO mice [$F_{(1,16)} = 210.0$, $p < 0.0001$], and in homozygous MOP-KO mice [$F_{(1,17)} = 9.50$, $p < 0.001$], although significant differences were observed between these genotypes [$F_{(2,24)} = 16.43$, $p < 0.0001$]. The remaining visceral chemical antinociceptive effects of butorphanol in homozygous MOP-KO mice were diminished by pretreatment with nor-BNI (5 mg/kg, s.c.). One-way factorial ANOVA revealed no significant difference between writhing counts in MOP-KO mice treated with nor-BNI and butorphanol and in MOP-KO mice treated with nor-BNI and saline. Furthermore, one-way factorial ANOVA revealed a significant difference between writhing counts in MOP-KO mice treated with butorphanol alone and writhing counts in MOP-KO mice treated with nor-BNI and butorphanol [$F_{(1,23)} = 6.57$, $p < 0.05$].

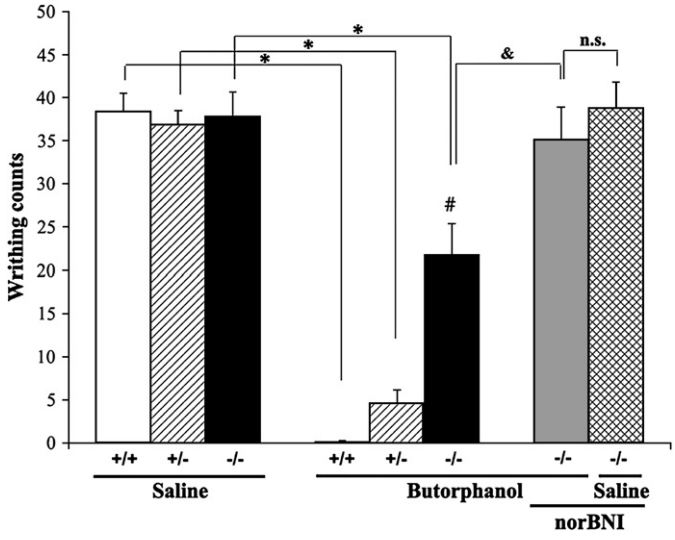

Fig. 3. Visceral chemical antinociceptive effects of butorphanol in wildtype, heterozygous, and homozygous MOP-KO mice. Writhing counts induced by 0.6% acetic acid (i.p.) with saline pretreatment in wildtype [+/+, $n = 9$ (male, 5; female, 4)], heterozygous [+/−, $n = 10$ (male, 5; female, 5)], and homozygous [−/−, $n = 7$ (male, 4; female, 3)] mice, butorphanol pretreatment (3 mg/kg, s.c.) in wildtype [+/+, $n = 8$ (male, 5; female, 3)], heterozygous [+/−, $n = 8$ (male, 4; female, 4)], and homozygous [−/−, $n = 12$ (male, 5; female, 7)] MOP-KO mice, and nor-BNI (5 mg/kg, s.c.) and butorphanol (3 mg/kg, s.c.) [−/−, $n = 13$ (male, 7; female, 6)] or saline pretreatment [−/−, $n = 13$ (male, 4; female, 5)] in homozygous MOP-KO mice. $^{\#}p < 0.05$, Significantly different from wildtype mice; $^{*}p < 0.05$, significantly different from saline pretreatment; $^{\&}p < 0.05$, significantly different from nor-BNI pretreatment; n.s., not significant. Data are expressed as mean ± S.E.M.

3.2. Binding characteristics

Butorphanol competition experiments using membranes prepared from MOP/CHO, DOP/CHO, and KOP/CHO cells revealed apparent binding affinities for each opioid receptor subtype (Fig. 4a, Table 1). Butorphanol bound with higher affinity than morphine to membranes prepared from MOP/CHO, DOP/CHO, and KOP/CHO cells. The morphine results were obtained from previous data (Ide et al., 2004) that were analyzed according to the present methods. The affinities of butorphanol for MOP and KOP were equivalent and higher than for DOP.

Table 1
Binding properties and agonistic effects of butorphanol and morphine on human opioid receptor subtypes

	MOP/CHO	DOP/CHO	KOP/CHO
Competitive binding assay			
K_i value (nM)			
Butotphanol	6.8 ± 2.3	34.7 ± 10.2	7.8 ± 4.1
Morphine	33.2 ± 7.2	355 ± 61	224 ± 11
cAMP assay			
IC_{50} (nM)			
Butotphanol	5.8 ± 2.9	64.4 ± 43.9	4.4 ± 3.0
Morphine	25.5 ± 9.7	364 ± 200	252 ± 231
I_{max} (%)			
Butotphanol	59.3 ± 10.8	77.9 ± 4.2	68.8 ± 8.2
Morphine	87.5 ± 2.8	83.6 ± 2.8	83.0 ± 1.3

Morphine data were obtained from reanalysis of data in Ide et al. (2004).

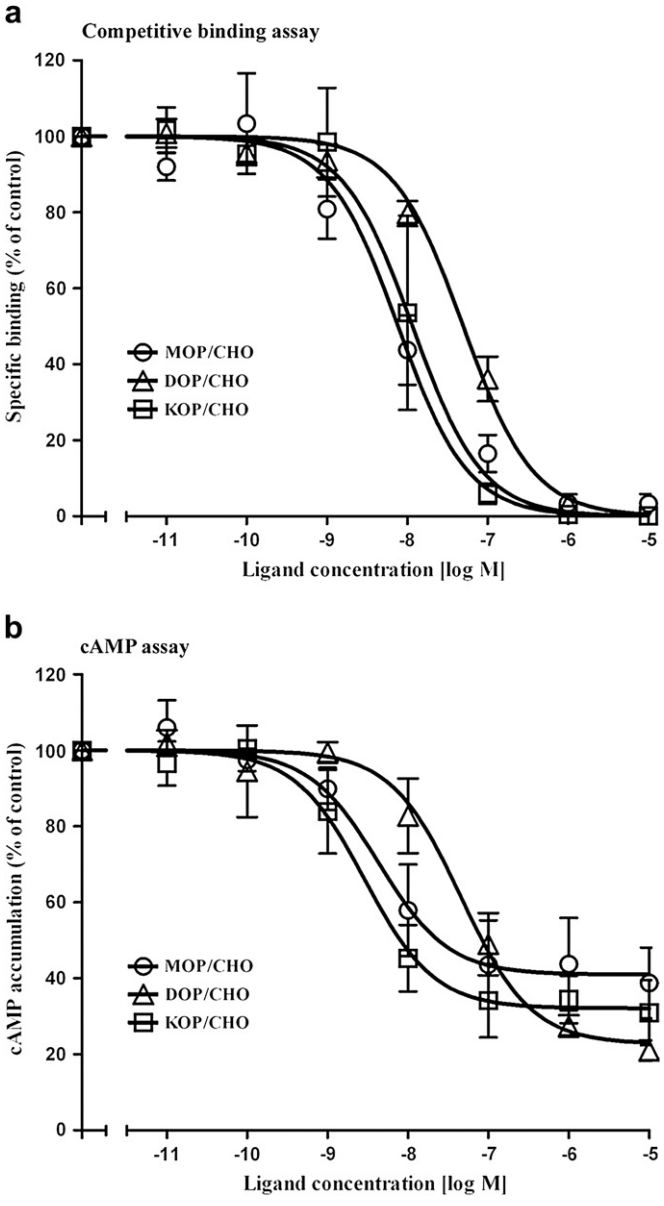

Fig. 4. (a) Binding properties of butorphanol for displacement of specific binding of 2 nM [^{3}H]DAMGO, 2 nM [^{3}H]DPDPE, and 3 nM [^{3}H]U69593 to the membranes of MOP/CHO (open circle, $n = 15$), DOP/CHO (open triangle, $n = 11$), and KOP/CHO (open square, $n = 12$), respectively. Data are expressed as mean ± S.E.M. (b) Agonistic effects of butorphanol on forskolin-stimulated cAMP production in MOP/CHO (open circle, $n = 5$), DOP/CHO (open triangle, $n = 3$), and KOP/CHO (open square, $n = 5$) cells. Intracellular cAMP levels in the cells incubated with 10 mM forskolin alone served as controls (100%). Data are expressed as mean ± S.E.M.

3.3. cAMP assay

Butorphanol effects on forskolin-stimulated cAMP accumulation in MOP/CHO, DOP/CHO, and KOP/CHO cells also were tested. Butorphanol concentration-dependently suppressed forskolin-stimulated cAMP accumulation in all three cell types (Fig. 4b). I_{max} values for butorphanol were apparently lower than those of morphine for all cell lines (Table 1). IC_{50} values of butorphanol were lower than those of morphine for MOP/CHO, DOP/CHO, and KOP/CHO cells (Table 1). The morphine results were obtained from previous data (Ide et al., 2004) that were analyzed according to the present methods.

4. Discussion

The thermal antinociceptive effects of butorphanol were significantly reduced in heterozygous and homozygous MOP-KO mice compared with wildtype mice in both the hot-plate and tail-flick tests. The thermal antinociceptive effects of butorphanol in both tests increased in a MOP gene dose-dependent fashion. The copy numbers of the MOP gene are zero in homozygous MOP-KO mice, one in heterozygous MOP-KO mice, and two in wildtype mice. In addition, the mechanical antinociceptive effects of butorphanol in these mice, analyzed by the Randall–Selitto test, were similar to the thermal antinociceptive effects. These results suggest that the MOP is the main opioid receptor involved in butorphanol-induced thermal and mechanical antinociception. This is consistent with previous reports. The selective MOP antagonist β-funaltrexamine was reported to antagonize the thermal antinociceptive effects of butorphanol in a tail-flick test, but pretreatment with nor-BNI did not reliably antagonize the butorphanol effects, and naltrindole, a DOP antagonist, failed to antagonize the effects of butorphanol (Garner et al., 1997).

The antinociceptive effects of morphine, an MOP agonist with low affinity for DOP and KOP, are reduced in several strains of heterozygous MOP-KO mice and completely abolished in homozygous MOP-KO mice (Loh et al., 1998; Sora et al., 1997b, 2001). Also, the antinociceptive effects of DPDPE, a DOP-preferring ligand with modest affinity for the MOP, are reduced in MOP-KO mice (Matthes et al., 1998; Sora et al., 1997a). CXBK mice, which express MOPs at approximately half of the level of C57BL/6 and BALB/c progenitor strains, show reduced analgesic effects in response not only to morphine but also to U50,488H, a κ-selective agonist (Ikeda et al., 1999). Furthermore, the thermal antinociception induced by buprenorphine, a nonselective partial agonist for opioid receptors, is abolished in MOP-KO mice, although the rewarding effects of the drug remain (Ide et al., 2004). In contrast, the antinociceptive effects of morphine are not altered in mice lacking DOPs (Zhu et al., 1999) or in mice lacking KOPs (Simonin et al., 1998). The present results, together with these previous reports, suggest that MOPs

play a critical role in the thermal and mechanical analgesia induced by opioid partial agonists. MOP tolerance and inactivation and/or individual differences in MOP number are thus important for most of the variation in the degree of thermal and mechanical analgesia induced by opioids.

The thermal antinociceptive effects of butorphanol were weak when compared with the effects in the tail-flick test. This is consistent with a previous report showing that butorphanol had weak analgesic activity in a mouse hot-plate test (Pircio et al., 1976). Antinociception in the hot-plate test is hypothesized to reflect analgesia at supraspinal level, whereas antinociception in the tail-flick test is hypothesized to reflect analgesia at spinal levels. Thus, the present results suggest that butorphanol may exert its antinociceptive effects spinally rather than supraspinally. Further studies of butorphanol using intracerebroventricular (i.c.v.) and intrathecal (i.t.) microinjection may provide novel insight. Butorphanol exhibited thermal antinociception more effectively with a low-temperature (50 °C) stimulus than with a high-temperature (55 °C) stimulus in warm-water tail-immersion tests in rhesus monkeys (Butelman et al., 1995). Further, our previous report showed that the thermal antinociceptive effects of buprenorphine in a hot-plate test were less effective than in a tail-flick test (Ide et al., 2004). Although we selected a relatively low-temperature (52 °C) in the hot-plate test, butorphanol-induced thermal antinociception was still weak in the hot-plate test. Far lower thermal stimuli (e.g. 48–50 °C) may be preferable for assessing butorphanol effects in hot-plate tests.

In the present study, the thermal and mechanical antinociceptive effects of butorphanol were assessed under the cumulative dose–response paradigm similar to previous reports (Ide et al., 2004; Sora et al., 1997b). This paradigm has the advantage of reducing the number of animals necessary for experiments. Because it is difficult to obtain a large number of genetically modified animals, the paradigm is especially useful for studies using these animals. However, the results obtained from the cumulative dose–response paradigm may not be comparable to those from paradigms using different animals for each dose. The cumulative dose–response paradigm can be used when the effect of the drug is expressed prior to the next injection and is retained until the end of the test. The paradigm may not be appropriate for analyzing drugs that are characterized by rapid tolerance or sensitization. In the present study, the effects of butorphanol were expressed early (<5 min) and were long-lasting (>3 h). Thus, the cumulative dose–response paradigm seems to have been appropriate for assessing the antinociceptive effects of butorphanol in the present study. In addition, the antinociceptive effects of butorphanol at 3 mg/kg in the cumulative dose–response paradigm was weak compared with the time-course analysis in both the hot-plate (about 10%MPE weak) and tail-flick (about 20%MPE weak) tests, although these differences were not statistically significant in the present study. The decreased effects of butorphanol in the cumulative dose–response paradigm may be attributable to both acute tolerance and blood level reduction by metabolism of butorphanol injected earlier. Cumulative dose–response paradigms may have relative weaknesses compared with other paradigms, but the present results indicated robust differences in the effects of butorphanol between genotypes.

In contrast to thermal and mechanical antinociception, butorphanol showed significant visceral chemical antinociceptive effects in homozygous MOP-KO mice, although the visceral chemical antinociceptive effects of butorphanol increased in a MOP gene dose-dependent fashion. The residual visceral chemical antinociception induced by butorphanol was abolished by pretreatment with nor-BNI, a selective KOP antagonist. These results indicate that both MOP and KOP play dominant roles in butorphanol-induced visceral chemical antinociception. This is also consistent with previous reports. The effectiveness of a KOP agonist in reducing visceral pain has been reported (Riviere, 2004). The enhanced response of KOP-KO mice in the acetic acid writhing test also has been demonstrated (Simonin et al., 1998). The nociceptive responses in the acetic acid writhing test were not altered in homozygous MOP-KO mice in the present study. Although the precise molecular mechanisms have not been revealed, KOPs rather than MOPs may regulate intrinsic visceral nociceptive sensations induced by endogenous opioids, and MOPs may regulate visceral nociception only with exogenously administered opioid drugs. The present results, together with previous reports, suggest that both MOPs and KOPs play important roles in visceral chemical analgesia mediated by opioid partial agonists. Furthermore, the present results suggest that varied visceral chemical pain can be controlled by nonselective opioids, such as bremazocine, pentazocine, and buprenorphine, acting through both MOPs and KOPs.

The results of our in vitro experiments using human MOP, DOP, and KOP cDNA suggest that butorphanol induces antinociceptive effects mainly via MOPs, and partially KOPs, in humans. Butorphanol bound to human MOPs with moderate affinity, approximately 4.9-fold greater than that displayed by morphine. Butorphanol binding affinity for MOPs was as high as that for KOPs and 5.1-fold higher than that for DOPs in human clones. In the cAMP assays, butorphanol also showed lower IC_{50} values for both MOPs and KOPs than for DOPs, although moderate I_{max} values were demonstrated for three opioid receptor subtypes. These results suggest that mainly MOPs, and partially KOPs but not DOPs, may be involved in the antinociceptive effects of butorphanol in humans as well as in rodents.

In conclusion, the present study demonstrated the abolition of thermal and mechanical antinociceptive effects of butorphanol in MOP-KO mice, suggesting that thermal and mechanical antinociception induced by butorphanol is completely mediated by partial agonistic effects of butorphanol on MOPs. We also demonstrated retention of butorphanol-induced visceral chemical antinociception in MOP-KO mice, abolition of butorphanol-induced visceral chemical antinociception by pretreatment with nor-BNI, and in vitro data showing that butorphanol more strongly acted on KOPs and MOPs than on DOPs, suggesting that butorphanol-induced visceral chemical antinociception is mediated by partial agonistic effects on both MOPs and KOPs. For clinical usage, butorphanol may be effective for controlling visceral pain, particularly in patients tolerant to MOP-selective opioid drugs or patients whose MOPs are hypoactive by genetic and/or other factors. Future studies elucidating the precise molecular mechanisms underlying the antinociceptive effects of butorphanol will contribute to the better usage of opioid drugs for pain management.

Acknowledgements

This study was supported by research grants from the Japanese Ministry of Health, Labour and Welfare (MHLW: H17-pharmaco-001); the Japanese Ministry of Education, Culture, Sports, Science, and Technology, Grant-in-Aid for Scientific Research (C), 19603021; and the National Institute on Drug Abuse Intramural Research Program from the National Institutes of Health. We thank Drs. Yoko Hagino, Yukio Takamatsu, and Keiko Matsuoka for technical support and animal care.

References

Butelman, E.R., Winger, G., Zernig, G., Woods, J.H., 1995. Butorphanol: characterization of agonist and antagonist effects in rhesus monkeys. J. Pharmacol. Exp. Ther. 272, 845–853.

Chang, K.J., Hazum, E., Cuatrecasas, P., 1981. Novel opiate binding sites selective for benzomorphan drugs. Proc. Natl. Acad. Sci. U.S.A. 78, 4141–4145.

Collier, H.O., Dinneen, L.C., Johnson, C.A., Schneider, C., 1968. The abdominal constriction response and its suppression by analgesic drugs in the mouse. Br. J. Pharmacol. Chemother. 32, 295–310.

D'Amour, F.E., Smith, D.L., 1941. A method for determining loss of pain sensation. J. Pharmacol. Exp. Ther. 72, 74–79.

Dykstra, L.A., 1990. Butorphanol, levallorphan, nalbuphine and nalorphine as antagonists in the squirrel monkey. J. Pharmacol. Exp. Ther. 254, 245–252.

Feng, Y.Z., Tseng, Y.T., Jaw, S.P., Hoskins, B., Ho, I.K., 1994. Tolerance development to butorphanol: comparison with morphine. Pharmacol. Biochem. Behav. 49, 649–655.

Garner, H.R., Burke, T.F., Lawhorn, C.D., Stoner, J.M., Wessinger, W.D., 1997. Butorphanol-mediated antinociception in mice: partial agonist effects and mu receptor involvement. J. Pharmacol. Exp. Ther. 282, 1253–1261.

Ide, S., Minami, M., Ishihara, K., Uhl, G.R., Sora, I., Ikeda, K., 2006. Mu opioid receptor-dependent and independent components in effects of tramadol. Neuropharmacology 51, 651–658.

Ide, S., Minami, M., Satoh, M., Uhl, G.R., Sora, I., Ikeda, K., 2004. Buprenorphine antinociception is abolished, but naloxone-sensitive reward is retained, in μ-opioid receptor knockout mice. Neuropsychopharmacology 29, 1656–1663.

Ikeda, K., Ichikawa, T., Kobayashi, T., Kumanishi, T., Oike, S., Yano, R., 1999. Unique behavioural phenotypes of recombinant-inbred CXBK mice: partial deficiency of sensitivity to μ- and κ-agonists. Neurosci. Res. 34, 149–155.

Jaw, S.P., Hoskins, B., Ho, I.K., 1993a. Opioid antagonists and butorphanol dependence. Pharmacol. Biochem. Behav. 44, 497–500.

Jaw, S.P., Makimura, M., Hoskins, B., Ho, I.K., 1993b. Effects of nor-binaltorphimine on butorphanol dependence. Eur. J. Pharmacol. 239, 133–140.

Katsumata, S., Minami, M., Nakagawa, T., Iwamura, T., Satoh, M., 1995. Pharmacological study of dihydroetorphine in cloned μ-, δ- and κ-opioid receptors. Eur. J. Pharmacol. 291, 367–373.

Loh, H.H., Liu, H.C., Cavalli, A., Yang, W., Chen, Y.F., Wei, L.N., 1998. μ Opioid receptor knockout in mice: effects on ligand-induced analgesia and morphine lethality. Brain Res. Mol. Brain Res. 54, 321–326.

Matthes, H.W., Maldonado, R., Simonin, F., Valverde, O., Slowe, S., Kitchen, I., Befort, K., Dierich, A., Le Meur, M., Dolle, P., Tzavara, E., Hanoune, J., Roques, B.P., Kieffer, B.L., 1996. Loss of morphine-induced analgesia, reward effect and withdrawal symptoms in mice lacking the μ-opioid-receptor gene. Nature 383, 819–823.

Matthes, H.W., Smadja, C., Valverde, O., Vonesch, J.L., Foutz, A.S., Boudinot, E., Denavit-Saubie, M., Severini, C., Negri, L., Roques, B.P., Maldonado, R., Kieffer, B. L., 1998. Activity of the δ-opioid receptor is partially reduced, whereas activity of the κ-receptor is maintained in mice lacking the μ-receptor. J. Neurosci. 18, 7285–7295.

Newman, L.C., Sands, S.S., Wallace, D.R., Stevens, C.W., 2002. Characterization of μ, κ, and δ opioid binding in amphibian whole brain tissue homogenates. J. Pharmacol. Exp. Ther. 301, 364–370.

Oh, K.W., Makimura, M., Jaw, S.P., Hoskins, B., Ho, I.K., 1992. Effects of β-funaltrexamine on butorphanol dependence. Pharmacol. Biochem. Behav. 42, 29–34.

Picker, M.J., Negus, S.S., Craft, R.M., 1990. Butorphanol's efficacy at mu and kappa opioid receptors: inferences based on the schedule-controlled behavior of nontolerant and morphine-tolerant rats and on the responding of rats under a drug discrimination procedure. Pharmacol. Biochem. Behav. 36, 563–568.

Pircio, A.W., Gylys, J.A., Cavanagh, R.L., Buyniski, J.P., Bierwagen, M.E., 1976. The pharmacology of butorphanol, a 3,14-dihydroxymorphinan narcotic antagonist analgesic. Arch. Int. Pharmacodyn. Ther. 220, 231–257.

Randall, L.O., Selitto, J.J., 1957. A method for measurement of analgesic activity on inflamed tissue. Arch. Int. Pharmacodyn. Ther. 111, 409–419.

Riviere, P.J., 2004. Peripheral kappa-opioid agonists for visceral pain. Br. J. Pharmacol. 141, 1331–1334.

Simonin, F., Valverde, O., Smadja, C., Slowe, S., Kitchen, I., Dierich, A., Le Meur, M., Roques, B.P., Maldonado, R., Kieffer, B.L., 1998. Disruption of the κ-opioid receptor gene in mice enhances sensitivity to chemical visceral pain, impairs pharmacological actions of the selective κ-agonist U-50,488H and attenuates morphine withdrawal. EMBO J. 17, 886–897.

Sora, I., Elmer, G., Funada, M., Pieper, J., Li, X.F., Hall, F.S., Uhl, G.R., 2001. μ opiate receptor gene dose effects on different morphine actions: evidence for differential in vivo mu receptor reserve. Neuropsychopharmacology 25, 41–54.

Sora, I., Funada, M., Uhl, G.R., 1997a. The μ-opioid receptor is necessary for [D-Pen^2, D-Pen^5]enkephalin-induced analgesia. Eur. J. Pharmacol. 324, R1–R2.

Sora, I., Takahashi, N., Funada, M., Ujike, H., Revay, R.S., Donovan, D.M., Miner, L.L., Uhl, G.R., 1997b. Opiate receptor knockout mice define μ receptor roles in endogenous nociceptive responses and morphine-induced analgesia. Proc. Natl. Acad. Sci. U.S.A. 94, 1544–1549.

Woolfe, G., MacDonald, A.D., 1944. The evaluation of the analgesic action of pethidine hydrochloride (demerol). J. Pharmacol. Exp. Ther. 80, 300–307.

Zhu, Y., King, M.A., Schuller, A.G., Nitsche, J.F., Reidl, M., Elde, R.P., Unterwald, E., Pasternak, G.W., Pintar, J.E., 1999. Retention of supraspinal delta-like analgesia and loss of morphine tolerance in δ opioid receptor knockout mice. Neuron 24, 243–252.

Animal models of depression in dopamine, serotonin, and norepinephrine transporter knockout mice: prominent effects of dopamine transporter deletions

Maria T.G. Perona[a], Shonna Waters[a], Frank Scott Hall[a], Ichiro Sora[b], Klaus-Peter Lesch[c], Dennis L. Murphy[d], Marc Caron[e] and George R. Uhl[a]

Antidepressant drugs produce therapeutic actions and many of their side effects via blockade of the plasma membrane transporters for serotonin (SERT/SLC6A2), norepinephrine (NET/SLC6A1), and dopamine (DAT/SLC6A3). Many antidepressants block several of these transporters; some are more selective. Mouse gene knockouts of these transporters provide interesting models for possible effects of chronic antidepressant treatments. To examine the role of monoamine transporters in models of depression DAT, NET, and SERT knockout (KO) mice and wild-type littermates were studied in the forced swim test (FST), the tail suspension test, and for sucrose consumption. To dissociate general activity from potential antidepressant effects three types of behavior were assessed in the FST: immobility, climbing, and swimming. In confirmation of earlier reports, both DAT KO and NET KO mice exhibited less immobility than wild-type littermates whereas SERT KO mice did not. Effects of DAT deletion were not simply because of hyperactivity, as decreased immobility was observed in DAT+/− mice that were not hyperactive as well as in DAT−/− mice that displayed profound hyperactivity. Climbing was increased, whereas swimming was almost eliminated in DAT−/− mice, and a modest but similar effect was seen in NET KO mice, which showed a modest decrease in locomotor activity. Combined increases in climbing and decreases in immobility are characteristic of FST results in antidepressant animal models, whereas selective effects on swimming are associated with the effects of stimulant drugs. Therefore, an effect on climbing is thought to more specifically reflect antidepressant effects, as has been observed in several other proposed animal models of reduced depressive phenotypes. A similar profile was observed in the tail suspension test, where DAT, NET, and SERT knockouts were all found to reduce immobility, but much greater effects were observed in DAT KO mice. However, to further determine whether these effects of DAT KO in animal models of depression may be because of the confounding effects of hyperactivity, mice were also assessed in a sucrose consumption test. Sucrose consumption was increased in DAT KO mice consistent with reduced anhedonia, and inconsistent with competitive hyperactivity; no increases were observed in SERT KO or NET KO mice. In summary, the effects of DAT KO in animal models of depression are larger than those produced by NET or SERT KO, and unlikely to be simply the result of the confounding effects of locomotor hyperactivity; thus, these data support reevaluation of the role that DAT expression could play in depression and the potential antidepressant effects of DAT blockade.
Behavioural Pharmacology **19:566–574**

Behavioural Pharmacology 2008, **19**:566–574

Keywords: DAT knockout, forced swim test, mouse, NET knockout, SERT knockout, sucrose intake, tail suspension test

[a]Molecular Neurobiology Branch, NIDA-IRP, NIH, Baltimore, Maryland, USA, [b]Division of Psychobiology, Department of Neuroscience, Tohoku University Graduate School of Medicine, Sendai, Japan, [c]Department of Psychiatry, University of Würzburg, Germany, [d]Laboratory of Clinical Science, NIMH-IRP, NIH, Bethesda, Maryland and [e]Departments of Cell Biology and Medicine, Duke University, Durham, North Carolina, USA

Correspondence to George R. Uhl, Molecular Neurobiology Branch, National Institute on Drug Abuse, 333 Cassell Drive, Baltimore, MD 21224, USA
E-mail: guhl@intra.nida.nih.gov

Received 28 January 2008 **Accepted as revised** 14 June 2008

Introduction

Inhibition of neurotransmitter reuptake by drugs acting at SERT, NET, and/or DAT can produce antidepressant effects (Skolnick *et al.*, 2003; Lucki and O'Leary, 2004), which, in part, has led to hypotheses that dysfunction of serotonin, norepinephrine, and/or dopamine systems might contribute to depression (Prange, 1964; Schildkraut, 1967; Akiskal and McKinney, 1973; van Praag, 1974; Willner, 1983a, b, c, 2000; Shelton, 2004; Dunlop and Nemeroff, 2007). Most drugs that are clinically effective antidepressants in humans produce reduced immobility in the rodent forced swim test (FST) (Porsolt, 1979). Modifications and extensions of the FST paradigm (Armario *et al.*, 1988; Cervo and Samanin, 1991; Detke *et al.*, 1995, 1997; Detke and Lucki; 1996) have sought to improve its specificity and predictive validity for human antidepressant efficacy (for review, see Cryan *et al.*, 2005a). These modified versions of the original test examine additional behavioral features and use slight modifications of the original apparatus that

0955-8810 © 2008 Wolters Kluwer Health | Lippincott Williams & Wilkins DOI: 10.1097/FBP.0b013e32830cd80f

allow assessment of a broader behavioral repertoire. Such assessments may be especially important for studies of experimental manipulations that may alter both depressive behavior and general activity. In studies of Fawn Hooded rats that exhibit both hyperactivity (Hall *et al.*, 1998b) and reduced immobility in forced swim testing (Hall *et al.*, 1998a), for example, the examination of several behavioral endpoints allowed dissociation of hyperactivity from antidepressant-like effects. Such considerations might thus be especially useful in studies of rodents with genetic manipulations that could alter both general levels of motor activity and depressive-like symptoms, such as dopamine transporter knockout (KO) mice (Giros *et al.*, 1996; Sora *et al.*, 1998).

Monoamine transporter knockouts are potentially of interest in the study of antidepressant actions because they chronically elevate extracellular monoamine levels (Gainetdinov *et al.*, 1998; Xu *et al.*, 2000; Mathews *et al.*, 2004; Shen *et al.*, 2004) in a manner similar to antidepressant treatments (Abercrombie *et al.*, 1988; Nomikos *et al.*, 1990; Kreiss and Lucki, 1995). Effects of SERT, NET, and DAT KO mice in antidepressant models may thus be of relevance in understanding the mechanisms that underlie antidepressant effects. Decreased immobility, a correlate of antidepressant activity, has been observed in NET KO mice (Xu *et al.*, 2000) and DAT KO mice (Spielewoy *et al.*, 2000). No difference or increased immobility has been observed SERT KO mice depending on the background strain examined (Holmes *et al.*, 2002). All of these studies, however, have only examined immobility in the FST. Examination of other behaviors in this test (e.g. climbing and swimming) should help in clarifying the nature of these effects. In the case of DAT KO mice this is essential because DAT KO mice are hyperactive (Giros *et al.*, 1996; Sora *et al.*, 1998). In an earlier study of DAT KO mice in the FST (Spielewoy *et al.*, 2000) it was suggested that reductions in immobility were produced by increased 'swimming', but those authors did not in fact measure any other behavior in the test, nor differentiate between climbing and swimming. The nature of this behavior is rather important as it might reflect one of two possible effects, general activity or antidepressant activity.

As hyperactivity may be a confounding issue in the FST it is important to validate the findings of that model in other models of depression. Another model that has been extensively validated with a wide range of antidepressants is the tail suspension test (TST) (Cryan *et al.*, 2005b). SERT KO mice showed reduced immobility in the TST, which was dependent on the background strain against which the knockout was expressed (Holmes *et al.*, 2002), similar to observations in the FST. A similar profile has been observed in NET KO mice in the TST (Dziedzicka-Wasylewska *et al.*, 2006), but this has not yet been assessed in DAT KO mice. Thus, to clarify and extend these data, we now report examination of behavior in DAT, SERT, and NET KO mice using both the FST and the TST under identical experimental conditions so that comparisons may be made between the relative magnitude of the effects of each of these monoamine transporter gene knockouts.

The TST, as well as the FST, might, however, be interpreted as being open to the confounding effects of hyperactivity. To further address this issue we examined another model, sucrose consumption, which should not be open to the same type of locomotor confound. The sucrose consumption model assesses a different aspect of depressive behavior, anhedonia, and was originally used to assess the depressive effects of chronic mild stress (Papp *et al.*, 1991), but has since been used to assess the effects of several other models of depression (El Yacoubi *et al.*, 2003; Wintink *et al.*, 2003; Shumake *et al.*, 2005).

Methods

Subjects

The KO mice used in these experiments were from the DAT-SERT (Sora *et al.*, 2001) and NET-SERT (Hall *et al.*, 2002) double KO lines described previously which were produced from crossing the original DAT (Sora *et al.*, 1998), SERT (Bengel *et al.*, 1998), and NET (Wang *et al.*, 1999) single KO lines. The DAT mice used in these experiments from the DAT-SERT line were wild type (WT) for SERT, the SERT mice from the DAT-SERT line were WT for DAT and NET mice from the NET-SERT line were WT for SERT. For simplicity the second genotype, always $+/+$, is not included in the descriptions. These KO lines are therefore of a mixed C57BL/6J-129Sv background. Wild-type mice ($+/+$), heterozygote KO mice ($+/-$), and homozygote KO mice ($-/-$) were genotyped by PCR, using two internal primers, one targeted at the knockout insertion sequence and the other targeted at the WT gene, and one external primer, which generated two products identifying the WT and KO genes. The DAT and SERT transgenic knockout insertion sequences contained a neomycin gene sequence (NEO), whereas the NET KO contained a green fluorescent protein gene insert. PCR using TaKaRa DNA polymerase (Takara Bio, Shiga, Japan) was performed on DNA that was eluted from tail biopsies after digestion overnight in Protease K. For DAT genotyping the external primer (5′ AGT GTG TGC AGG GCA TGG TGT A 3′) and the WT primer (5′ TAG GCA CTG CTG ACG ATG ACT G 3′) produced a 500-bp band, whereas the external primer and the NEO primer (5′ CTC GTC GTG ACC CAT GGC GAT 3′) produced a 600-bp band. For SERT genotyping the external primer (5′ GCT CTC AGT CTT GTC TCC ATA AC 3′) and the WT primer (5′ TGC TGA CTG GAG TAC AGG CTA G 3′) produced a 620-bp band, whereas the external primer and the NEO

primer (5′ CTC GTC GTG ACC CAT GGC GAT 3′) produced a 800-bp band. For NET genotyping the external primer (5′ GCT CTG TCC CTG TGC TTC ACG 3′) and the WT primer (5′ TGA GGC CTA AGC TGG AGC TCG 3′) produced a 601-bp band, whereas the external primer and the green fluorescent protein primer (5′ CGG TGA ACA GCT CCT CGC CC 3′) produced a 470-bp band.

Forced swim test

This experiment used the FST (Porsolt *et al.*, 1977) modified and validated in a manner similar to that described earlier for rats (Hall *et al.*, 1998a). On two successive days, DAT, SERT, and NET KO mice (n = 8–10/genotype) were placed in 3-l cylindrical beakers (diameter 19 cm) that were filled to a depth of 14 cm with 25°C water. On the pretest day, mice were placed in the water for 15 min, towel-dried, placed under a warming lamp until completely dry, and then returned to their home cages. On the test day, the mice were placed into the water for 5 min and their behavior was recorded digitally. Their behavior was scored by observation of these recordings, blind to genotype. Durations of immobility, swimming, and climbing behaviors were measured using the TIMER behavioral scoring program (National Institutes of Health). 'Immobility' was defined as being stationary with only enough motion of the tail or forepaws to keep the head above water. The forepaws usually remained at the animal's sides. 'Swimming' was defined as active use of the forepaws with forward movement, in the center or along the sides of the cylinder, which did not involve lifting the paws above the surface of the water. The body was usually oriented parallel to the sides of the cylinder. 'Climbing' was defined as active pawing of the side of the cylinder, lifting the paws above the surface of the water. The body was oriented with the head toward the wall and the body oriented perpendicularly to the side of the cylinder. Inter-rater reliability estimates for these three measures were calculated by comparing the scores of two observers for 32 subjects. Reliability estimates for immobility ($r = 0.88$, $P < 0.001$), climbing ($r = 0.86$, $P < 0.001$), and swimming ($r = 0.81$, $P < 0.001$) were similar to the inter-rater reliability estimates obtained previously for rats (Hall *et al.*, 1998a).

As strain has been shown to affect responses to SERT and NET blockers in the FST (Lucki *et al.*, 2001; David *et al.*, 2003; Dulawa *et al.*, 2004), an additional experiment was performed to determine the sensitivity of WT mice from the DAT-SERT line to selective transporter blockers. The effects of pretreatment with saline (1 ml/100g IP), fluoxetine (30 mg/kg IP), desipramine (20 mg/kg IP), or GBR12909 (20 mg/kg IP), 30 min prior to the 5 min test on the second day were examined in WT mice (n = 8–9 per condition). In all other respects the experiment was identical to that described above.

Tail suspension test

In the TST DAT, SERT, and NET KO mice (n = 8–13/genotype) were suspended by the tail from a horizontal metal rod (8 mm diameter) for 5 min. The duration of immobility was measured by an observer with a stopwatch.

Sucrose consumption test

In the sucrose consumption test DAT KO (n = 7–11 per genotype), SERT KO (n = 7–13 per genotype), and NET KO (n = 6–10 per genotype), were placed in a sucrose consumption chamber (DM-8 lick counter, Columbus Instruments, Columbus, OH) each day with access to water and sucrose. The number of licks for sucrose and water were monitored for 30 min. In a preliminary experiment the volume consumed as well as the number of licks was monitored. The correlation between licks and volume was found to be highly significant ($r = 0.85$, $P < 0.01$); thus only the number of licks is presented. To account for differing weight of the subjects the number of licks is presented as licks/100 g body weight. The subjects were tested over 9 days, 3 days at each concentration of sucrose (0.7, 7, and 34% sucrose).

Locomotor activity

Earlier studies found that DAT−/− mice were profoundly hyperactive (Giros *et al.*, 1996), whereas locomotor activity was reduced in NET KO mice (Xu *et al.*, 2000). No basal differences in activity were found in SERT KO mice or in DAT+/− mice (Giros *et al.*, 1996; Bengel *et al.*, 1998; Xu *et al.*, 2000). Nonetheless, because differences in locomotor activity between genotypes might be thought to affect the paradigms described above, basal locomotion was assessed in DAT, SERT, and NET KO mice. For each gene knockout +/+, +/− and −/− mice (n = 9–11 per genotype) were assessed for locomotor activity for 1 h under novel conditions. Total distance traveled was measured in Optovarimax activity monitors (Columbus Instruments) under dark, sound-attenuated conditions using methods identical to our earlier publications with DAT KO, SERT KO, and DAT/SERT KO mice (Sora *et al.*, 1998, 2001).

Data analysis

The data were analyzed using analysis of variance (ANOVA) with the between-subjects factor of 'genotype', followed by Fisher's protected least significant difference (PLSD) for post-hoc comparisons where appropriate. For analysis of the sucrose consumption data, the additional within-subjects factors of 'sucrose' (sucrose vs. water) and 'concentration' (0.7, 7 and 34% sucrose) were included in the ANOVA. The data for the 3 days of testing at each concentration were averaged and the average values submitted to ANOVA. The effects of saline, fluoxetine, desipramine, and GBR12909 were compared by ANOVA followed by post-hoc comparison with Fisher's PLSD.

Results

Forced swim test

Deletion of the dopamine transporter gene profoundly affected FST behavior. The duration of immobility was decreased by DAT KO (Fig. 1a) so that DAT −/− mice exhibited virtually no immobility [$F(2,27) = 4.9$, $P < 0.02$]. These results were significantly different from those obtained from littermate DAT +/+ mice ($P < 0.05$). Immobility was also reduced in DAT −/− mice. Immobility in these mice was intermediate between values for DAT +/+ and DAT −/− mice, although post-hoc comparisons did not reach statistical significance. The duration of swimming was also greatly reduced in DAT KO mice (Fig. 1b) [$F(2,27) = 4.9$, $P < 0.02$]. DAT −/− mice exhibited virtually no swimming behavior. These differences achieved significance in comparison with DAT +/+ ($P < 0.05$) and DAT +/− mice ($P < 0.05$). The duration of swimming was unaltered in DAT +/− mice compared with DAT +/+ mice. DAT −/− mice exhibited climbing behavior for almost the entire period of testing. Six of the 10 DAT −/− subjects tested struggled to escape the cylinder for the entire session (Fig. 1c). The duration of climbing was greatly increased in DAT KO mice [$F(2,27) = 12.7$, $P < 0.001$]. In this case, as for immobility, DAT +/− mice exhibited behavior that was intermediate between DAT +/+ and DAT −/− mice. The duration of climbing was significantly greater in DAT −/− mice than in either DAT +/+ or DAT +/− mice ($P < 0.05$). DAT +/− mice also exhibited significantly more climbing than WT DAT +/+ mice ($P < 0.05$).

Fig. 1

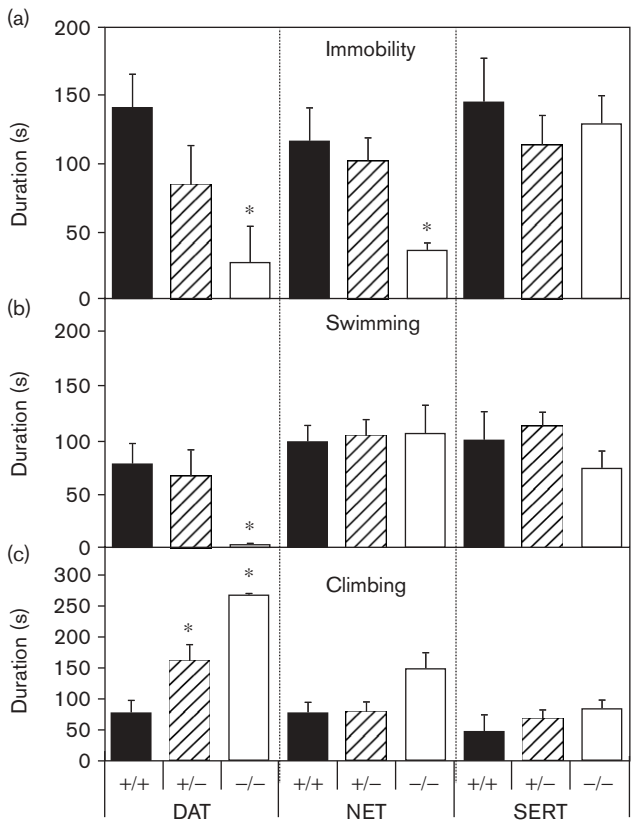

Behavior in the modified forced swim test in DAT KO, SERT KO, and NET KO mice. The duration of immobility (a), swimming (b), and climbing (c) in DAT KO, SERT KO, and NET KO mice (+/+, +/−, and −/− genotypes for each strain), expressed as mean ± the standard error of mean. *Significant difference from +/+ mice, Fisher's protected least significant difference.

Deletion of the NET gene also reduced the duration of immobility in the FST [Fig. 1a; $F(2,27) = 4.9$, $P < 0.02$]. NET −/− mice exhibited substantially reduced immobility when compared with NET +/+ mice ($P < 0.05$). NET +/− mice did not differ significantly from WT mice. The duration of swimming was unaffected by NET KO [Fig. 1b; $F(2,24) = 0.1$, NS]. Although climbing showed a trend toward increase in NET −/− mice, this did not reach statistical significance [Fig. 1c; $F(2,24) = 2.1$, NS].

Deletion of the SERT gene had no effect on any FST behavior. Figure 1a-c shows that SERT KO failed to affect the duration of immobility [$F(2,25) = 0.3$, NS], the duration of swimming [$F(2,25) = 0.8$, NS], or the duration of climbing [$F(2,25) = 0.8$, NS].

In WT mice a significant difference was observed between drug treatment groups for immobility [Table 1; $F(3,28) = 10.2$, $P < 0.001$] and swimming followed by [Table 1; $F(3,28) = 5.4$, $P < 0.005$], but not for climbing [Table 1; $F(3,28) = 1.4$, NS]. Desipramine significantly reduced immobility ($P < 0.05$ vs. saline, Fisher's PLSD), and increased swimming ($P < 0.05$ vs. saline, Fisher's PLSD). Desipramine treatment also increased climbing but this difference was not statistically significant. In contrast, neither of the other two drugs, fluoxetine or GBR 12909, had any statistically significant effects, although a trend for GBR 12909 to decrease immobility and to increase climbing was observed.

Tail suspension test

Deletion of all three monoamine transporter genes decreased immobility in the TST (Fig. 2): DAT

Table 1 Effects of fluoxetine, desipramine, and GBR 12909 in the modified forced swim test in WT mice

	Behavioral measure		
Drug	Immobility	Swimming	Climbing
Saline	181.5 ± 13.4	105.9 ± 12.6	11.1 ± 7.6
Desipramine	69.1 ± 15.7[a]	193.5 ± 20.7[a]	34.8 ± 10.0
Fluoxetine	183.6 ± 17.7	100.1 ± 19.4	14.1 ± 5.2
GBR 12909	144.0 ± 19.6	121.0 ± 20.4	31.3 ± 14.7

The duration of immobility, swimming, and climbing in WT mice treated with saline, fluoxetine, desipramine, or GBR 12909 expressed as mean ± the standard error of mean.
WT, wild type.
[a]Significant difference from saline-treated mice, Fisher's protected least significant difference.

[$F(2,34) = 6.5$, $P < 0.01$], SERT [$F(2,31) = 3.5$, $P < 0.05$], and NET [$F(2,23) = 3.9$, $P < 0.05$]. In SERT KO mice, however, only homozygous mice exhibited a significant reduction in immobility ($P < 0.05$ Fisher's PLSD), whereas in DAT and NET KO mice both heterozygous and homozygous KO mice had reduced immobility compared with WT mice. The magnitude of the difference between +/+ and −/− mice differed between the knockout strains; the magnitude of the effect of a homozygous knockout was 74% in DAT KO mice, but only 51% in SERT KO and NET KO mice.

Sucrose consumption test

Deletion of the DAT gene increased sucrose consumption at all of the concentrations tested (Fig. 3a). An overall preference for sucrose over water was observed for all subjects [sucrose: $F(1,23) = 16.9$, $P < 0.001$]. DAT −/− mice had greater fluid consumption overall [genotype: $F(2,23) = 6.2$, $P < 0.01$], which was the result of greater consumption of sucrose, but not water at all concentrations tested [genotype × sucrose: $F(2,23) = 6.4$, $P < 0.01$], especially at higher concentrations [genotype × sucrose × concentration: $F(4,46) = 2.8$, $P < 0.05$]. DAT +/− mice were not different from WT mice.

Sucrose consumption was not affected by SERT KO (Fig. 3b) or NET KO (Fig. 3c). Although SERT KO mice showed a trend toward a reduction in sucrose consumption at the middle concentration, neither the main effect of genotype nor the interaction terms were significantly different in the ANOVA.

Locomotor activity

DAT −/− mice were profoundly hyperactive [Table 2; genotype: $F(2,27) = 14.4$, $P < 0.001$, $P < 0.05$ Fisher's PLSD], but there was no difference in activity between DAT +/− and DAT +/+ mice. No significant differences in baseline activity were observed in NET KO or SERT KO mice, although both had strong trends toward reduced locomotion [Table 2; NET: $F(2,26) = 3.2$, $P = 0.06$; SERT: $F(2,27) = 3.1$, $P = 0.06$].

Fig. 2

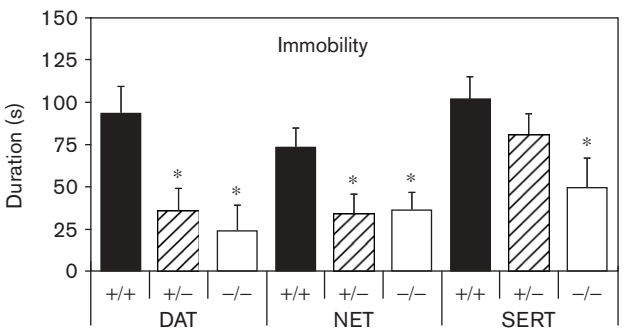

Immobility in the tail suspension test in DAT KO, SERT KO, and NET KO mice. The duration of immobility in DAT KO, SERT KO, and NET KO mice (+/+, +/−, and −/− genotypes for each strain) expressed as mean ± the standard error of mean. *Significant difference from +/+ mice, Fisher's protected least significant difference.

Fig. 3

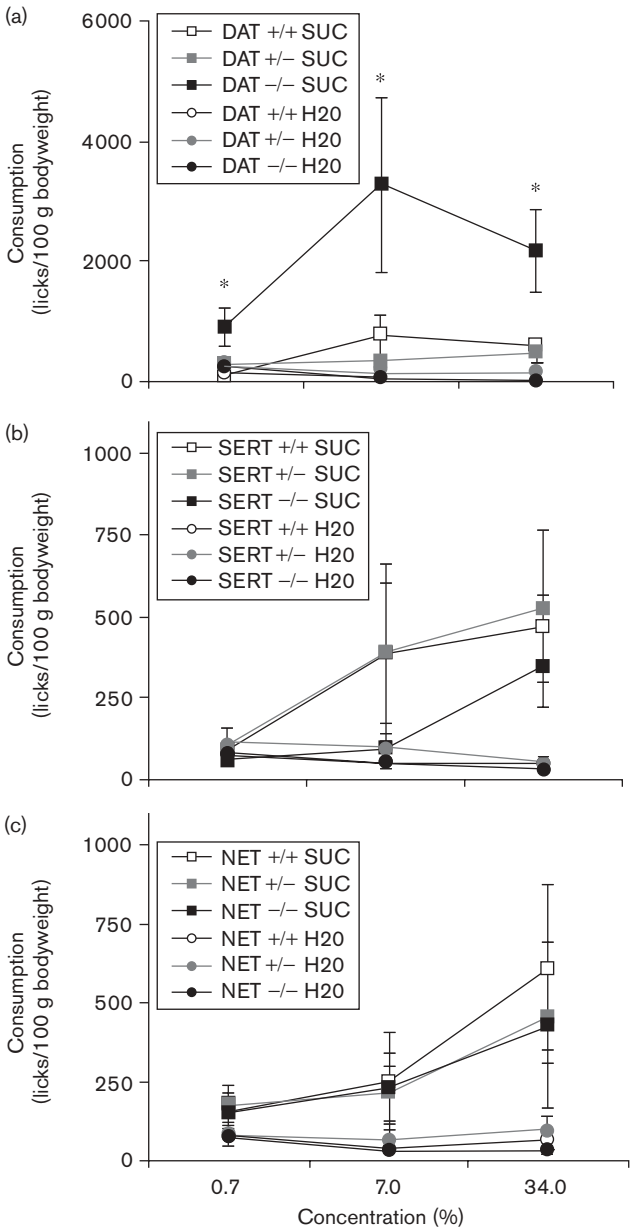

Sucrose consumption in DAT, SERT and NET KO mice. Consumption of sucrose (0.7, 7, and 34%) and water in DAT (a), SERT (b), and NET (c) KO mice (+/+, +/− and −/− genotypes) expressed as average licks per 100 g body weight. The data are expressed as the mean ± the standard error of mean. *Significant difference from +/+ mice, Fisher's protected least significant difference.

Discussion

In this study, deletion of the DAT gene produced changes in behavior in three behavioral tests sensitive to

Table 2 Locomotor activity in DAT, SERT, and NET KO mice

	Genotype		
Knockout	+/+	+/−	−/−
DAT KO	12387 ± 1009	13140 ± 1365	32219 ± 4796[a]
NET KO	8536 ± 1025	6622 ± 825	5108 ± 1015
SERT KO	8273 ± 768	10847 ± 2103	6191 ± 564

Locomotor activity in +/+, +/−, and −/− genotypes of DAT, SERT, and NET KO mice. The data are expressed as the mean ± the standard error of mean.
[a]Significant difference from +/+ mice, Fisher's protected least significant difference.

antidepressant drugs. These effects were quite profound. In the FST and TST, homozygous DAT KO mice spent nearly the entire duration of the test struggling to escape whereas sucrose consumption was greatly enhanced, consistent with increased rewarding effects (e.g. reduced anhedonia). Contrary to what might be supposed, based on naive preconceptions of the relative importance of each of these neurotransmitter systems in depression and the mechanisms of the majority of commonly used antidepressant compounds, although similar effects were observed in NET KO mice in both the FST and TST and in SERT KO mice in the TST, these effects were less pronounced than those observed in DAT KO mice. Such a comparison must, however, be considered in light of potential interactions with genetic background, as discussed below, but suggests at the very least that under some circumstances DAT manipulations can have greater effects on antidepressant-like phenotypes than previously appreciated.

DAT knockout almost completely eliminated immobility in the FST, consistent with an earlier finding (Spielewoy *et al.*, 2000). That report suggested that increased immobility was associated with increased swimming, but those authors did not actually measure any other behavior; in particular, there was no attempt to dissociate general activity (swimming) from specific activity aimed at escaping from the cylinder (climbing). In this experiment both immobility and swimming behavior were almost completely eliminated in DAT KO mice, replaced with persistent and almost continuous climbing (e.g. escape attempts). As DAT KO mice are hyperactive (Giros *et al.*, 1996; Sora *et al.*, 1998), it might be supposed that differences in behavior in the FST between DAT +/+ and DAT −/− mice merely reflects this hyperactivity; indeed, this was the conclusion of the study mentioned earlier (Spielewoy *et al.*, 2000). Those authors interpreted the persistent attempts to escape of DAT KO mice in the FST as 'inappropriate' as opposed to the 'adaptive' strategy of immobility, in accordance with one interpretation of the paradigm (Borsini *et al.*, 1986). This interpretation is not generally accepted [see discussion of this subject in the review by Cryan *et al.* (2005a)]. To some extent the use of a single-exposure forced swim paradigm in the Spielewoy *et al.* (2000) study, compared with a two exposure-forced swim paradigm in this study might lead to different interpretations of the results, the former relating more to acute stress, and the latter to 'behavioral despair'. Of course, the type of paradigm used in this study should be more related to antidepressant actions, which was one of the conclusions of the review mentioned earlier (Cryan *et al.*, 2005a).

Returning to the issue of hyperactivity, several lines of evidence weigh against such a simple explanation of the effects of DAT KO in the FST. Reduced immobility and increased climbing were observed in both homozygous and heterozygous DAT KO mice, yet heterozygous DAT KO mice are not hyperactive (Table 2). Decreased immobility, although to a lesser extent, was also observed in NET KO mice, which are also not hyperactive (Table 2). In addition, decreased immobility in DAT KO mice was also observed in the TST, as was reduced immobility in both SERT KO and NET KO mice, consistent with earlier reports (Holmes *et al.*, 2002; Dziedzicka-Wasylewska *et al.*, 2006), and hyperactivity was not observed in either of those knockout strains.

In any case, the description of DAT KO mice as hyperactive is probably not an accurate depiction of their behavior. This is based upon the placement of DAT KO mice in a novel environment in which exploratory activity would be the dominant initial response tendency. More accurately, DAT KO, like amphetamine treatment (Evenden and Robbins, 1983), may increase the dominant response tendency. According to this view, escape behavior in TST and FST would be enhanced, and the present results would not be the result of hyperactivity *per se*. Behavior in a sucrose consumption test would not be confounded by locomotor hyperactivity in the same way as the other tests; indeed, pronounced locomotor hyperactivity should reduce sucrose consumption by producing a competing behavior. In contrast, DAT KO mice had increased consumption of sucrose when compared with WT mice. Increased sucrose consumption, particularly at low concentrations (e.g. 0.7% as in Fig. 3), has generally been taken to indicate differences in the hedonic properties of sucrose (Papp *et al.*, 1991; El Yacoubi *et al.*, 2003; Wintink *et al.*, 2003; Shumake *et al.*, 2005). This additional evidence further indicates that the effects of DAT KO in the FST and the TST are probably not the result of the confounding effects of hyperactivity. No differences were found in sucrose consumption in SERT or NET KO mice, consistent with the lack of effect of SERT KO in the FST, and somewhat reduced effects of NET KO in both tests.

The meaning of the relative lack of effect of NET KO and SERT KO in the present experiments must be interpreted with caution, however, as substantial strain differences have been reported in the response to antidepressants in both FST and TST (Liu and Gershenfeld, 2001, 2003; David *et al.*, 2003; Ripoll *et al.*,

2003; Dulawa *et al.*, 2004; Lucki and O'Leary, 2004; Crowley *et al.*, 2005). In particular, both C57BL/6 and 129Sv mice do not exhibit antidepressant-like effects in response to fluoxetine in the FST (Lucki *et al.*, 2001; Dulawa *et al.*, 2004), although both strains seem to be responsive to a wide range of SERT, NET, and DAT blockers in the TST (Ripoll *et al.*, 2003; Crowley *et al.*, 2005). In an interesting parallel to the present results, one study found that C57BL/6 mice were unresponsive to NET or SERT blockers in the FST, but did respond to GBR 12909 (David *et al.*, 2003). In the current experiments, mixed C57BL/6-129Sv background WT mice did respond to desipramine in the FST, but not fluoxetine, consistent with findings in C57BL/6 mice (Lucki *et al.*, 2001), so that the effects of SERT KO in the present experiments should be treated with particular caution.

Comparison of pharmacological antagonism of transporters and constituitive gene knockouts should, however, be treated with caution in any case. Results of tests performed on adult KO mice need to be potentially interpreted in light of the effects of absence of the gene during development as well as at the time of testing. In DAT KO mice, in particular, it might be supposed that differences in depressive phenotypes may largely reflect developmental consequences of the deletion. However, there is substantial evidence of the role of dopamine in depression and in depressive phenotypes in animal models of depression (Randrup *et al.*, 1975; Willner, 1983a,b,c, 2000; Dunlop and Nemeroff, 2007), much of it involving acute alterations in dopamine function. In humans the relatively selective DAT blocker, bupropion, and its metabolites, produce clinically effective antidepressant actions (Ascher *et al.*, 1995; Jefferson *et al.*, 2005; Volkow *et al.*, 2005). These findings are supported by numerous studies in animal models. Dopamine is also involved in anhedonia in the sucrose consumption model (Papp *et al.*, 1991), and in the FST dopamine agonists and selective dopamine reuptake blockers have antidepressant-like effects (Cooper *et al.*, 1980; Vaugeois *et al.*, 1996; Hemby *et al.*, 1997; Damaj *et al.*, 2004; Siuciak and Fujiwara, 2004; Basso *et al.*, 2005). In addition to reduced immobility, GBR 12909 selectively increased climbing behavior, but not swimming in the FST (Hemby *et al.*, 1997). Dopamine agonists also enhance the antidepressant-like effects of selective serotonin reuptake inhibitors (Renard *et al.*, 2001). The effects of DAT blockers are not the result of generally enhanced activity, as the effects of bupropion in the FST occur at doses that do not affect spontaneous locomotion (Cooper *et al.*, 1980; David *et al.*, 2003).

The present findings are consistent with earlier findings in DAT, SERT, and NET KO mice, while extending them in several respects. NET KO mice have been reported to have reduced immobility in the FST and TST (Xu *et al.*, 2000; Dziedzicka-Wasylewska *et al.*, 2006), as was observed in this study. The present data are also consistent with some earlier results using SERT KO mice, which were reported to have decreased immobility in the TST, but increased immobility in the FST when bred onto a 129S6 background, but did not display any differences in these tests when bred onto a C57BL/6J background (Holmes *et al.*, 2002). It is interesting to note that in the TST, the mixed background strain from this study had reduced immobility in the TST, similar to SERT KO mice on a 129S6 background in the Holmes *et al.* (2002) study, whereas no effect was observed in the FST, similar to C57BL/6J congenic mice in that study. This suggests somewhat different underlying genetic substrates for the TST and FST, consistent with some of the pharmacological findings in inbred strains discussed above.

In the FST antidepressants that act primarily at the serotonin transporter have been reported to increase swimming, whereas those that act primarily at the norepinephrine transporter have been reported to increase climbing (Detke *et al.*, 1995, 1997; Detke and Lucki, 1996; Page *et al.*, 1999; Cryan *et al.*, 2002, 2003). This was not found in desipramine-treated WT mice in this experiment. Nonetheless, it seems that changes in either type of active behavior and concomitant reductions in immobility may be associated with antidepressant-like effects. However, several models of depression, including those produced by withdrawal from amphetamine, ovarian hormone treatments that simulate pregnancy, and estrogen deficiencies caused by aromatase knockout, increase FST immobility and decrease climbing without affecting swimming (Galea *et al.*, 2001; Cryan *et al.*, 2003; Dalla *et al.*, 2004). These depressive-like effects are mirrored by the opposite, antidepressant-like effects of amphetamine administration, pregnancy, or estradiol: decreased immobility and increased climbing, in the absence of substantial changes in swimming (Galea *et al.*, 2001; Molina-Hernandez and Tellez-Alcantara, 2001; Cryan *et al.*, 2003). The pattern of antidepressant effects in these models is very similar to that observed in DAT KO mice, whereas the effects in models of depression are opposite to those observed in DAT KO mice.

The current results thus support a prominent role for DAT, and dopamine, in the mediation of antidepressant-like behavior, as assessed by the models used here. The striking magnitude of the effects of DAT KO, particularly in comparison with the more modest consequences or lack of consequences of NET or SERT KO, each support reevaluation of the clinically proven effects of DAT blockade on depression, and the role of the DAT gene or differences in DAT gene expression in individual differences in depression and responses to effective antidepressant treatments. The pronounced effects of background strain in both pharmacological and transgenic studies indicate that these very strong DAT effects may

be limited to certain genetic backgrounds, but the data suggest that, under these circumstances, DAT may have more importance than SERT or NET. It remains to be seen whether such profound and prominent effects may be observed for NET or SERT gene knockout when it is expressed on other genetic backgrounds in which SERT and NET blockers have more pronounced effects. Taken together, these data suggest that manipulations of DAT, SERT, and NET genes are highly dependent on genetic background and raise the possibility that this may influence both baseline depressive behavior and response to antidepressants acting selectively at each of these transporters.

Acknowledgements

This research was supported by the Intramural Research Program of the National Institute on Drug Abuse (NIH/DHHS). The authors thank the contract staff of Charles River Laboratories for their expert care of the mice and especially the breeder-geneticist Kriss Knestaut. The authors also thank Joshua Schwarzbaum for his technical assistance in the later stages of these studies.

References

Abercrombie ED, Keller RW Jr, Zigmond MJ (1988). Characterization of hippocampal norepinephrine release as measured by microdialysis perfusion: pharmacological and behavioral studies. *Neuroscience* **27**:897–904.

Akiskal HS, McKinney WT Jr (1973). Depressive disorders: toward a unified hypothesis. *Science* **182**:20–29.

Armario A, Gavalda A, Marti O (1988). Forced swimming test in rats: effect of desipramine administration and the period of exposure to the test on struggling behavior, swimming, immobility and defecation rate. *Eur J Pharmacol* **158**:207–212.

Ascher JA, Cole JO, Colin JN, Feighner JP, Ferris RM, Fibiger HC, *et al.* (1995). Bupropion: a review of its mechanism of antidepressant activity. *J Clin Psychiatry* **56**:395–401.

Basso AM, Gallagher KB, Bratcher NA, Brioni JD, Moreland RB, Hsieh GC, *et al.* (2005). Antidepressant-like effect of D(2/3) receptor-, but not D(4) receptor-activation in the rat forced swim test. *Neuropsychopharmacology* **30**: 1257–1268.

Bengel D, Murphy DL, Andrews AM, Wichems CH, Feltner D, Heils A, *et al.* (1998). Altered brain serotonin homeostasis and locomotor insensitivity to 3, 4-methylenedioxymethamphetamine ('Ecstasy') in serotonin transporter-deficient mice. *Mol Pharmacol* **53**:649–655.

Borsini F, Volterra G, Meli A (1986). Does the behavioral 'despair' test measure 'despair'? *Physiol Behav* **38**:385–386.

Cervo L, Samanin R (1991). Effect of chronic treatment with 8-OH-DPAT in the forced swimming test requires the integrity of presynaptic serotonergic mechanisms. *Psychopharmacology (Berl)* **103**:524–528.

Cooper BR, Hester TJ, Maxwell RA (1980). Behavioral and biochemical effects of the antidepressant bupropion (Wellbutrin): evidence for selective blockade of dopamine uptake in vivo. *J Pharmacol Exp Ther* **215**:127–134.

Crowley JJ, Blendy JA, Lucki I (2005). Strain-dependent antidepressant-like effects of citalopram in the mouse tail suspension test. *Psychopharmacology (Berl)* **183**:257–264.

Cryan JF, Page ME, Lucki I (2002). Noradrenergic lesions differentially alter the antidepressant-like effects of reboxetine in a modified forced swim test. *Eur J Pharmacol* **436**:197–205.

Cryan JF, Hoyer D, Markou A (2003). Withdrawal from chronic amphetamine induces depressive-like behavioral effects in rodents. *Biol Psychiatry* **54**: 49–58.

Cryan JF, Mombereau C, Vassout A (2005a). The tail suspension test as a model for assessing antidepressant activity: review of pharmacological and genetic studies in mice. *Neurosci Biobehav Rev* **29**:571–625.

Cryan JF, Valentino RJ, Lucki I (2005b). Assessing substrates underlying the behavioral effects of antidepressants using the modified rat forced swimming test. *Neurosci Biobehav Rev* **29**:547–569.

Dalla C, Antoniou K, Papadopoulou-Daifoti Z, Balthazart J, Bakker J (2004). Oestrogen-deficient female aromatase knockout (ArKO) mice exhibit depressive-like symptomatology. *Eur J Neurosci* **20**:217–228.

Damaj MI, Carroll FI, Eaton JB, Navarro HA, Blough BE, Mirza S, *et al.* (2004). Enantioselective effects of hydroxy metabolites of bupropion on behavior and on function of monoamine transporters and nicotinic receptors. *Mol Pharmacol* **66**:675–682.

David DJ, Renard CE, Jolliet P, Hascoet M, Bourin M (2003). Antidepressant-like effects in various mice strains in the forced swimming test. *Psychopharmacology (Berl)* **166**:373–382.

Detke MJ, Lucki I (1996). Detection of serotonergic and noradrenergic antidepressants in the rat forced swimming test: the effects of water depth. *Behav Brain Res* **73**:43–46.

Detke MJ, Rickels M, Lucki I (1995). Active behaviors in the rat forced swimming test differentially produced by serotonergic and noradrenergic antidepressants. *Psychopharmacology (Berl)* **121**:66–72.

Detke MJ, Johnson J, Lucki I (1997). Acute and chronic antidepressant drug treatment in the rat forced swimming test model of depression. *Exp Clin Psychopharmacol* **5**:107–112.

Dulawa SC, Holick KA, Gundersen B, Hen R (2004). Effects of chronic fluoxetine in animal models of anxiety and depression. *Neuropsychopharmacology* **29**:1321–1330.

Dunlop BW, Nemeroff CB (2007). The role of dopamine in the pathophysiology of depression. *Arch Gen Psychiatr* **64**:327–337.

Dziedzicka-Wasylewska M, Faron-Gorecka A, Kusmider M, Drozdowska E, Rogoz Z, Siwanowicz J, *et al.* (2006). Effect of antidepressant drugs in mice lacking the norepinephrine transporter. *Neuropsychopharmacology* **31**:2424–2432.

El Yacoubi M, Bouali S, Popa D, Naudon L, Leroux-Nicollet I, Hamon M, *et al.* (2003). Behavioral, neurochemical, and electrophysiological characterization of a genetic mouse model of depression. *Proc Natl Acad Sci U S A* **100**:6227–6232.

Evenden JL, Robbins TW (1983). Increased response switching, perseveration and perseverative switching following d-amphetamine in the rat. *Psychopharmacology (Berl)* **80**:67–73.

Gainetdinov RR, Jones SR, Fumagalli F, Wightman RM, Caron MG (1998). Re-evaluation of the role of the dopamine transporter in dopamine system homeostasis. *Brain Res Brain Res Rev* **26**:148–153.

Galea LA, Wide JK, Barr AM (2001). Estradiol alleviates depressive-like symptoms in a novel animal model of post-partum depression. *Behav Brain Res* **122**:1–9.

Giros B, Jaber M, Jones SR, Wightman RM, Caron MG (1996). Hyperlocomotion and indifference to cocaine and amphetamine in mice lacking the dopamine transporter. *Nature* **379**:606–612.

Hall FS, Huang S, Fong GF, Pert A (1998a). The effects of social isolation on the forced swim test in Fawn hooded and Wistar rats. *J Neurosci Methods* **79**:47–51.

Hall FS, Huang S, Fong GW, Pert A, Linnoila M (1998b). Effects of isolation-rearing on locomotion, anxiety and responses to ethanol in Fawn Hooded and Wistar rats. *Psychopharmacology (Berl)* **139**:203–209.

Hall FS, Li XF, Sora I, Xu F, Caron M, Lesch KP, *et al.* (2002). Cocaine mechanisms: enhanced cocaine, fluoxetine and nisoxetine place preferences following monoamine transporter deletions. *Neuroscience* **115**:153–161.

Hemby SE, Lucki I, Gatto G, Singh A, Thornley C, Matasi J, *et al.* (1997). Potential antidepressant effects of novel tropane compounds, selective for serotonin or dopamine transporters. *J Pharmacol Exp Ther* **282**:727–733.

Holmes A, Yang RJ, Murphy DL, Crawley JN (2002). Evaluation of antidepressant-related behavioral responses in mice lacking the serotonin transporter. *Neuropsychopharmacology* **27**:914–923.

Jefferson JW, Pradko JF, Muir KT (2005). Bupropion for major depressive disorder: pharmacokinetic and formulation considerations. *Clin Ther* **27**:1685–1695.

Kreiss DS, Lucki I (1995). Effects of acute and repeated administration of antidepressant drugs on extracellular levels of 5-hydroxytryptamine measured in vivo. *J Pharmacol Exp Ther* **274**:866–876.

Liu X, Gershenfeld HK (2001). Genetic differences in the tail-suspension test and its relationship to imipramine response among 11 inbred strains of mice. *Biol Psychiatry* **49**:575–581.

Liu X, Gershenfeld HK (2003). An exploratory factor analysis of the Tail Suspension Test in 12 inbred strains of mice and an F2 intercross. *Brain Res Bull* **60**:223–231.

Lucki I, O'Leary OF (2004). Distinguishing roles for norepinephrine and serotonin in the behavioral effects of antidepressant drugs. *J Clin Psychiatry* **65** (**Suppl 4**):11–24.

Lucki I, Dalvi A, Mayorga AJ (2001). Sensitivity to the effects of pharmacologically selective antidepressants in different strains of mice. *Psychopharmacology (Berl)* **155**:315–322.

Mathews TA, Fedele DE, Coppelli FM, Avila AM, Murphy DL, Andrews AM (2004). Gene dose-dependent alterations in extraneuronal serotonin but not dopamine in mice with reduced serotonin transporter expression. *J Neurosci Methods* **140**:169–181.

Molina-Hernandez M, Tellez-Alcantara NP (2001). Antidepressant-like actions of pregnancy, and progesterone in Wistar rats forced to swim. *Psychoneuroendocrinology* **26**:479–491.

Nomikos GG, Damsma G, Wenkstern D, Fibiger HC (1990). In vivo characterization of locally applied dopamine uptake inhibitors by striatal microdialysis. *Synapse* **6**:106–112.

Page ME, Detke MJ, Dalvi A, Kirby LG, Lucki I (1999). Serotonergic mediation of the effects of fluoxetine, but not desipramine, in the rat forced swimming test. *Psychopharmacology (Berl)* **147**:162–167.

Papp M, Willner P, Muscat R (1991). An animal model of anhedonia: attenuation of sucrose consumption and place preference conditioning by chronic unpredictable mild stress. *Psychopharmacology (Berl)* **104**: 255–259.

Porsolt RD (1979). Animal model of depression. *Biomedicine* **30**:139–140.

Porsolt RD, Le Pichon M, Jalfre M (1977). Depression: a new animal model sensitive to antidepressant treatments. *Nature* **266**:730–732.

Prange AJ Jr (1964). The pharmacology and biochemistry of depression. *Dis Nerv Syst* **25**:217–221.

Randrup A, Munkvad I, Fog R, Gerlach J, Molander L, Kjellberg B, Scheel-Kruger J (1975). Mania, Depression and brain dopamine. In: Essman WB, Vazelli L, editors. *Current developments in pyschpharmacology*. **Vol. 2**. New York: Spectrum. pp. 206–248.

Renard CE, Fiocco AJ, Clenet F, Hascoet M, Bourin M (2001). Is dopamine implicated in the antidepressant-like effects of selective serotonin reuptake inhibitors in the mouse forced swimming test? *Psychopharmacology (Berl)* **159**:42–50.

Ripoll N, David DJ, Dailly E, Hascoet M, Bourin M (2003). Antidepressant-like effects in various mice strains in the tail suspension test. *Behav Brain Res* **143**:193–200.

Schildkraut JJ (1967). The catecholamine hypothesis of affective disorders. A review of supporting evidence. *Int J Psychiatry* **4**:203–217.

Shelton RC (2004). The dual-action hypothesis: does pharmacology matter? *J Clin Psychiatry* **65** (**Suppl 17**):5–10.

Shen HW, Hagino Y, Kobayashi H, Shinohara-Tanaka K, Ikeda K, *et al.* (2004). Regional differences in extracellular dopamine and serotonin assessed by in vivo microdialysis in mice lacking dopamine and/or serotonin transporters. *Neuropsychopharmacology* **29**:1790–1799.

Shumake J, Barrett D, Gonzalez-Lima F (2005). Behavioral characteristics of rats predisposed to learned helplessness: reduced reward sensitivity, increased novelty seeking, and persistent fear memories. *Behav Brain Res* **164**:222–230.

Siuciak JA, Fujiwara RA (2004). The activity of pramipexole in the mouse forced swim test is mediated by D2 rather than D3 receptors. *Psychopharmacology (Berl)* **175**:163–169.

Skolnick P, Popik P, Janowsky A, Beer B, Lippa AS (2003). 'Broad spectrum' antidepressants: is more better for the treatment of depression? *Life Sci* **73**:3175–3179.

Sora I, Wichems C, Takahashi N, Li XF, Zeng Z, Revay R, *et al.* (1998). Cocaine reward models: conditioned place preference can be established in dopamine- and in serotonin-transporter knockout mice. *Proc Natl Acad Sci U S A* **95**:7699–7704.

Sora I, Hall FS, Andrews AM, Itokawa M, Li XF, Wei HB, *et al.* (2001). Molecular mechanisms of cocaine reward: combined dopamine and serotonin transporter knockouts eliminate cocaine place preference. *Proc Natl Acad Sci U S A* **98**:5300–5305.

Spielewoy C, Roubert C, Hamon M, Nosten-Bertrand M, Betancur C, Giros B (2000). Behavioural disturbances associated with hyperdopaminergia in dopamine-transporter knockout mice. *Behav Pharmacol* **11**:279–290.

van Praag HM (1974). Toward a biochemical classification of depression. *Adv Biochem Psychopharmacol* **11**:357–368.

Vaugeois JM, Pouhe D, Zuccaro F, Costentin J (1996). Indirect dopamine agonists effects on despair test: dissociation from hyperactivity. *Pharmacol Biochem Behav* **54**:235–239.

Volkow ND, Wang GJ, Fowler JS, Learned-Coughlin S, Yang J, Logan J, *et al.* (2005). The slow and long-lasting blockade of dopamine transporters in human brain induced by the new antidepressant drug radafaxine predict poor reinforcing effects. *Biol Psychiatry* **57**:640–646.

Wang YM, Xu F, Gainetdinov RR, Caron MG (1999). Genetic approaches to studying norepinephrine function: knockout of the mouse norepinephrine transporter gene. *Biol Psychiatry* **46**:1124–1130.

Willner P (1983a). Dopamine and depression: a review of recent evidence. I. Empirical studies. *Brain Res* **287**:211–224.

Willner P (1983b). Dopamine and depression: a review of recent evidence. II. Theoretical approaches. *Brain Res* **287**:225–236.

Willner P (1983c). Dopamine and depression: a review of recent evidence. III. The effects of antidepressant treatments. *Brain Res* **287**:237–246.

Willner P (2000). Dopaminergic mechanisms in depression and mania. In: Watson, editor Psychopharmacology: The Fourth Generation of Progress, On-Line edition, Lippincott Williams & Wilkins: New York. http://www.acnp.org/citations/GN401000093.

Wintink AJ, Young NA, Davis AC, Gregus A, Kalynchuk LE (2003). Kindling-induced emotional behavior in male and female rats. *Behav Neurosci* **117**:632–640.

Xu F, Gainetdinov RR, Wetsel WC, Jones SR, Bohn LM, Miller GW, *et al.* (2000). Mice lacking the norepinephrine transporter are supersensitive to psychostimulants. *Nat Neurosci* **3**:465–471.

ORIGINAL ARTICLE

Genome-Wide Association for Methamphetamine Dependence

Convergent Results From 2 Samples

George R. Uhl, MD, PhD; Tomas Drgon, PhD; Qing-Rong Liu, PhD; Catherine Johnson, MSc; Donna Walther, MSc; Tokutaro Komiyama, MD; Mutsuo Harano, MD; Yoshimoto Sekine, MD, PhD; Toshiya Inada, MD; Norio Ozaki, MD, PhD; Masaomi Iyo, MD, PhD; Nakao Iwata, MD, PhD; Mitsuhiko Yamada, MD; Ichiro Sora, MD, PhD; Chih-Ken Chen, MD, PhD; Hsing-Cheng Liu, MD, PhD; Hiroshi Ujike; Shih-Ku Lin, MD

Context: We can improve understanding of human methamphetamine dependence, and possibly our abilities to prevent and treat this devastating disorder, by identifying genes whose allelic variants predispose to methamphetamine dependence.

Objective: To find "methamphetamine dependence" genes identified by each of 2 genome-wide association (GWA) studies of independent samples of methamphetamine-dependent individuals and matched controls.

Design: Replicated GWA results in each of 2 case-control studies.

Setting: Japan and Taiwan.

Participants: Individuals with methamphetamine dependence and matched control subjects free from psychiatric, substance abuse, or substance dependence diagnoses (N=580).

Main Outcome Measures: "Methamphetamine dependence" genes that were reproducibly identified by clusters of nominally positive single-nucleotide polymorphisms (SNPs) in both samples in ways that were unlikely to represent chance observations, based on Monte Carlo simulations that corrected for multiple comparisons, and subsets of "methamphetamine dependence" genes that were also identified by GWA studies of dependence on other addictive substances, success in quitting smoking, and memory.

Results: Genes identified by clustered nominally positive SNPs from both samples were unlikely to represent chance observations (Monte Carlo $P<.00001$). Variants in these "methamphetamine dependence" genes are likely to alter cell adhesion, enzymatic functions, transcription, cell structure, and DNA, RNA, and/or protein handling or modification. Cell adhesion genes *CSMD1* and *CDH13* displayed the largest numbers of clustered nominally positive SNPs. "Methamphetamine dependence" genes overlapped, to extents much greater than chance, with genes identified in GWA studies of dependence on other addictive substances, success in quitting smoking, and memory (Monte Carlo P range $<.04$ to $<.00001$).

Conclusion: These data support polygenic contributions to methamphetamine dependence from genes that include those whose variants contribute to dependence on several addictive substances, success in quitting smoking, and mnemonic processes.

Arch Gen Psychiatry. 2008;65(3):345-355

METHAMPHETAMINE abuse is a growing problem in many regions of the United States and a long-standing concern in Taiwan and Japan. Elucidating which genetic variants enhance individuals' vulnerability should increase our understanding of methamphetamine dependence.

Recent reviews suggest that addictive substance dependence is likely to display a polygenic genetic architecture.[1-3] Psychostimulant dependence displays strong familial and genetic influences in family and twin studies.[4-18] Individual differences in vulnerability to methamphetamine are thus likely to display substantial genetic determinants. Since much of the genetic vulnerability to stimulant abuse overlaps with the genetics of vulnerability to other classes of addictive substances, it is likely that methamphetamine dependence displays such genetic overlaps as well.[13-16,19] However, there is no evidence that any single gene's variants mediate a large portion of vulnerability to psychostimulant dependence.

Identifying the genes that harbor allelic variants that contribute to human individual differences in vulnerabilities to methamphetamine dependence will help us to understand processes that underlie human addictions. We may improve understanding of the relative contributions of variants in the brain systems that underlie

Author Affiliations are listed at the end of this article.

reward vs mnemonic components of addictions, for example.[20] Increasing our ability to determine which constellation of genetic and environmental factors plays a role in the methamphetamine dependence of each affected individual should improve "personalized" targeting of treatment and prevention efforts to those most likely to benefit from them.

Genome-wide association (GWA) can help to elucidate chromosomal regions and genes that contain allelic variants that predispose to substance abuse. This approach does not require family member participation. It gains power as densities of genomic markers increase.[21-24] Association identifies smaller chromosomal regions than linkage-based approaches. Genome-wide association fosters pooling strategies that preserve confidentiality and reduce costs, including those that we have previously validated.[25-28] This approach provides ample genomic controls that can minimize the chances of unintended ethnic mismatches between disease and control samples (eg, stratification). The large numbers of assessments that are key components of GWA do mandate careful use of statistical approaches that correct for multiple comparisons and studies in multiple independent samples, such as those that we now report.

We thus now describe GWA in 2 samples of methamphetamine-dependent and control individuals. These studies test the a priori hypothesis that marker allele frequency differences between methamphetamine-dependent and control individuals will help us to identify genes whose alleles predispose to development of dependence on methamphetamine. Sample 1 contrasts (1) Han Chinese methamphetamine-dependent individuals from the Taipei region of Taiwan with (2) age- and sex-matched Han Chinese Taiwanese control individuals free from any histories of abuse or dependence on any legal or illegal addictive substance. Sample 2 contrasts (1) Japanese methamphetamine-dependent individuals with (2) age- and sex-matched Japanese control individuals free from any histories of abuse or dependence on any legal or illegal addictive substance. We used standard statistical approaches to document the power that these samples provided to identify genetic influences of different magnitudes. We identified striking convergence of the data from sample 1 and sample 2, in ways that are never attained by chance in many Monte Carlo simulation trials. We discuss the convergence that these data provide with recently reported GWA studies of related phenotypes that include polysubstance abuse, nicotine dependence, alcohol dependence, success in quitting smoking, and individual differences in memory. To our knowledge, these results provide the first replicated GWA study that identifies "methamphetamine dependence" genes.

METHODS

RESEARCH VOLUNTEERS

Sample 1

Subjects recruited in Taipei provided informed consent for genetic studies under protocols approved by ethics committees at the respective institutions; 30% were female and the mean (SD) age was 32.5 (10) years. One hundred forty individuals were diagnosed independently by each of 2 psychiatrists based on interviews, review of records, and Chinese versions of the Diagnostic Interview for Genetic Studies[29] and the Family Interview for Genetic Studies[30] using *DSM-IV* criteria.[31] These individuals were of ethnic Han Chinese origin and older than 17 years, reported methamphetamine use more than 20 times per year (unless they described well-documented methamphetamine psychosis), and denied histories of psychosis either prior to methamphetamine use or in relation to other psychedelic drugs. Most reported use of at least 1 other addictive substance. Two hundred forty Han Chinese controls, who were matched for sex and age, were older than 17 years, and denied either illegal drug use or psychotic symptoms to psychiatric interviewers, were recruited in Taipei from hospital and pharmacy staffs, blood donation centers, and an electric company.

Sample 2

Subjects who were born and resided in the northern Kyushu, Setouchi, Chiba, Tokai, or Kanto regions of Japan provided informed consent for genetic studies under protocols approved by ethics committees at the respective institutions. Twenty-one percent of subjects were female and the mean (SD) age was 39.9 (13) years. One hundred methamphetamine-dependent subjects were inpatients or outpatients of psychiatric hospitals in these regions that participate in the Japanese Genetics Initiative for Drug Abuse[32-45] and met *International Statistical Classification of Diseases, 10th Revision, Diagnostic Criteria for Research*[46] criteria F15.2 and F15.5 for methamphetamine dependence in independent diagnoses made by each of 2 trained psychiatrists based on interviews and review of records. Ninety-one percent revealed histories of methamphetamine psychosis, 89% used methamphetamine intravenously, 62% also abused organic solvents, and most abused at least 1 other substance. Subjects who displayed clinical diagnoses of schizophrenia, other psychotic disorders, or organic mental syndromes were excluded. Controls were 100 age-, sex-, and geographically matched staff recruited at the same institutions, who denied use of any illegal substance, abuse or dependence on any legal substance, any psychotic psychiatric illness, or any family history of substance dependence or psychotic psychiatric illness during interviews with trained psychiatrists.

DNA PREPARATION AND ASSESSMENT OF ALLELE FREQUENCIES

Genomic DNA was prepared from blood,[28,32,47,48] quantitated,[28,32] and combined into pools representing 20 individuals of the same ethnicity and phenotype. Relative allele frequencies were assessed using Affymetrix (Santa Clara, California) microarrays.

Hybridization probes were prepared from the genomic DNA pools (as described in the Affymetrix GeneChip Mapping Assay manual), with precautions to avoid contamination that included dedicated preparation rooms and hoods. Briefly, 50 ng of pooled genomic DNA was digested by *Xba*I or *Hind*III (100K) or by *Sty*I or *Nsp*I (500K), ligated to appropriate adaptors, and amplified using a GeneAmp PCR System 9700 (Applied Biosystems, Foster City, California) with a 3-minute 94°C hot start; 30 cycles of 30 seconds at 94°C, 45 seconds at 60°C, and 60 seconds at 68°C (100K) or 15 seconds at 68°C (500K); and a final 7-minute 68°C extension. Polymerase chain reaction (PCR) products were purified (MinElute 96 UF kits; Qiagen, Valencia, California) and quantitated. Forty micrograms of PCR product were digested for 35 minutes at 37°C with 0.04-unit/μL deoxyribonuclease I to produce 30– to 100–base pair fragments, which were end-labeled using terminal deoxynucleotidyl trans-

ferase and biotinylated dideoxynucleotides and hybridized to the appropriate 100K (*Xba*I or *Hind*III arrays) or 500K (*Sty*I or *Nsp*I arrays) array (early-access Centurion and commercial Mendel array sets; Affymetrix). Arrays were stained and washed as described in the Affymetrix GeneChip Mapping Assay manual using immunopure strepavidin (Pierce, Milwaukee, Wisconsin), biotinylated antistreptavidin antibody (Vector Labs, Burlingame, California), and R-phycoerythrin strepavidin (Molecular Probes, Eugene, Oregon). Arrays were scanned and fluorescence intensities were quantitated using an Affymetrix array scanner, as described previously.[28] Estimates for "genomic coverage" for these marker densities were almost 0.8 (sample 1) and almost 0.9 (sample 2).[49]

Chromosomal positions for each single-nucleotide polymorphism (SNP) were sought using NCBI (build 36.1; National Center for Biotechnology Information, Bethesda, Maryland) and NetAffyx (Affymetrix) data. Allele frequencies for each SNP in each DNA pool were assessed based on hybridization intensity signals from 4 arrays, allowing assessment of hybridization to the 20 (100K arrays) or 12 (500K arrays) "perfect match" cells on each array that were complementary to the PCR products from alleles "A" and "B" for each diallelic SNP on sense and antisense strands. We eliminated (1) SNPs with minor allele frequencies less than 0.02 determined using Affymetrix data; (2) SNPs on sex chromosomes; and (3) SNPs whose chromosomal positions could not be adequately determined. We thus analyzed data from the remaining 371 820 and 466 883 SNPs (for sample 1 and sample 2, respectively) in detail. Each array was analyzed, as described previously,[28] subtracting background values, normalizing to the highest values noted on the array, averaging the hybridization intensities from the array cells that corresponded to the perfect match "A" and "B" cells, calculating "A/B ratios" by dividing average normalized A values by average normalized B values, performing arctangent transformations to aid combination of data from arrays hybridized and scanned on different days, and determining the average arctan value for each SNP from the 4 replicate arrays. This approach is thus based on hybridization intensity data from Affymetrix scanners rather than relative allele score (RAS) or k corrections derived from RAS scores.[50,51]

The analyses presented in this work use standard methods for correcting hybridization values for each perfect match feature based on chip-to-chip differences in background fluorescence and in total fluorescence intensity. These approaches have generated good, approximately 0.95, correlations between individually genotyped and pooled-genotype values in extensive validation experiments.[32,52] Other approaches to analysis of pooling-based GWA studies have focused on the RAS measurements that derive from Affymetrix software to generate k correction scores for each SNP that attempt to correct for probe × probe variation (ie, that induced by, or consistent with, differential hybridization effects).[50,51] In studies that have used these corrections, correlations between individually and pooled genotyped SNP allelic frequencies can equal or exceed those that we have observed in validation experiments.[53,54] However, RAS scores have been used less and less as the genotype-calling algorithms for successive generations of Affymetrix arrays have improved their accuracy. Initial RAS scores are based in part on data from mismatch cells, which have again been eliminated from successive generations of Affymetrix arrays because of their inconsistent effects on accuracy. The k corrections based on RAS scores that are generated in different laboratories produce differing results.[55] Further, we have found that substantial numbers of the array features that provide information for the RAS scores are saturated under conditions used to conduct individual genotyping (Q-R.L., D.W., and G.R.U., unpublished data, 2005), leading us to use smaller amounts of input DNA and hybridization probes for the pooled assays reported herein. The k corrections may prove to be useful for experiments in which saturation is controlled carefully and where data from heterozygote control individuals are generated in the same experiments and in the same laboratories as the pooling data. However, in the present analysis, this adds to the variation that we already parse as quantified by replicate pools (ie, biological haplotype replication), applications of different chips to the same pool (ie, chip-oriented technical replication), and different samples altogether (ie, overall association replication).

ANALYSES

We compared data for all the pools from methamphetamine-dependent individuals with all of the pools from control individuals separately for sample 1 and sample 2, as previously described.[28] A *t* statistic for the differences between abusers and controls was generated, as described previously,[28] for each SNP for each sample. For each sample, we focused on "nominally positive" SNPs that displayed *t* statistics with $P < .05$ for abuser-control differences. We first sought evidence for clustering of the nominally positive SNPs from each sample. We focused on chromosomal regions in which at least 3 of these nominally positive SNPs, assessed by at least 2 different array types, lay within 25 kilobases (kb) of each other. We term these clustered nominally positive SNPs *clustered positive SNPs* and focus our analyses on regions in which they lie. The degree of clustering within each single sample provides a technical control (eg, assurance that there are haplotypes that occur at different frequencies in dependent vs control samples) that could result from stochastic differences in haplotypes as well as differences related to the methamphetamine-dependence phenotype.

To seek the SNPs within the strongest positive support from both data sets, we sought convergence between data from sample 1 and sample 2 (**Table**).[56] Analyses focused on genes identified by clustered positive results from both samples, rather than on individual SNPs whose informativeness might differ between samples 1 and 2. Clustering of positive results in the same gene in each of 2 independent samples is unlikely to represent purely stochastic effects for most genes and is thus likely to reflect differences related to dependence on methamphetamine (and/or to dependence on addictive substances in general).

Monte Carlo simulation trials assessed the significance of the results in ways that correct for the number of repeated comparisons made herein, as described previously.[28] These empirical statistical approaches do not require assumptions about the underlying distribution of the data sets, as do statistical approaches such as analysis of variance, and allow correction for the hundreds of thousands of repeated comparisons in ways that would provide difficulties for repeated analyses of variance. For each trial, a randomly selected set of SNPs from the current data set was assessed to see if it provided results equal to or greater than the results that we actually observed (eg, to see how frequently randomly selected sets of 15 565 SNPs from sample 1 and 25 538 SNPs from sample 2 contained nominally positive SNPs that lie clustered within 25 kb of each other on the chromosomes, see "Results" section). The number of trials for which the randomly selected SNPs displayed the same features of observed results was then tallied to generate an empirical *P* value. These simulations thus corrected for the number of repeated comparisons made in these analyses, an important consideration in evaluating this large association genome scanning data set. We used a similar approach to assess the likelihood that the convergences between the current data and data obtained from other samples might occur by chance.

To seek possible generalization of these results, we sought locations where the clustered positive data from both sample 1 and sample 2 lie at chromosomal positions near clustered positive results from studies that compared allelic frequencies in

Table. Selected "Methamphetamine Dependence" Genes Identified by Clustered Positive Results From Both Sample 1 and Sample 2[a]

Gene	Class	Description	SNPs[b]	*P* Value[c]
SGCZ	CAM	Sarcoglycan, zeta	3, 20	<.00001
DAF/CD55	ENZ	Decay-accelerating factor for complement system	1, 4	<.00001
ACSL6	ENZ	Acyl-CoA synthetase long-chain family member 6	9, 5	<.00001
FKBP15	ENZ	FKBP15	4, 4	<.00001
PDE6C	ENZ	cGMP phosphodiesterase 6C α′	4, 7	<.00001
POU5F1	TF	POU-domain 5 transcription factor 1	1, 5	<.00001
SH3MD4	PROT	SH3 multiple domains 4	9, 7	<.00001
RALY	RNA	Autoantigenic RNA binding protein	5, 3	<.00001
PRKG1	ENZ	cGMP-dependent protein kinase I	14, 5	.00001
LARGE	ENZ	Like-glycosyltransferase	11, 3	.00001
PCOLCE2	STR	Procollagen C endopeptidase enhancer 2	3, 2	.00001
MOSC2	ENZ	MOCO sulphurase C-terminal domain containing 2	4, 5	.00002
ZNF423	TF	Zinc finger protein 423	5, 4	.00002
MAP2K5	ENZ	Mitogen-activated protein kinase kinase 5	5, 3	.00003
USP48	PROT	Ubiquitin-specific peptidase 48	3, 2	.00003
SMYD3	TF	SET MYND domain containing 3	7, 5	.00007
CCHCR1	REC	Coiled-coil α-helical rod protein 1	2, 4	.00009
LRRN6C	CAM	Leucine-rich repeat neuronal 6C	4, 13	.00010
CENPC2	STR	Centromere protein C2	2, 3	.00012
RAPGEF5	REC	Rap guanine nucleotide exchange factor 5	4, 1	.00016
SERPINA5	ENZ	Serpin peptidase inhibitor A 5	4, 1	.00018
PRDM2	TF	PR domain containing 2 with ZNF domain	6, 3	.00022
ASTN2	CAM	Astrotactin 2	12, 3	.00037
TM7SF4	PROT	Transmembrane 7 superfamily member 4	2, 3	.00037
TRPM3	CHAN	Transient receptor potential cation channel, subfamily M, member 3	4, 10	.00039
RGS17	ENZ	Regulator of G-protein signaling 17	4, 3	.00047
COL28A1	STR	Collagen, type XXVIII, alpha 1	4, 3	.00047
MOSC1	ENZ	MOCO sulphurase C-terminal domain containing 1	5, 1	.00048
PDE4B	ENZ	Phosphodiesterase 4B	8, 4	.00049
AOAH	ENZ	Acyloxyacyl hydrolase	3, 4	.00049
PDE4D	ENZ	Phosphodiesterase 4D	6, 6	.00057
ZNF659	TF	Zinc finger protein 659	6, 9	.00060
NRG1	CAM	Neuregulin 1	5, 3	.00064
HS3ST4	ENZ	Heparan sulfate (glucosamine) 3-O-sulfotransferase 4	3, 7	.00064
MYO5B	STR	Myosin 5B	4, 11	.00065
PSD3	REC	Pleckstrin and sec7 domain containing 3	3, 15	.00078
AK5	ENZ	Adenylate kinase 5	6, 3	.00080
CUBN	REC	Cubilin	6, 6	.00085
FHIT	ENZ	Fragile histidine triad gene	8, 20	.00088

Abbreviations: Acyl-CoA, acyl coenzyme A; CAM, cell adhesion molecule; cGMP, cyclic guanine monophosphate; CHA, channels; DIS, disease associated; ENZ, enzymes; PROT, protein processing; REC, receptors (combining single TM, 7 TM, and ligand-gated channel families); RNA/DNA, RNA/DNA handling or modification; SNP, single-nucleotide polymorphism; STR, structural proteins; TF, transcriptional regulation; TRANSP, transporter.

[a] Each gene listed here contains at least 5 clustered positive SNPs with $P < .05$ from sample 1 and/or sample 2, has a function that can be inferred, and displays a Monte Carlo *P* value <.001. Genes are grouped by the class of the function to which they appear to contribute: CAM, ENZ, STR, TF, PROT, REC, RNA/DNA, TRANSP, CHA, and DIS. The Monte Carlo *P* value represents probabilities of chance discovery of clustered nominally positive SNPs in segments of randomly selected genes that sum to the same size as the true gene identified in the present work. Genes listed in this Table are selected because their Monte Carlo *P* values are <.001 and/or because they are identified in other samples in ways that are discussed in the text (see eTable [available at http://www.archgenpsychiatry.com] for full table, in which correction for 109 repeated comparisons would require $P < .0004$ for significance).

[b] Numbers of clustered nominally positive SNPs from samples 1 and 2 that lie within the gene's exons or 10-kilobase flanks.

[c] Monte Carlo *P* value for the number of nominally significant SNPs lying within a gene region of the same size.

polysubstance abusers vs controls,[32] alcohol-dependent individuals vs controls,[57] nicotine-dependent individuals vs nondependent smokers,[58] individuals successful in quitting smoking vs those unsuccessful,[59] and individuals with better or poorer scores in memory testing[55] (Table).

To provide controls for the alternative possibilities that the results obtained herein could come from (1) occult racial/ethnic stratification or (2) assay noise, we compared the clustered positive SNPs from sample 1 and from sample 2 with SNPs that displayed the largest allele frequency differences between (1) European American vs African American control individuals, as previously described[32]; (2) HapMap Japanese (JPT) and Han Chinese (HCB) samples; and (3) SNPs that displayed the largest variances from array to array, as previously described.[32]

To assess the statistical power of our analysis, we used the program PS version 2.1.31[60] with (1) $\alpha = .05$, (2) sample sizes equal to the numbers of pools from the current data set, (3) mean abuser-control differences of 0.05 and 0.1, and (4) standard deviations from the SNPs that provided the largest differences between control and abuser population means from the current data set. We also present data from the Genetic Power Calculator.

Power Calculations

There is no single standard for calculation of the power of GWA; we have thus presented calculations based on allele frequency differences in the body of this article. An alternative approach,

the Genetic Power Calculator, assumes substantial additional information about the genetic architecture and marker frequencies for the disorder being studied and is adapted to use with allele frequency information from individual genotyping. Using a reasonable set of assumptions about the genetic architecture and linkage disequilibrium between markers and disease alleles, we obtained powers of 0.63 and 0.4 for samples 1 and 2 from this approach.[61]

Alternative Means for Analyzing GWA Data

The experiments presented herein compare (1) disease/nondisease pools (a group factor); (2) multiple case and control pools (a within–disease group factor); (3) for each pool, multiple chip assays (a within-pool factor); and (4) sample 1 vs sample 2 results. While there is no single consensus for how to treat issues raised by so many multiple comparisons, there is also no reason to assume that there is such underlying normality of the data that parametric tests, or tests that make assumptions about underlying distributions of the data (eg, analysis of variance), should be used. Monte Carlo approaches used herein provide empirical statistical values that are based on the data sets that are actually generated in these experiments and provide tests for most of the hypotheses. In previous work, these results have correlated reasonably well with those from permutation and false discovery rate tests.[32]

Use of Detailed Linkage Disequilibrium Data From HapMap Samples as a Proxy for the Detailed Linkage Disequilibrium for the Present Samples

While general patterns of linkage disequilibrium are readily inferred from HapMap data, the detailed patterns of linkage disequilibrium from a number of samples that we have previously investigated have differed, often significantly, from those in HapMap samples. Use of HapMap data as a primary basis for calculation of linkage disequilibrium in the present samples complicates the Monte Carlo simulation paradigms that we used. We have thus used chromosomal distances as a primary metric in ways that allow crisp Monte Carlo simulations for the SNPs that are well localized and eliminated data from SNPs that are not well localized.

RESULTS

A number of features of the genotyping data support the validity of the approach used herein.[32] From sample 1, 371 820 SNPs (of 489 922 on 2 array types) and, from sample 2, 466 614 SNPs (of 609 431 on 4 array types) lie on chromosomes 1 to 22 and displayed minor allele frequencies of 0.02 or less. In the data from samples 1 and 2, 368 811 SNPs overlapped. Pooled genotyping for these SNPs displays features that support modest variability. Mean SEMs for the differences among the 4 replicate measurements of each DNA pool were ±0.040 and 0.038 for samples 1 and 2. The SEMs for pool-to-pool differences were ±0.025 and 0.029. Power calculations that used the observed variability from these samples, $\alpha = .05$, and the observed within-group standard deviations document 0.92 and 1 and 0.7 and 0.99 power to detect 5% and 10% differences in mean abuser vs control allele frequencies in samples 1 and 2, respectively.

A number of SNPs displayed nominally significant allele frequency differences between methamphetamine-dependent vs control individuals. In samples 1 and 2, 15 565 and 25 538 SNPs displayed t values with $P < .05$ (**Figure**). We term these SNPs *nominally positive SNPs*; since these P values are not corrected for multiple comparisons, these data do not allow us to distinguish these values from chance.

We obtained results that differed from those expected by chance; however, when we evaluated the extent to which 3 or more of these nominally positive SNPs "cluster" together with 25 kb or more separating them, 846 clusters contained 3749 of the 15 569 nominally positive SNPs from sample 1 and 1787 clusters contained 8388 of the 25 538 nominally positive SNPs from sample 2. Such clustering is found in no Monte Carlo trial of how frequently randomly selected sets of either 15 565 SNPs from sample 1 or 25 538 SNPs from sample 2 lie clustered within 25 kb of each other. With correction for the multiple comparisons made herein, the empirical P value for clustering of nominally positive SNPs is thus $< .00001$ for both samples 1 and 2. This degree of clustering within each single sample provides a control for the fact that we identified bona fide haplotypes that occur at different frequencies in the pools constructed from methamphetamine-dependent vs control samples. Stochastic differences in the frequencies at which these haplotypes occurred in our methamphetamine-dependent vs control samples that are independent of the addiction phenotype could conceivably contribute to some of the clustering in each individual sample, however.

We obtained evidence for replication and results that could not be expected by chance alone when we evaluated the genes that were identified by clustered nominally positive results from both sample 1 and sample 2 (Table and eTable, available at http://www.archgenpsychiatry.com). The degree of convergent identification of genes by data from each of these 2 samples was never observed by chance in any of 100 000 Monte Carlo simulation trials ($P < .00001$). The clustering of positive results in the same genes in both samples is thus very unlikely to represent stochastic effects. We term the genes identified in 2 samples in this way *"methamphetamine dependence" genes*. We use this term in quotation marks because variants in at least some of these genes are also likely to alter vulnerabilities to addictions for other substances (see later). The Monte Carlo P values assigned to each gene in the Table identify the probabilities that random segments of genes that have the same size as the true gene identified in each of these 2 samples would display at least the numbers of nominally positive SNPs actually identified in the true gene (see correction for multiple comparisons in the Table legend).

These "methamphetamine dependence" genes displayed convergence with genes identified by (1) clustered positive results from 639 000 SNP GWA studies of polysubstance abuse in National Institute on Drug Abuse European American and African American samples,[32] (2) nominally positive SNPs from 100 000 GWA studies of alcohol dependence,[57,58] and (3) nominally positive SNPs in comparisons of nicotine-dependent vs nondependent smokers (Table).[58] Data from samples 1 and 2 converge with these previously reported data sets, with Monte Carlo P values of (1) .0412, (2) .0016, and (3) .0003, re-

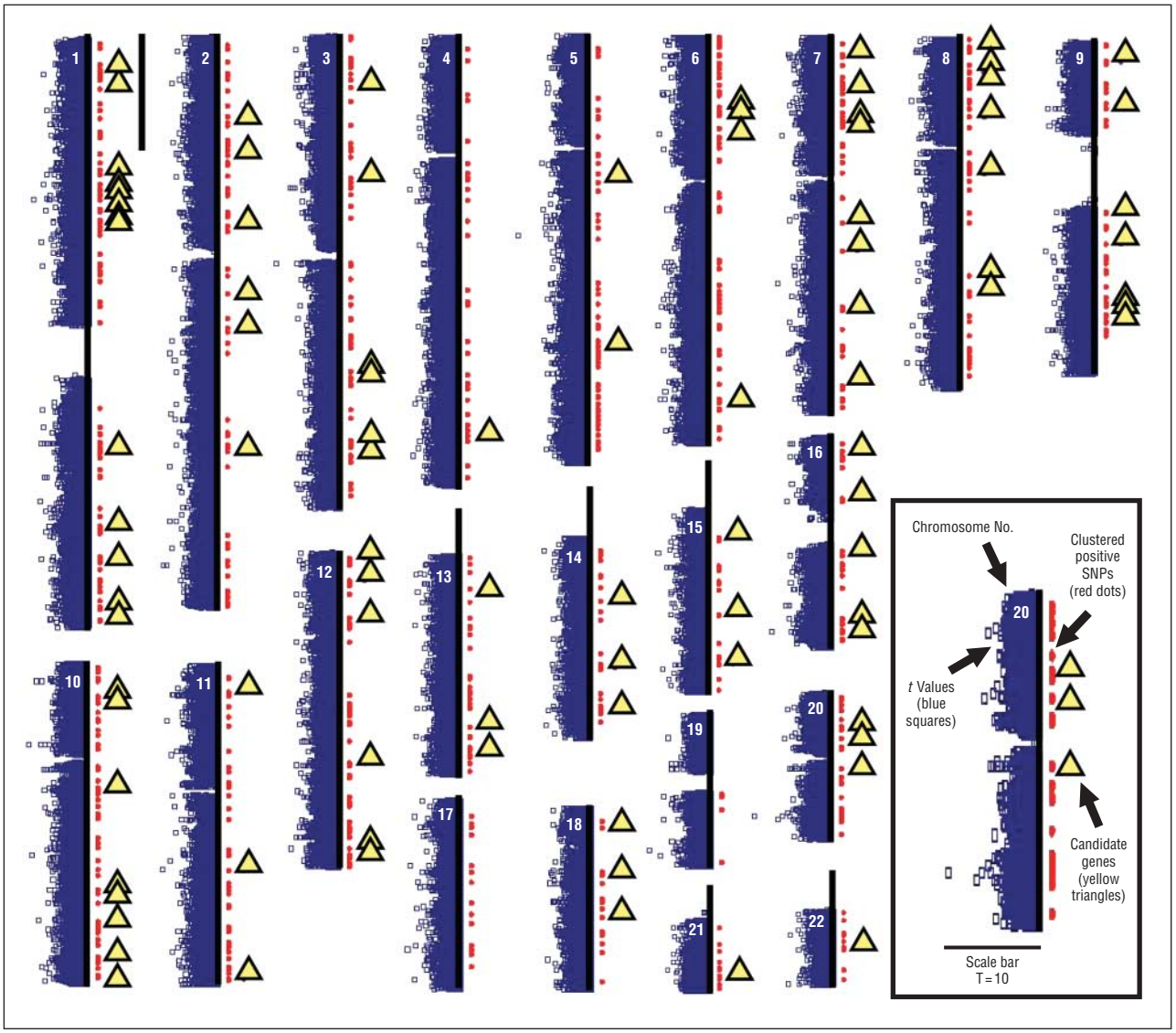

Figure. Cartoons of chromosomes 1 to 22. The blue squares to the left of the axis represent *t* values for the methamphetamine-dependent vs control allele frequency ratios mapped to the chromosomal position of each corresponding single-nucleotide polymorphism (SNP). The SNPs for which abuser-control differences display *P* values >.05 and that pass the clustering criteria of 3 outlier SNPs from 2 array types with less than a 25-kilobase inter-SNP distance are marked with red dots to the right of the axis. Clustered SNPs in genes with convergent evidence from both sample 1 and sample 2 are marked by yellow triangles to the right of the axis. The scale bar represents 50 Mb, with chromosomal positions based on National Center for Biotechnology Information (Bethesda, Maryland) MAPVIEWER coordinates and supplemental data from NetAffyx. The chromosomes are ordered in rows from left to right by chromosome number.

spectively. These analyses both correct for the multiple comparisons made and provide substantial additional support for many of the genes identified herein.

A number of the reproducibly positive genes identified in the current study are also identified by clustered positive results from 500 000 GWA studies of European American smokers who were successful vs unsuccessful in abstaining from smoking during clinical trials for smoking cessation ($P = .002$[59] and $P < .00001$ [G.R.U., unpublished data, 2007]).

The large differences between these observed results and chance clustering makes it highly unlikely that most of the clustered positive SNPs resulted from misgenotyping, for which there should be no reason that results should cluster. The SNPs that displayed clustered positive results in the current study failed to overlap appreciably more than expected by chance with the SNPs that displayed the largest variances from array to array (391 SNPs identified vs 386 expected by chance). Many of the positive SNPs in this report were thus likely to cluster since they lie near and display linkage disequilibrium with functional variants that contribute to individual differences in vulnerability to methamphetamine dependence. Convergence with observations made in other samples supports this idea and suggests that some of the functional variants that were identified by these clustered positive SNPs are likely to contribute to vulnerability to addictions to other substances as well as to methamphetamine.

There is also no evidence that most of the SNPs identified herein were found because of occult racial/ethnic stratification between methamphetamine-dependent and control groups. There was no significant overlap between clustered reproducibly positive SNPs from samples 1 and 2 with the SNPs that provided the largest racial/

ethnic differences from comparisons between European American and African American controls or between Japanese and Chinese HapMap samples (though 523 and 737 of the outlier SNPs from samples 1 and 2 do lie in the top 2.5% of the SNPs that distinguish JPT [Japanese from Tokyo] from CHB [Han Chinese from Beijing] HapMap samples, when 389 and 532 would be expected by chance; $.06 > P > .05$).

COMMENT

This report identifies chromosomal regions that are likely to contain allelic variants that alter vulnerability to methamphetamine dependence. The validity of these observations is supported by the clustering of nominally positive SNPs and from the convergence of data from 2 independent samples. The clustered positive markers from this work identify "methamphetamine dependence" genes whose products are involved in cell adhesion, enzymatic, transcriptional regulation, and other processes. The classes of genes identified and convergence with results from other GWA studies point toward substantial roles for individual differences in mnemonic, as well as rewarding, brain systems and individual differences in vulnerability to methamphetamine dependence.[20]

The reliability and validity of the current approach are supported by many lines of evidence. These include data for clinical assessments made by multiple observers, the reliability and validity of the microarray-based genotyping approaches used herein,[32,52,57,62] the extent to which the markers that displayed nominally positive differences between abusers and controls clustered together in specific chromosomal regions, the extent to which observations made in these 2 samples converge with each other, and the extent to which these results converge with those from other studies that compare dependent vs control individuals. We have also confirmed many of the results from these approaches using individual genotyping (A. Hishimoto, MD, PhD, T.D., and G.R.U., unpublished data, 2007).

Modeling studies indicate that the experimental designs used herein have significant statistical power to detect modest differences in allelic frequencies between methamphetamine-dependent individuals and controls. Nonetheless, there remains the likelihood of both false-positive and false-negative results. Power calculations indicate that our current approach will fail to identify 1% and 38% of the alleles that actually have 10% and 5% abuser vs control differences, respectively, in both samples; other calculations support higher false-negative rates (see "Power Calculations" subsection). As always, larger samples would help to reduce these false-negative results. However, independent of the separate statistical considerations for each population studied herein, the degree of replication and convergence between the 2 samples and with other drug-abusing populations provides additional confidence in results obtained.

Monte Carlo analyses indicate that we never, by chance, could identify a group of SNPs as large as the group in the Table that (1) display nominally significant *P* values, (2) cluster together in groups of 3 or more within small chromosomal regions, and (3) provide replication so that clustered nominally positive SNPs from comparisons in sample 1 fit with the clustered nominally positive SNPs in comparisons from sample 2. These statistical arguments are buttressed by technical convergence. Each of the clusters of nominally positive SNPs identified herein contain positive SNPs that are independently identified on at least 2 array types, each determined in quadruplicate.

In addition to the overall statistical confidence in the set of the genes identified herein, a number of these "methamphetamine dependence" genes overlap with genes identified in other GWA studies of addiction vulnerability and related phenotypes. More than half of the 23 cell adhesion genes identified in the current work are identified by prior GWA studies of polysubstance and alcohol dependence (8 genes), nicotine dependence (1 gene), memory (1 gene), and/or smoking cessation success (4 genes) in samples collected in the United States and Australia from individuals of self-reported European and African ancestries. Clustered positive markers in *DAB1* thus also distinguish those successful in quitting smoking vs those unsuccessful; *CLSTN2* (OMIM *611323) markers also identify success in quitting smoking and individual differences in memory; *NRXN1* markers also identify vulnerability to nicotine dependence among smokers; markers in *CRIM1*, *CSMD1*, *SGCZ*, *PTPRD*, and *LRRN6C* identify vulnerability to polysubstance use and to alcohol dependence; and markers in *CDH13* (OMIM *601364) and *DSCAM* (OMIM *602523) identify vulnerability to polysubstance use, alcohol dependence, and success in quitting smoking. These molecules join neurexin 3,[52,63] *NrCAM*,[64] and *PTPRB* (H. Ishiguro, MD, PhD, and G.R.U., unpublished data, 2007) and other cell adhesion molecule genes that display addict vs control associations in at least 3 different samples. Such results support careful use of *"methamphetamine dependence" genes* to describe genes likely to contain variants that predispose to methamphetamine dependence rather than to describe gene variants that predispose to vulnerability to only this drug.

Enzyme genes that are identified herein and also by repeated substance abuse GWA studies include *DAF/CD55*, *FHIT*, *PDE4D*, and *PRKG1* (OMIM *176894). The putative transcription factor *ZNF423* is also identified by comparisons between those successful and unsuccessful in smoking cessation.

The channel gene *RYR3*, the transporter gene *XKR4*, the gene for RNA processing *A2BP1* (OMIM *605104), and the structural genes *ELMO1*, *SORCS1*, and *TACC2* are also identified by clustered positive results from repeated comparisons between substance-dependent and control samples. Markers at *A2BP1* also distinguish smokers who are successful vs unsuccessful in quitting.

The genes that contain markers whose frequencies distinguish the methamphetamine-dependent vs control subjects in the present report and also distinguish dependent vs nondependent subjects and those successful vs unsuccessful in quitting smoking represent an especially interesting group. These genes include *CDH13*, *DSCAM*, *PRKG1*, and *A2BP1*. Cadherin 13 is a glycosyl phosphatidylinositol–anchored cell adhesion molecule that is expressed in neurons in brain regions that are known to have a role in addiction, including the hippo-

campus, frontal cortex, and ventral midbrain.[65] *CDH13* can inhibit neurite extension from select neuron populations[65,66] and activate a number of signaling pathways.[67-70] It is thus a strong candidate for roles in brain mechanisms important for both developing and quitting addictions.

DSCAM is a single transmembrane domain cell adhesion molecule with immunoglobulin and fibronectin domains that is expressed strongly in the brain[71,72] and hippocampus in ways that are required for appropriate neuronal connections to form in memory-associated circuits in model organisms.[73,74] Flies with altered *Dscam* expression display alterations in memories of both rewarded and punished behaviors.[74]

PRKG1 is expressed in the brain and hippocampus and other neurons.[75,76] Nitric oxide dramatically modulates brain cyclic guanine monophosphate systems; *PRKG1* thus provides a major target for the products of nitric oxide synthases. Mnemonic and addictive functions can each be altered by changes in cyclic guanine monophosphate–dependent protein kinase and/or nitric oxide synthases.[77-79]

The *A2BP1* gene is highly expressed in neurons in brain regions that include the hippocampus.[80] *A2BP1* binds to a UGCAUG splicing enhancer element found 3′ to a substantial number of neuron-specific exons and thus acts as a specific regulator of the splicing processes that form mature messenger RNAs.[81] *A2BP1* itself contains a number of splicing variants that are likely to alter its functions.

Identifying *CLSTN2* markers in the present repeated comparisons between methamphetamine-dependent vs control subjects in repeated comparisons of success in quitting smoking and in relation to individual differences in memory is also interesting. *CLSTN2* is well positioned to provide calcium-dependent cell-adhesion functions in brain regions that include the hippocampus and in the postsynaptic densities where it is highly expressed. The identification of this and other genes whose variants are good candidates to contribute to mnemonic aspects of addiction support the view that substantial components of the individual difference in vulnerability to dependence on addictive substances relate to individual differences in mnemonic systems.[20]

The convergence between the genes identified by these samples and by genes identified in previous GWA studies for dependence on other legal and illegal addictive substances supports roles for allelic variants that are well represented in chromosomes from African, European, and Asian racial/ethnic groups.[32,57] Genes identified by these methamphetamine-dependence studies, but not as strongly by any of these other GWA comparisons, are also of interest. Neuregulin 1 is a strong candidate gene for vulnerability to schizophrenia in Icelandic and related populations.[82-84] Conceivably, variants in neuregulin 1 might even provide a generalized vulnerability to psychosis that could manifest itself in the presence of either methamphetamine or other risk factors for schizophrenia.

It is important to consider limitations of this convergent replicated GWA data for methamphetamine dependence. (1) The sample sizes available for this work provide moderate power to detect gene variants related to methamphetamine dependence in each sample. False-negative results are likely since we required positive data from each of the 2 samples. The likelihood of false negatives is also increased since we required positive results from several SNPs from at least 2 array types that cluster within small chromosomal regions, making it easier to miss modest association signals within small genes that contain few SNPs or genes whose SNPs lie on only 1 array type. (2) We focused only on data from autosomal regions herein. This focus allowed us to combine data from male and female subjects but may have neglected potentially important contributions from genes on sex chromosomes. (3) Differences in allele frequencies in different populations could explain why some genes were strongly associated with methamphetamine dependence in the Asian samples studied herein but not as strongly with related substance-dependence phenotypes studied in European American or African American samples. (4) Many of the subjects for this work came to clinical attention because of methamphetamine psychosis. They might thus not be totally representative of all methamphetamine-dependent individuals. (5) While each of these individuals was methamphetamine dependent, many also reported use of additional addictive substances, such as inhalants. These clinical considerations, as well as the overlap between the "methamphetamine dependence" genes identified herein and the genes identified in other GWA work, support the idea that many, but not all, of these loci are likely to contain allelic variants that provide a more general vulnerability to addictive substances. While we term these genes *"methamphetamine dependence" genes* to denote the fact that variants in these genes are likely to alter vulnerability to developing dependence on this substance, we use the term in quotation marks to denote the probability that many of these allelic variants may predispose individuals to dependence on other addictive substances as well. (6) None of the controls for this study reported any significant use of methamphetamine. The genes identified herein thus could influence vulnerabilities to initiation of methamphetamine use, persistence of this use, and/or the transition from persistent use to methamphetamine dependence. (7) The current report uses only one of a number of current approaches to analysis of data from GWA. Additional discussion of the limits of techniques for identifying polygenic influences in complex disorders and traits can be found elsewhere.[85-87] Despite these cautions, however, the replicated positive results that we document herein and the failure of control experiments to support alternative hypotheses do provide substantial confidence in roles for most of the genes reported.

The current data, and results of classic genetic studies, thus support polygenic influences on vulnerability to methamphetamine dependence from genes that, as a group, are highly unlikely to represent chance observations. *P* values for individual genes, based on the data from the current work, suggest that some of these genes are very strongly supported and some more modestly supported by these current data. Genes identified by both the current results and by data from other related reports appear especially worthy of further evaluation. Taken together, the data point toward the likelihood that brains of individuals who are most vulnerable to this addiction are likely to differ in a number of ways from those of in-

dividuals who are least vulnerable. Understanding these differences in increasing detail should aid us in improving understanding, prevention, and treatments for methamphetamine dependence.

Submitted for Publication: May 8, 2007; final revision received September 14, 2007; accepted September 17, 2007.
Author Affiliations: Molecular Neurobiology Branch, National Institutes of Health Intramural Program, Department of Health and Human Services, Baltimore, Maryland (Drs Uhl, Drgon, and Q-R. Liu and Mss Johnson and Walther); Division of Psychiatry, National Center Hospital for Mental, Nervous, and Muscular Disorders, National Center of Neurology and Psychiatry, Tokyo, Japan (Dr Komiyama); Department of Neuropsychiatry, Kurume University School of Medicine, Kurume, Japan (Dr Harano); Department of Psychiatry and Neurology, Hamamatsu University School of Medicine, Hamamatsu, Japan (Dr Sekine); Department of Psychiatry, Nagoya University Graduate School of Medicine, Nagoya, Japan (Drs Inada and Ozaki); Department of Psychiatry, Teikyo University School of Medicine, Chiba Medical Center (Dr Inada), and Department of Psychiatry, Graduate School of Medicine, Chiba University (Dr Iyo), Chiba, Japan; Department of Psychiatry, Fujita Health University School of Medicine, Aichi, Japan (Dr Iwata); Department of Psychiatry, Showa University Northern Yokohama Hospital, Yokohama, Japan (Dr Yamada); Department of Biological Psychiatry, Tohoku University Graduate School of Medicine, Sendai, Japan (Dr Sora); Japanese Genetics Initiative on Drug Abuse (Drs Komiyama, Harano, Sekine, Inada, Ozaki, Iyo, Iwata, Yamada, Sora and Ujike); Department of Psychiatry, Chang Gung Memorial Hospital, Keelung, Taiwan (Dr Chen); Department of Psychiatry, Taipei City Hospital, and Taipei City Psychiatric Center, Taipei, Taiwan, Republic of China (Drs H-C. Liu and Lin); Department of Neuropsychiatry, Graduate School of Medicine and Dentistry, Okayama University, Okayama, Japan (Dr Ujike).
Correspondence: George R. Uhl, MD, PhD, Molecular Neurobiology, 333 Cassell Dr, Ste 3510, Baltimore, MD 21224 (guhl@intra.nida.nih.gov).
Financial Disclosure: None reported.
Funding/Support: Financial support was received from National Institutes of Health Intramural Program (National Institute on Drug Abuse), Department of Health and Human Services, and the Taiwanese and Japanese Ministries for Science and Technology and the participating Japanese and Taiwanese institutions.
Additional Information: The eTable is available at http://www.archgenpsychiatry.com.
Additional Contributions: We acknowledge the invaluable assistance of the subjects and their families.

REFERENCES

1. Uhl GR. Molecular genetic underpinnings of human substance abuse vulnerability: likely contributions to understanding addiction as a mnemonic process. *Neuropharmacology*. 2004;47(suppl 1):140-147.
2. Uhl GR. Molecular genetics of substance abuse vulnerability: remarkable recent convergence of genome scan results. *Ann N Y Acad Sci*. 2004;1025:1-13.
3. Uhl GR, Drgon T, Johnson C, Fatusin OO, Liu QR, Contoreggi C, Li CY, Buck K, Crabbe J. Higher order addiction molecular genetics: convergent data from genome-wide association in humans and mice [published online ahead of print July 25, 2007]. *Biochem Pharmacol*. 2008;75(1):98-111.
4. Uhl GR, Elmer GI, Labuda MC, Pickens RW. Genetic influences in drug abuse. In: Gloom FE, Kupfer DJ, eds. *Psychopharmacology: The Fourth Generation of Progress*. New York, NY: Raven Press; 1995:1793-2783.
5. Uhl GR, Gold LH, Risch N. Genetic analyses of complex behavioral disorders. *Proc Natl Acad Sci U S A*. 1997;94(7):2785-2786.
6. Uhl GR. Molecular genetics of substance abuse vulnerability: a current approach. *Neuropsychopharmacology*. 1999;20(1):3-9.
7. Cadoret RJ, Troughton E, O'Gorman TW, Heywood E. An adoption study of genetic and environmental factors in drug abuse. *Arch Gen Psychiatry*. 1986; 43(12):1131-1136.
8. Cadoret RJ, Yates WR, Troughton E, Woodworth G, Stewart MA. Adoption study demonstrating two genetic pathways to drug abuse. *Arch Gen Psychiatry*. 1995; 52(1):42-52.
9. Goldberg J, Henderson WG, Eisen SA, True W, Ramakrishnan V, Lyons MJ, Tsuang MT. A strategy for assembling samples of adult twin pairs in the United States. *Stat Med*. 1993;12(18):1693-1702.
10. Grove WM, Eckert ED, Heston L, Bouchard TJ Jr, Segal N, Lykken DT. Heritability of substance abuse and antisocial behavior: a study of monozygotic twins reared apart. *Biol Psychiatry*. 1990;27(12):1293-1304.
11. Gynther LM, Carey G, Gottesman II, Vogler GP. A twin study of non-alcohol substance abuse. *Psychiatry Res*. 1995;56(3):213-220.
12. Tsuang MT, Lyons MJ, Eisen SA, Goldberg J, True W, Lin N, Meyer JM, Toomey R, Faraone SV, Eaves L. Genetic influences on *DSM-III-R* drug abuse and dependence: a study of 3,372 twin pairs. *Am J Med Genet*. 1996;67(5):473-477.
13. Tsuang MT, Lyons MJ, Meyer JM, Doyle T, Eisen SA, Goldberg J, True W, Lin N, Toomey R, Eaves L. Co-occurrence of abuse of different drugs in men: the role of drug-specific and shared vulnerabilities. *Arch Gen Psychiatry*. 1998;55(11): 967-972.
14. Karkowski LM, Prescott CA, Kendler KS. Multivariate assessment of factors influencing illicit substance use in twins from female-female pairs. *Am J Med Genet*. 2000;96(5):665-670.
15. Kendler KS, Prescott CA. Cocaine use, abuse and dependence in a population-based sample of female twins. *Br J Psychiatry*. 1998;173:345-350.
16. Kendler KS, Karkowski LM, Corey LA, Prescott CA, Neale MC. Genetic and environmental risk factors in the aetiology of illicit drug initiation and subsequent misuse in women. *Br J Psychiatry*. 1999;175:351-356.
17. Woodward CE, Maes HH, Silberg JL, Meyer JM, Eaves LJ. Tobacco, alcohol and drug use in 8-16 year old twins. *NIDA Res Monogr*. 1996;162:309.
18. Merikangas KR, Stolar M, Stevens DE, Goulet J, Preisig MA, Fenton B, Zhang H, O'Malley SS, Rounsaville BJ. Familial transmission of substance use disorders. *Arch Gen Psychiatry*. 1998;55(11):973-979.
19. True WR, Heath AC, Scherrer JF, Xian H, Lin N, Eisen SA, Lyons MJ, Goldberg J, Tsuang MT. Interrelationship of genetic and environmental influences on conduct disorder and alcohol and marijuana dependence symptoms. *Am J Med Genet*. 1999;88(4):391-397.
20. Uhl GR. Molecular genetics of addiction vulnerability. *NeuroRx*. 2006;3(3):295-301.
21. Cervino AC, Hill AV. Comparison of tests for association and linkage in incomplete families. *Am J Hum Genet*. 2000;67(1):120-132.
22. Sham PC, Cherny SS, Purcell S, Hewitt JK. Power of linkage versus association analysis of quantitative traits, by use of variance-components models, for sibship data. *Am J Hum Genet*. 2000;66(5):1616-1630.
23. Risch N, Merikangas K. The future of genetic studies of complex human diseases. *Science*. 1996;273(5281):1516-1517.
24. Schork NJ, Nath SK, Fallin D, Chakravarti A. Linkage disequilibrium analysis of biallelic DNA markers, human quantitative trait loci, and threshold-defined case and control subjects. *Am J Hum Genet*. 2000;67(5):1208-1218.
25. Barcellos LF, Klitz W, Field LL, Tobias R, Bowcock AM, Wilson R, Nelson MP, Nagatomi J, Thomson G. Association mapping of disease loci, by use of a pooled DNA genomic screen. *Am J Hum Genet*. 1997;61(3):734-747.
26. Germer S, Holland MJ, Higuchi R. High-throughput SNP allele-frequency determination in pooled DNA samples by kinetic PCR. *Genome Res*. 2000;10(2): 258-266.
27. Hacia JG, Fan JB, Ryder O, Jin L, Edgemon K, Ghandour G, Mayer RA, Sun B, Hsie L, Robbins CM, Brody LC, Wang D, Lander ES, Lipshutz R, Fodor SP, Collins FS. Determination of ancestral alleles for human single-nucleotide polymorphisms using high-density oligonucleotide arrays. *Nat Genet*. 1999;22(2):164-167.
28. Uhl GR, Liu QR, Walther D, Hess J, Naiman D. Polysubstance abuse-vulnerability genes: genome scans for association, using 1,004 subjects and 1,494 single-nucleotide polymorphisms. *Am J Hum Genet*. 2001;69(6):1290-1300.

29. Chen WJ, Liu SK, Chang CJ, Lien YJ, Chang YH, Hwu HG. Sustained attention deficit and schizotypal personality features in nonpsychotic relatives of schizophrenic patients. *Am J Psychiatry*. 1998;155(9):1214-1220.
30. Bucholz KK, Cadoret R, Cloninger CR, Dinwiddie SH, Hesselbrock VM, Nurnberger JI Jr, Reich T, Schmidt I, Schuckit MA. A new, semi-structured psychiatric interview for use in genetic linkage studies: a report on the reliability of the SSAGA. *J Stud Alcohol*. 1994;55(2):149-158.
31. American Psychiatric Association. *Diagnostic and Statistical Manual of Mental Disorders*. 4th ed. Washington, DC: American Psychiatric Association; 1994.
32. Liu QR, Drgon T, Johnson C, Walther D, Hess J, Uhl GR. Addiction molecular genetics: 639,401 SNP whole genome association identifies many "cell adhesion" genes. *Am J Med Genet B Neuropsychiatr Genet*. 2006;141(8):918-925.
33. Itoh K, Hashimoto K, Shimizu E, Sekine Y, Ozaki N, Inada T, Harano M, Iwata N, Komiyama T, Yamada M, Sora I, Nakata K, Ujike H, Iyo M. Association study between brain-derived neurotrophic factor gene polymorphisms and methamphetamine abusers in Japan. *Am J Med Genet B Neuropsychiatr Genet*. 2005;132(1):70-73.
34. Iwata N, Inada T, Harano M, Komiyama T, Yamada M, Sekine Y, Iyo M, Sora I, Ujike H, Ozaki N. No association is found between the candidate genes of t-PA/plasminogen system and Japanese methamphetamine-related disorder: a collaborative study by the Japanese Genetics Initiative for Drug Abuse. *Ann N Y Acad Sci*. 2004;1025:34-38.
35. Morita Y, Ujike H, Tanaka Y, Uchida N, Nomura A, Ohtani K, Kishimoto M, Morio A, Imamura T, Sakai A, Inada T, Harano M, Komiyama T, Yamada M, Sekine Y, Iwata N, Iyo M, Sora I, Ozaki N, Kuroda S. A nonsynonymous polymorphism in the human fatty acid amide hydrolase gene did not associate with either methamphetamine dependence or schizophrenia. *Neurosci Lett*. 2005;376(3):182-187.
36. Hashimoto T, Hashimoto K, Matsuzawa D, Shimizu E, Sekine Y, Inada T, Ozaki N, Iwata N, Harano M, Komiyama T, Yamada M, Sora I, Ujike H, Iyo M. A functional glutathione S-transferase P1 gene polymorphism is associated with methamphetamine-induced psychosis in Japanese population. *Am J Med Genet B Neuropsychiatr Genet*. 2005;135(1):5-9.
37. Ujiie H, Inada T, Harano M, Komiyayama T, Yamada M, Sekine Y, Sora I, Iwata N, Iyo M, Ozaki N. Genetic studies on substance dependence [in Japanese]. *Seishin Shinkeigaku Zasshi*. 2004;106(12):1598-1603.
38. Nishiyama T, Ikeda M, Iwata N, Suzuki T, Kitajima T, Yamanouchi Y, Sekine Y, Iyo M, Harano M, Komiyama T, Yamada M, Sora I, Ujike H, Inada T, Furukawa T, Ozaki N. Haplotype association between GABAA receptor gamma2 subunit gene (GABRG2) and methamphetamine use disorder. *Pharmacogenomics J*. 2005;5(2):89-95.
39. Morita Y, Ujike H, Tanaka Y, Uchida N, Nomura A, Otani K, Kishimoto M, Morio A, Inada T, Harano M, Komiyama T, Yamada M, Sekine Y, Iwata N, Iyo M, Sora I, Ozaki N. The X-box binding protein 1 (XBP1) gene is not associated with methamphetamine dependence. *Neurosci Lett*. 2005;383(1-2):194-198.
40. Ikeda M, Iwata N, Suzuki T, Kitajima T, Yamanouchi Y, Kinoshiya Y, Sekine Y, Iyo M, Harano M, Komiyama T, Yamada M, Sora I, Ujike H, Inada T, Ozaki N. Positive association of AKT1 haplotype to Japanese methamphetamine use disorder [published online ahead of print June 28, 2005]. *Int J Neuropsychopharmacol*. 2006;9(1):77-81.
41. Ide S, Kobayashi H, Tanaka K, Ujike H, Sekine Y, Ozaki N, Inada T, Harano M, Komiyama T, Yamada M, Iyo M, Ikeda K, Sora I. Gene polymorphisms of the mu opioid receptor in methamphetamine abusers. *Ann N Y Acad Sci*. 2004;1025:316-324.
42. Harano M, Uchimura N, Abe H, Ishibashi M, Iida N, Yanagimoto K, Tanaka T, Maeda H, Sora I, Iyo M, Komiyama T, Yamada M, Sekine Y, Inada T, Ozaki N, Ujike H. A polymorphism of DRD2 gene and brain atrophy in methamphetamine psychosis. *Ann N Y Acad Sci*. 2004;1025:307-315.
43. Inada T, Iijima Y, Uchida N, Maeda T, Iwashita S, Ozaki N, Harano M, Komiyama T, Yamada M, Sekine Y, Iyo M, Sora I, Ujikec H. No association found between the type 1 sigma receptor gene polymorphisms and methamphetamine abuse in the Japanese population: a collaborative study by the Japanese Genetics Initiative for Drug Abuse. *Ann N Y Acad Sci*. 2004;1025:27-33.
44. Koizumi H, Hashimoto K, Kumakiri C, Shimizu E, Sekine Y, Ozaki N, Inada T, Harano M, Komiyama T, Yamada M, Sora I, Ujike H, Takei N, Iyo M. Association between the glutathione S-transferase M1 gene deletion and female methamphetamine abusers. *Am J Med Genet B Neuropsychiatr Genet*. 2004;126(1):43-45.
45. Ujike H, Harano M, Inada T, Yamada M, Komiyama T, Sekine Y, Sora I, Iyo M, Katsu T, Nomura A, Nakata K, Ozaki N. Nine or fewer repeat alleles in VNTR polymorphism of the dopamine transporter gene is a strong risk factor for prolonged methamphetamine psychosis. *Pharmacogenomics J*. 2003;3(4):242-247.
46. World Health Organization. *ICD-10: International Statistical Classification of Diseases and Related Health Problems: Tenth Revision*. 2nd ed. Geneva, Switzerland: World Health Organization; 2004.
47. Smith SS, O'Hara BF, Persico AM, Gorelick DA, Newlin DB, Vlahov D, Solomon L, Pickens R, Uhl GR. Genetic vulnerability to drug abuse: the D2 dopamine receptor Taq I B1 restriction fragment length polymorphism appears more frequently in polysubstance abusers. *Arch Gen Psychiatry*. 1992;49(9):723-727.
48. Persico AM, Bird G, Gabbay FH, Uhl GR. D2 dopamine receptor gene TaqI A1 and B1 restriction fragment length polymorphisms: enhanced frequencies in psychostimulant-preferring polysubstance abusers. *Biol Psychiatry*. 1996;40(8):776-784.
49. Mägi R, Pfeufer A, Nelis M, Montpetit A, Metspalu A, Remm M. Evaluating the performance of commercial whole-genome marker sets for capturing common genetic variation. *BMC Genomics*. 2007;8:159.
50. Wilkening S, Chen B, Wirtenberger M, Burwinkel B, Forsti A, Hemminki K, Canzian F. Allelotyping of pooled DNA with 250 K SNP microarrays. *BMC Genomics*. 2007;8:77.
51. Macgregor S, Visscher PM, Montgomery G. Analysis of pooled DNA samples on high density arrays without prior knowledge of differential hybridization rates. *Nucleic Acids Res*. 2006;34(7):e55.
52. Liu QR, Drgon T, Walther D, Johnson C, Poleskaya O, Hess J, Uhl GR. Pooled association genome scanning: validation and use to identify addiction vulnerability loci in two samples. *Proc Natl Acad Sci U S A*. 2005;102(33):11864-11869.
53. Meaburn E, Butcher LM, Schalkwyk LC, Plomin R. Genotyping pooled DNA using 100K SNP microarrays: a step towards genomewide association scans. *Nucleic Acids Res*. 2006;34(4):e27.
54. Butcher LM, Meaburn E, Knight J, Sham PC, Schalkwyk LC, Craig IW, Plomin R. SNPs, microarrays and pooled DNA: identification of four loci associated with mild mental impairment in a sample of 6000 children. *Hum Mol Genet*. 2005;14(10):1315-1325.
55. Papassotiropoulos A, Stephan DA, Huentelman MJ, Hoerndli FJ, Craig DW, Pearson JV, Huynh KD, Brunner F, Corneveaux J, Osborne D, Wollmer MA, Aerni A, Coluccia D, Hanggi J, Mondadori CR, Buchmann A, Reiman EM, Caselli RJ, Henke K, de Quervain DJ. Common Kibra alleles are associated with human memory performance. *Science*. 2006;314(5798):475-478.
56. Bansal A. Trends in reporting of SNP associations. *Lancet*. 2001;358(9298):2016.
57. Johnson C, Drgon T, Liu QR, Walther D, Edenberg H, Rice J, Foroud T, Uhl GR. Pooled association genome scanning for alcohol dependence using 104,268 SNPs: validation and use to identify alcoholism vulnerability loci in unrelated individuals from the collaborative study on the genetics of alcoholism. *Am J Med Genet B Neuropsychiatr Genet*. 2006;141(8):844-853.
58. Bierut LJ, Madden PA, Breslau N, Johnson EO, Hatsukami D, Pomerleau OF, Swan GE, Rutter J, Bertelsen S, Fox L, Fugman D, Goate AM, Hinrichs AL, Konvicka K, Martin NG, Montgomery GW, Saccone NL, Saccone SF, Wang JC, Chase GA, Rice JP, Ballinger DG. Novel genes identified in a high-density genome wide association study for nicotine dependence. *Hum Mol Genet*. 2007;16(1):24-35.
59. Uhl GR, Liu QR, Drgon T, Johnson C, Walther D, Rose JE. Molecular genetics of nicotine dependence and abstinence: whole genome association using 520,000 SNPs. *BMC Genet*. 2007;8(1):10.
60. Dupont WD, Plummer WD Jr. Power and sample size calculations: a review and computer program. *Control Clin Trials*. 1990;11(2):116-128.
61. Purcell S, Cherny SS, Sham PC. Genetic Power Calculator: design of linkage and association genetic mapping studies of complex traits. *Bioinformatics*. 2003;19(1):149-150.
62. Butcher LM, Meaburn E, Liu L, Fernandes C, Hill L, Al-Chalabi A, Plomin R, Schalkwyk L, Craig IW. Genotyping pooled DNA on microarrays: a systematic genome screen of thousands of SNPs in large samples to detect QTLs for complex traits. *Behav Genet*. 2004;34(5):549-555.
63. Hishimoto A, Liu QR, Drgon T, Pletnikova O, Walther D, Zhu XG, Troncoso JC, Uhl GR. Neurexin 3 polymorphisms are associated with alcohol dependence and altered expression of specific isoforms. *Hum Mol Genet*. 2007;16(23):2880-2891.
64. Ishiguro H, Liu QR, Gong JP, Hall FS, Ujike H, Morales M, Sakurai T, Grumet M, Uhl GR. NrCAM in addiction vulnerability: positional cloning, drug-regulation, haplotype-specific expression, and altered drug reward in knockout mice. *Neuropsychopharmacology*. 2006;31(3):572-584.
65. Takeuchi T, Misaki A, Liang SB, Tachibana A, Hayashi N, Sonobe H, Ohtsuki Y. Expression of T-cadherin (CDH13, H-Cadherin) in human brain and its characteristics as a negative growth regulator of epidermal growth factor in neuroblastoma cells. *J Neurochem*. 2000;74(4):1489-1497.
66. Fredette BJ, Miller J, Ranscht B. Inhibition of motor axon growth by T-cadherin substrata. *Development*. 1996;122(10):3163-3171.
67. Kipmen-Korgun D, Osibow K, Zoratti C, Schraml E, Greilberger J, Kostner GM, Jurgens G, Graier WF. T-cadherin mediates low-density lipoprotein-initiated cell proliferation via the Ca(2+)-tyrosine kinase-Erk1/2 pathway. *J Cardiovasc Pharmacol*. 2005;45(5):418-430.
68. Philippova M, Ivanov D, Allenspach R, Takuwa Y, Erne P, Resink T. RhoA and Rac mediate endothelial cell polarization and detachment induced by T-cadherin. *FASEB J*. 2005;19(6):588-590.

69. Hug C, Wang J, Ahmad NS, Bogan JS, Tsao TS, Lodish HF. T-cadherin is a receptor for hexameric and high-molecular-weight forms of Acrp30/adiponectin. *Proc Natl Acad Sci U S A*. 2004;101(28):10308-10313.
70. Ivanov DB, Philippova MP, Tkachuk VA. Structure and functions of classical cadherins. *Biochemistry (Mosc)*. 2001;66(10):1174-1186.
71. Yamakawa K, Huot YK, Haendelt MA, Hubert R, Chen XN, Lyons GE, Korenberg DSCAM Jr. A novel member of the immunoglobulin superfamily maps in a Down syndrome region and is involved in the development of the nervous system. *Hum Mol Genet*. 1998;7(2):227-237.
72. Barlow GM, Micales B, Lyons GE, Korenberg JR. Down syndrome cell adhesion molecule is conserved in mouse and highly expressed in the adult mouse brain. *Cytogenet Cell Genet*. 2001;94(3-4):155-162.
73. Chen BE, Kondo M, Garnier A, Watson FL, Puettmann-Holgado R, Lamar DR, Schmucker D. The molecular diversity of Dscam is functionally required for neuronal wiring specificity in Drosophila. *Cell*. 2006;125(3):607-620.
74. Keene AC, Krashes MJ, Leung B, Bernard JA, Waddell S. Drosophila dorsal paired medial neurons provide a general mechanism for memory consolidation. *Curr Biol*. 2006;16(15):1524-1530.
75. Feil S, Zimmermann P, Knorn A, Brummer S, Schlossmann J, Hofmann F, Feil R. Distribution of cGMP-dependent protein kinase type I and its isoforms in the mouse brain and retina. *Neuroscience*. 2005;135(3):863-868.
76. Demyanenko GP, Halberstadt AI, Pryzwansky KB, Werner C, Hofmann F, Maness PF. Abnormal neocortical development in mice lacking cGMP-dependent protein kinase I. *Brain Res Dev Brain Res*. 2005;160(1):1-8.
77. Weitzdoerfer R, Hoeger H, Engidawork E, Engelmann M, Singewald N, Lubec G, Lubec B. Neuronal nitric oxide synthase knock-out mice show impaired cognitive performance. *Nitric Oxide*. 2004;10(3):130-140.
78. Itzhak Y, Martin JL, Black MD, Huang PL. The role of neuronal nitric oxide synthase in cocaine-induced conditioned place preference. *Neuroreport*. 1998; 9(11):2485-2488.
79. Kleppisch T, Wolfsgruber W, Feil S, Allmann R, Wotjak CT, Goebbels S, Nave KA, Hofmann F, Feil R. Hippocampal cGMP-dependent protein kinase I supports an age- and protein synthesis-dependent component of long-term potentiation but is not essential for spatial reference and contextual memory. *J Neurosci*. 2003; 23(14):6005-6012.
80. Allen Institute for Brain Science Allen Brain Atlas. http://brain-map.org/. Accessed January 23, 2007.
81. Underwood JG, Boutz PL, Dougherty JD, Stoilov P, Black DL. Homologues of the Caenorhabditis elegans Fox-1 protein are neuronal splicing regulators in mammals. *Mol Cell Biol*. 2005;25(22):10005-10016.
82. Stefansson H, Sarginson J, Kong A, Yates P, Steinthorsdottir V, Gudfinnsson E, Gunnarsdottir S, Walker N, Petursson H, Crombie C, Ingason A, Gulcher JR, Stefansson K, St Clair D. Association of neuregulin 1 with schizophrenia confirmed in a Scottish population. *Am J Hum Genet*. 2003;72(1):83-87.
83. Stefansson H, Sigurdsson E, Steinthorsdottir V, Bjornsdottir S, Sigmundsson T, Ghosh S, Brynjolfsson J, Gunnarsdottir S, Ivarsson O, Chou TT, Hjaltason O, Birgisdottir B, Jonsson H, Gudnadottir VG, Gudmundsdottir E, Bjornsson A, Ingvarsson B, Ingason A, Sigfusson S, Hardardottir H, Harvey RP, Lai D, Zhou M, Brunner D, Mutel V, Gonzalo A, Lemke G, Sainz J, Johannesson G, Andresson T, Gudbjartsson D, Manolescu A, Frigge ML, Gurney ME, Kong A, Gulcher JR, Petursson H, Stefansson K. Neuregulin 1 and susceptibility to schizophrenia. *Am J Hum Genet*. 2002;71(4):877-892.
84. Stefansson H, Steinthorsdottir V, Thorgeirsson TE, Gulcher JR, Stefansson K. Neuregulin 1 and schizophrenia. *Ann Med*. 2004;36(1):62-71.
85. Wellcome Trust Case Control Consortium. Genome-wide association study of 14,000 cases of seven common diseases and 3,000 shared controls. *Nature*. 2007; 447(7145):661-678.
86. Dudbridge F, Gusnanto A, Koeleman BP. Detecting multiple associations in genome-wide studies. *Hum Genomics*. 2006;2(5):310-317.
87. NHLBI Research and Policy Update, number 35, November 2006. www.nhlbi.nih.gov/resources/listserv/number35.htm. Accessed January 23, 2007.